QUANTIFICATION
OF
METAMERISM AND COLOUR CONSTANCY

By

Wen-Guey Kuo

A Doctoral Thesis

Submitted in partial fulfilment of the requirements for the award of

Doctor of Philosophy

of the Loughborough University of Technology

August 1995

ACKNOWLEDGEMENTS

I wish to express my most sincere thanks to my supervisor Dr. H. E. Bez for his work on administration, and proof reading my thesis. I am greatly indebted to my external supervisor Dr. M. R. Luo for his guidance and constructive criticism in the writing of this thesis. Thanks are also due to Dr. B. Rigg together with the other members in the Colour Measurement Committee (CMC) for providing technical advices.

Particular thanks are due to Miss W. Li, Miss K. Li, Miss L. Yu, Miss Q. Wang, Miss M. C. Lo, Mr. Q. Ma, Mr. K. Ho, Mr. W. Kung, Dr. T. M. Zimina, Dr. J. H. Xin, Dr. X. Wang, Dr. H. Jiang, Dr. P. Yu and Dr. A. S. Goh for taking part as observers in many experimental sessions.

Special thanks are due to financial assistance from the National Science Council and the University of Chinese Culture, Taiwan, R. O. C. , and the Society of Dyers and Colourists, U.K.

I am grateful to Professor J. Blanshard, Mrs. J. Blanshard, Mr. and Mrs. R. and P. Waters, Miss V. Thompson together with the brothers and sisters of the Loughborough Chinese Christian Fellowship for their spiritual support.

I offer my gratitude and sincere thanks to my wife Lihua for her enduring encouragement and to my baby son Ziying who arrived in time to give me much encouragement, and made so many efforts to keep his "quiet" during my writing.

Above all, I wish to express my most sincere gratitude to God the Almighty, the Creator and source of everything.

To God be the Glory.

ABSTRACT

Reliable colour constancy and metamerism indices are highly desired by industry for colour quality control. Two experiments were conducted to quantify the degree of colour constancy and metamerism.

In the colour constancy experiment, 240 wool samples were prepared and scaled using a magnitude estimation method by a panel of 5 experienced observers under sources D65, A and TL84. 2 corresponding data sets derived from the experimental results were used to test various chromatic adaptation transforms. The results clearly show that the BFD transform gave the most precise prediction than the other transforms. Attempts were also made to derive 4 new transforms from four independent data sets. These gave similar performance as that of the BFD, but overcome the BFD's problem (incapable of predicting some of the high saturated colours). Hence, these transforms should be used with confidence for predicting the degree of colour constancy.

This experimental results were also used to test various uniform colour spaces and colour appearance models. The Hunt94 model gave the most precise prediction to the colourfulness and hue results. Modification was made to its lightness scale for improving the fit.

In the metamerism experiment, 76 pairs of wool samples were prepared and assessed with 20 observations using a grey scale under 7 sources: D65, A, TL84, TL83, P27, W and WW. The experimental results were used to test 3 types of illuminant metamerism indices derived here. It was found that calculating colour difference using 3 colour difference formulae, i.e. CMC, BFD and CIE94 gave the most precise prediction to the visual results. The degree of precision is quite satisfactory in comparison with typical observer precision.

A new standard deviate observer (SDO) was also derived. This together with the CIE SDO and 1964 Observer were tested using the author's and the Obande's data. The results showed that the new SDO predicted results more accurate than those from the other two CIE Observers. An Observer Metamerism Index (OMI) was also derived to indicate the degree of metamerism based upon the new SDO. The results showed that the new SDO was more suitable for indicating the degree of observer metamerism.

COLOUR is a gift of God.

TO

my family,

Lihua

and

my son, Ziying

CONTENTS

LIST OF TABLES

LIST OF FIGURES

Figure 3.5.3 The ΔE values calculated using the new SDO for the CIEL*a*b*, CMC(1:1), CIE94 and BFD(1:1) formulae (from top to bottom) plotted against the D65 ΔV results.

LIST OF APPENDICES

CHAPTER 1

CHAPTER 1

INTRODUCTION

1.1 General Introduction

Colour vision makes life more enjoyable and the world more colourful by providing information that would not exist in a monochromatic visual system. Chromatic sensation occurs due to the absorption of visible electromagnetic radiation in cone receptors with three different, but overlapping, spectral sensitivities. Millions of colours can be distinguished by those who have normal colour vision, but less than several thousand colours can be memorised or described using natural words. Although colour scientists have established methods for quantifying colour, colour specification is still a problem. This is mainly caused by the change of an object's colour appearance under different conditions of illumination. Obviously, there is a need to have an effective and reliable method to precisely define a colour under various viewing conditions.

In 1931, the International Commission on Illumination (CIE, Commission Internationale de l'Eclairage) recommended the CIE Standard Observer, illuminants and reflectance for defining object colour, on which the colorimetry is based. Since then, colour measurement has played an important role in colour specification in manufacturing industries. With advanced technology, the modern spectrophotometer driven by a computer with suitable software has considerably contributed towards automation and total colour management in industries. However, the performance of colour measurement is still considered to be unsatisfactory. For example, the standardisation of observer data has made colour measurement easier and more precise, but disagreement still exists between visual judgement and instrumental measurement. The phenomenon is more profound for colour objects with a metameric nature. A metameric pair may appear to be a perfect match to one observer, but be a

complete mis-match to another. Similarly, the match may no longer hold when the angular subtense by the sample pair to the same observer changes. It is common in industrial practice to control production within a tolerance under different illuminants. However, this tolerance is accepted solely on the basis of illuminant effects without any regard for observer variation. Thus, the end results could be still invalid when the metameric pair is exposed to the eyes of a random purchaser or a different observer. In many cases this may result in the rejection of the product.

The CIE systems specify each colour in terms of *tristimulus values* (described in the next Section) under a fixed set of viewing conditions such as observer and illuminant. In practice, the viewing conditions frequently vary. This indicates that the CIE systems cannot account for the change in appearance of a colour due to variation of viewing conditions. Hence, the tristimulus values must be regarded as a measure of the quality of the stimulus rather than of the quality of the sensation (Wright 1964). In industrial practice, specifying colour appearance under different viewing conditions is vital for quantifying the colour constancy of an object colour. For most coloured materials such as textiles, painted surfaces, plastic materials, the precise colour is important. A purchaser of coloured articles may carefully select the item by its colour, and would not be satisfied by a perceived change in the colour under a different light source. These goods are considered to be colour non-constant. The visual mechanism whereby approximate compensation is made for changes in the colours of stimuli, especially in the case of changes in illuminants, is named chromatic adaptation (CIE 1987). A reliable colour constancy index, associated with a chromatic adaptation transform, is required. This would enable the predicted recipes to provide coloured objects showing little or no change in colour appearance when viewed under different light sources. Brockes (1968); Bartleson (1978); Luo et al. (1991a, 1991b) found that none of chromatic adaptation transforms gave satisfactory prediction to the experimental results. Kuehni (1980) also pointed out that colour

constancy or chromatic adaptation evaluation is still one of the most pressing unsolved problems of applied colour science.

The prediction of colour constancy and chromatic adaptation effects would be useful for a number of practical reasons:

(1) It allows designers to choose their colours in such a way that the harmonious effect which they are trying to achieve, for instance, in clothing or interior design, is preserved under various types and levels of illumination.
(2) Together with a better colour difference formula, it helps to determine more precise colour differences seen under a wide range of light sources rather than the one in which the colour difference formula has originally been based.
(3) It can also assist to determine the degree of metamerism due to change in illuminant, and to make the metamerism index more meaningful to the user.

1.2 Colour Specification Systems

This section introduces various colour specification systems. The CIE Colorimetric System forms the basis of colorimetry. In addition, colour order systems, which are used to describe and arrange colours in an orderly manner, also play an important role in colour appearance specification and communication. Three colour order systems are used in this work: Munsell, Natural and Optical Society of America (OSA) colour order systems.

1.2.1 The CIE Colorimetric System

The CIE recommended a standard system for colour measurement and specification in 1931 known as the CIE Colorimetric System. This is based on the principle of additive colour mixing, and includes the specification of the colorimetric observer, illuminants, and illuminating and viewing geometriers. The system has been well

documented elsewhere by Judd and Wyszecki (1975), Wright (1964), Billmeyer (1981), and Wyszecki and Stiles (1982).

The CIE Colorimetric System comprises the essential standards and procedures for colour measurement that are necessary to make colorimetry a useful tool. The CIE 1931 Standard Observer was defined by averaging the results from the investigations by Wright (1928 - 1929) and Guild (1931) on the colour matching of spectral colours in a 2^0 field. Fig. 1.2.1.1 shows that the standard observer data in terms of distribution coefficients $\bar{r}(\lambda)$, $\bar{g}(\lambda)$, $\bar{b}(\lambda)$ which are the amounts of three monochromatic primaries with fixed wavelengths at 700 nm (R), 546.1 nm (G) and 435.8 nm (B) required to match each stimulus across visible spectrum. It is necessary to avoid the negative quantities in the $\bar{r}(\lambda)$, $\bar{g}(\lambda)$, $\bar{b}(\lambda)$ functions which produces problems in computation of colorimetric values. A linear transformation was derived to convert the $\bar{r}(\lambda)$, $\bar{g}(\lambda)$, $\bar{b}(\lambda)$ functions to a new set of positive functions, $\bar{x}(\lambda)$, $\bar{y}(\lambda)$, $\bar{z}(\lambda)$, based on three imaginary primaries (X), (Y) and (Z). These functions can be calculated using Eq. 1.2.1 given below.

$$\begin{vmatrix} \bar{x}(\lambda) \\ \bar{y}(\lambda) \\ \bar{z}(\lambda) \end{vmatrix} = A \begin{vmatrix} \bar{r}(\lambda) \\ \bar{g}(\lambda) \\ \bar{b}(\lambda) \end{vmatrix} \qquad (1.2.1)$$

where

$$A = \begin{vmatrix} 0.49000 & 0.31000 & 0.20000 \\ 0.17697 & 0.81240 & 0.01063 \\ 0.00000 & 0.01000 & 0.99000 \end{vmatrix}$$

These values shown in Fig. 1.2.1.2 (plotted using solid circles) are named the CIE 1931 colour-matching functions. They represent the colour matching properties of the CIE 1931 Standard Colorimetric Observer, often referred to the 2^0 Observer which applies to colour matching fields of angular subtense less than 4^0. The $\bar{y}(\lambda)$ function

was chosen to coincide with the CIE 1924 V(λ) function (i.e. the spectral luminance efficiency function) developed by Coblentz and Emerson (1918) and Gibson and Tyndall (1923).

Three standard illuminants A, B and C were recommended to represent tungsten filament light, direct sunlight and average daylight respectively. The CIE illuminants are defined in terms of relative spectral power distribution (SPD) across visible spectrum (380 nm - 780 nm).

The CIE also recommended that the colorimetric specification of opaque specimens should be measured to correspond to one of the following standard illuminating/viewing geometries: 45°/normal (45/0), normal/45° (0/45), diffuse/normal (d/0), and normal/diffuse (0/d), as shown in Fig. 1.2.1.3 (Wyszecki and Stiles 1982). Each object colour is defined as reflectance factors across the visible spectrum. The reflectance factor is a ratio of the radiant flux reflected by the sample into a defined cone to the radiant flux similarly reflected by the perfect diffuser (CIE 1987). The 'reflectance' will be used hereafter instead of 'reflectance factor'.

In the CIE 1931 colorimetric system, a colour light can be defined using Eq. 1.2.2, and an object colour can be computed by Eq. 1.2.3:

$$X_1 = \int_\lambda P(\lambda)\ \bar{x}(\lambda)\ d\lambda$$
$$Y_1 = \int_\lambda P(\lambda)\ \bar{y}(\lambda)\ d\lambda$$
$$Z_1 = \int_\lambda P(\lambda)\ \bar{z}(\lambda)\ d\lambda\ , \qquad (1.2.2)$$

and

$$X_2 = \int_\lambda S(\lambda)\ \bar{x}(\lambda)\ R(\lambda)\ d\lambda$$
$$Y_2 = \int_\lambda S(\lambda)\ \bar{y}(\lambda)\ R(\lambda)\ d\lambda$$
$$Z_2 = \int_\lambda S(\lambda)\ \bar{z}(\lambda)\ R(\lambda)\ d\lambda \qquad (1.2.3)$$

where $\{P(\lambda)d\lambda\}$ defines the spectral power distribution of a colour light. $S(\lambda)$ and $R(\lambda)$ are the spectral distribution of a particular CIE illuminant and the reflectance of the object in question respectively. X_1, Y_1, Z_1 represent the tristimulus values of a colour light, and X_2, Y_2, Z_2 are those of the object.

Hunt (1991) states that although the Y tristimulus value correlates approximately with brightness or, more usually, with lightness, X and Z tristimulus values do not correlate, even approximately, with any perceptual attributes. Important colour attributes are related to the relative magnitudes of the tristimulus values. Hence, it is useful to calculate a type of relative tristimulus values called chromaticity co-ordinates, as follows:

$$\begin{aligned} x &= X / (X + Y + Z) \\ y &= Y / (X + Y + Z). \\ z &= Z / (X + Y + Z) \end{aligned} \qquad (1.2.4)$$

and

$$x + y + z = 1. \qquad (1.2.5)$$

If x and y are known, z can always be deduced from 1 - x - y. The interpretation of colours is facilitated by expressing a colour using chromaticity co-ordinates x, y and the luminance factor Y. A plot of x against y is known as the chromaticity diagram as shown in Fig. 1.2.1.4 (the CIE 1931 (x, y)-chromaticity diagram plotted using solid circles). All real colours lie within the boundaries of the spectrum locus which is the line joining the x, y values of the spectrum colours.

The colour-match conditions for two test colours can be expressed as follows:

$$\begin{aligned} k \int_\lambda P_1(\lambda)\, \bar{x}(\lambda)\, d\lambda &= k \int_\lambda P_2(\lambda)\, \bar{x}(\lambda)\, d\lambda \\ k \int_\lambda P_1(\lambda)\, \bar{y}(\lambda)\, d\lambda &= k \int_\lambda P_2(\lambda)\, \bar{y}(\lambda)\, d\lambda \\ k \int_\lambda P_1(\lambda)\, \bar{z}(\lambda)\, d\lambda &= k \int_\lambda P_2(\lambda)\, \bar{z}(\lambda)\, d\lambda \end{aligned} \qquad (1.2.6)$$

or

$$
\begin{aligned}
k \int_{\lambda} S(\lambda)\, \bar{x}(\lambda)\, R_1(\lambda)\, d\lambda &= k \int_{\lambda} S(\lambda)\, \bar{x}(\lambda)\, R_2(\lambda)\, d\lambda \\
k \int_{\lambda} S(\lambda)\, \bar{y}(\lambda)\, R_1(\lambda)\, d\lambda &= k \int_{\lambda} S(\lambda)\, \bar{y}(\lambda)\, R_2(\lambda)\, d\lambda \qquad (1.2.7) \\
k \int_{\lambda} S(\lambda)\, \bar{z}(\lambda)\, R_1(\lambda)\, d\lambda &= k \int_{\lambda} S(\lambda)\, \bar{z}(\lambda)\, R_2(\lambda)\, d\lambda
\end{aligned}
$$

Both Eqs. 1.2.6 and 1.2.7 also show a typical metameric match between two stimuli and objects respectively.

In 1964 the CIE introduced an alternative set of standard colour-matching functions, denoted by $\bar{x}_{10}(\lambda)$,$\bar{y}_{10}(\lambda)$, and $\bar{z}_{10}(\lambda)$, as a supplement to those of the 1931 Standard Observer, referred to the CIE 1964 Supplementary Standard Colorimetric Observer (or simply 10° Standard Observer). The colour-matching functions are shown in Fig. 1.2.1.2 plotted using open circle symbols. It is intended for use with colours of large angular areas (i.e. larger than 4°). The colour-matching functions of the CIE 1964 Standard Observer are based on experimental investigations made by Stiles and Burch (1959) and Speranskaya (1959). Stiles and Burch used a trichromatic colorimeter with monochromatic primary stimuli to determine for forty nine observers the tristimulus values of monochromatic stimuli of equal energy and of wavelengths from approximately 390 to 830 nm. In the course of the investigation different sets of primary stimuli (all monochromatic stimuli) were employed, but the final mean results were all transformed to refer to the primary stimuli R (645.2 nm), G (526.3 nm, and B (444.4 nm). Stiles and Burch measured the radiant power, $P(\lambda)$ in Eq. 1.2.2 of each monochromatic test stimulus presented to the observer. The colour-matching functions were obtained directly from the observations.

The transformation equations for converting the 10° colour-matching functions $\bar{r}_{10}(\lambda)$, $\bar{g}_{10}(\lambda)$, $\bar{b}_{10}(\lambda)$ to the tristimulus values $\bar{x}_{10}(\lambda)$,$\bar{y}_{10}(\lambda)$, $\bar{z}_{10}(\lambda)$ are as follows (Wyszecki and Stiles 1982):

$$\begin{vmatrix} \bar{x}_{10}(\lambda) \\ \bar{y}_{10}(\lambda) \\ \bar{z}_{10}(\lambda) \end{vmatrix} = M \begin{vmatrix} \bar{r}_{10}(\lambda) \\ \bar{g}_{10}(\lambda) \\ \bar{b}_{10}(\lambda) \end{vmatrix} \qquad (1.2.8)$$

where

$$M = \begin{vmatrix} 0.341080 & 0.189145 & 0.387529 \\ 0.139058 & 0.837460 & 0.073316 \\ 0.000000 & 0.039553 & 2.026200 \end{vmatrix}$$

In the CIE 1964 colorimetric system, the chromaticity co-ordinates and the colour-match conditions for two test colours are the same as those given in Eqs. 1.2.4 to 1.2.7 by replacing X, Y, Z and $\bar{x}(\lambda)$, $\bar{y}(\lambda)$, $\bar{z}(\lambda)$ with X_{10}, Y_{10}, Z_{10} and $\bar{x}_{10}(\lambda)$, $\bar{y}_{10}(\lambda)$, $\bar{z}_{10}(\lambda)$ respectively.

Dissatisfaction arose over the reproduction of daylight by illuminant C for measuring fluorescent materials. (Illuminant C has deficiencies in the blue and ultraviolet ranges in comparison with daylight.) Hence, the CIE recommended the standard illuminant D65 representing a phase of daylight with a correlated colour temperature of about 6504 K, together with a range of D illuminants representing other correlated colour temperatures. The CIE illuminants A, B, C and D65 are specified by the tabulated SPD data throughout the visible spectrum. In practice, there are not any real light sources that agree with those SPD. Some sources produced to simulate those illuminants only have a close match to their chromaticity co-ordinates. In the following part of the thesis, the words 'illuminant' and 'light source' represent that defined by the CIE, and a physical lamp respectively. Nowadays, in practice, B and C illuminants are obsolete.

1.2.2 Munsell Colour Order System

The Munsell system, the oldest colour order system considered in terms of continuously available physical exemplifications, is also the

most extensively studied of all colour order systems. The system was originated by Albert H. Munsell and was published in 1905. In 1915, the first physical exemplification, named the Altas of the Munsell Colour System was also published. The Committee on colorimetry of the Optical Society of America carried out further development of the Munsell system which culminated in the final report of the Committee (Newhall et al. 1943), and established the Munsell Renotation System in 1943.

There are three variables (or attributes) considered in the Munsell system. The first variable, Hue, appears as a variable in all colour order systems. It is defined as 'the attribute of a visual sensation according to which an area appears to be similar to one, or proportions of two, of the perceived colours red, yellow, green, or blue' by the CIE (1987).

The second Munsell variable is Value which is associated with lightness. The CIE (1987) defines lightness as 'the brightness of an area judged relative to the brightness of a similarly illuminated area that appears to be white or highly transmitting'. Munsell defined the third variable in his system, which he called Chroma, as the degree of departure of the colour from an achromatic colour of the same lightness. This is related to that defined by the CIE (1987) as 'the colourfulness of an area judged as a proportion of the brightness of a similarly illuminated area that appears to be white or highly transmitting'.

Fig. 1.2.2.1 shows that these three variables are arranged in a familiar fashion, in which the Value axis is vertical, with white (having a Value of 10) at the top and black (0) at the bottom, the greys being in between. In Fig. 1.2.2.2, hues are arranged around a circle having constant Chroma. All colours in this plane have a fixed Value. Munsell, impressed by the merits of the decimal system, chose five primary hues [red (R), yellow (Y), green (G), blue (B), and purple (P)] and five secondary hues [yellow-red (5YR), green-yellow (5GY), blue-green (5BG), purple-blue (5PB), and red-purple (5RP)] to obtain

10 major hues, which are divided into 100 steps known as Munsell 100 Hues. Chroma scale starts at the neutral axis (0) and progressed in the direction of each Hue until reaches the limit of real colours. The distances between two neighbouring pairs of samples are intended to represent an equal perceived chroma difference.

The equality of visual spacing is arranged such that one Value step (on a scale of 10 between black, 0, and white, 10) equals to two steps of Chroma as shown in Fig. 1.2.2.3. Hue spacing was meant to be in equal steps around the Hue circle, and one Value step (Nickerson 1936) equals to 0.3 Hue steps at Chroma 5.

The relation between the Munsell colour co-ordinates and the CIE colorimetric values is a complicated one, and cannot be presented by a simple equation. The simplest relation is between the Munsell Value and the CIE luminance factor Y, which approximates perceived lightness. The Munsell renotation definition of Value is in the form of a fifth-order polynomial as shown in Eq. 1.2.9.

$$Y = 1.2219\ V - 0.23111\ V^2 + 0.23951\ V^3 - 0.021009\ V^4 + 0.0008404\ V^5 \qquad (1.2.9)$$

where Y value is calculated relative to a reference white, which is a magnesium oxide tile, assigned an absolute Y value of 1.026 using $45^0/0^0$ illuminating/viewing geometry. This equation requires a slightly modification to correspond to the present CIE recommendation using the perfect reflecting diffuser, assigned a value of 1.000, as the white reference. It is also desirable to have an equation to calculate V in terms of Y. Eq. 1.2.10 derived by Hesselgren (1954) and Hård and Sivik (1981) can be used:

$$V = 0.01612\ Y + 2.5649\ Y^{1/6} + 1.3455\ Y^{1/3} + 0.08797\ Y^{-1} - (2.685 \times 10^{-7})\ Y^3 - 3.116 \qquad (1.2.10)$$

The equation is quite accurate (within 0.01 in V for $Y > 2.5$) and should be useful in practice.

The complete Munsell specification of a sample is expressed as H V/C. For instance, the colour of 5R 5/8 has 5R, 5 and 8 for Hue, Value and Chroma respectively.

1.2.3 NCS Colour Order System

The origins of the Natural Colour System (NCS) can be traced back to the six primary colours suggested by Leonardo da Vinci and to the opponent-type colour scales proposed by Hering (1964). The modern Natural Colour Order System was based on the work of Johansson (1937, 1952) and Hesselgren (1952, 1954). As outlined by Hård and Sivik (1981), research and development on the NCS began in 1964. This led to a set of notations adopted as the Swedish Standard for Colour Notation (SS 01 91 00) in 1972-1973 and an colour atlas including 1412 samples (Swedish Standard Colour Atlas, SS 01 91 02) in 1979.

The NCS is the system of the resemblances of colours to the six elementary colours red (r), yellow (y), Green (g), blue (b), black (s), and white (w). Of these, the four chromatic colours are those in which no trace of the others can be seen, for example, the red that contains no trace of either yellow or blue, and so on. Similarly, White and black do not have any trace of the other chromatic elementary colours.

The variables of the NCS system are defined in terms of resemblances. Hue (ϕ) is defined in terms of the resemblance of the test colour to the two nearest chromatic elementary colours. Fig. 1.2.3.1 shows the arrangement of the hue circle. The four elementary hues are arranged 90^0 apart on the hue circle and form the basis for red-green and yellow-blue opponent axes. For instance, a violet hue might be said to bear a 30 % resemblance to red and a 70 % resemblance to blue, and would have the notation R70B, as shown in Fig. 1.2.3.1.

A second variable of the NCS system is chromaticness (c), that is, the resemblance of the test colour to the colour of the same hue having the maximum possible chromatic content. The third variable is blackness (s), that is, the resemblance of the test colour to the perfect black. In addition, whiteness (w) is defined as resemblance to white. The scales of the resemblances are chosen so that the sum of the chromaticness, blackness and whiteness is 100(%):

$$w + s + c = 100 \qquad (1.2.11)$$

Colours having only combinations of hue (say red), blackness, and whiteness are represented in a triangular array, as shown in Fig. 1.2.3.2. The three sides of the triangle are of equal length, with white represented by the point, W, at the top, black by the point, S, at the bottom, and red by the point C. Colours that are perceived to have only redness and whiteness are situated on the line WC, and their positions along this line represents the proportions of redness and whiteness. Similarly, points on the line SC represent colours having only blackness and redness; and points on WS, those having only whiteness and blackness (the greys). Points lying within the triangle represent a colour having some whiteness, blackness and redness. For example, colour A in Fig. 1.2.3.2 is defined by the w, s and c distances. The w, s, and c always add up to 100, (see Eq. 1.2.11). Hence, it is only necessary to quote two numbers. The NCS specification of a colour is expressed as sc-ϕ.

For a colour is perceived to have 80% yellow and 20% red with zero whiteness and blackness, it would locate on the point C in Fig. 1.2.3.2. This point corresponds to the Y20R position in Fig. 1.2.3.1. For a colour had 10% whiteness , 30% blackness, 30% yellowness and 30% redness, its hue would be determined by the ratio of its two hue contents, i.e. 30 : 30, which equals to 50 : 50. The two chromatic primaries need to add up to 100 so that the hue is Y50R triangle for this colour. Its position in the triangle is point A in Fig. 1.2.3.2. The c of 60% in this case is the sum of the two hue contents, and represents the NCS chromaticness, c.

1.2.4 OSA UCS Colour System

The OSA UCS Colour System was developed by the Committee on Uniform Colour Scales of the Optical Society of America during 1947 - 1974 period. It is primarily dedicated to produce a system in which samples are arranged in a regular rhombohedral lattice as shown in Fig. 1.2.4.1 (Judd and Wyszecki 1975). The distances between a sample and each of its 12 nearest neighbours correspond to equal perceived colour differences at any point in the lattice. An OSA specification includes three numbers such as 1,-1,1, that is, L, j, g as shown in Fig. 1.2.4.2 (Foss 1978). The first number represents the lightness L, ranging from about -7 to +5 with 0 standing for a medium lightness. The second, j, (from French jaune) represents the yellowness-blueness of the colour; j is positive for yellowish colours and negative for bluish colours. Values of j range from about -6 to +11. The third number, g, represents the greenness-redness of the colour; g is positive for greenish colours and negative for reddish colours. Values of g range from about -10 to +6.

1.3 Colour Measurement Instruments

Advanced colour measurement instruments provide the spectral data and colorimetric data such as the reflectance values, tristimulus values and chromaticity co-ordinates of a given colour. There are three types of instruments: the spectroradiometer, the spectrophotometer, and the tristimulus-filter colorimeter. These are commercially available in a variety of makes, degrees of sophistication, and specialisations to suit specific applications. The spectrophotometer and tele-spectroradiometer (one of the spectroradiometers) were used in the author's study. The detail information of their design and operation can be obtained from the manufactures, so only a brief description is given here.

1.3.1 Tele-Spectroradiometer

A tele-spectroradiometer is an apparatus designed to measure radiometric quantities as a function of wavelength. In a tele-spectroradiometer system, the radiant power emitted by a test colour (which may be a surface colour or a light source) in a preselected direction enters the entrance slit of the monochromator through a telescope which receives light from the target colour, and is connected with a monochromator by means of optic fibres or other materials. The monochromator disperses the incoming radiant power via a diffraction grating or a prism, and transmits it via a narrow band of wavelengths through the exit slit which is optically coupled with the photodetector which converts the light to electronic signal. These signals is then analysed by the computer with suitable software.

In practice, measuring spectral radiometric quantity involves the comparison of the test source with a suitable reference source of known spectral radiant power distribution. Reference sources, most often in the form of tungsten filament lamps, are usually available from national standardising laboratories. The spectral radiant power distributions of these sources are determined, directly or indirectly, by a spectroradiometric comparison with a blackbody (Planckian) radiator operating at a known temperature, or with some other primary standard sources.

A typical output of a tele-spectroradiometer system includes:

- the spectral radiant power distribution of the test source,
- the tristimulus values and chromaticity with respect to either the CIE 1931, or CIE 1964 colorimetric system, or both,
- the CIE colour-rendering indices,
- the correlated colour temperature,
- and photometric quantities such as luminance (cd/m^2).

1.3.2 Spectrophotometer

A spectrophotometer is an apparatus designed to measure the spectral transmittance and spectral reflectance factors of objects. It is similar in design to the spectroradiometer, but has a rather different objective, namely, to compare at each wavelength the radiant power leaving the object with that incident on it.

In the author's study, the Macbeth MS2020 spectrophotometer was used to measure reflectance of test samples. For measuring a specimen, diffuse illumination from a Xenon pulse source is used, which produces a pulse of intense radiation of short duration within an integrating sphere. The sample is viewed at 8^0 to the normal in the integrating sphere. The amount of radiation from the sample is further dispersed by a diffraction grating into 16 wavelengths (from 400 to 700 nm with 20 nm interval via an array of 16 photodiode detectors, and the corresponding reference signals are obtained from a reference detector that samples the diffuse illuminating radiation by viewing the inside wall of the integrating sphere (coated with $BaSO_4$ white colour). The resulting reflectance data are then passed to a microprocessor for further data analysis.

1.4 Metamerism

Metamerism is the phenomenon exhibited by two colour stimuli with the same tristimulus values but different spectral radiant power distributions, and such stimuli are defined as metameric colour stimuli (CIE 1987). In colorimetric terms, a pair of metameric object colours (say a metamer) with different spectral reflectances $R_1(\lambda)$ and $R_2(\lambda)$ must satisfy the Eq. 1.2.7. Such a non-spectral colour match for a given observer is said to be a metameric match. On the other hand, if the spectral reflectance values of the two coloured objects are equal, i.e. $R_1(\lambda) = R_2(\lambda)$, the match would hold regardless of the change of illuminant and observer. This is known as a non-metameric match. In practice, the metamerism does not exist due to the definition of 'identical' tristimulus values between the two

samples considered. In this work, the definition of metamerism is loosen as two samples having 'similar' tristimulus values but spectrally differed.

1.4.1 Types of Metamerism

Metamerism occurs due to the change in illuminant, observer, and the geometry of illumination and viewing. There are four types of metamerism which are described below (Billmeyer 1967; McDonald 1987; Badcock 1992):

(1) Illuminant metamerism

Illuminant metamerism occurs when two objects, which match under one set of conditions, no longer match when the illuminant is changed, for example, from daylight to tungsten lamp or some other sources such as Philips TL84.

(2) Observer metamerism

Observer metamerism takes place when two objects, which match by one observer, mis-match with another observer. This arises because of the difference in colour-matching functions of two observers.

(3) Field size metamerism

Field size metamerism occurs when field size is changed, say from 2^0 to 10^0, i.e. a metameric pair produces a match at a distance (small field size) but mis-match when seen at a closer distance (large field view).

(4) Geometric metamerism

Geometric metamerism takes place when two objects, which match under one set of conditions, no longer match when the illuminating/viewing geometry is changed. This frequently occurs with paint films containing metallic pigments and moulded plastics which contain metal flakes or glassy material.

1.4.2 Problems from Metamerism

Metamerism occurs when two metameric samples (or a metamer) with identical or very similar tristimulus values have different reflectance curves with at least three cross-over wavelengths. As mentioned earlier, the typical effect is that a metamer matches when viewed by an observer under a particular light source, but fails to match when viewed by a different observer or by the same observer under a second source. Using a combination of three fixed colorants (say red, blue, and yellow), it is possible to match a wide range of colours for a particular observer and light source. However, in most cases the matches will be metameric, i.e. will fail to hold for a different observer or a second source. In practice, a small degree of metamerism might be tolerable but not to a large degree.

Attempts are made to set up standard viewing conditions such as illuminating samples with special matching lamps in a viewing cabinet for visual assessment. However, for highly metameric pairs, a slight variation of the light source could result in a mis-match. In addition, the differences in colour vision between observers may also cause problems although these observers have normal colour vision. Ideally, these difficulties should be overcome by colour measurement which gives results calculated from a range of standard illuminants and standard observers. Unfortunately, these difficulties still remain due to the limitation in precisely quantifying colour difference for metameric pairs (Berns et al. 1988).

For industrial colour quality control, matches made under a reference source (frequently daylight) are checked under a test source (say tungsten). If the match is still preserved, the sample is assumed to be satisfactory. With the introduction of fluorescent lamps the problem becomes worse. It could well be a good match under daylight and tungsten light, but a very poor match under a fluorescent lamp. Hence, it is a common practice to check the degree of metamerism for a pair under at least three light sources, such as a daylight, a tungsten, and a three narrow-band fluorescent (TL84).

In commercial recipe formulation systems, it is usual for recipes to be calculated for several different combinations of dyes. The criteria for selecting dye combinations to be used is usually based upon the cost and the predicted degree of metamerism; the cheapest with an acceptable degree of metamerism is selected. Again, the problems mentioned above occur. A metameric match for a target colour (say the standard) under a particular set of conditions may be a mis-match for another observer, or under a different light source or with different viewing geometry. This often causes disagreement between manufactures and customers, and results in production delay and loss, and money spent in vain. The problem lies in a lack of reliable means to estimate the degree of metamerism.

1.4.3 Metamerism indices

Metamerism index is a method of quantifying the degree of metamerism for a pair of samples. The CIE (1986) has recommended that the degree of metamerism for changes of illuminant be evaluated by an Illuminant Metamerism Index (IMI), in which colour difference values (ΔE) of a metamer are computed under one or more test illuminants. When computed under the reference illuminant, the ΔE is always quite small. The method assumes that if a match holds for these illuminants, it will remain for all other illuminants or sources, and all observers. However, the results from Berns et al. (1988) showed that a three-chromatic-colorant match aimed to the reference source may not persist under a second test source. Furthermore, a colour-difference formula must be used to calculate the ΔE values. The current CIE (1986) recommendation in evaluating colour difference for surface colours is CIEL*a*b*. Many new sets of experimental results such as Clarke et al. (1984), Luo and Rigg (1987a, 1987b), Berns et al. (1991) have shown that it gives poor predictions to small to moderate size visual colour differences. The more advanced formulae such as *CMC(l:c)* (Clarke et al. 1984), *BFD(l:c)* (Luo and Rigg 1987a, 1987b), and *CIE94* (Berns et al. 1991) are based almost entirely on work carried out under daylight and

may well be inaccurate if used for other sources. An alternative method would be to transform the tristimulus values under the test illuminant to those under the reference illuminant by a chromatic-adaptation transform, and subsequently to compute ΔE between the transformed and measured tristimulus values from one of the above advanced colour-difference formulae. There are many chromatic adaptation transforms available. There is no official standard being recommended. Another approach proposed by Nimeroff and Yurow (1965), and Moradian and Rigg (1987) uses the weighted reflectance differences or lightness difference of two samples by the three CIE standard observer functions, $\bar{x}_\lambda$, $\bar{y}_\lambda$, and $\bar{z}_\lambda$, or its derivatives $\bar{u}_\lambda$, $\bar{v}_\lambda$, and $\bar{w}_\lambda$. However, these methods did not give satisfactory predictions to the visual results (Moradian and Rigg 1987; Badcock 1992).

1.4.4 Colour Difference Formulae

In many industrial applications, the difference between two colours requires to be precisely quantified. This difference is a combination of differences in lightness, chroma and hue. A reliable colour-difference formula is required to provide close agreement with visual assessment. Many colour-difference formulae have been suggested in the past two decades. In this work, four CIEL*a*b*, CMC (1:1), BFD(1:1) and CIE94 were tested. These formulae are described below.

1976 CIEL*a*b* formula

This is a cube-root formula recommended by the CIE (1978), and is a simplification of the Adams-Nickerson (ANLAB) (Adams 1942) colour space. In 1976, the Colour Measurement Committee (CMC) of the Society of Dyers and Colourists (SDC) recommended the CIEL*a*b* to replace the existing ANLAB to promote the uniformity of practice (McLaren 1976). The CIEL*a*b* equation is as given below:

$$L^* = 116\, f(Y/Y_n) - 16,$$
$$a^* = 500\, [f(X/X_n) - f(Y/Y_n)], \qquad (1.4.1)$$
$$b^* = 200\, [f(Y/Y_n) - f(Z/Z_n)],$$

where

$f(X/X_n)=(X/X_n)^{1/3}$, $X/X_n > 0.008856$

$f(X/X_n)=7.787(X/X_n) + 16/116$, $X/X_n < 0.008856$

$f(Y/Y_n)=(Y/Y_n)^{1/3}$, $Y/Y_n > 0.008856$

$f(Y/Y_n)=7.787(Y/Y_n) + 16/116$, $Y/Y_n < 0.008856$

$f(Z/Z_n)=(Z/Z_n)^{1/3}$, $Z/Z_n > 0.008856$

$f(Z/Z_n)=7.787(Z/Z_n) + 16/116$, $Z/Z_n < 0.008856$

where X, Y, Z are the tristimulus values of the sample considered, and X_n, Y_n and Z_n are those of the perfect reflecting diffuser (which are the same as those of the illuminant).

Colour difference between a pair of samples can be calculated using Eq. 1.4.2 shown below:

$$\Delta E = [\ (\Delta L^*)^2 + (\Delta a^*)^2 + (\Delta b^*)^2\ ]^{1/2} \qquad (1.4.2)$$

The values of chroma (denoted by C*) and hue (h in degree) can be calculated using the following equations.

$$C^* = [(a^*)^2 + (b^*)^2]^{1/2}, \qquad (1.4.3)$$

and

$$h = \arctan\ (b^*/a^*). \qquad (1.4.4)$$

CMC(l : c) formula

CMC(l : c) formula is a revised version of the CIEL*a*b* colour-difference formula, containing the two variables l and c that are the relative weights of the lightness to the chromatic differences. Its colour difference is calculated using Eq. 1.4.5:

$$\Delta E = [\ (\Delta L/\ l\ S_L)^2 + (\Delta C/\ c\ S_c)^2 + (\Delta H/\ S_H)^2\ ]^{1/2} \qquad (1.4.5)$$

where $S_L = 0.040975L_1/(1 + 0.01765L_1)$,
unless $L_1 < 16$ when $S_L = 0.511$,
$S_c = 0.0638C_1/(1 + 0.0131C_1) + 0.638$,
$S_H = S_c (Tf + 1 - f)$,
$f = \{(C_1)^4 / [(C_1)^4 + 1900]\}^{1/2}$,
$T = 0.36 + |0.4 \cos(h_1 + 35)|$,
unless h_1 is between 164^0 and 345^0 when
$T = 0.56 + |0.2 \cos(h_1 + 168)|$,

where L_1, C_1 and h_1 refer to the CIEL*a*b* L*, C* and h values of the standard sample. The ΔL, ΔC and ΔH are calculated from the CIEL*a*b* formula. The l and c are constants and can be optimised to achieve the best correlation with visual assessment results for different industries. The l and c weights are normally set to either (1:1) for perceptibility or (2:1) for acceptability assessments.

There is no corresponding colour space for CMC(l : c) colour difference formula. A uniform colour space (abbreviated as UCS) similar in form to CIEL*a*b* space has been derived by Luo and Rigg (1986b) in which distances agree closely with the corresponding ΔE(CMC) values. The formulae for the CMC(l : c) UCS are given below:

$$L_{ucs} = (1/l) [21.75 \ln L^* + 0.3838 L^* - 38.54], \qquad (1.4.6)$$

unless $L^* < 16$ when $L_{ucs} = 1.744 L^* / l$,

$$C_{ucs} = (l / c) \{0.162 C^* + 10.92 [\ln(0.638 + 0.07216 C^*)] + 4.907\}, \qquad (1.4.7)$$

$$h_{ucs} = h + Df, \qquad (1.4.8)$$

$$a_{ucs} = C_{ucs} \cos h_{ucs}, \qquad (1.4.9)$$

$$b_{ucs} = C_{ucs} \sin h_{ucs}, \qquad (1.4.10)$$

and

$$C_{ucs} = (a^2_{ucs} + b^2_{ucs})^{1/2}, \qquad (1.4.11)$$

$$h_{ucs} = \arctan(b_{ucs} / a_{ucs}), \qquad (1.4.12)$$

where

$$D = k_1 + k_2 P |P|^{k_3}, \quad (1.4.13)$$

$$P = \cos(k_4 h + k_5), \quad (1.4.14)$$

$$f = \{(C^*)^4 / [(C^*)^4 + 1900]\}^{1/2}, \quad (1.4.15)$$

where the values of the k_1 to k_5 for different ranges of h are as follows:

h (degrees)	k_1	k_2	k_3	k_4	k_5 (degrees)
0-49	133.87	-134.50	-0.924	1.727	340
49-110	11.78	-12.70	-0.218	2.120	333
110-269.5	13.87	10.93	0.140	1.000	-83
269.5-360	0.14	5.23	0.170	1.610	233.

The CMC UCS will be compared with the other two UCSs (CIEL*a*b* and RLAB (see Section 1.5.6 (6)) and two colour appearance models (Nayatani and Hunt94 (see Section 1.5.6 (3) and (4) respectively) in predicting the colour appearance data for the samples prepared in this study.

CIE94 formula

CIE94 formula (CIE 1995) has the same structure as CMC (l :c) formula except for different functions of S_L , S_c and S_H as shown below:

$$S_L = 1,$$
$$S_c = 1 + 0.045\, C_{ab}, \quad (1.4.16)$$
$$S_H = 1 + 0.015\, C_{ab},$$

where the colour difference between a pair of samples is calculated using Eq. 1.4.5. For textile application, the recommended weights are l = 2 and c=1.

BFD(*l* : c)

The BFD colour difference formula was derived by Luo and Rigg (1987a, 1987b) at Bradford University. They quantified a number of small colour difference pairs of object colours. The formula was derived from two sets of data (combined perceptibility and acceptability data) accumulated by Luo and Rigg (1986a, 1987a). The BFD colour difference formula is a further modification to the CMC(*l* : c). The formula was constructed to avoid discontinuities such as those present in the S_L and T scales of lightness and hue in the CMC formula. The form of the BFD colour difference formula is given below.

$$\Delta E\,(\mathrm{BFD}\,(\,l:c\,)) = \{\,[\,\Delta L\,(\mathrm{BFD})\,/\,l\,]^2 + [\,\Delta C^*\,/\,(cD_c)\,]^2 + (\Delta H^*\,/\,D_H)^2 + R_T\,(\Delta C^*\,/\,D_c)\,(\Delta H^*\,/\,D_H)\,\}^{1/2} \qquad (1.4.17)$$

where

$$D_c = 0.035\,\bar{C}^*\,/\,(1 + 0.00365\,\bar{C}^*) + 0.521$$

$$D_H = D_c\,(GT' + 1 - G)$$

$$G = \{(\bar{C}^*)^4\,/\,[(\bar{C}^*)^4 + 14000]\,\}^{1/2}$$

$$T' = 0.627 + 0.055\cos(\bar{h} - 254^o) - 0.040\cos(2\bar{h} - 136^o) + 0.070\cos(3\bar{h} - 32^o) + 0.049\cos(4\bar{h} + 114^o) - 0.015\cos(5\bar{h} - 103^o)$$

$$R_T = R_H R_C$$

$$R_H = -0.194\cos(5\bar{h} + 280^o) - 0.260\cos(\bar{h} - 308^o) - 0.379\cos(2\bar{h} - 160^o) - 0.636\cos(3\bar{h} + 254^o) - 0.226\cos(4\bar{h} - 140^o)$$

$$R_C = \{(\bar{C}^*)^6\,/\,[(\bar{C}^*)^6 + 7 \times 10^7]\,\}^{1/2}$$

$$L(\mathrm{BFD}) = 54.6\log(Y+1.5) - 9.6$$

where $\bar{C}^*$ and $\bar{h}$ refer to the mean of the C* and h values for the standard and sample. The ΔC^* and ΔH^* are calculated from the CIEL*a*b* formula.

The illuminant metamerism indices used in this work are based on the four colour difference formulae described above, and are divided into three types. The Type I index applies a colour difference formula to calculate the ΔE values under the reference and test light sources. The Type II index additively corrects both measurement and visual results to make a zero colour difference under the reference (i.e. D65) source, followed by calculating the ΔE value under the test source (for instance source A). The Type III index first transforms the tristimulus values from the test to the reference sources via a chromatic adaptation transform, followed by calculating the ΔE value under the reference source. A more detailed description of the three index types will be given in Chapter 3.

1.5 Colour Constancy

Human beings have the remarkable capability of seeing objects as having essentially the same colour under various illumination conditions. A white dove looks white in a rosy light at sunset, in a bright noon daylight or in a greenish-blue light of an approaching thunderstorm. His memory and knowledge of the colour of a white dove undoubtedly assists him to make a judgement of what its colour appearance should be. Most importantly, there is an 'adaptation' mechanism, which affects change of colour appearance due to variation of viewing conditions. In addition, people have a lot of similar experiences from their environment. A blue wall looks blue, for instance, despite a pattern of dappled sun and shadow. A lump of coal looks black and a piece of chalk white, regardless of the various light sources. Such experiences demonstrate the existence of stable perceptions of object colours. This phenomenon is known as *colour constancy*. The adaptation process is one of the most important properties of our visual mechanism. The visual mechanism adjusts itself to the conditions under which the eyes are exposed to radiant energy (Judd and Wyszecki 1975).

Colour constancy is defined by CIE (1987) as "The effect of visual adaptation whereby the appearance of colours remains approximately constant when the level and colour of the illumination are changed."

In real life, colour constancy makes a very important contribution to the stability of appearance of objects. Without it, our constantly changing perceptions correlated with the changing stimulation from objects would be intolerable. Fortunately, natural objects appear to be more colour constant than manufactured artifacts. Technology has made a wide variety of colourants and artificial light sources available. This produces more non-constant colour goods and increasing problems in industrial colour control.

1.5.1 Colour Constancy and Metamerism

Colour constancy and metamerism are closely linked and sometimes easily confused. The distinction between them is that colour constancy is a property of a single sample while metamerism refers to a pair of samples or colours. If two samples are a metameric match under a reference illuminant, they will be a mismatch under a second illuminant. Also, at least one of the two samples must exhibit a lack of colour constancy. If both were perfectly colour-constant, they would remain a match for all illuminants, and be a non-metameric match.

1.5.2 Chromatic Adaptation

The visual adaptation mechanism is a major factor associated with colour constancy. Many studies on colour constancy have intended to investigate or formulate the adaptation effect. The adaptation can be divided into three types: dark (scotopic) adaptation, light (photopic) adaptation, and chromatic adaptation. The two former types consider the adjustment of the visual mechanism to changes in the rate at which radiant energy enters the eyes. Chromatic adaptation refers primarily to the adjustment of the visual mechanism to changes in

radiant energy spectral distribution. This phenomenon is of great important in predicting object colour appearance and in maintaining the colour constancy of objects seen under different qualities of light sources.

1.5.3. Theories

The earliest chromatic adaptation research can be traced back to the last century. Interest in colour constancy is as strong today as it ever was. The best summary of the problem of colour constancy comes from Judd (1940):

> 'The visual mechanism of a normal observer is so constructed that objects keep their daylight colors even when the illuminant departs from average daylight. The processes by means of which the observer adapts to the illuminant or discounts most of the effect of a nondaylight illuminant are complicated; they are to be partly retinal and partly cortical.'

Colour constancy has been investigated by many researchers over years. Their aim was to describe colour constancy precisely via a mathematical model. Many models derived from the earlier works can be divided into three main categories: linearity, non-homogeneous linearity, and non-linearity.

1.5.3.1 The Linearity Theory

The earliest and best known hypothesis on chromatic adaptation is the proportionality rule of von Kries (Wyszecki and Stiles 1982). The von Kries hypothesis assumes that different adaptations of a particular retinal area modify the overall sensitivities of three fundamental colour-response mechanisms, whose relative spectral sensitivities $\bar{r}(\lambda)$, $\bar{g}(\lambda)$, $\bar{b}(\lambda)$ are a particular fixed set of the colour-

matching functions applicable to the area in question. Thus, $\bar{r}(\lambda)$, $\bar{g}(\lambda)$, $\bar{b}(\lambda)$ are related by a linear transformation with matrix M (with non-zero determinant) to the colour-matching functions $\bar{x}(\lambda)$, $\bar{y}(\lambda)$, $\bar{z}(\lambda)$. The fundamental tristimulus values R, G, B of a stimulus are then related to X, Y, Z by the same matrix M (Wyszecki and Stiles 1982).

For general colour matching, the conditions of colour matching are said to be symmetric if all factors involved in the match are the same. A symmetric match can be expressed in the form of the equation in Eq. 1.2.7. It can also be represented using functional forms as given in Eq. 1.5.1.

$$\begin{aligned} F_1(X, Y, Z; A) &= F_1(X', Y', Z'; A) \\ F_2(X, Y, Z; A) &= F_2(X', Y', Z'; A) \\ F_3(X, Y, Z; A) &= F_3(X', Y', Z'; A) \end{aligned} \qquad (1.5.1)$$

where X, Y, Z and X', Y', Z' represent the tristimulus specification for two test colour respectively under A referring to a particular illuminant.

Wyszecki and Stiles (1982) state that for chromatic adaptation, a state of equal colour response under two different conditions of illumination is described as an asymmetric match. In this case the two stimuli are physically different, but appear to be the same. It may be assumed that by some means a colour match is obtained for two different stimuli which are imaged on the same area of the retina under two different conditions of illumination to which the observer is adapted. Such an asymmetric match may be expressed using the functional notations as seen in Eq. 1.5.2.

$$\begin{aligned} F_1(X, Y, Z; A) &= F_1(X', Y', Z'; A') \\ F_2(X, Y, Z; A) &= F_2(X', Y', Z'; A') \\ F_3(X, Y, Z; A) &= F_3(X', Y', Z'; A') \end{aligned} \qquad (1.5.2)$$

The colour match may be transitive or not, depending on the methods of asymmetric matching. Using a colour naming or memory scaling method (Section 1.5.4), two different stimuli perceived under two different adapted illuminants are assumed to stimulate the same retinal area but on entirely distinct occasions; A and A' are the two sets of values assumed on these occasions by a single set of conditioning variables. In these circumstances, asymmetric matching is transitive, that is, if stimulus (X, Y, Z) presented under conditions A matches (X', Y', Z') presented under conditions A', and if (X', Y', Z') under A' matches (X", Y", Z") under A", then (X", Y", Z") under A" matches (X, Y, Z) under A. On the other hand, if an asymmetric match is formed by the sense that besides different illumination conditions, different retinal areas are stimulated as in monocular and binocular matching (Section 1.5.4) respectively, there is no basis for assuming that transitivity of the match will be obtained (Bartleson 1977). There might be interaction between condition A and A' because the response to (X, Y, Z) by the left eye in binocular matching might not only depend on the adapting stimuli applied to the left eye, but also on the stimuli applied to the right eye. In monocular matching, a pre-exposed adapting stimulus applied to one half of the retina area may affect the condition of the other half (Wyszecki and Stiles 1982).

The classical hypothesis on chromatic adaptation is based on the three-components theory of colour vision proposed by Young-Helmholtz (Judd and Wyszecki 1975). This theory postulates three types of cones; one is sensitive to the short-wavelength (blue) part of the spectrum, the second to the middle-wavelength (green) and the third to the long-wavelength (red). When the eye is exposed sufficiently long to a light source such as tungsten light with a high proportion of long wavelengths, the red-sensitive receptors are somewhat desensitised, the green-sensitive receptors are affected to a lesser extent, while the blue-sensitive receptors are only slightly affected by the relatively low stimulation from the short-wavelength part of the spectrum of the adapting stimulus. This means that adaptation to a reddish-yellow stimulus results in a relative gain in sensitivity to violet and blue stimuli.

Accepting the Young-Helmholtz theory, von Kries formulated the persistence law: 'Different composed stimuli, which look equal for the nonfatigued eye' as stated by Terstiege (1972), which means that colour equations are independent of the state of chromatic adaptation. In 1904, von Kries further formulated the Helmholtz's ideas on chromatic adaptation, which is a combination of the persistence law and Grassman's (linearity) law as stated by Judd and Wyszecki (1975). He postulated that although the responses of the three cone mechanisms are differently affected by chromatic adaptation, the relative spectral sensitivities of each of the three cone mechanisms remain unchanged. In other words, chromatic adaptation may be explained as a reduction of sensitivity by a constant factor. This factor differs for each of the three cone channels, and its magnitude depends on the colour of the stimulus to which the observer is adapted. The well-known von Kries coefficient law is as given in Eq. 1.5.3 as shown below.

$$\begin{aligned} R' &= \alpha R \\ G' &= \beta G \\ B' &= \gamma B \end{aligned} \qquad (1.5.3)$$

In Eq. 1.5.3 all tristimulus values are in terms of the fundamental primaries of the Young-Holmholtz theory. R, G, B represent the colour of the stimulus perceived under the original adapting light, and R', G', B' specify the colour of the same stimulus perceived by the same observer adapted to another light. The coefficients α, β, γ are the von Kries coefficients corresponding to the reduction in sensitivity of the three cone mechanisms respectively due to chromatic adaptation.

Wyszecki and Stiles (1982) state that although the linearity laws are not generally true for asymmetric matching, within the limits of some investigations confined to certain pairs of conditioning stimuli, these have been found to be approximately valid. The implication of obedience to the linearity laws for asymmetric matching have played a vital part in the study of chromatic adaptation.

1.5.3.2 The Non-homogeneous Linearity Theory

This theory was devised by Burham et al. (1957). A haploscopic (or binocular) matching technique was used to measure changes in colour appearance under daylight or incandescent illumination of the two test areas by different surround fields. In this study, a sophisticated computational method was used to investigate whether the 'random errors' are responsible for any deviations of the observations from the von Kries theory. Their results agreed well with those of the other studies such as Hunt (1952, 1953). They presented charts of *corresponding colours* (i.e. pairs of colours that look alike when one is seen in one set of adaptation conditions, and the other is seen in another set. (CIE 1987)), and derived linear relationships between tristimulus values under daylight and incandescent illumination. They obtained a better representation of their asymmetric matches by means of the non-homogeneous relations as shown in Eq. 1.5.4.

$$\begin{aligned} X &= t_{11} X' + t_{12} Y' + t_{13} Z' + t_{14} \\ Y &= t_{21} X' + t_{22} Y' + t_{23} Z' + t_{24} \\ Z &= t_{31} X' + t_{32} Y' + t_{33} Z' + t_{34} \end{aligned} \qquad (1.5.4)$$

These equations were designed to relate CIE tristimulus values, but not to represent a model of visual function.

1.5.3.3 The Non-linearity Theory

MacAdam (1956) employed a monocular bipartite field with differential adaptation of the retina in two halves. Extensive asymmetric data was collected with pairs of adapting sources, i.e. tungsten light, daylight, green, pink, red, greenish-yellow, and blue. His results showed considerable systematic deviations from the predictions of any von Kries scheme. These deviations were found to be of such a kind that if the linearity of asymmetric matching is true, it would indicate that there existed more than three independent

fundamental spectral sensitivities. The concept of only three fundamentals is restored by admitting non-linearity. Meanwhile, MacAdam (1956) pioneered in proposing the non-linear hypothesis which disagrees with the von Kries law. This can be expressed by Eq. 1.5.5.

$$\begin{aligned} a_R + b_R(R)^{P_R} &= a'_R + b'_R(R')^{P_{R'}} \\ a_G + b_G(G)^{P_G} &= a'_G + b'_G(G')^{P_{G'}} \\ a_B + b_B(B)^{P_B} &= a'_B + b'_B(B')^{P_{B'}} \end{aligned} \qquad (1.5.5)$$

where the nine coefficients, a_R, a_G, a_B, b_R, b_G, b_B, p_R, p_G and p_B, are dependent on the adapting conditions A of one half-field of the retina adapted, and the similar primed coefficients depend on the adapting conditions A' of the other half-field.

1.5.4 Techniques for Studying Chromatic Adaptation and Describing Colour Appearance

As mentioned in the last section, various methods have been used for describing colour appearance under different sets of adapting conditions. Wright (1981) and Bartleson (1977) have reviewed how chromatic adaptation has been studied. These methods can be divided into four groups: (a) haploscopic matching (Burnham et al. 1952; Hunt 1952, 1953; Wassef 1965; Breneman 1977), (b) local adaptation (or differential retinal conditioning) (MacAdam 1956), (c) magnitude estimation (or direct scaling) (Bartleson 1979a, 1979b; Pointer 1977, 1980; de Mattiello 1987; Nayatani et al. 1972; Luo et al. 1991a, 1991b), and (d) memory matching (Helson et al. 1952; Pitt and Winter 1974; Lam 1985). Some of these techniques have been mentioned in Section 1.5.3. They are briefly summarised below.

Methods (a) and (b) are carried out using specially designed visual colorimeters. The validity of these methods is dependent on a certain assumption. Firstly, in haploscopic matching, it is assumed that the adaptation of one eye does not affect the sensitivity of the other eye. Secondly, in the local adaptation method, it is assumed

that a pre-exposed adapting stimulus applied to one part of the retinal area has a negligible effect on the condition of the juxtaposed part. These methods impose unnatural viewing conditions and so are considered impractical for industrial applications.

Methods (c) and (d) are carried out under normal viewing conditions using both eyes, and without the interposition of any optical devices. Both methods require longer training periods for each observer than for methods (a) and (b). For the memory matching method, there can be some shortcomings: (a) observers only have a limited ability for remembering colours; (b) some memory distortion could occur; and (c) some stimuli may lie outside the gamut of sample colours used, such as those in the Munsell System. In the magnitude estimation method, observers are asked to make estimates of the magnitudes of some perceptual attributes such as lightness, colourfulness and hue. It is essential that each observer clearly understands the perceptual attributes being scaled otherwise the reliability of the results can be in doubt.

Luo et al.'s (1991a, 1991b) studies indicated that the colour matching results were more accurate than the magnitude estimation results. However, when using magnitude estimation, observer precision improves with efficient training and experimental experience. They summarised the main advantages in using magnitude estimation as follows:

(1) The method provides absolute perceptual values for colour attributes in the context of the interaction of various parameters, for instance, luminance levels, light sources, media and induction colours. However, short-term memory matching can only be used when two adapting fields considered have similar luminances and chromaticities.
(2) The results obtained are, in perceptual terms, equivalent to those predicted by colour appearance models. The results can be used directly to test various existing colour models

or, consequently, for deriving a completely new colour model.

(3) The method is a kind of knowledge representation of colour appearance because it expresses colour in a reportable form.

These points are in agreement with those found by other researchers such as Nayatani et al. (1972) and Takahama et al. (1984).

1.5.5 Experimental Data From Chromatic Adaptation Studies

Bartleson (1978, 1979b) divided the experimental data obtained from different methods into two groups, depending on the character of stimuli presented in each experiment. Some of those results derived from stimuli consisting of coloured lights are referred to type I results, and others generally obtained from coloured objects as type II results. In general, the type II results imply a much higher degree of object colour constancy than do the type I results. Inevitably, there are differences in appearance between the two kinds of stimuli in that the chromaticities of objects are more dependent on illumination than those coloured lights. In addition, the coloured objects tend to have textured surfaces with very small areas of specular reflectance. These may provide clues to the colour of the illuminant and thereby allowing for more effective "discounting of the illuminant" (Bartleson 1979b). This could lead to the greater constancy of object colours than for the homogeneous, textureless stimuli common to type I results. For instance, high constancy can usually be found on textile samples.

Of the published type I and type II results, some of those representing different experimental techniques which have been tested by many researchers are described as follows:

1.5.5.1 Type I Results (Using Coloured Lights)

(1) MacAdam data (1956)
MacAdam used a monocular bipartite field with differential retinal conditioning in the two halves (as described in Section 1.5.3.3). Two observers were used, and each repeated the matching process three or more times. This data set was not used in this study due to the limited number of observers available.

(2) Breneman data (1987)
Breneman designed an instrument that allowed a transparency to be back-illuminated by two different light sources. The device was constructed such that light from one of the sources enters only the right eye and light from the other source enters only the left eye. While each of observer's two eyes was independently adapted to a different illuminant in viewing a complex visual field, each observer matched a series of test colours seen by one eye with a juxtaposed variable stimulus seen by the other eye. Breneman used 2^0 test and matching stimuli located centrally in the complex adapting field which subtended an angle of 31^0 x 24^0. In making the matches, each observer viewed the test and matching stimuli for a series of brief intervals (about one second) while viewing the complex adapting field with normal eye movements. Nine experiments were completed with different pairs of illuminants and different luminances ranging from that of an average living room to that of a scene illuminated with hazy sunlight. In three other experiments each of the observer's two eyes was adapted to a different luminance of D55. The results obtained from eight observers by adapting to the illuminants D65 and A with the luminance of white 350 cd/m^2 were used to test various chromatic adaptation transforms (introduced in the next Section) investigated in the author's work. The correlated colour temperatures of 6500K and 2850K are for sources D65 and A respectively.

1.5.5.2 Type II Results (Using Object Colours)

(1) Helson et al. data (1952)

Helson et al. used memory matching technique in their chromatic adaptation experiment. Six observers were trained to describe colours in terms of Munsell colour co-ordinates under illuminant C and A. The luminances were 73 and 57 foot-candles (about 250 and 195 cd/m^2) for illuminant C illuminant A respectively. Sixty Munsell samples with one inch squares were used. Eleven samples were exposed in a random order during each observation. Each sample was viewed successively on each of three neutral backgrounds (white, grey and black) having Y values of 3, 21 and 78 % respectively. The results obtained from grey background (i.e. with the Y of 21%) were used here to test various chromatic adaptation transforms.

(2) Lam and Rigg data

Lam and Rigg (1985) studied the degree of colour constancy for object colours with change of light sources. Fifty-eight dyed plain wool samples having various degrees of colour constancy were described by a panel of five colour normal observers in terms of Munsell Value, Chroma, and Hue using a memory matching method under D65 and A light sources. For visual assessment, a viewing cabinet fitted with suitable light sources was used. The interior of the cabinet was finished in BS/5097 grey emulsion paint which gives a medium grey background of Munsell value 4. Twenty nine samples were presented at a time to simulate natural viewing conditions in each experimental session. The luminances were 1170 lm/m^2 (i.e. 372 cd/m^2) for the simulating artificial daylight and 1000 lm/m^2 (i.e. 318 cd/m^2) for the simulating illuminant A. A total of 3480 visual estimations were made. The results were also used to test various chromatic adaptation transforms in this thesis.

1.5.6. Chromatic Adaptation Transforms

Many chromatic adaptation transforms have been proposed over the years. These are used to predict the corresponding chromaticity co-ordinates or tristimulus values. A pair of corresponding colours represent samples having the same colour appearance when an observer is adapted to different conditions of illumination. Some of the most frequently used chromatic adaptation transforms were used in this study and are described below.

(1) Helson et al. Transform (1952)
Helson et al. (1952) formulated a theoretical transform based on the von Kries coefficient law, as shown in Eq. 1.5.6:

$$\begin{aligned} X' &= \beta X + 2.954\,(\alpha - \beta)\,Y + 0.220\,(\gamma - \beta)\,Z \\ Y' &= \alpha Y \\ Z' &= \gamma Z \end{aligned} \qquad (1.5.6)$$

where α, β, γ are the von Kries coefficients, and the X, Y, Z tristimulus values are referred to the stimuli perceived under one illuminant while X', Y', Z' as the stimuli giving the same colour appearance under another illuminant. The von Kries coefficients α, β, γ can be calculated by Eq. 1.5.7 :

$$\begin{aligned} \alpha &= R_0' / R_0 \\ \beta &= G_0' / G_0 \\ \gamma &= B_0' / B_0 \end{aligned} \qquad (1.5.7)$$

where R_0', G_0', B_0' and R_0, G_0, B_0 refer to the fundamental tristimulus values of illuminants computed by Eq. 1.5.8,

$$\begin{aligned} R &= 1.00\,Y \\ G &= -0.46\,X + 1.36\,Y + 0.10\,Z \\ B &= 1.00\,Z \end{aligned} \qquad (1.5.8)$$

In 1974, the CIE (1974) technical committee on colour rendering chose to use this transform in making small adjustments to account for differences in light sources to be compared for colour-rendering properties. This transform is designated as the von Kries transform hereafter.

(2) Bartleson Transform (1979)

Bartleson (1979a, 1979b) gave an empirical scheme that is based on the notion of the von Kries hypothesis to which is added a non-linear compression of the response of the "blue" fundamental as shown in Eq. 1.5.9 .

$$\begin{aligned} R' &= \alpha R \\ G' &= \beta G \\ B' &= k\,(\gamma B)^{p} \end{aligned} \qquad (1.5.9)$$

where α, β, γ are von Kries coefficients which are determined from the fundamental tristimulus values of the two conditioning stimuli that control the two adaptation states A and A' (e.g. A: daylight (D65), A': tungsten-light (A)). In this transform, the two conditioning stimuli are calculated using a single set of König-type fundamental primaries shown in Eq. 1.5.10 :

$$\begin{aligned} R &= 0.0713\,X + 0.9625\,Y - 0.0147\,Z \\ G &= -0.3952\,X + 1.1668\,Y + 0.0815\,Z \\ B &= \ 0.5610\,Z \end{aligned} \qquad (1.5.10)$$

Hence, the von Kries coefficients α, β, γ can be computed using Eq. 1.5.7 in which R_0' , G_0' , B_0' and R_0 , G_0 , B_0 calculated using Eq. 1.5.10 above.

In addition, the exponent p in Eq. 1.5.9 that compresses the response of the "blue" fundamental to show a post-receptor neural activity, can be obtained from Eq. 1.5.11:

$$p = 0.326\,\alpha^{27.45} + 0.325\,\beta^{-3.91} + 0.340\,\gamma^{-0.45} \qquad (1.5.11)$$

The coefficient k in Eq. 1.5.9 is given by

$$k = \gamma B_A / (\gamma B_A)^p \qquad (1.5.12)$$

where B_A is the fundamental tristimulus value of the stimulus under adaptation condition A (i.e. daylight D65 adaptation, in Bartleson's case). From the transferred fundamental tristimulus values R', G', B', the CIE tristimulus values X', Y', Z' can be obtained using the Eq. 1.5.13 in which the coefficients are obtained by inverse of Eq. 1.5.10:

$$\begin{aligned} X' &= 2.5170\ R' - 2.0763\ G' + 0.3676\ B' \\ Y' &= 0.8525\ R' + 0.1538\ G' + 0.0000\ B' \\ Z' &= 0.0000\ R' + 0.0000\ G' + 1.7825\ B' \end{aligned} \qquad (1.5.13)$$

(3) CIE (Nayatani) Transform

The CIE transform is based upon the Nayatani et al.'s (1981, 1990), Takahama et al.'s (1984) and Nayatani (1995) studies. This has been proposed by the CIE for field trials. It is a non-linear chromatic adaptation transform that predicts corresponding colours by transforming CIE 1931 tristimulus values through a non-linear function involving fundamental tristimulus values that are linearly related to those of the CIE 1931 colour matching functions. The fundamental tristimulus values are based on the fundamental primaries reported by Hunt and Pointer (1985).

The transform consists of two stages. The first stage is a modified von Kries transformation, and the second is a non-linear transformation corresponding to a compression in response of each mechanism. It also takes level of luminance into account. The prediction of corresponding colours is computed by using the following three steps:

Step 1: The tristimulus values (X_1, Y_1, Z_1) of a colour under test field are transformed to fundamental tristimulus values (R_1, G_1, B_1) by Eq. 1.5.14 .

$$\begin{aligned} R_1 &= 0.40024\ X_1 + 0.70760\ Y_1 - 0.08081\ Z_1 \\ G_1 &= -0.22630\ X_1 + 1.16532\ Y_1 + 0.04570\ Z_1 \\ B_1 &= 0.91822\ Z_1 \end{aligned} \qquad (1.5.14)$$

Step 2: The fundamental tristimulus values of the corresponding colour under reference field (R_2, G_2, B_2) are derived using Eq. 1.5.15 :

$$\begin{aligned} R_2 &= (Y_0\xi_2+1) \times K^{1/\beta_1 (R_{02})} \times [(R_1+1)/(Y_0\xi_1+1)]^{\beta_1 (R_{01}) / \beta 1 (R_{02})} - 1 \\ G_2 &= (Y_0\eta_2+1) \times K^{1/\beta_1 (G_{02})} \times [(G_1+1)/(Y_0\eta_1+1)]^{\beta_1 (G_{01}) / \beta 1 (G_{02})} - 1 \\ B_2 &= (Y_0\zeta_2+1) \times K^{1/\beta_2 (B_{02})} \times [(B_1+1)/(Y_0\zeta_1+1)]^{\beta_2 (B_{01}) / \beta 2 (B_{02})} - 1 \end{aligned} \qquad (1.5.15)$$

where the transformed relative chromaticity co-ordinates (ξ_1, η_1, ζ_1) are calculated by Eq. 1.5.16 under test illuminant using (x_{01}, y_{01}). The same calculation is used for obtaining (ξ_2, η_2, ζ_2) by replacing (ξ_1, η_1, ζ_1) and (x_{01}, y_{01}) with (ξ_2, η_2, ζ_2) and (x_{02}, y_{02}) respectively. The x_{02} and y_{02} represents the chromaticity co-ordinates of the reference illuminant.

$$\begin{aligned} \xi_1 &= (0.48105\ x_{01} + 0.78841\ y_{01} - 0.08081) / y_{01} \\ \eta_1 &= (-0.27200\ x_{01} + 1.11962\ y_{01} + 0.04570) / y_{01} \\ \zeta_1 &= 0.91822\ (1 - x_{01} - y_{01}) / y_{01} \end{aligned} \qquad (1.5.16)$$

In addition, the effective adapting responses under test field (R_{01}, G_{01}, B_{01}) are calculated using Eq. 1.5.17.

$$\begin{aligned} R_{01} &= (Y_0E_{01} / 100\pi)\ \xi_1 \\ G_{01} &= (Y_0E_{01} / 100\pi)\ \eta_1 \\ B_{01} &= (Y_0E_{01} / 100\pi)\ \zeta_1 \end{aligned} \qquad (1.5.17)$$

where E_{01} is the illuminance (lux) of the test field and Y_0 is the luminance factor of the background (Y_0 = 100 for the perfect reflecting diffuser). The same equation was used to obtain R_{02}, G_{02}, B_{02} for the reference field by replacing E_{01} and ξ_1, η_1, ζ_1 with E_{02} and ξ_2, η_2, ζ_2.

The exponents of red, green and blue transformations $\beta_1(R_{01})$, $\beta_1(G_{01})$, $\beta_2(B_{01})$ in Eq. 1.5.15 are calculated from the effective adapting responses of the test field R_{01}, G_{01}, B_{01}, respectively. These are obtained using Eq. 1.5.18 .

$$\beta_1(R_{01}) = (6.469 + 6.362\ R_{01}^{0.4495}) / (6.469 + R_{01}^{0.4495})$$
$$\beta_1(G_{01}) = (6.469 + 6.362\ G_{01}^{0.4495}) / (6.469 + G_{01}^{0.4495})$$
$$\beta_2(B_{01}) = 0.7844\ [(8.414 + 8.091\ B_{01}^{0.5128}) / (8.414 + B_{01}^{0.5128})] \quad (1.5.18)$$

Similarly, the $\beta_1(R_{02})$, $\beta_1(G_{02})$, $\beta_2(B_{02})$ for the reference field are calculated using Eq. 1.5.18 by replacing R_{01}, G_{01}, B_{01} with R_{02}, G_{02}, B_{02}.

Finally, the coefficient K is computed by Eq. 1.5.19.

$$K = \{[(Y_0\xi_1 + 1)/(20\xi_1 + 1)]^{(2/3)\beta 1\ (R01)} / [(Y_0\xi_2 + 1)/(20\xi_2 + 1)]^{(2/3)\beta 1\ (R02)}\}$$
$$\times \{[(Y_0\xi_1 + 1)/(20\xi_1 + 1)]^{(2/3)\beta 1\ (R01)} / [(Y_0\xi_2 + 1)/(20\xi_2 + 1)]^{(2/3)\beta_1(R_{02})}\} \quad (1.5.19)$$

For Y_0 = 20, the relation of K = 1 holds irrespective of the test and reference illuminants and luminances.

Step 3: The values (R_2, G_2, B_2) are transformed to (X_2, Y_2, Z_2) by Eq. 1.5.20.

$$X_2 = 1.85995\ R_2 - 1.12939\ G_2 + 0.21990 B_2$$
$$Y_2 = 0.36119\ R_2 + 0.63881\ G_2$$
$$Z_2 = 1.08906 B_2 \quad (1.5.20)$$

Nayatani (1995) extended his chromatic adaptation transform to become a colour appearance model to predict colour appearance attributes for colours perceived under various viewing conditions. These attributes include lightness, chroma, colourfulness, hue, and brightness, etc.

(4) The Hunt Transform (Hunt Colour Appearance Model)

This transform is based on the studies of Hunt (1991, 1994) on colour appearance modelling. He devised a colour appearance model which is capable of predicting the colour appearance under various conditions of illumination, background colour and surrounding for *related colours* and *unrelated colours*. Related Colour is defined by CIE (1987) as "Colour perceived to belong to an area seen in relation to other colours." Unrelated Colour is defined by CIE (1987) as "Colour perceived to belong to an area seen in isolation from other colours." In this thesis, the former case was used. The Hunt (1991, 1994) model can also compute the corresponding X', Y', Z' tristimulus values using its reverse form derived by Wang (1994) Hence, the Hunt colour appearance model can also be considered as a chromatic adaptation transform. The Hunt colour appearance model will be designated as Hunt94 hereafter.

The computational procedure for the Hunt94 is described as follows:

Step 1: Calculate X, Y, Z values from CIE chromaticity co-ordinates (x, y) if necessary for the reference white, background, and the sample considered.

$$X = (x / y)\, Y$$
$$Y = Y$$
$$Z = (1-x-y)\, Y / y \qquad (1.5.21)$$

Step 2: Calculate ρ, γ, β cone responses for the reference white, background, and the sample considered.

$$\rho = 0.38971\ X + 0.68898\ Y - 0.07868\ Z$$
$$\gamma = -0.22981\ X + 1.18340\ Y + 0.04641\ Z$$
$$\beta = 1.00000\ Z \qquad (1.5.22)$$

Where if account is being taken of simultaneous contrast or assimilation, the values for the reference white, $\rho_W, \gamma_W, \beta_W$, for the background, $\rho_b, \gamma_b, \beta_b$, and for the proximal field, $\rho_p, \gamma_p, \beta_p$, are used to calculate values for a modified reference white, $\rho'_W, \gamma'_W, \beta'_W$:

$$\rho'_W = \rho_W[(1-p)r + (1+p) / r]^{1/2} / [(1+p)r + (1-p) / r]^{1/2}$$
$$\gamma'_W = \gamma_W[(1-p)g + (1+p) / g]^{1/2} / [(1+p)g + (1-p) / g]^{1/2}$$
$$\beta'_W = \beta_W[(1-p)b + (1+p) / b]^{1/2} / [(1+p)b + (1-p) /b]^{1/2} \qquad (1.5.23)$$

where

$$r = (\rho_p/\rho_b)$$
$$g = (\gamma_p/\gamma_b)$$
$$b = (\beta_p/\beta_b). \qquad (1.5.24)$$

The values of p are between 0 and -1 for simultaneous contrast, and between 0 and +1 for assimilation.

Step 3: Calculate $\rho/\rho_W, \gamma/\gamma_W, \beta/\beta_W$, for the samples. $\rho_W, \gamma_W, \beta_W$, are the values of ρ, γ, β, for the reference white, or the modified reference white, as appropriate.

Step 4: Calculate F_L:

$$F_L = 0.2k^4(5L_A) + 0.1(1-k^4)^2(5L_A)^{1/3} \qquad (1.5.25)$$

where

$$k = 1 / (5L_A + 1). \qquad (1.5.26)$$

F_L is the luminance-level adaptation factor, and L_A is the luminance of the adapting field.

Step 5: Calculate F_ρ, F_γ, F_β, the chromatic adaptation factors.

$$h_\rho = 3\rho_W / (\rho_W + \gamma_W + \beta_W)$$
$$h_\gamma = 3\gamma_W / (\rho_W + \gamma_W + \beta_W)$$
$$h_\beta = 3\beta_W / (\rho_W + \gamma_W + \beta_W) \qquad (1.5.27)$$

$$F_\rho = (1 + L_A^{1/3} + h_\rho) / (1 + L_A^{1/3} + 1 / h_\rho)$$
$$F_\gamma = (1 + L_A^{1/3} + h_\gamma) / (1 + L_A^{1/3} + 1 / h_\gamma)$$
$$F_\beta = (1 + L_A^{1/3} + h_\beta) / (1 + L_A^{1/3} + 1 / h_\beta) \qquad (1.5.28)$$

Where for the equi-energy stimulus (defined as 'Stimulus consisting of equal amounts of power per small constant-width wavelength interval throughout the spectrum.' by CIE (1987), S_E, $\rho_W = \gamma_W = \beta_W$ and hence $h_\rho = h_\gamma = h_\beta$, and $F_\rho = F_\gamma = F_\beta = 1$. The colour of the illuminant is discounted.

Step 6: Calculate ρ_D, γ_D, β_D, the Helson-Judd effect factors (Helson-Judd effect is defined by the CIE (1987) as 'Tendency, in coloured illumination, for light colours to be tinged with the hue of the illuminant, and for dark colours to be tinged with the complementary hue.'

$$\rho_D = f_n[(Y_b / Y_W)F_L F_\gamma] - f_n[(Y_b / Y_W)F_L F_\rho]$$
$$\gamma_D = 0$$
$$\beta_D = f_n[(Y_b / Y_W)F_L F_\gamma] - f_n[(Y_b / Y_W)F_L F_\beta] \qquad (1.5.29)$$

Where $f_n[I]$ represents the cone response functions.

$$f_n[I] = 40[I^{0.73} / (I^{0.73} + 2)] \qquad (1.5.30)$$

If the colour of the illuminant is discounted, $\rho_D = \gamma_D = \beta_D = 0$.

Step 7: Calculate ρ_a, γ_a, β_a, the cone responses after adaptation for a related colour,

$$\begin{aligned}\rho_a &= B_\rho[f_n(F_L F_\rho \rho / \rho_W) + \rho_D] + 1 \\ \gamma_a &= B_\gamma[f_n(F_L F_\gamma \gamma / \gamma_W) + \gamma_D] + 1 \\ \beta_a &= B_\beta[f_n(F_L F_\beta \beta / \beta_W) + \beta_D] + 1 \end{aligned} \qquad (1.5.31)$$

where

$$\begin{aligned}B_\rho &= 10^7 / [\ 10^7 + 5\ L_A(\rho_W / 100)] \\ B_\gamma &= 10^7 / [\ 10^7 + 5\ L_A(\gamma_W / 100)] \\ B_\beta &= 10^7 / [\ 10^7 + 5\ L_A(\beta_W / 100)], \end{aligned} \qquad (1.5.32)$$

and $f_n[I]$ is defined as shown in Eq. 1.5.30. B_ρ, B_γ, B_β are the cone bleach factors providing reduced cone responses at very high levels of illumination, where appreciable bleaching of the cone pigments occurs.

Step 8: Calculate colour difference signals (C_1, C_2, C_3):

$$\begin{aligned}C_1 &= \rho_a - \gamma_a \\ C_2 &= \gamma_a - \beta_a \\ C_3 &= \beta_a - \rho_a\ . \end{aligned} \qquad (1.5.33)$$

For the criterion adopted for achromatic colours is $\rho_a = \gamma_a = \beta_a$, all the three signals are equal to zero, that is, $C_1 = C_2 = C_3 = 0$. Colourfulness increases as C_1, C_2, and C_3 increase. In addition, the criterion for four unique hues: red, green, yellow, and blue, is that the signals are in constant ratios to each other as shown below:

$$\begin{aligned}&\text{Unique red} && C_1 = C_2 \\ &\text{Unique green} && C_1 = C_3 \\ &\text{Unique yellow} && C_1 = C_2 / 11 \\ &\text{Unique blue} && C_1 = C_2 / 4\ . \end{aligned} \qquad (1.5.34)$$

Step 9: Calculate hue angle h_s:

$$h_s = \arctan \{ [1/9 (C_2 - C_3)] / [C_1 - (C_2 / 11)] \}$$
$$= \arctan (t / t'), \quad (1.5.35)$$

where

$0^o \leq h_s < 90^o$ when $t \geq 0$ and $t' > 0$,
$90^o < h_s < 180^o$ when $t > 0$ and $t' < 0$,
$180^o \leq h_s < 270^o$ when $t < 0$ and $t' < 0$,
$270^o < h_s < 360^o$ when $t < 0$ and $t' > 0$.

Step 10: Calculate hue H:

$$H = H_i + 100 A / (A + B), \quad (1.5.36)$$
$$A = (h_s - h_i) / e_i, \quad (1.5.37)$$
$$B = (h_{i+1} - h_s) / e_{i+1}, \quad (1.5.38)$$

where

	Red	Yellow	Green	Blue	Red
i	1	2	3	4	5
H_i	0	100	200	300	400
h_i	20.14	90.0	164.25	237.53	380.14
e_i	0.8	0.7	1.0	1.2	0.8

Step 11. Calculate eccentricity factor e_s:

$$e_s = e_i + [(e_{i+1} - e_i) (h_s - h_i)] / (h_{i+1} - h_i), \quad (1.5.39)$$

where the values of e_i and h_i are given in Eq. 1.5.37.

Step 12: Calculate the low luminance tritanopia factor F_t:

$$F_t = L_A / (L_A + 0.1) \quad (1.5.40)$$

Step 13: Calculate Yellow-Blueness response M_{YB} and Red-Greenness response M_{RG}:

$$M_{YB} = 100\ [\ 1/2\ (C_2 - C_3) / 4.5\ ]\ [e_s\ (10/13)\ N_c N_{cb} F_t\ ], \quad (1.5.41)$$
$$M_{RG} = 100\ [\ C_1 - (C_2/11)]\ [e_s\ (10/13)\ N_c\ N_{cb}], \quad (1.5.42)$$

where

$$N_{cb} = 0.725\ (Y_w / Y_b)^{0.2}, \quad (1.5.43)$$
$$N_c = 1\ . \quad (1.5.44)$$

Step 14: Calculate colourfulness content factor M:

$$M = (M^2_{YB} + M^2_{RG})^{1/2} \quad (1.5.45)$$

Step 15: Calculate relative Yellowness-Blueness m_{YB}, relative Redness-Greenness m_{RG}, and Saturation s:

$$m_{YB} = M_{YB} / (A + \gamma_a + \beta_a), \quad (1.5.46)$$
$$m_{RG} = M_{RG} / (A + \gamma_a + \beta_a), \quad (1.5.47)$$
$$s = 50\ M / (A + \gamma_a + \beta_a). \quad (1.5.48)$$

Step 16: Calculate scotopic luminance level adaptation factor F_{LS}:

$$F_{LS} = 3800\ j^2\ (5L_{AS} / 2.26) + 0.2\ (1 - j^2)^4\ (5L_{AS} / 2.26)^{1/6}, \quad (1.5.49)$$

where

$$j = 0.00001\ /\ [(5L_{AS} / 2.26) + 0.00001]\ . \quad (1.5.50)$$

Step 17: Calculate rod bleach or saturation factor B_s:

$$B_s = 0.5\ /\ [\ 1 + 0.3(5L_{AS} / 2.26)\ (S/S_w)^{0.3}\ ]$$
$$+ 0.5\ /\ [\ 1 + 5(5L_{AS} / 2.26)\ ], \quad (1.5.51)$$

where S/S_w are the scotopic luminances relative to that of the reference white. If the true values of S/S_w are not known, the

equivalent photopic values, Y/Y_w, can usually be used as an approximation instead.

Step 18: Calculate rod response after adaptation A_s:

$$A_s = B_s\ (3.05)\ \{f_n[F_{LS}\ (S / S_w)]\} + 0.3, \qquad (1.5.52)$$

where f_n is calculated by Eq. 1.5.32.

Step 19: Calculate photopic part of the achromatic signal A_a:

$$A_a = 2\rho_a + \gamma_a + (1/20)\beta_a - 3.05 + 1\ . \qquad (1.5.53)$$

Step 20: Calculate total achromatic signal A:

$$A = N_{bb}\ [\ A_a - 1 + A_s - 0.3 + (\ 1^2 + 0.3^2)^{1/2}], \qquad (1.5.54)$$

where

$$N_{bb} = 0.725\ (\ Y_w / Y_b\ )^{0.2}\ . \qquad (1.5.55)$$

Step 21: Calculate Brightness Q:

$$Q = \{7\ [A + (M/100)]\}^{0.6}\ N_1 - N_2, \qquad (1.5.56)$$

where

$$N_1 = (7A_w)^{0.5} / 5.33\ N_b^{0.13}, \qquad (1.5.57)$$

$$N_2 = 7A_w N_b^{0.362} / 200, \qquad (1.5.58)$$

and A_w is the value of A for the reference white.

Step 22: Calculate lightness J and J_{new}:

$$J = 100\ (Q / Q_w)^z, \qquad (1.5.59)$$

where Q_w is the value of brightness for the reference white and $z = 1 + (Y_b / Y_w)^{1/2}$ for the reflectance colours;

z = 0.85 for the cut-sheet transparency colours under darker background;
z = 1 for the cut-sheet transparency colours under lighter medium-grey background;
For the 35 mm projected slide colours z = 1.2 and

$$J_{new} = J \{1.14 [1 - (J / 100)^3] + (J / 100)^5\} \quad (1.5.60)$$

Step 23: Calculate the chroma C and colourfulness Mc:

$$C = 2.44 s^{0.69} (Q / Q_w)^{Yb/Yw} (1.64 - 0.29^{Yb/Yw}) \quad (1.5.61)$$

$$Mc = C F_L 0.15, \quad (1.5.62)$$

where F_L is calculated using Eq. 1.5.25.

Step 24: Calculate whiteness-Blackness Q_{WB}:

$$Q_{WB} = 20 (Q^{0.7} - Q_b^{0.7}), \quad (1.5.63)$$

where Q_b is the value of Q for the background.

Two procedures were used to obtain the predicted corresponding colours from the Hunt94 model. First, the tristimulus values of a test colour and a test illuminant, and the parameters defining the test conditions were programmed to calculate the colour appearance values of L C H under the test illuminant for the test colour. Subsequently, these colour appearance values, the tristimulus values of the reference illuminant (D65) and the parameters defining the reference conditions were put into the reverse Hunt model to calculate the tristimulus values of corresponding colours. The reverse Hunt model was derived by Wang (1994).

The values of the Hunt94 model chromatic and brightness surround induction factors (i.e. N_c and N_b respectively) for different viewing conditions are given as follows:

(1) Small areas in uniform light backgrounds and surrounds, N_c = 1.0; N_b = 300, (these are used in the author's work for Breneman data).
(2) Normal scenes, N_c = 1.0; N_b = 75, (these are used in the author's work for surface colours).
(3) Television and VDU display in dim surrounds, N_c = 0.95; N_b = 25.
(4) Projected photographs in dark surrounds, N_c = 0.9; N_b = 10.
(5) Arrays of adjacent colour in dark surrounds, N_c = 0.75; N_b = 5.

(5) The Bradford Transform

The Bradford transform (abbreviated as BFD) was derived by Lam and Rigg (1985) from their experimental data (as mentioned in Section 1.5.5.2). The transform is similar to that of Bartleson (1979a, 1979b). The results gave a good prediction for the five independent data sets based on object colours. The computational procedure of the transform is given as follows:

Step 1: Transformation from the tristimulus values X, Y, Z to the fundamental tristimulus values R, G, B and for the test colours.

$$\begin{aligned} R &= 0.8951X + 0.2664Y - 0.1614Z \\ G &= -0.7502X + 1.7135Y + 0.0367Z \\ B &= 0.0389X - 0.0685Y + 1.0296Z \end{aligned} \qquad (1.5.64)$$

Step 2: The tristimulus values of the corresponding colour in the reference field (R', G', B') are computed by Eq. 1.5.65 :

$$\begin{aligned} R' &= R'_0(R / R_0) \\ G' &= G'_0(G / G_0) \\ B' &= B'_0(B / B_0)(B_0 / B'_0)^{0.0834} \end{aligned} \qquad (1.5.65)$$

where quantities R_0, G_0, B_0, and R'_0, G'_0, B'_0, are calculated from the tristimulus values of the test and reference illuminants respectively through Eq. 1.5.64.

Step 3: Transform the tristimulus values of the corresponding X', Y', Z' from R', G', B' using Eq. 1.5.66 as shown below.

$$\begin{aligned} X' &= 0.9870R' - 0.1470G' + 0.1600B' \\ Y' &= 0.4323R' + 0.5184G' + 0.0493B' \\ Z' &= -0.0085R' + 0.0401G' + 0.9685B' \end{aligned} \qquad (1.5.66)$$

(6) The RLAB Transform

The RLAB transform is based on the studies of Fairchild and Berns (1993) and Fairchild (1994) on the RLAB colour space for image colour-appearance specification. The colour space is an extension of the CIEL*a*b* colour space. It is capable of predicting corresponding colours under different sets of viewing conditions such as those for viewing reflective and self-luminous stimuli. It can also take into account the change of surroundings. The following equations describe the RLAB transform.

Step 1: Convert CIE tristimulus values (Y = 100 for white) to fundamental tristimulus values as illustrated in Eqs. 1.5.67 and 1.5.68.

$$\begin{vmatrix} R \\ G \\ B \end{vmatrix} = M \begin{vmatrix} X \\ Y \\ Z \end{vmatrix} \qquad (1.5.67)$$

where

$$M = \begin{vmatrix} 0.4002 & 0.7076 & -0.0808 \\ -0.2263 & 1.1653 & 0.0457 \\ 0.0 & 0.0 & 0.9182 \end{vmatrix} \qquad (1.5.68)$$

Step 2: Calculate the A matrix used to model the chromatic adaptation transform.

$$A = \begin{vmatrix} a_R & 0.0 & 0.0 \\ 0.0 & a_G & 0.0 \\ 0.0 & 0.0 & a_B \end{vmatrix} \qquad (1.5.69)$$

where

$$a_R = [\, p_L + D(1.0 - p_L)] \,/\, R_n \qquad (1.5.70)$$

$$p_L = (1.0 + Y_n^{1/3} + l_E) \,/\, (1.0 + Y_n^{1/3} + 1.0 \,/\, l_E) \qquad (1.5.71)$$

$$l_E = [3.0(R_n \,/\, 102.70)] \,/\, (R_n/102.70 + G_n/98.47 + B_n/91.82) \qquad (1.5.72)$$

where Y_n is the absolute adapting luminance in cd/m^2. Terms with an n subscript refer to values for the adapting illuminant. The D factor in Eq. 1.5.70 allows to vary the proportion of cognitive 'discounting-the-illuminant'. D should be set equal to 1.0 for hard-copy images, 0.0 for soft-copy display, and an intermediate value such as 0.5 for situations such as projected transparencies in completely darkened rooms.

Step 3: The corresponding tristimulus values of a stimulus colour under reference viewing conditions can be obtained by using Eq. 1.5.73 .

$$\begin{vmatrix} X_{ref} \\ Y_{ref} \\ Z_{ref} \end{vmatrix} = R\,A\,M \begin{vmatrix} X \\ Y \\ Z \end{vmatrix} \qquad (1.5.73)$$

where

$$R = \begin{vmatrix} 186.01 & -112.95 & 21.98 \\ 36.12 & 63.88 & 0.0 \\ 0.0 & 0.0 & 108.89 \end{vmatrix} \quad (1.5.74)$$

The RLAB co-ordinates are then calculated using Eqs. 1.5.75 to 1.5.79:

$$L^R = 100\,(Y_{ref} / 100.00)^{\sigma} \quad (1.5.75)$$

$$a^R = 430[(X_{ref} / 95.05)^{\sigma} - (Y_{ref} / 100.00)^{\sigma}] \quad (1.5.76)$$

$$b^R = 170[(Y_{ref} / 95.05)^{\sigma} - (Z_{ref} / 100.00)^{\sigma}] \quad (1.5.77)$$

$$C^R = [(a^R)^2 + (b^R)^2]^{1/2}, \quad (1.5.78)$$

$$h^R = \arctan(b^R / a^R), \quad (1.5.79)$$

where σ = 1/2.3 for an average surround, σ = 1/2.9 for a dim surround, and σ = 1/3.5 for a dark surround.

(7) The CIEL*a*b* Transform

The CIEL*a*b* transform is the same as the CIEL*a*b* colour space recommended by the CIE in 1976 for use as a colour difference metric. Although CIEL*a*b* was developed solely for quantifying colour difference in colours under near-daylight, it also provides colour appearance attributes through its cylindrical specification of lightness (L*), chroma (C*) and hue angle (h) (see Section 1.4.4), and can be used with different illuminants by changing values of X_n, Y_n, Z_n. Hence, it can also be considered as a chromatic adaptation transform through a modified form of the von Kries model. The inverse form of CIEL*a*b* formula has been derived and can compute the corresponding X Y Z tristimulus values from the lightness, chroma and hue angle predicted by the CIEL*a*b* colour space under specific viewing conditions. By combining the formula of CIEL*a*b* colour space (as mentioned in Section 1.4.4) and its inverse, a transformation is formed.

All the chromatic adaptation transforms described above have been used to test their performance. The results obtained by many researchers such as Lam (1985), Hunt (1987), Nayatani et al. (1987, 1990), and Luo et al. (1991a, 1991b) indicate that the reliability of all the transforms is still unsatisfactory in predicting the experimental data.

1.6 Aims of the Work

As mentioned in Sections 1.4 and 1.5, the reliability of the various metamerism indices and chromatic adaptation transforms is still unsatisfactory. The research work was intended to carry out experiments to verify these indices and transforms, and aimed to recommend reliable methods for industrial application. The work was divided into two parts: metamerism and colour constancy.

For metamerism study, the primary strategic aim was to derive a reliable index for quantifying metamerism. Five tasks were defined:

(1) to prepare a number of metameric pairs covering a wide range of colours,
(2) to conduct visual assessments in quantifying degree of metamerism,
(3) to evaluate the precision of available metamerism indices using the experimental data,
(4) to derive a reliable method in predicting the degree of metamerism,
(5) to develop a new standard deviate observer for indicating the degree of observer metamerism.

In colour constancy study, the primary strategic aim was to derive a reliable index for quantifying the degree of colour constancy. Five tasks were defined:

(1) to prepare a set of colour constancy samples covering a wide colour gamut,
(2) to conduct visual assessments in quantifying colour appearance,
(3) to derive the corresponding chromaticities under the three light sources studied: D65, A and TL84.
(4) to test the performance of various available chromatic adaptation transforms using the experimental grids obtained.
(5) to derive a reliable chromatic adaptation transform for predicting the degree of colour constancy.

In this chapter, ' metamerism is explained prior to colour constancy. However, the details of colour constancy and metamerism studies are given in Chapters 2 and 3 respectively. This arrangement is due to the sequence of the experimental work and the chromatic adaptation transform derived from Chapter 2 being used in the Chapter 3.

CHAPTER 2

CHAPTER 2

COLOUR CONSTANCY STUDY

A reliable Colour Constancy Index (CCI) is important for surface colour industries. In the textile trade, seasonal fashion palettes are the primary target shades for all dye houses and are selected long before the actual production. These shades often need to be produced onto a wide range of material, such as polyester, cotton and wool. In product design, the same shade is required to be produced onto various other types of materials such as textile and plastics. In both cases, the CCI is required for selecting the most colour constant recipes in order that the colour matches for these materials hold under various light sources. In the lighting industry, CCI can also be used to evaluate the colour rendering property of light sources (typically fluorescent tubes). In the colour reproduction industry, there are problems in precisely reproducing a colour from colour monitor using an electronic printer. One cause of the problem is that the observer's state of adaptation is often different when viewing the hardcopy compared to that when viewing the original scene on the display. Using the CCI, it is possible to predict what the tristimulus values of the hardcopy colour must be to ensure a reasonable colour match under the two different states of adaptation.

The common method for achieving CCI is to use a chromatic adaptation transform to predict corresponding colours under a reference source (usually D65) and a second source (tungsten lamp, A). Subsequently, at least one colour difference formula described in Section 1.4.4 can be used to compute the colour differences between the predicted corresponding colours and the measured colours under reference light source. This colour difference represents the degree of colour constancy for the test colour. The larger the difference, the greater the degree of colour non-constancy. Hence, the reliability of both chromatic adaptation transform and colour difference formula is

essential to achieve a successful CCI. The experimental results produced here together with three other data sets were accumulated to evaluate the chromatic adaptation transforms and colour appearance models described in Section 1.5.6. Attempts were also made to derive a chromatic adaptation transform to fit these results.

In this study, 240 wool samples were prepared. Each was assessed by a panel of five experienced observers under three light sources (i.e. D65, A and TL84) using a magnitude estimation method The mean visual data in terms of lightness, colourfulness and hue were obtained and used to derive corresponding chromaticities.

2.1 Experimental

2.1.1 Preparation of Samples

Some of the samples used were produced with the assistance of the Scottish College of Textiles. The general strategy is to produce a set of wool samples well distributed over CIEL*a*b* colour space. The L* scale was divided into ten intervals (with 10 L* units from 0 to 100). The a* and b* axes were also divided into 10 unit intervals within the maximum to the minimum achievable dye ranges. In total, two hundred and ninety three colours were achieved. The number of samples for each L* plane are given below:

L* Plane	80-70	70-60	60-50	50-40	40-30	30-20	20-10
No. of samples	28	69	57	60	49	26	4.

It can be seen that there are insufficient samples in very light region due to the inherent yellowish colour of substrate. A second set of samples (including 200 colours), previously used at the University of Bradford for investigating small to medium colour differences, was also used to extend the colour gamut.

The choice of samples was somewhat arbitrary but guided by the following points:

a. The samples chosen were evenly distributed over CIE L*a*b* colour space, i.e. without large gaps between samples.
b. Samples should cover a wide colour gamut by including the most saturated, light and dark achievable colours.

After a careful screening process, a lack of colours in light area (i.e. L*> 80) was still found. Hence, it was decided to use some bright cotton samples. Eleven samples were prepared. There are four samples within the 100-90 L* range and seven within the 90-80 L* range. These cotton samples have a plain texture which appears quite similar to that used for wool samples. Finally, a total of 240 colours were selected. The number of samples for each L* plane are given below.

L* Plane	90-75	75-65	65-55	55-45	45-35	35-25	25-15	15-0
Samples	16	25	43	49	43	41	20	3

These samples are plotted on CIE a*b* diagram under D65 and A, and TL84 light sources as shown in Figs. 2.1.1 (a), (b) and (c) respectively. The samples selected covered a wide range colour space and lightness direction.

2.1.2 Colour Measurement

The colour measurements for the 240 samples were carried out using a Macbeth MS-2020 Spectrophotometer. The dyed wool serge was mounted onto hard white cardboard with three inch squares. Four layers of the sample were used as it was found that there was no change in the measured readings beyond this thickness. The reflectance values were measured at 20 nm intervals (400 - 700 nm) with specular component included, without the UV cut-off filter, and using a large aperture. The average of four measurements was taken

for each sample by rotating it through 90 degrees between measurements. These results are given in Appendix A.1.

2.1.3 Visual Assessment

Three light sources were used in this study: the Thorn D65, Philips TL84 and tungsten lamp (A). The engineering information for the three sources are shown in Table 2.1.1. A VeriVide viewing cabinet with a grey background (with Y about 12) was used for visual assessment. Each colour was judged, in terms of lightness, colourfulness and hue, by a panel of five experienced observers using a magnitude estimation method as mentioned in Section 1.5.4. The total number of colour samples used was 240 (section 2.1.1), and in each observing session thirty colours were used. For each light source, nine sessions were required for each observer, in which one session was repeated to investigate the repeatability of visual results. Table 2.1.2 summarises the experimental conditions for the three sources used. In total, 135 sessions were carried out and 10,770 estimations were made.

2.1.3.1 Viewing Conditions

The experiments performed in a darkened room in which each observer viewed the samples presented in the viewing cabinet at a distance of about 45 cm, with a viewing geometry of $0^0/45^0$ (illuminating/viewing). This makes sample subtending about 10^0 to observer's eye.

2.1.3.2 Magnitude Estimation Method

As mentioned earlier, a panel of five observers participated in the experiment. All observers had normal colour vision according to the Ishihara and City University tests. Their ages ranged from twenty to forty. They were either research assistants or members of staff in the Loughborough University of Technology. All of them were also quite experienced in the magnitude estimation scaling technique. At

the beginning of each observing session, each observer was asked to adapt to the experimental condition for three minutes. Subsequently, 30 samples randomly generated from all 240 samples were given to each observer. He or she was asked to rank them in terms of the lightness, colourfulness and hue attributes, and then gave the scaled value for each test colour. Definitions of these attributes were described in Section 1.2.2, and are summarised below:

Lightness is the brightness of an area judged relative to the brightness of a similarly illuminated area that appears to be white or highly transmitting.

Colourfulness is the attribute of a visual sensation according to which an area appears to exhibit more or less of its own hue.

Hue is the attribute of a visual sensation according to which an area appears to be similar to one, or to proportions of two, of the perceived colours red, yellow, green and blue.

2.1.3.3 Experimental Procedure

After the three-minute adaptation, each observer commenced judging the three attributes, Lightness, Colourfulness and Hue. There was no constraint to each observer as which attribute should be first judged. The following instructions were given to each observer:

INSTRUCTIONS

You will be shown 30 samples randomly generated from all 240 ones. Your task will be to rank them by each of three attributes (i.e., lightness, colourfulness and hue), and then to report the quantities of lightness, colourfulness and hue for each sample you see.

Lightness scaling

Use the reference white as a standard which has a lightness of 100 and your imaginary black has a lightness of zero as anchoring points to scale lightness for each sample.

Colourfulness scaling

A neutral colour has no colourfulness, represented by zero on your scale. You are asked to assign a reasonable number to describe the colourfulness of each sample. This is an open-ended scale since no top limit is set. A reference colourfulness sample is also used. Hence, all samples can be related on the same visual scale.

Hue scaling

There are four psychological primaries: red, yellow, green and blue. These four colours can be arranged as points around a circle and lying at opposite ends of x and y axes. Hues lying at opposite ends of each axis cannot be sensed simultaneously. You are asked to describe a hue as a proportion of two neighbouring primaries. Firstly, decide whether or not you can perceive any hue at all. If not, please reply " neutral." On the other hand, if the sample does not appear neutral, then decide which of the four primaries is predominant. Next, decide whether or not you see a trace of any other primary hue. If so, identify it. Finally, estimate the proportions in which the two primaries stand, *e.g.*, an orange colour may be 60% yellow and 40% red.

The results were recorded for further data analysis.

For colourfulness scaling, a different reference colourfulness sample was used under each light source. All results were on a common visual scale in relation to the reference colourfulness sample used under D65 source, a colourfulness of 40 being assigned to this sample. For example, before commencing a session under a new light source, observers were first asked to readapt under D65 and to fix in

memory the reference colourfulness sample with magnitude of 40. Again, after a three-minute adaptation period under the new light source, observers were asked to estimate a new reference colourfulness sample against the previous one under D65 from memory. The reference colourfulness samples used under D65, A and TL84 were red, bluish green and blue respectively. These were selected with similar colourfulness but different hue.

2.2 Data Analysis

The data analysis was carried out using a method similar to those used by Bartleson (1979a, 1979b), Pointer (1980), Troscianko (1979) and Luo et al. (1991a, 1991b).

For the colourfulness results, an unconstrained scale was used. Computation of the geometric mean was used to determine the mean visual results. This automatically establishes a basis for normalising the results of an individual's data. If S_i is the individual observer's rating of the test colour i, and $\bar{S}_i$ is the geometric mean of all observers' ratings of the same test colour, then $\log S_i$ can be plotted against $\log \bar{S}_i$ for all the test colours. A regression line can be established to determine the a and b factors of each observer, as shown in Eq. 2.2.1.

$$\log \bar{S}_i = b \log S_i + a \qquad (2.2.1)$$

where a is a scaling factor and b is a compression (or expansion) factor.

The constants a and b for each observer enable each observer's data to be adjusted to a common scale. The factor (a) indicates the multiplicative constants used in each observing session. The fact that they vary between observers means that each observer chose a somewhat different modulus. However, the exponent (b) representing

scale compression can be used to evaluate the consistency of each individual observer between similar experimental conditions. For some of the test colours, the colourfulness results were zero. The observers estimated the stimuli colours as being neutral and so these were assigned a value of 1 in order to enable the geometric mean to be calculated.

The arithmetic mean values of lightness and hue for each colour were calculated. The arithmetic mean was used to calculate the mean result because all the observers were using the same numerical scale with the same fixed end points. For lightness, the results are within 0 (imaginary black) and 100 (reference white). For the hue scale, all the results were transformed onto a 0-400 scale. That is, 0-100 for R-Y, 100-200 for Y-G, 200-300 for G-B and 300-400 for B-R. These mean visual results are given in Appendix A.2.

2.2.1 Precision and Repeatability of Visual Results

The deviation between the individual and the mean visual results representing corporate panel results was examined using the statistical measures. That is the correlation coefficient (r) and coefficient of variation (CV) proposed by Coates et al. (1973), which were calculated for each light source between each observer's results and the mean results. The two measures are described below.

Correlation Coefficient (r)

This is the product moment correlation coefficient and has been widely used. It is a measure of the tendency of X to increase as Y increases, and can be defined as:

$$r = \frac{N\Sigma(XY) - \Sigma X \Sigma Y}{\{ [N\Sigma X^2 - (\Sigma X)^2] [N\Sigma Y^2 - (\Sigma Y)^2] \}^{1/2}} \qquad (2.2.1)$$

where X and Y are the individual and mean results respectively.
For perfect correlation, r should be 1.

Coefficient of Variation (CV)

If the X values are plotted against the Y values, the points ought to lie on a straight line. The more the points are scattered about the line, the poorer the formula. CV is a measure of the distance of the points from the best straight line through the points and expresses the root mean square deviation of the points from the line as a percentage of the mean Y values. For two sets of the X and Y values, the relationship between X_i and Y_i for one particular pair is given by

$$X_i = fY_i + T \qquad (2.2.2a)$$

and

$$S^2 = (X_i - fY_i - T) \qquad (2.2.2b)$$

where f is a proportionality constant. T is the intercept on the X against Y plot, and S^2 is the sum of squares of the distances of the points from the straight line. The best f and T values can be obtained using following equations.

$$f = (N\Sigma (XY) - \Sigma X \Sigma Y) / [N\Sigma Y^2 - (\Sigma Y)^2] \qquad (2.2.2c)$$

$$T = (\Sigma X - f\Sigma Y) / N \qquad (2.2.2d)$$

The coefficient of variation (CV) is expressed as Eq. 2.2.2e:

$$CV\ (\%) = 100\ [(\Sigma S^2 / N)^{1/2} / \bar{Y}\ ] \qquad (2,2,2e)$$

where $\bar{Y}$ is the mean of the Y values from a particular colour difference formula. For a perfect agreement, CV should be zero. The larger the value, the poorer the formula. For comparing individual and mean results, the f and T equal 1.0 and 0.0 respectively due to assuming that all the individual and mean visual results obtained in this work were on the same scale.

Each observer's precision performance is summarised in Table 2.2.1. The mean r values are 0.97, 0.94 and 1.00 for lightness, colourfulness and hue respectively, which indicate a high degree of

correlation between the individual result and the mean result, especially for huė. The mean CV values are 11, 17 and 7 for lightness, colourfulness and hue respectively. These values generally agree with those found by Bartleson (1979b), Pointer (1980) and Luo et al. (1991a).

All of the above findings indicate that the hue results are the most consistent throughout the whole experiment, and the colourfulness results show that colourfulness is the most difficult of the three attributes to scale, about twice as difficult to scale as hue. These results imply that for a satisfactory colour appearance model or space it seems to be unlikely to achieve better than 89%, 83% and 93% agreement to the lightness, colourfulness and hue visual results respectively.

As mentioned earlier, 30 samples were assessed a second time by each observer with a one-month gap. Table 2.2.2 summarises individual repeatability performance. The mean r values are 0.98, 0.92 and 1.00, and the mean CV values are 11, 23 and 6 for lightness, colourfulness and hue respectively. These values indicate that the individual result is highly repeatable. The results also show that each observer's precision and repeatability performance are very similar except for colourfulness, in which the result obtained from each observer's repeat assessment is slightly more varied than that from each against the mean results.

As mentioned earlier, the exponent factor b was used to scale the individual colourfulness results onto a common scale. These factors can also be used to indicate the consistency of an individual's colourfulness results for each experimental condition. For each observer, the ratios between maximum and minimum exponent factors under all sources (D65, A and TL84) were calculated. The results are summarised in Table 2.2.3. The ratio for all five observers ranged from 1.07 to 1.20 with a mean value of 1.12, that is, a 12% difference from unity. The results are slightly better than those

obtained in the Luo et al's (1991a) surface non-luminous mode experiment in which 17% was found.

2.2.2 Deriving Corresponding Chromaticities

Several researchers (Bartleson 1979a, 1979b; Pointer 1977, 1980; Luo et al. 1991b) described their colour appearance results by constructing experimental grids in the CIE u'v' chromaticity diagram. These grids were produced visually by interpolating the u'v' chromaticity co-ordinates of each test colour with mean hue and colourfulness visual results under a particular set of adaptation conditions. Loci of constant hue and contours of constant colourfulness were then drawn in by hand.

However, Luo et al. (1991a, 1991b) pointed out that there are some disadvantages in constructing a grid in the CIE u'v' chromaticity diagram. These are: (1) it is only an approximate uniform colour space; (2) it is only strictly applicable to illuminants of near-daylight colour; thus the chromaticities for the test stimuli in experimental phases of light sources (W and A) are very close together when plotted; plotting the values of mean hue and colourfulness produced an almost unreadable diagram. Hence, the precision of the experimental grids is in doubt; (3) the u'v' diagram is only valid for presenting samples having equal luminance factors. They adopted the CIEL*a*b* space to establish their experimental grids.

It was decided in this work to construct the experimental grids in the CIEL*a*b* colour space. There are some major advantages for this approach:

(1) CIEL*a*b* allows for the effects of luminance factor (Y);
(2) CIEL*a*b* has an imbedded chromatic adaptation transformation in order to account for adaptation in different light sources (i.e., X/Xn, Y/Yn, Z/Zn, where n refers to the reference light source). The CIEL*a*b* system, however, was only intended for illuminants of near-daylight colour. Hence, the test stimuli

plotted would be reasonably distributed in the a*b* diagram with the neutral point at its origin;

(3) This enables the author's results directly to compare with those of Luo et al.'s (1991a, 1991b).

The constant colourfulness contours were constructed using a slightly different technique from that used in earlier publications such as Bartleson (1979a), Pointer (1977, 1980). The software was developed to first select visual colourfulness results corresponding to stimuli close to a particular colourfulness (e.g. within ± 10 colourfulness range) and then to generate a set of hypothetical points corresponding to a particular colourfulness. For instance, if Cp_i represents the CIE L*a*b* chroma of a hypothetical point (i) corresponding to a particular perceived colourfulness (such as 30), this can be calculated using Eq. 2.2.3. Its CIE a*b* co-ordinates can then be computed (Ap_i and Bp_i) using the Eqs. 2.2.3 to 2.2.5 given below:

$$Cp_i = 30\ C^*_i\ /\ C_{vi} \qquad (2.2.3)$$

$$Ap_i = Cp_i\ \text{Cos}\ h_i \qquad (2.2.4)$$

$$Bp_i = Cp_i\ \text{Sin}\ h_i \qquad (2.2.5)$$

where C_{vi} is a colour's visual colourfulness results selected, corresponding to the measured results of h_i , C^*_i (CIE L*a*b* hue angle and C*).

The Ap_i , Bp_i for each colour is plotted in the a*b* diagram. The loci of constant colourfulness were drawn by hand to go through these hypothetical points. More weighting was placed on the test colours having L* close to 50. This method is easy to use and provides an accurate contour. For example, Fig. 2.2.1 shows the contour having a particular perceived colourfulness value of 30 with L* of 50 under light source D65. The colours having visual colourfulness ranging from 20 to 40 (i.e. 30 ± 10) were selected to obtain the hypothetical points with a particular perceived colourfulness value (30 in this case). Similar contours corresponding to 10 to 60 colourfulness values at 10 unit intervals were also constructed under each of the three light

sources used. In Fig. 2.2.1, the 'o', '*' and 'x' symbols represent the hypothetical points having the lightness values within the range of 0 - 35, 35 - 65, and 65 - 100 respectively. All the symbols in this diagram represent all the hypothetical points having the same perceived colourfulness of 30.

For constructing constant hue loci, the lines with constant hue (representing unique red (R), yellow (Y), green (G) and blue (B), together with equal mixtures of R-Y, Y-G, G-B and B-R), the mean visual hue result for a particular colour was initially plotted in a*b* diagrams. This is followed by carefully drawing loci by hand guided by visual interpolation, as shown in Fig. 2.2.2 for the lines marked with R (0/100), YR (12.5), Y (25), GY (37.5), G (50), BG (62.5), B (75), and RB (87.5). These hue loci are reasonably accurate due to careful selection of the samples, in which many cover the unique hues and their equal mixture areas. The neutral point of the experimental grid was placed at the origin of the a*b* diagram. This was done because the Helson - Judd (1938) effect did not seem to occur for neutral colours in the current experimental results. Many near neutral samples (varying in L*) were used under each light source. The results show that these remain neutral appearance.

The experimental grids are given in Figs. 2.2.3a to 2.2.3c for D65, A, TL84 light sources respectively, with constant L* value of 50. The cross points between constant hue loci and colourfulness contours in each grid were used to construct a set of corresponding a*b* values. These values are given in Appendix A.3. By plotting the corresponding cross points in two different grids, say D65 and A, or D65 and TL84, a pair of corresponding colours was formed. A vector between each two corresponding points was drawn. These vectors are plotted in Figs. 2.2.4a and 2.2.4b, and show the direction and magnitude of the shift in visual results from adaptation to D65, into adaptation to A and TL84 respectively. The '*' symbol represents colour appearance under light source D65 and the '+' symbol represents the same colour appearance under either A or TL84 source.

The corresponding cross points in Figs. 2.2.3 (a) and (b) and those from Luo et al.'s study (1991b) were respectively compared to reveal any difference between the two sets of results. Figs. 2.2.5a and 2.2.5b show the author's data plotted using '*' symbols and Luo et al.'s plotted using '+' symbols under sources D65 and A respectively. The TL84 source was not investigated in their study so that those were not compared. In their experiments, the OSA small glossy paint samples subtending 2^0 visual angle were used. This differs from that used in the author's study in which large samples of wool woven fabric with a size of three inch square subtending 10^0 visual angle (usually used in textile industry) were used. In addition, one sample was assessed at one time in their experiment, unlike the 30 samples judged at one time in this experiment. Furthermore, the reference sample was placed apart from the test colour in their work, but the samples were arranged to touch each other side by side in the author's work with a more complex viewing field than theirs.

2.2.3 Methods for Comparing Chromatic Adaptation Transforms

The 41 cross points of constant hue loci and colourfulness contours from the A and TL84 experimental grids (Figs. 2.2.3b and 2.2.3c) were transformed to those under the D65 light source using a particular chromatic adaptation transform. 45 corresponding a*b* vectors were derived, but four of them are out of the colour gamut of CIEL*a*b* space when using the BFD transform to predict their corresponding chromaticities from A or TL84 to D65 source. Hence, these four were removed in this study. The difference between the predicted and the D65 experimental grid data provides a measure of precision for this transform. For a close agreement between the experimental results and a particular transform, these differences should be small.

Both qualitative and quantitative methods were used in comparing the seven transforms described. For the qualitative analysis, the predicted shift for a particular transform and the corresponding experimental shift are plotted in CIE a*b* diagram. Figs.

2.2.6(a) to 2.2.6(f) show the transformation from light source A to light source D65, where the alphabetical subscripts represent transform indices, that is, (a) for von Kries, (b) for Bartleson, (c) for BFD, (d) for CIE, (e) for Hunt94 and (f) for RLAB. Similarly, Figs. 2.2.7(a) to 2.2.7(f) show the transformation from light source TL84 to light source D65. The '*' and '+' symbols represent experimental results viewed under the D65 and A or TL84 light sources, respectively. The 'o' symbol represents predicted chromaticity from one particular transform. The line between '*' and '+' represents the corresponding a*b* vectors, or expected shift, and the line between 'o' and '+' represents the predicted shift. The distance between each corresponding 'o' and '*' indicates the error of prediction. For a close agreement between experimental results and a particular transformation, the two vectors should overlap. Figs. 2.2.4a and 2.2.4b depict the qualitative performance of CIEL*a*b* transform. For a perfect agreement between CIEL*a*b* and the experimental results, each vector plotted in the two figures should have a zero length. In other words, the two corresponding colours should overlap, and become one single point. As it can be seen, such perfect agreement is not found. On the other hand, there is a clear pattern of colour shift to be found in each of Figs. 2.2.4 (a) and 2.2.4 (b), i.e., the colour shift increases as C* increases. This was also found in Luo et al.'s (1991b) study.

For the quantitative comparison, the colour difference between the 'o' and '*' points in each of Figs. 2.2.6 (a) to 2.2.6 (f) and 2.2.7 (a) to 2.2.7 (f) was calculated for each pair. Two colour difference formulae, CIEL*a*b* and CMC(1:1), were used. The mean colour difference and root-mean-square (rms) for each transform were calculated. The rms is calculated using Eq. 2.2.6 as shown below.

$$rms = [\sum_{j=1}^{N} (\Delta E_j)^2 / N]^{1/2} \qquad (2.2.6)$$

where ΔE_j is the CIEL*a*b* or CMC (1:1) colour difference for the jth pair and N represents the number of corresponding colours used. The rms seems to be a superior measure to the mean colour difference

because the former gives a better indication of the variance of the error involved.

This results in four different kinds of measure. These are the mean and rms, represented in both CIEL*a*b* and CMC(1:1) colour-difference units. For a perfect agreement between experimental results and a given transformation, all four measures should be zero. The results are summarised in Table 2.2.4 together with average ranks.

2.3 Results and Discussion

2.3.1 Constant Hue Loci and Colourfulness Contours

In Fig. 2.2.1, all symbols represent the hypothetical points having the same visual colourfulness of 30. For a perfect agreement, all these points should be very close to or on the circular contour. In fact, these points scattered very widely. The lighter colours are located outside the contour and the darker inside. This indicates that when colours having the same a*b* values but varying in L*, the lighter colours ('x' points) are perceived more colourful than the darker colours ('o' points). Similar results can also be seen in the other colourfulness plots under the three light sources used. This scatter implies that CIEL*a*b* colour space cannot fit well with the visual colourfulness results. In addition, Figs. 2.2.3a to 2.2.3c show that these grids can not overlap with each other. By comparing the grid under the light source D65 with those under A and TL84, the latter two shift towards the red (turned clockwise). This indicates that the precision of CIEL*a*b* in predicting colour appearance is unsatisfactory. Furthermore, the constant hue lines in all the three grids are not straight lines, especially for the blue contours. For a perfect agreement, these iso-colourfulness contours should be circular and be an equal distance apart. Actually, these appear to be oval and the regions of blue are more compressed. This implies that CIEL*a*b* colour space is far from an ideal uniform colour space.

2.3.2 Comparing Experimental Grids

The comparison was made between these experimental grids and those obtained by Luo et al. In Figs. 2.2.5a and 2.2.5b, each vector of the corresponding cross points represents the difference between the these experimental grids under D65 and A respectively. The colourfulness contours obtained by Luo et al. (1991b) were scaled by factors of 1.21 and 1.06 for D65 and A results respectively to bring the two sets of results onto a common visual scale. For a close agreement, each vector should be very small or with zero length. Figs. 2.2.5a and 2.2.5b show that the magnitude of each vector clearly increases as C* increases, especially for the equal mixture colours under the light source D65. The average difference between these experimental results under D65 and A sources are 6.8 and 4.1 in terms of CIEL*a*b* and CMC(1:1) units respectively. This discrepancy could be caused by different experimental conditions such as simple and complex viewing fields, glossy and textured samples, and physical sizes. The results, to some extent, agree with the previous findings of other researchers: the magnitude estimation method (the direct-scaling method) is the easiest to use to quantify colour appearance, but a larger experimental error could occur. Lam (1985) also addressed the visual results obtained from different studies of chromatic adaptation which also varied unlike those obtained from say colour difference.

2.3.3 Performance of Various Chromatic Adaptation Transforms

The performance of the transforms from adaptation to A into adaptation to D65 is first compared. These two particular light sources have been investigated by many researchers for studying chromatic adaptation. In Table 2.2.4, the rms ΔE values ranged from 6.7 to 13.9 and 4.5 to 8.9 in terms of the CIEL*a*b* and CMC (1:1) units respectively. This indicates that large differences occur between the seven transforms studied. The BFD transform gave the least error of prediction in all measures and performed the best, and

the Bartleson transform the worst. The difference between these two transforms can be clearly seen in Fig. 2.2.6 (b) (Bartleson) and Fig. 2.2.6 (c) (BFD). The BFD transform gave much smaller errors of prediction (the distances between '*' and 'o' points for each corresponding colour) than the Bartleson transform. The Hunt transform performed the second best for both measures. As shown in Fig. 2.2.6 (e), the predicted hue shifts are in reasonable agreement with those of the experimental data (slightly larger errors in the G and GY regions), and also for colourfulness prediction (but with the largest discrepancy around the Y region). The CIE and CIEL*a*b* transforms gave similar performance for the CMC(1:1) measures but not for CIEL*a*b* measures. The order of merit changed according to which colour-difference formula was used. This was mainly due to the differences between the two formulae used. The largest discrepancy between the two formulae is that CIEL*a*b* predicts larger colour differences for high chroma samples than CMC (1:1) (Luo and Rigg 1986b). Close inspection of the CIE transform (Fig. 2.2.6 (d)) shows that the predicted chroma shifts are much compressed in the YR to GY regions, leading to a large error of prediction around this area. The predicted shifts for the von Kries (Fig. 2.2.6 (a)) and RLAB (Fig. 2.2.6 (f)) transforms are very similar, and they shift only along the a* axis. The errors of predictions from both von Kries and RLAB transforms increased as colourfulness increased.

In Fig. 2.2.6 (b), the predicted shifts from the Bartleson transform are all compressed towards the a* axis. This behaviour is quite different from the other transforms. It could be closely associated with type I and type II results found by Bartleson (1978), Pointer (1982), Lam(1985) and Luo et al. (1991b). They found that different transforms are required for the prediction of corresponding chromaticities for mixed coloured light in an isolated viewing field (type I results) and for real surface colours (type II results). The Bartleson transform was derived to predict his experimental data based on the mixed light stimuli, or Type I data.

The performance of the transforms from adaptation to TL84 into adaptation to D65 was also compared. The four measures to indicate the predictive error from each transform are given in Table 2.2.4. The results indicated that the Hunt transform performed the worst according to the rms ΔE and mean ΔE units of CIEL*a*b* and CMC (1:1). As Fig. 2.2.7 (e) shows, the errors of predictions from the Hunt transform increased as colourfulness increased. The BFD transform still gave the best performance. However, the ranges of rms colour difference measures were from 4.4 to 7.7 and from 3.3 to 4.5 for CIEL*a*b* and CMC (1:1) formulae respectively, much smaller than those from adaptation to A into adaptation to D65. It was difficult to draw definite conclusions as to whether one transform was better than another. In addition, the distances between the 'o' and '*' points in Figs. 2.2.7 (a) to 2.2.7 (f) were much smaller than those in Figs. 2.2.6 (a) to 2.2.6 (f). This indicates that all transforms can have a better agreement with the visual results under TL84 than under A. In other words, if the two light sources in question have a smaller colour temperature difference, the predictive precision from different transforms would increase.

In general, as shown in Table 2.2.4, the BFD transform (average rank 1.0) gave a quite reasonable fit to the experimental grids data, especially from adaptation to A into adaptation to D65. The Bartleson transform (average rank 7.0) was the least effective. The CIEL*a*b* and von Kries (average ranks 2.0 and 2.5 respectively) had a very similar performance as did the CIE and Hunt transforms (average rank 3.0). The smallest measures of mean colour differences obtained from the best transform (BFD) in the two adapting conditions studied are around 4.2 and 3.1 respectively in terms of CMC (1:1) unit. As mentioned earlier, a large discrepancy occurred between the experimental results from the author's and Luo et al.'s studies using the same magnitude estimation technique. This strongly suggests that the BFD transform is good enough to be used in industry for predicting corresponding colours under various light sources. However, there exists a problem for the BFD transform in predicting high colourfulness corresponding colours, in which these colours

surrounding YR, Y and GY regions cannot be predicted due to negative values occurring in Eq. 1.5.64. This was not found for the other transforms. It may result from deriving the fundamental primary transformation system of its own (matrix coefficients in Eq. 1.5.64). Hence, a more reliable and accurate transform than that of the BFD is still anticipated.

2.3.4 Deriving New Chromatic Adaptation Transforms

All transforms previously tested cannot give a satisfactory prediction for chromatic adaptation. This indicates that there could still be room for further improving these transforms.

The BFD transform is a modified version of the Bartleson transform. In Fig. 2.2.6 (b), the Bartleson transform shows much more compression in almost all ranges of CIEL*a*b* colour space, and gives the worst prediction in relationship to the author's results. Although this is much improved by using the BFD transform, the BFD still has the problem in predicting high colourfulness corresponding colours around the YR, Y and GY regions. With regard to the form of the BFD model (see Section 1.5.6 (5), Eq. 1.5.65), only the Blue response is given with an exponent. This is in accordance with the non-linear form for chromatic adaptation originally proposed by MacAdam (Eq. 1.5.5) using three non-linearity coefficients, P_r, P_g and P_b, for the three independent responses, R, G and B respectively. In addition, the CIE transform recommended for further field trials by CIE also uses the similar fashion as the MacAdam transform. The new model developed here also keeps the non-linearities for the three responses.

Furthermore, the concept of noise components for the three responses originally introduced by Helmholtz was restored in the CIE transform (Nayatani et al. 1981). The noise components are independent of the test stimulus. Nayatani et al. (1981) postulated that the values of the noise components (R_n, G_n, B_n, see Eq. 1.5.15) are equal to each other in unity for the three kinds of response

mechanism. However, the Young-Helmholtz three-component theory assumes the existence of three independent cone types with different spectral sensitivities. The signals generated in these cones are transmitted directly to the brain where "colour sensations" are experienced. It may be assumed that the values of those noise components are unequal to each other with a small magnitude.

In terms of CMC(1:1) unit, the KUO1 chromatic adaptation transform was derived by minimising the colour difference between the predicted results and the visual data. The visual data included the author's experimental data and the other three sets of data: Lam and Rigg (1985), Helson et al. (1952) and Breneman (1987). The optimising technique used was the 'E04JAF' routine in the NAG Library at the Computer Centre, Loughborough University of Technology, which is an easy-to-use quasi-Newton algorithm (Gill and Murray 1976). The computation procedure of the new chromatic adaptation transform is given below.

Step 1: to transform X, Y, Z to R, G, B.

$$\begin{aligned} R &= 0.91376X + 0.30240Y - 0.13303Z \\ G &= -0.75621X + 1.74487Y + 0.01362Z \\ B &= 0.04867X - 0.04904Y + 1.04497Z \end{aligned} \qquad (2.3.1)$$

Step2: to calculate R', G', B' from R, G, B.

$$\begin{aligned} R' &= R'_0(R / R_0)^{(R_0 / R'_0)^{P_r}} + R_n \\ G' &= G'_0(G / G_0)^{(G_0 / G'_0)^{P_g}} + G_n \\ B' &= B'_0(B / B_0)^{(B_0 / B'_0)^{P_b}} + B_n \end{aligned} \qquad (2.3.2)$$

where

$$P_r = 0.01724, \quad P_g = 0.03502, \quad P_b = -0.02594,$$
$$R_n = -0.00370, \quad G_n = -0.00925, \quad B_n = -0.02317,$$

and R_0, G_0, B_0 and R'_0, G'_0, B'_0 are computed from the tristimulus values of the test and reference illuminants respectively using Eq. 2.3.1.

Step 3: to compute X', Y', Z' from R', G', B'.

$$\begin{aligned} X' &= 0.96213R' - 0.15834G' + 0.12696B' \\ Y' &= 0.42144R' + 0.51520G' + 0.04797B' \\ Z' &= -0.00686R' + 0.05541G' + 0.97913B' \end{aligned} \qquad (2.3.3)$$

The coefficients, P_r, P_g, P_b, R_n, G_n, B_n, in Eq. 2.3.2, and the constants in Eq. 2.3.1 and 2.3.3 are all optimised. The reversibility of the new transform was also examined during optimisation in terms of CMC(1:1) ΔE unit. The result showed that the exact inverse was not found for the new transform (KUO1). The reversibility performance was evaluated by comparing two sets of tristimulus values. One set under test illuminant was transformed to that under reference illuminant using a forward transform. This was further transformed back to that under test illuminant using a reverse transform. The latter transformed and original sets under test illuminant were compared. The reversibility of the KUO1 is about 0.1 of CMC(1:1) ΔE unit. This is the same as that of the BFD transform. Normally, for surface colours, if the colour difference between two colours in CMC(1:1) ΔE unit is less than 0.5, the two colours have a unnoticeable difference. This implies that the KUO1 and BFD transforms have a reasonable reversibility performance.

The KUO1 transform can be considered as a simplified version of the CIE transform, and combines the advantages of the other three transforms, CIE, MacAdam and BFD.

To compare the performance of the KUO1 transform with that of the seven transforms tested in Section 2.3.3, the KUO1 was firstly tested using the visual results of the author's study. As mentioned in Section 2.3.3, the BFD transform performed the best and gave the smallest measures in terms of mean colour differences with 4.2 and 3.1 CMC(1:1) units for A to D65 and TL84 to D65 conditions respectively. Comparing these results with those shown in Table 2.3.1, there is an improvement in the condition from A to D65 from the BFD's 4.2 CMC(1:1) units to the new model's 3.5 units while the two transforms gave the same performance in the condition from TL84 to D65. Although the improvement is limited, the prediction error from the KUO1 transform is smaller than the experimental error (4.1 CMC(1:1) units) as mentioned in Section 2.3.2. In addition, the problem for the BFD transform in predicting high colourfulness corresponding colours as mentioned in Section 2.3.3 is still remained in the KUO1 transform. However, the KUO1 can predict higher colourfulness samples surrounding YR, Y, and GY regions (C* less than around 80) than those predicted by the BFD (C* less than 70).

Figs. 2.3.1 (a) and 2.3.1 (b) show the discrepancies between the experimental shifts and the predictive shifts from KUO1 transform for adaptations from A to D65 and from TL84 to D65 respectively. In comparison with Figs. 2.2.6 (c) and 2.2.7 (c) of the BFD transform, it shows that the KUO1 gives a slightly better predictive precision than the BFD. Most distances between '*' and 'o' points for all test colours in Figs. 2.3.1 (a) and (b) are slightly closer than those in Figs. 2.2.6 (c) and 2.2.7 (c). Meanwhile, the compression given by some transforms such as the Bartleson, the CIE and the Hunt transforms is not found for the KUO1.

The other three sets of experimental data mentioned earlier (i.e. the Lam and Rigg, Helson et al. and Breneman) were also accumulated to compare the performance of the new transform KUO1 with those previously tested. The results in terms of the four measures used earlier are given in Table 2.3.2. It shows that almost all transforms had a worse prediction to fit the Breneman data than

that for the other two sets. The Bartleson transform gave the worst agreement with the Lam and Rigg's and the Helson et al.'s data. This further confirmed the difference between the Type I and Type II data. The von Kries transform had the same performance as that of the CIE with an average rank of 4.0. The result was very similar to the finding obtained in the last Section. This again confirmed that no improvement was found from the von Kries to the CIE. The results agreed well with the findings obtained by the other researchers (Bartleson 1978; Pointer 1982; Lam 1985). The result also agreed well with the finding of Luo et al.'s (1991b) study on evaluating performance of colour models using LUTCHI colour appearance data.

The BFD model gave the most accurate prediction of the transforms for the Lam and Helson et al. data. This was because the BFD transform was derived using these two data sets. The KUO1 transform derived here gave a very similar performance to that of the BFD.

The Pitt (Lam 1985; Nayatani et al. 1987) and Estèvez-Hunt-Pointer (Hunt and Pointer 1985) fundamental primaries have been widely used to derive chromatic adaptation transforms or colour appearance models by many researchers such as Fairchild (1994), Hunt and Pointer (1985) and Nayatani et al. (1987). Two new transforms were also derived using these two types of primaries separately. These have the same form as the KUO1 transform but with different fundamental primaries. The two new transforms were designated as KUO2 for Pitt primaries and KUO3 for Estèvez-Hunt-Pointer primaries respectively. The parameters for these transforms are given below:

Parameters used for the KUO2 transform are:

$$P_r = 0.00046, \quad P_g = 0.04053, \quad P_b = 0.03247,$$
$$R_n = 0.00006, \quad G_n = 0.00046, \quad B_n = 0.01133;$$

Parameters used for the KUO3 transform are:

$$P_r = 0.03665, \quad P_g = 0.04054, \quad P_b = 0.03353,$$
$$R_n = 0.00034, \quad G_n = 0.00021, \quad B_n = 0.01170 \ .$$

The Pitt fundamental primary transform is given in Eq. 2.3.4:

$$\begin{aligned} R &= \ 0.07114X + 0.94940Y + 0.01562Z \\ G &= -0.44617X + 1.31733Y + 0.09794Z \\ B &= \ 0.00000X + 0.00000Y + 0.91876Z \ , \end{aligned} \qquad (2.3.4)$$

and, the Estèvez-Hunt-Pointer fundamental primary transform:

$$\begin{aligned} R &= \ 0.40024X + 0.70760Y - 0.08081Z \\ G &= -0.22630X + 1.16532Y + 0.04570Z \\ B &= \ 0.00000X + 0.00000Y + 0.91822Z \ . \end{aligned} \qquad (2.3.5)$$

In addition, the BFD transform was also modified in a similar manner as above. It is designated as BFD2 for Pitt fundamental primaries and BFD3 for Estèvez-Hunt-Pointer fundamental primaries. The exponent P_b values for BFD2 and BFD3 are -0.01681 and -0.01229 respectively. The optimising technique and the four data sets used in deriving these new chromatic adaptation transforms were the same as those used for KUO1. The reversibility of these new transforms was also examined in terms of CMC(1:1) ΔE unit. The results also showed that these four new transforms gave almost exact reversibility performance (with about 0.1 CMC(1:1) ΔE unit).

The four data sets mentioned earlier were also used to test these new transforms. The results are summarised in Table 2.3.3. In comparison with the results of KUO1 in Tables 2.3.1 and 2.3.2, the performance of KUO2 and KUO3 was slightly improved for the Breneman data, but became worse for the other three sets of data. For BFD2 and BFD3 transforms, the performance became significantly worse in comparison with that of the BFD transform in all of the

experimental data sets. Nevertheless, it can be seen that KUO2 and KUO3 transforms can still give reasonable prediction to these data sets, and predict significantly more accurate than BFD2 and BFD3 transforms. The problem in predicting high colourfulness colours for BFD and KUO1 as mentioned earlier was not found in these new transforms. The BFD2 and BFD3 performed significantly worse than the BFD. This seemed to indicate the unsatisfaction of the form of the BFD transform.

By rearranging and averaging all four measures presented in Tables 2.3.1 to 2.3.3 (except those for adaptation from TL84 to D65 due to similar performance of all transforms obtained in this condition) for each transform, Table 2.3.4 summarises overall mean values of the four measures in terms of CIEL*a*b* and CMC(1:1) units. A further mean value of the four measures was also computed for each transform. An average of the further mean values from the three transforms, BFD, BFD2 and BFD3, was used to represent the performance of the BFD type transform. Similarly, the average from the three new transforms, KUO1, KUO2 and KUO3, represented the performance of the KUO type transform.

The results clearly showed that the KUO type transform (average rank 1.0) derived here gave a better fit to the four independent data sets of experimental data than the others tested. On the whole, the KUO type transform derived here was considered to be more reliable for predicting corresponding colours than the others at least under the viewing conditions investigated. The KUO2 transform had similar performance in predicting the four data sets accumulated to that of the KUO1 transform, and slightly better than that of the KUO3 transform. The KUO2 can also predict high colourfulness colours within YR, Y and GY regions. Hence, the KUO2 transform is more suitable for applications than the KUO1 and KUO3 transforms.

2.4 Testing Various Colour Spaces and Models

The new set of colour appearance data in terms of lightness (L), colourfulness (C) and hue (H) obtained from the author's study can also be used to evaluate the predictive performance of uniform colour spaces and colour appearance models. Three uniform colour spaces, CIEL*a*b*, CMC(1:1) and RLAB, and two colour appearance models, Nayatani and Hunt94, were investigated. The correlation coefficient (r) and coefficient of variation (CV) described in Section 2.2.1 were again used to indicate the agreement between the visual results and those predicted by the spaces and models. To compare the visual with the predicted lightness and hue results, no scaling factor (SF) was used for each colour space or model. For comparing the visual colourfulness with the predicted chroma or colourfulness, different individual SFi and mean SFm were used respectively to adjust predicted results from each space or model onto the same scale as the visual results. This was necessary for different magnitudes in the spaces and models studied. The SF was calculated using the following Eq. 2.4.1:

$$SF = \Sigma X_i Y_i / \Sigma X^2_i \qquad (2.4.1)$$

where X_i represents the predicted colourfulness or chroma from a particular space or model, and Y_i the mean visual colourfulness for the sample *i*. Tables 2.4.1 to 2.4.4 summarise the comparison results for lightness, chroma, colourfulness and hue attributes respectively. For testing space or model's colourfulness scales, only the Hunt94 and Nayatani models provide this attribute, and hence these were tested.

Colour spaces are mainly used to describe the colour difference between two stimuli. For instance, equal hue angle (ranging from 0^0 to 360^0) intervals represent approximately equal perceived hue differences. This scale is designed to quantify the hue difference, not appearance. Thus, comparing between visual and predicted hue using

uniform colour spaces is meaningless. On the other hand, the models of colour vision were designed to estimate the colour appearance hue in terms of the percentage of four unitary hues. This used the same definition as that being scaled in the visual assessment.

2.4.1 Lightness Predictions

Table 2.4.1 shows the results for comparing the five lightness scales. The r values are about 0.98 which suggests that all lightness scales for the results from D65, A and TL84 light sources are linearly related to the perceived lightness. The visual responses are plotted against the predicted results from the five lightness scales tested in Figs. 2.4.1 to 2.4.3 for sources D65, A and TL84 respectively. These figures show that the predictions by the Hunt scale are slightly darker (with a mean CV value of 16) than the visual responses while the CMC scale predicts a much lighter response (with a mean CV value of 28). The other lightness scales, CIE, Nayatani and RLAB, fit very well to the visual data with a mean CV value around 7. This was better than the typical observer's precision of 11 CV units, as found in Section 2.2.1. An attempt was also made to further modify the Hunt94 lightness scale for surface colours which will be described in Section 2.4.4.

2.4.2 Chroma and Colourfulness Predictions

As mentioned earlier, for comparing space or model's chroma predictions with visual results, a scaling factor (SF) for each space and model under each of the D65, A and TL84 sources was required, and was computed using Eq. 2.4.1. These individual SFi for each space or model and their SFm across the three sources are given in Tables 2.4.2 and 2.4.3. These scaling factors were used to adjust predicted data onto the same scale as the visual data. The final comparison was made using a mean CV value for all spaces and models respectively.

The comparison of the chroma predictions from the spaces and models shows that the predictive precision of Hunt94 chroma scale is the best, with the mean CV value of 19, which is very close to the typical observer's precision with 17 CV units for colourfulness. The RLAB colour space gave the worst agreement with the visual results, with the mean CV value of 42. Figs. 2.4.4 to 2.4.6 show the perceived colourfulness plotted against the predicted chroma by the five chroma scales investigated for sources D65, A and TL84 respectively. It can be seen that the Hunt94 model has the smallest spread while the largest spread for RLAB space under D65 and TL84 sources, and for the Nayatani model under A. Table 2.4.3 shows that the performance of the colourfulness predictions by the Hunt94 model is the same as that of its chroma scale, which is also better than that of the Nayatani's colourfulness scale. For the Nayatani model, the precision of the colourfulness scale is slightly worse than the chroma scale by 2 CV units.

2.4.3 Hue Predictions

Table 2.4.4 summarises the performance of the hue predictions from Hunt94 and Nayatani models under D65, A and TL84 sources. The results indicate that the precision of the Hunt94 hue scale is much better than that of the Nayatani's by 5 CV units. Fig. 2.4.7 shows the models' predictions plotted against visual results under the three light sources. It clearly shows that all data points under each light source are closer to the 45° line for the Hunt94 model than those for the Nayatani, especially under A source. The results demonstrate that the Hunt94 model can give satisfactory prediction of hue results for surface colours with the deviation of 9 CV units, which is close to the typical observer's precision with 7 CV units.

2.4.4 Modification to the Hunt94's Lightness Scale

The Hunt94 colour appearance model gave the best performance in quantifying colour appearance for object colours used in this study,

except for the lightness attribute. An attempt was therefore made to empirically modify this model to improve its predictive precision in quantifying lightness for object colours.

The Hunt94 model's (see Section 1.5.6 (4)) lightness scale (J) is calculated using Eq. 1.5.59, that is,

$$J = 100\ (Q / Q_w)^z,$$

where Q and z are obtained by using Eq. 1.5.56 to 1.5.58 rewritten here:

$$Q = \{7\ [A + (M/100)]\}^{0.6}\ N_1 - N_2,$$
$$N_1 = (7A_w)^{0.5} / 5.33\ N_b^{0.13},$$
$$N_2 = 7A_w N_b^{0.362} / 200,$$

and

$$z = 1 + (Y_b / Y_w)^{1/2}\ . \qquad (2.4.2)$$

where Q and Q_w are the brightness of the stimulus considered and reference white respectively. A and A_w are the achromatic signals of the sample and reference white respectively. M is the colourfulness of the stimulus. Y_b and Y_w are the luminance factors for the background and reference white respectively. N_b is the brightness induction factor. For object colours in normal scenes, N_b should be approximately equal to 75, mentioned in Section 1.5.6 (4).

It is easy to empirically modify the lightness scale of the Hunt94 model by changing the z value until a minimum of CV value calculated between the visual and predicted data was reached. For object colours, it was found that the factor z was 1.0 with an N_b value of 75. Hence, the originally suggested value for N_b was confirmed and the new z value was obtained. The comparison using the new z value was carried out. The results are r of 0.98 for all the three light sources used, and CV values of 8, 8 and 7 for sources D65, A and TL84 respectively, with the mean value of 8 CV units as shown in Table 2.4.1 under 'Modified Hunt94'. This indicated that the new z

value gave about 150% improvement in predicting lightness of the visual results obtained in the author's work.

Again, the scatter diagram between the visual and predicted data were plotted. Fig. 2.4.8 shows the visual responses plotted against those predicted by the Hunt94 model (plotted on the left) and those obtained using the modified lightness scale (plotted on the right) for the viewing conditions under D65, A and TL84 sources. It is obvious that all data points in the figures on the right are closer to the 45° line than those on the left. The results strongly suggest that the new z value 1.0 should be used instead of the original z value determined by Eq. 2.4.2 for object colours under the adapting conditions studied.

2.5 Conclusions

The Colour Constancy Study forms the first part of this work. All tasks set out in the preliminary strategy have been completed. In addition, further results were also obtained.

A set of 240 colour constancy samples covering a wide colour gamut were prepared. A series of visual experiments were conducted to quantify each colour's colour appearance in terms of the three attributes: lightness, colourfulness and hue using a magnitude estimation method under three light sources D65, A and TL84. Each colour was assessed by 5 experienced observers. Data analysis for the experimental results was carried out to investigate each individual observer's precision and repeatability performance. The results showed that the visual results were highly reliable.

Three experimental grids were constructed by constant hue contours and colourfulness loci under three light sources D65, A and TL84. Two sets of corresponding chromaticities were derived, and represented the corresponding colours of the adapting conditions from source A to D65, and from source TL84 to D65. These were used to test seven chromatic adaptation transforms. The results showed

that the BFD transform gave the best agreement to the visual results obtained from the author's study, having the predictive precision of 4.2 and 3.1 CMC(1:1) colour difference units for the two adapting conditions from A to D65 and from TL84 to D65 respectively. These magnitudes were close to, or were less than the typical experimental error of 4.1 units for the adapting condition from A to D65. These results agreed with the findings from other researchers. It implied that the BFD transform was good enough to predict corresponding colours for various adapting conditions. However, there exists a problem for the BFD transform in predicting high colourfulness corresponding colours, in which these colours surrounding YR, Y and GY regions cannot be predicted due to negative values occurred in the computation of the fundamental tristimulus values.

Efforts were made to improve the shortcoming of the BFD transform. The KUO1 transform, a simplified version of the CIE transform, was developed. Compared with the BFD, slight improvement of agreement with the author's visual results was found. The KUO1 gave more precise prediction (3.5 CMC(1:1) ΔE units) than that of the BFD (ΔE of 4.2) for the adapting conditions from source A to D65. This degree of precision was even better than the typical experimental error (ΔE of 4.1).

Another attempt to improve the performance of the KUO1 transform and the BFD was made. Four new transforms were derived, designated as KUO2, KUO3, BFD2 and BFD3 which had the same form as the KUO1 and the BFD transforms but different fundamental primaries. The KUO2 and BFD2 used the Pitt primaries while the KUO3 and BFD3 used the Estèvez-Hunt-Pointer primaries. Again, the four independent sets of corresponding colours were used to test these new transforms. The results were also compared with those from the other transforms investigated. The KUO type transform (with an average rank 1.0) gave a more precise prediction to these four sets of experimental results than the other transforms tested. The problem of predicting high colourfulness corresponding colours was not found for all four new transforms. However, the

performance of BFD2 and BFD3 became much worse than that of the original BFD transform. This confirmed the unsatisfaction of the form of the BFD transform. The results implied that the KUO type transform was more suitable for dealing with chromatic adaptation problems involving commonly encountered illuminants than the others studied. The KUO2 transform performed slightly better than that of KUO3 and without the problem in predicting high colourfulness colours. Hence, it is preferred to be used.

In addition, the colour appearance data of the author's study was also used to test three uniform colour spaces and two colour appearance models. The results showed that the Hunt94 model gave a more accurate prediction to the colour appearance data than the other spaces and model studied, except for the lightness predictions. An attempt was made to improve the lightness scale of the Hunt94 model in lightness predictions for object colours under the adapting conditions studied by using an empirical method. Finally, a z value of 1.0 for predicting the lightness of object colours was found. Using the new value of z, the precision of the Hunt94 model on lightness predictions to the author's visual results was significantly improved. This strongly suggested that the new z value 1.0 should be used in the Hunt94 model for object colours with a large viewing field.

CHAPTER 3

CHAPTER 3

METAMERISM STUDY

The importance of studying metamerism has been stated in Section 1.4. Computer recipe formulation systems are widely used. However, there are still many problems such as human factors, the disposition of experienced and conservative colourists, a too strict colour tolerance set by a conventional executive with high expectations, and insufficiency of the CIE system. One of these problems is the disagreement between the visual and instrumental assessment, and variations between observers in judging metameric pairs. This problem is associated with the weighting functions used in the recipe formulation systems that represent a standard CIE observer and a particular illuminant. However, in practice, the viewing conditions used for visual assessment, and the differences in colour vision between observers may be largely different from those defined by CIE. One of the aims of this work was to investigate the possible causes of differences between visual and instrumental assessments for metameric pairs by providing guidelines for minimising these differences in order to maximise the benefit of computer colour recipe formulation system. Most importantly, the primary goal was to investigate various methods for quantifying the degree of metamerism including illuminant and observer metamerism indices.

3.1 Experimental

For investigating the problems arising in metameric matching, metamers were prepared, which were instrumental or visual matches under a reference illuminant or source, but had a large colour difference under a second one. Visual assessment was carried out under different light sources using two scaling methods which applied a grey scale to quantify the degree of metamerism for these metamers. Furthermore, the Davison and Hemmendinger

(abbreviated D-H) Color Rule was used to test the deficiency of observers' vision.

3.1.1 Preparation of Metameric Pairs

3.1.1.1 Materials

Plain wool serge supplied by the Society of Dyers and Colourists for use in wash-fastness tests was used for preparing colour samples.

3.1.1.2 Dyes

Eleven Sandoz acid dyes were used due to their ease in application. These dyes are commonly used in industry as shown below:

	Name		
1.	SANDOLAN	YELLOW	E-2GL
2.	TECTILON	YELLOW	4R200
3	SANDOLAN	ORANGE	E-GL
4.	SANDOLAN	RHODINE	E-2GL172
5.	SANDOLAN	RUBINOL	E-3GPL
6.	SANDOLAN	VIOLET	E-2R
7.	SANDOLAN	BLUE	E-HRL
8.	SANDOLAN	BLUE	E-2GL200
9.	SANDOLAN	TURQUOISE	E-VR300
10.	SANDOLAN	BRILLIANT	GREEN E-B400
11.	LISS	SCARLET	3B

Five calibration samples were prepared for each dye using concentrations of 0.1, 0.25, 0.5, 0.75 and 1.5 % o.w.f. These samples were used for establishing a database for computer recipe formulation purposes and were measured using a Macbeth MS-2020 spectrophotometer in terms of reflectances ranging from 400 to 700 nm at 20 nm intervals. The measuring conditions were: large aperture, specular and UV included. The same set of conditions was used throughout this work. Fig. 3.1.1 shows the calibration samples for the 11 dyes used in this work plotted in CIE a*b* diagram. It

clearly indicates that these samples give a good coverage of colour space, and these dyes can produce a wide range of colours.

3.1.1.3 Dyeing Method

Ten gram pieces of plain wool serge were weighed out and pre-treated in 5 % Synperonic N for 30 minutes at boiling point. These pre-treated pieces of wool serge were then cold rinsed with water and the excess was squeezed out using a centrifuge. The materials were put into the high pressure dyeing pots of the Rapid dyeing machine using 1:15 ratio with the following recipe (o.w.f.):

x % Acid Dye	
10 c.c.	Glauber salt (10% W/W)
5 c.c.	Sulphuric Acid (5% W/W)

The dyeing pots were safely clamped onto the rotating device and dyeing started at 40 °C. The temperature was then raised to 100 °C at a constant rate for 40 minutes and boiled for 60 minutes. The dyeing pots were cooled down, and the dyed wool pieces were then taken out, rinsed in cold water and iron-dried.

3.1.2 Selection of Dye-Combinations for Preparing Highly Metameric Pairs

In order to clearly exhibit the possible problems in metameric colour matching highly metameric pairs were desirable.

About 100 glossy paint samples covering a wide range of lightness and colour were initially selected from the OSA Uniform Colour Scales (MacAdam 1974). Each colour was measured and recipes predicted using a Coats recipe formulation system. All tertiary recipes from available dyes given an exact colorimetric match to the target colour under the CIE D65 illuminant and 1964 Standard Colorimetric Observer were listed together with their CMC(2:1) ΔE values under illuminant A and source TL84. If two

recipes corresponding to a target colour showed a potential metameric pair as indicated by the ΔE values, these were dyed. Another method to produce metameric pair proposed by Badcock (1992) was also employed. The method suggested that binary shades produced using only two dyes might exhibit a high degree of metamerism. Hence, these binary colours exhibiting large degree of colour non-constancy were initially dyed. Subsequently, a three-dye colour with high colour constancy was produced to match a particular binary colour. This method was used here to produce a series of metameric pairs in the blue region under D65 because highly metameric pairs in this area are more difficult to prepare using three-dye combinations.

From these dyeings, two groups of metamers according to different matching criteria were produced. In group one, 55 *instrumental metamers* were obtained. Instrumental metamer means that a pair of samples gives very close instrumental match in terms of CMC(2:1) ΔE value under CIE D65 illuminant, but large mismatch under CIE illuminant A. For the other group, 21 visual metamers were prepared by an experienced colourist. For each pair, the recipe was iteratively adjusted and the sample was dyed until an acceptable visual match viewed under a Thorn Artificial Daylight source was reached. Each sample was then mounted in four layers on three inch square stiff white cardboard in the same way as those samples used in the Colour Constancy Study. Four layers of the sample were used so that there was no change in the measured readings beyond this thickness.

In total, 76 metamers were obtained which are plotted in CIE a*b* diagram shown in Figs. 3.1.2 and 3.1.3 for the sources D65 and A respectively. Each vector represents a pair including a standard and a batch. The open and symbol ends of each vector represent the standard and the sample of a metamer respectively. Three different symbols are used to represent three L* ranges: '*' for 60 - 80, 'o' for 40 - 60, and 'x' for below 40. These figures clearly show that these pairs cover a very wide range of lightness and colour gamut. In Fig.

3.1.2, the majority of pairs under source D65 are very close match between the standard and the sample. Most of the pairs under source A in Fig. 3.1.3 show large colour difference and shift in the red or green direction.

3.1.3 Colour Measurement

Each three inch square sample was measured using the Macbeth MS-2020 Spectrophotometer. For each sample, an average of four measurements was taken by rotating it through 90^0 between measurements. For evaluating the short-term repeatability of the MS-2020 used, the CMC(1:1) colour difference between the average and the individual measurement was calculated. The mean of the four differences was computed. Finally, the mean from all samples' differences was obtained to represent the short-term repeatability. All 76 pairs of samples were also measured three times during a two-month experimental period, and the mean value of these three measurements was used to represent colour measurement results. The long-term repeatability was examined in a similar fashion as the short-term one by replacing the previous four by these three measurements. The results are shown in Table 3.1.1. For the short term repeatability, the mean of 0.06 in terms of CMC(1:1) ΔE unit was found with a maximum of 0.23 and a minimum of 0.02. This indicates an excellent short-term repeatability and no directional effect concerning the samples used. For the long term repeatability from the three measurements with a two-month period, an average of 0.09 in CMC(1:1) ΔE unit was found with a maximum of 0.25 and a minimum of 0.01. This means good long-term repeatability, and colours being hardly changed during the experimental period. The mean reflectance values for the 76 metamers used are given in Appendix B.

3.1.4 Preparation of a Five-Step Grey Scale

A grey scale including five samples was also produced. Each sample in the scale had the same size and material as those of the metamers prepared in this Study. Several dye combinations were tried and a scale was finally obtained to give a neutral appearance and a consistent colour difference for all of the steps under the sources studied. Table 3.1.2 lists the CIEL*a*b* co-ordinates, ΔL^* and ΔE values between each sample and the 'standard' under CIE D65, A illuminants and Philips TL84 source.

The scale used was different from the standard scale used in fastness testing for assessing colour change, which was also used in the Luo and Rigg's (1987a) study. This was necessary for judging some of the metamers under source A which had larger colour differences than those exhibited in the standard scale. Hence, the ΔE value in each grade was extended. As shown in Table 3.1.2, six neutral samples (each marked with a Grade number) were produced varying in lightness except for Grade 5 having a close match to the standard (SD) colour. The measured differences increase from Grades 5 to 1. The CIEL*a*b* ΔL^* values agree almost exactly with those of ΔE values indicating that all of the samples were essentially neutral.

3.1.5 Artificial Light Sources

Initially, nine light sources were obtained and measured using a Bentham tele-spectroradiometer (TSR, as mentioned in Section 1.3.1) against a $BaSO_4$ tile with a $0^0/45^0$ illuminating/viewing geometry. Their spectral power distributions (SPD) were recorded ranging from 380 to 780 nm with 5 nm interval. These results are given in Appendix C.1. For each source, its CIE 1964 tristimulus values, x, y chromaticity co-ordinates, luminance (cd/m^2), correlated colour temperature, colour rendering index, and lamp group and type are given in Table 3.1.3. The CIE (1986) has divided the fluorescent sources into three groups: normal, broad and three bands, and twelve types: F1 to F12. Figs. 3.1.4 (a) to 3.1.4 (d) are the SPD values plotted

against the wavelength for the tungsten, the Thorn Artificial Daylight, the Thorn White Fluorescent and the Philip TL84 sources, respectively. These were selected to represent the three typical lamp groups used in this work. The commercial names of these sources will be abbreviated to A, D65, W and TL84 sources. The word 'illuminant ' is to be used only for those specified by the CIE without real sources, i.e. the CIE D65 and A illuminants.

These measured SPD were first multiplied by the functions of the CIE 1964 Standard Colorimetric Observer, and further abridged at 20 nm intervals ranging from 400 to 700 nm. These abridged weights were calculated by Luo and Lo (1992), and were used to calculate the tristimulus values from a given sample's reflectance data. These are given in Appendix C.2. For each metamer, the CMC(2:1) ΔE values were calculated for the nine sources together with the CIE D65 and A illuminants. The mean ΔE values for the instrumental, visual, and overall metamers are summarised in Table 3.1.4.

For instrumental metamers, these were specially prepared to give a close instrumental match under the illuminant D65 (a mean ΔE of 0.9) and very large ΔE values (6.0) under illuminant A. Although there were nine metamers with ΔE exceeding 1.0 unit under D65 illuminant, these still provided a good visual match under real source D65. Hence, these were included. The mean ΔE for the visual metamers was much larger than that of the instrumental metamers as expected. In total, 76 metamers were obtained and used in the visual assessment. The mean ΔE results indicated that source A gave the largest degree of metamerism; followed by P27, P30, TL83, WW, TL84, W, while CW the smallest. It was also found that for each metamer, the ΔE values calculated from the P30 and WW sources were very similar. Only the WW source was used in the experiment. (These two sources are categorised as the 'normal' type.) Finally, it was decided to use seven sources in the experiment: D65, A, TL83, TL84, P27, W and WW. These covered a wide range of colour temperatures, lamp groups and types.

3.2 Visual Assessment

3.2.1 Viewing Conditions

The visual assessments were carried out in a Verivide viewing cabinet by a panel of 13 observers using a grey scale method under seven light sources as described in the last section. Five of them were research staff, and others were research students. The five former observers had more experience in scaling colour than the others. The range of these observers' age was from 20 to 45.

Each observer was required to adapt to the experimental conditions in each session for two minutes before the actual assessments. The viewing distance was about 50 cm with an illuminating/viewing geometry about $0^0/45^0$ varied depending on the height of the observer. Each sample subtended about 10^0 at the eyes. Each sample pair was assessed twice by each observer.

3.2.2 Colour Vision Test

Detection of colour deficiency was carried out by means of the Ishihara colour chart and the City University colour vision test. The results showed that all observers had normal colour vision. In addition, the D-H Color Rule experiment by Kaiser and Hemmendinger's (1980) was also performed by each observer. The match points on the D-H Color Rule under D65, TL84 and A sources are given in Table 3.2.1. Both the lettered and numbered scales were included in the D-H Color Rule, and marked by letters from A to V and numbers from 1 to 24 respectively. These scales were further divided into two by the author. A match point, for example, judged in the half way between A and B was represented as A-B. Similarly, 4.5 represented that in the half way between 4 and 5, i.e. 4-5. The results are also plotted in Fig. 3.2.1. It is obvious that the range of match points for each light source is quite wide. The results roughly agreed with Lam and Rigg's (1985) and Kaiser and Hemmendinger's (1980) findings.

In order to quantify these ranges, the lettered scale was converted to a numerical scale using a method similar to that used by Lam and Rigg (1985) by assigning A=1.0, A-B=1.5, B=2.0, C=3.0, etc. In Lam and Rigg's study, they divided each scale into four in the form of A=1.0, A-B = 1.25, 1.50, or 1.75, B=2.0. Each match point was converted to a total score which was the sum of the two scales. Hence, a match point of numbered scale 10 and lettered scale E-F had a total score of 15.5 in the author's study. These values are also given in Table 3.2.1 under 'Total Score'. The difference between the mean total scores for two sources (say D65 and A or TL84) represented the distance between the two sources. The distance between maximum and minimum scores under each source represented the range of the observation.

The results showed that the ranges of observation in total score units were: 4.0, 4.5 and 7.0 for D65, TL84 and A sources respectively. the distances of 1.0 and 18.3 were for those between D65 and TL84 sources and between D65 and A, respectively. The results between D65 and A sources differed from the findings of the Kaiser and Hemmendinger's (1980), the Billmeyer and Saltzman's (1980) and Lam and Rigg's (1985) studies. They found that the range of observation under source D65 (which can be referred to observer metamerism) was about 3/4 for the Kaiser and Hemmendinger study, 8/9 for the Billmeyer and Saltzman study, and 1/2 for the Lam and Rigg study of the distance between D65 and A sources (as illuminant metamerism). For the author's study, the ratio is around 2/9 (i.e. 4.0/18.3). However, from the results under D65 and TL84 in the author's study, the range of observation under source D65 was much larger than the distance between the two sources, in the ratio of 4 (4.0/1.0, as observer metamerism/illuminant metamerism, for D65 and TL84). This seemed to imply that the variation of presenting observer and illuminant metamerism using the D-H Color Rule was very large. This finding agreed with those of Nayatani et al. (1985). They found that the D-H Color-Rule samples cannot be representative

for determining the relation between observer metamerism and illuminant metamerism indices.

Kaiser and Hemmendinger (1980) carried out an intensive study on the relationship between the predicted match points for 25 observer-illuminant pairs on the D-H Color Rule. The pairs were chosen from the two CIE Standard Observers (1931 and 1964) and the D series of the daylight simulators together with A illuminant and two CW fluorescents. They plotted these predicted match points by letter scale against number scale. The plot indicated that almost all the predicted match points fell very close to a straight line except for the two points falling far from that line. The two points were the predicted match points for the two CW fluorescents. Kaiser and Hemmendinger also plotted those predicted match points excluding the two points for the two CW fluorescents by total score against reciprocal colour temperature in megakelvins (MK^{-1}). Their results showed the total score on the Color Rule as a linear function of reciprocal colour temperature (MK^{-1}) of the illuminant. There was a change of 6.5 units in the total score per 100-MK^{-1} change in the illuminant. This was also confirmed by Lam and Rigg (1985). In their study, they also only used the total score results for D65 and A sources. Therefore, they all concluded that analogies could be drawn between variations of illuminant colour temperature and variations of observer Color Rule settings.

The linear relationship between reciprocal colour temperature of illuminant and the total score on the Color Rule found by Kaiser and Hemmendinger and Lam and Rigg was expected because their results were only obtained from two kinds of illuminants and sources: the daylight simulators (D series) and the tungsten lamp(A). Therefore, this linear relationship seemed to be uncertain. From their findings, the total score for TL84 source should be about 24.90, but only 14.2 was found. The total score for TL84 was slightly different from that for D65 by 1.0 unit found in the author's work, not by 6.5 units as found by Kaiser and Hemmendinger (1980), and Lam and Rigg (1985). Fig. 3.2.2 shows the total score of the author's results on the

Color Rule plotted as a non-linear function of reciprocal colour temperature in megakelvins (MK^{-1}) of illuminant. Further D-H Color Rule experiments using light sources with a wide range of colour temperatures is required to verify this finding.

3.2.3 Psychophysical Experiments for Quantifying Metamerism

Prior to the real experiment, each observer was required to attend a two-hour training session to familiarise themselves with the scaling techniques for quantifying metamerism against a grey scale. Firstly, a Munsell Book of Color was used. The author explained the colour specification employed in this system as described in Section 1.2.2. This allowed each observer to understand the three colour attributes, lightness, chroma and hue. The author also showed the difference between colour chips along each of lightness, chroma and hue axis to assist observers to realise the concept of colour difference. Subsequently, the procedures for assessing colour difference via a grey scale were illustrated. These will be described in Sections 3.2.3.1 and 3.2.3.2. Ten metamers were used in the training session under D65 and A sources. Their results indicated each observer's understanding of the scaling technique. A further explanation was required for some observers until the author was satisfied with their performance.

The experiment was divided into two parts referred to Experiments I and II according to the different scaling techniques used. Visual assessment was carried out over a six-month period using a Verivide viewing cabinet. Its background was painted with a grey matt paint with a Y value of about 12. In each Experiment, each metamer was assessed twice by ten observers. However, some observers only participated in one of the two Experiments. In total, 13 observers were used. 200 sessions were carried out, and 28880 assessments were made.

3.2.3.1 Experiment I

The grey scale method used by Luo and Rigg (1987a) was employed to scale colour difference of each metamer. Fig. 3.2.3 illustrates the sample arrangement. The samples in each metamer (marked as a 'sample pair') were interchanged (left and right) and the sequence was randomised in each observing session. The observer was asked to choose a sample from the grey scale alongside the 'STD' giving a colour difference closest to that of the metamer. Each observer was encouraged to give intermediate grades where possible. For instance, a difference of 2.2 indicated that this pair was slightly smaller than that between 'STD' and Grade '2'. This scaling technique was used in Experiment I under the seven sources investigated. The instruction for this experiment is given below.

Assessment Instructions

Given a pair of samples exhibiting a colour difference, you are going to quantify this total colour difference with the aid of a grey scale. The scale consists of a standard and five grey samples which are marked 'STD' and 1 to 5 on the back respectively. When a sample is taken from the scale to compare with the standard, a visual difference is formed. The greater the number of the sample, the smaller is the visual difference. Conversely, the smaller the number of the sample, the greater is the visual difference.

EXAMPLE: If 4 is picked to go with the standard and the colour difference from the sample pair is larger than that, you need to exchange 4 with 3 from the scale to give a bigger difference. Fine judgement is required between 4 and 3 to see whether it is nearer to 4 (smaller difference) or 3 (bigger difference). Any intermediate steps can be given, e.g. 3.8, 3.5, or 3.2 in this case. If the colour difference of the sample pair is equal to the difference of 4 and standard, then you just read out 4.

NB: 1. If you do not understand, please ask.
2. Please do not change the position of the sample pair.

3.2.3.2 Experiment II

A modified grey scale method was used. Besides assessing the total colour difference of a metamer (as used in Experiment I), each observer was further asked to judge the lightness, chroma, and hue colour-difference components in terms of percentages and descriptors. For assessing each metamer, the conductor first assigned the 'sample' and 'standard' in each pair. Each observer was asked to describe the three colour-difference components of the sample with respect to the standard using eight terms: lighter or darker, stronger or weaker, and redder, yellower, greener, or bluer, for lightness, chroma, and hue respectively. Finally, they gave the percentage for each component. A typical answer could be ' This pair has 25%, 35%, and 40% lightness, chroma, and hue differences, respectively. The sample is darker, weaker, and redder than the standard.' The sum of these three components must be 100%. The Experiment II was only conducted under D65, TL84 and A sources. The instruction for this experiment is given below.

Assessment Instructions

Each assessment is divided into two steps. Step one is to judge the total colour difference of a sample pair. Step two is to estimate the percentage of the three components resulting in the total colour difference, i.e. lightness, chroma and hue differences.

Step one: Given a pair of samples exhibiting a colour difference, you are going to quantify this total colour difference with the aid of a grey scale. The scale consists of a standard and five grey samples which are marked 'STD' and 1 to 5 on

the back respectively. When a sample is taken from the scale to compare with the standard, a visual difference is formed. The greater the number of the sample, the smaller is the visual difference. Conversely, the smaller the number of the sample, the greater is the visual difference.

Step two: The sample pair also consists of a standard and a batch samples. These will be clearly specified by the experimentist. You need to further judge the percentage of the three colour-difference components: lightness, chroma and hue. (These add up as 100%.) When assessing each component, the lightness of the batch sample will need to be judged as lighter or darker than that of the standard, stronger or weaker for chroma difference, and redder, yellower, greener or bluer for hue difference.

EXAMPLE: If 4 is picked to go with the standard and the colour difference from the sample pair is larger than that, you need to exchange 4 with 3 from the scale to give a bigger difference. Fine judgement is required between 4 and 3 to see whether it is nearer to 4 (smaller difference) or 3 (bigger difference). Any intermediate steps can be given, e.g. 3.8, 3.5, or 3.2 in this case. If the colour difference of the sample pair is equal to the difference of 4 and standard, then you just read out 4. Subsequently, quantify the percentage of the three components, which form the total colour difference. For instance, the total difference of a pair results from 40% lightness, 40% chroma and 20% hue differences. Finally, between the sample pair, judge the lightness of the batch is lighter or darker than the standard, stronger or weaker for chroma, and redder, yellower, greener or bluer for hue.

NB:
1. If you do not understand, please ask.
2. Please do not change the position of the sample pair.

3.3 Data Analysis

3.3.1 Visual Colour Difference and Mean Visual Results

Following visual assessment experiment, the mean of individual's grey scale ratings (GS) were computed. In Table 3.1.2, the grey-scale ratings are obviously not proportional to the difference seen, but their corresponding ΔE values should be. A pair with a GS value of 2 should correspond to about 200% of the visual difference for a pair with a GS value of 3 (ΔE values of 11.2 and 5.2 in Table 3.1.2). A standard curve-fitting technique was used to derive a third-order polynomial equation Eq. 3.3.1 to approximate the relationship shown in Fig. 3.3.1 between the GS and all measured ΔE values in Table 3.1.2.

$$\Delta E = 45.772 - 25.928\ GS + 5.1261\ GS^2 - 0.3518\ GS^3 \qquad (3.3.1)$$

Subsequently, the individual observer's grey scale rating (GS_i) for each pair was transformed to the individual visual difference (designated as ΔV_i) for the pair by Eq. 3.3.2.

$$\Delta V_i = 45.772 - 25.928\ GS_i + 5.1261\ GS_i^2 - 0.3518\ GS_i^3 \qquad (3.3.2)$$

As shown in Eqs. 3.3.1 and 3.3.2, the ΔV_i value has the same unit as the CIEL*a*b* ΔE or ΔL^*. The mean of ΔV_i values for each metamer was calculated to represent the mean visual results (designated as ΔV_T) for the metamer.

In Experiment II, each observer also judged three colour-difference components (lightness, chroma and hue) for each metamer. Eqs. 3.3.3 to 3.3.5 were derived to obtain each individual's visual results, ΔV_{Li}, ΔV_{Ci} and ΔV_{Hi}, in relation to the ΔV_T values:

$$\Delta V_{Li} = (f_i\, l_i^{\,2})^{1/2} \qquad (3.3.3)$$

$$\Delta V_{Ci} = (f_i\, c_i^{\,2})^{1/2} \qquad (3.3.4)$$

$$\Delta V_{Hi} = (f_i\, h_i^{\,2})^{1/2} \qquad (3.3.5)$$

where l_i , c_i, h_i are the percentages of the lightness, chroma, and hue differences for pair i ($l_i + c_i + h_i = 1$). The value of f_i is calculated using $\Delta V^2_{Ti} / (1 - 2\, l_i c_i - 2 c_i h_i - 2\, l_i h_i)$. The Eqs. 3.3.3 to 3.3.5 are obtained by solving the Eqs. 3.3.6 to 3.3.8.

$$\Delta V_{Ti} = (\Delta V_{Li}^2 + \Delta V_{Ci}^2 + \Delta V_{Hi}^2)^{1/2} \qquad (3.3.6)$$

$$\Delta V_{Ti} = [f_i (l_i^2 + c_i^2 + h_i^2)]^{1/2} \qquad (3.3.7)$$

$$l_i + c_i + h_i = 1 \qquad (3.3.8)$$

The signs of the three colour-difference components (ΔV_{Li}, ΔV_{Ci} and ΔV_{Hi}) for individual observer were decided by the descriptors. If the sample is lighter than the standard, ΔV_L is positive, or negative when the sample is darker. Similarly, if the sample is stronger than the standard, ΔV_C is positive, and weaker negative. For determining the ΔV_H component, the two samples' CIEL*a*b* hue angles in each pair were first plotted in the CIE a*b* diagram. If the sample is located in the anti-clockwise direction from the standard, ΔV_H is positive, otherwise negative. Finally, for each pair, the individual observer's ΔV_{Li} , ΔV_{Ci} and ΔV_{Hi} components were averaged to give ΔV_L, ΔV_C and ΔV_H, and a new total difference (designated as ΔV_I) was obtained using Eq. 3.3.9.

$$\Delta V_I = (\Delta V_L^2 + \Delta V_C^2 + \Delta V_H^2)^{1/2} \qquad (3.3.9)$$

On the whole, the visual results of Experiment II consist of ΔV_T, ΔV_I, ΔV_L, ΔV_C, and ΔV_H values for each pair. The mean visual results in terms of ΔV_T obtained from Experiments I and II under seven light sources are listed in Appendix D.1. The visual results in terms of ΔV_I from Experiment II under D65, A and TL84 sources are also listed in Appendix D.2.

3.3.2 Statistical Measures

In this study, many comparisons between two sets of data were made. There is a need to use a statistic measure for indicating the

agreement between the two sets of data compared. The Performance Factor (PF) developed by Luo and Rigg (1987b) was used in this study and is given in Eq. 3.3.10:

$$PF = 100\ [\gamma + V_{AB} + (CV / 100) - r] \qquad (3.3.10)$$

where r represents the correlation coefficient; CV and γ measures were proposed by Coates et al. (1973); V_{AB} was derived by Schultze (1971, 1972). The r and CV measures were described in Section 2.2.1. The γ and V_{AB} measures are given below. The PF measure combines the four statistical measures of fit (suitably weighted) into one value for ease of comparison. For perfect agreement between two sets of data, the PF should be equal to zero. The higher PF value indicates a lesser agreement between data sets. It was decided to use PF/4 in the author's study. The magnitude is similar to the percentage error, unlike PF value always giving too large values which may be larger than 100. For example, a PF/4 value of 30 indicates a standard deviation of 30% between two sets of data. For the mean of twenty observation, the standard error is therefore $30/20^{1/2}$ or 6.5% of the PF/4 value.

Gamma Factor (γ)

For visual data expressed in the form of ΔV values, the ΔE values should be directly proportional to the ΔV values. That means ΔE should equal $f\Delta V$, and $\Delta E/\Delta V$ and ln $(\Delta E/\Delta V)$ should be constant. The best f value could be calculated from the mean values of $\Delta E/\Delta V$, and the standard deviation could be used to determine the agreement between ΔE and ΔV. The logarithm of $\Delta E/\Delta V$ may well form a normal distribution (Coates et al. 1972, 1973). Hence, the standard deviation of ln $(\Delta E/\Delta V)$ can be used as the basis of a measure of fit.

$$\ln(\gamma) = \{\Sigma\ [\ \ln(\Delta E/\Delta V) - \overline{\ln(\Delta E/\Delta V)}\ ]^2 / N\ \}^{1/2} \qquad (3.3.11)$$

where $\overline{\ln(\Delta E/\Delta V)}$ is the mean value of ln $(\Delta E/\Delta V)$.

However, γ is more readily interpreted than ln γ and hence is preferred. For a perfect agreement, γ should be 1.

V_{AB}

This measure was proposed by Schultze (1971, 1972) to assess the agreement between two colour difference formulae. It was used by Strocka, Brockes and Paffhausen (1983) and is defined below.

$$V_{AB} = \{\Sigma [(\Delta E_A - F\Delta E_B)^2 / (\Delta E_A F\Delta E_B)] / N \}^{1/2} \qquad (3.3.12)$$

where

$$F = [\Sigma (\Delta E_A / \Delta E_B) / \Sigma (\Delta E_B / \Delta E_A)]^{1/2} ,$$

and ΔE_A and ΔE_B are the ΔE values for sets A and B. This equation was simply modified by substituting ΔV for ΔE_B in the present work so that the ΔE_A calculated from a particular formula and ΔV visual results can be directly compared. For visual data analysis, F equals 1.0 due to that all visual results obtained in this work were on the same scale.

The V_{AB} value corresponding to an average deviation, expressed as a fraction, between the ΔE and ΔV values. For a perfect agreement, the value should be zero. The larger the value, the poorer the formula. Very roughly, $V_{AB} = \gamma - 1 = CV / 100$.

Three examples shown in Figs. 3.3.2 (a) to (c) illustrate the PF/4 measures in relation to the typical scatters between the two sets of data, say A and B. For a perfect agreement, both sets of data would lie on the 45° line as it is assumed that the two sets of data are on the same scale. Fig. 3.3.2 (a) shows that both sets agree with each other well with a PF/4 measure of 15. Similarly, the PF/4 value is around 34 for the two data sets plotted in Figs. 3.3.2 (b) and (c). In Fig. 3.3.2 (b), two sets of data have a high linear correlation with each other, but set A results are consistently lower than those in set B (depart from the 45° line). This indicates a systematic discrepancy occurred. In Fig. 3.3.2 (c), two sets of data are located around the 45°

line, but a very large scatter can be found. This represents a large random error existing in the experimental data.

3.4 Results and Discussion

3.4.1 Barocentric Wavelengths

The cross-over wavelengths from 76 instrumental and visual metamers were examined, and the results are summarised in Table 3.4.1. Stiles and Wyszecki (1968) verified that there are at least three cross points between two reflectance curves of metameric samples. Fig. 3.4.1a shows a typical example of cross-over reflectance curves for one of the 76 metamers studied. Several researchers, Thornton (1986), Ohta (1987), and Berns and Kuehni (1990), carried out further studies to investigate the cross-over wavelengths of metameric pairs. Generally, their results showed that these three wavelengths were concentrated in three spectral regions, 430-480 nm, 500-580 nm, and 550-640 nm. Additionally, as the degree of metamerism increased, the three wavelengths converged to or near the three barocentric wavelengths 450, 540 and 610 nm. Our results agreed with the earlier findings with mean cross-overs converged around 455, 536 and 605 nm, as shown in Fig. 3.4.1b. Further examination was carried out by grouping pairs into four classes according to the degree of metamerism (using the CMC(2:1) ΔE values under the illuminant A as an indicator). The results are summarised below.

Case	Number of Samples	Mean CMC (2:1) ΔE	Converged Wavelength
Other studies			450 540 610
All pairs	76	6.1	455 536 605
$\Delta E>7$	30	9.6	455 534 604
$\Delta E>10$	13	11.6	454 531 603
The largest ΔE	5	13.5	454 529 601

The results seemed to suggest that when the metamerism increased, the cross-overs slightly moved away from those

barocentric wavelengths. This was particularly marked for the longer wavelengths, 530 nm and 600 nm. This tendency was similar to that found by Berns and Kuehni (1990). Nevertheless, more experimental results are required to verify this.

3.4.2 Observer Variations

Various analyses were carried out to investigate observer variations. The first analysis aimed to establish the typical observer precision. In the experiment, each metamer was assessed twice by ten observers for a particular source, i.e. twenty observations in total. For each source, the results from each observation for all 76 pairs were compared with those of the mean visual results using the PF/4 measure. Each observer's two PF/4 measures were then averaged to represent his or her precision performance. The mean measure for each observer is listed in Tables 3.4.2 (a) and 3.4.2 (b) for Experiments I and II respectively. The results showed that a typical observer precision was 29 ranging from about 20 to 40 of PF/4 measure. The experimental sequence was followed those in Tables 3.4.2 (a) and 3.4.2 (b) from left (D65) to right (P27 and TL84 respectively). There is a tendency for some observers, such as RL, YU, LI, GR, TY, HN and WK, to improve their precision through experience. The mean measure for each observer across all sources was also calculated and ranked according to their performance. Furthermore, it showed that all observers had larger variations for D65 source than the other sources. The experiment carried out under D65 of Experiment II was conducted after the completion of Experiment I. The D65 results again showed the largest observer variation. This implied that all metamers intended to match under the D65 source had a large observer metamerism effect. Fig. 3.4.2 gives examples which are the worst (a) and the best (b) cases of observer precision under A source in the two Experiments. The worst case seems to result from both systematic discrepancy (prediction too high compared to that for mean results) and random error (large scatter of data points).

Within Observer Error was also analysed by calculating the PF/4 measure between each observer's repeated results for each source. The average measure for each observer under all sources is given in Tables 3.4.3a and 3.4.3b for Experiments I and II respectively representing individual's repeatability performance. In comparison with the observer precision results in Tables 3.4.2a and 3.4.2b, the repeatability results were slightly larger, but each observer had very similar rank in both cases. Again, it was found that observer's repeatability improved when more experiments were carried out. In addition, Fig. 3.4.3 shows the worst (a) and the best (b) situations of observer repeatability under A source between Experiment I and Experiment II. The worst situation seems to also involve both systematic discrepancy and random error.

Between Observer Error was also examined by comparing each individual's and the other observers' results. Again, the average measure for each observer under all sources is given in Tables 3.4.4a and 3.4.4b for Experiments I and II respectively representing individual's between-observer performance. Compared with observer precision and individual repeatability, the between-observer variation were the largest, but each observer still had very similar rank to those in the former two cases. Again, it was found that between-observer variation improved by having more experience for those observers mentioned earlier. Fig. 3.4.4 exhibits examples for the worst (a) and the best (b) agreement between observers under TL84 in Experiment II. The worst case seems to result mainly from systematic discrepancy.

All observer's mean PF/4 values were averaged for each source in both Experiments. These are summarised in Table 3.4.5 including the three types of observer variations described above. The PF/4 values found here indicated that the typical experimental errors were 29, 32 and 37 for observer precision, within-observer and between- observer, respectively. This degree of error was considered to be quite reasonable and was similar to those found in Luo and Rigg's (1986a, 1987a) study. It also established a basis in which a

reliable index of metamerism has to meet the same or greater degree of precision in predicting the experimental data.

Another analysis was also made for the results of the three colour-difference components (ΔV_{Li}, ΔV_{Ci} and ΔV_{Hi}) in Experiment II by using correlation coefficient (r) and wrong decision (WD%). The measure of wrong decision was proposed by McLaren (1970). Here, a modified method for computing the value of wrong decision was used. As mentioned in Experiment II (see Section 3.2.3.2), each observer was asked to describe three colour-difference components (ΔV_L, ΔV_C, ΔV_H) of the sample with respect to the standard, in terms of lighter or darker, stronger or weaker, and redder, yellower, greener, or bluer for lightness, colourfulness and hue respectively. Here, for the values of ΔV_L and ΔV_C,, if the sample was judged lighter and stronger than the standard, these values would be defined as positive. On the contrary, the values would be negative. If there was no difference perceived, the values would be zero.

For the value of ΔV_H, if the co-ordinate of the sample 'o' in the CIE a*b* diagram is anticlockwise to that of the standard 'x' as shown in the figure below, the value would be noted as positive. Conversely, this value would be negative. Similarly, if the sample has the same hue as that of the standard, i.e. no difference in hue between the pair of samples, the value would be zero.

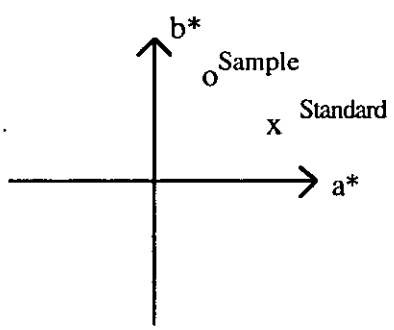

The WD% for a particular metamer was determined by subtracting the largest percentage out of 20 observations for one of the three signs (positive, zero, negative) of each of the three colour-

difference components from 100. For example, if 60% of observations judging the lightness colour-difference component (ΔV_L) is positive, the value of 40% would be the WD%. If the largest percentage 40% is for positive, the value of 60% for both negative and zero decisions would be the WD%. Similarly, if 50% is for positive, 50% would certainly be the WD%. For a perfect agreement between observers, the mean WD% value for the 76 metamers used should be zero, and the correlation coefficient should be unity. The results are summarised in Table 3.4.6.

The values of WD% under A and TL84 sources for ΔV_C and ΔV_H components are smaller than those under D65 source and those for ΔV_L under all the three sources due to larger colour differences for each metamer in chroma and hue occurring under the two sources (A and TL84). In general, each metamer had a small lightness difference. In addition, because all metamers were intended to match under D65, observers gave larger visual wrong decision under this source than that under the other two sources. This implied that a large observer metamerism effect occurred under D65 source. Furthermore, the mean values of WD%, 30, 20 and 9 for ΔV_L, ΔV_C and ΔV_H respectively, indicate that observers can more easily identify a hue difference for each metamer than chroma and lightness differences under the three light sources studied. In general, the same tendency can be found using the measure of correlation coefficient (r).

The final analysis was to compare the mean visual results (ΔV_T) from the Experiments I and II. The PF/4 values are 11, 9 and 7 for sources D65, TL84 and A respectively. The plots for the two sets of experimental results under the three sources are given in Figs. 3.4.5 (a) and 3.4.5 (b). The agreement is considered to be very satisfactory. The same comparison was also made for the total ΔV_T (obtained by averaging the two ΔV_T results of both Experiments I and II) and the ΔV_I results of Experiment II. There is a systematic trend that the total ΔV_T data are larger than the ΔV_I data by a factor about 1.2 as shown in Fig. 3.4.5 (b). This is caused by the methods to compute the

ΔV_1 results. (When observers gave the disagreement on descriptors (say lighter or darker), the sum from all observers' results used to calculate the mean result would be reduced.) However, the difference is very small.

3.4.3 Comparison of Illuminants and their Corresponding Light Sources

As mentioned in Section 3.1.5, for computing the tristimulus values under the seven sources investigated, weighting functions were calculated from the spectral power distribution (SPD) measured by a TSR. In addition, the weighting functions computed using the SPD of the CIE D65 and A illuminants were also used together with those published by the ASTM (CIE 1987) for the TL84 (or F11) source. All these weights were further abridged to correspond to wavelengths ranging from 400 to 700 nm with a 20 nm interval using the interpolation method developed by Luo and Lo (1992).

For each metamer, its colour differences were calculated using four colour difference formulae (CIEL*a*b*, CMC(1:1), CIE94 and BFD(1:1) under the seven sources studied. In addition, the colour differences under the CIE D65, A illuminants and TL84 source (using ASTM weights) were also calculated. The PF/4 measure was used to indicate the agreement between the ΔV and ΔE values from a particular formula. These results are summarised in Table 3.4.7. The results show a large variation in PF/4 values between different weighting functions used. The ASTM's TL84 weights agreed with visual results slightly better than those calculated from the real source for all colour difference formulae tested. However, the weights calculated from D65 and tungsten (A) sources give more precise prediction to the visual results than those from the CIE illuminants. In particular under D65 source, the PF/4 values for real source were markedly better than those for the CIE illuminant by a factor about 1.5. Fig. 3.4.6 shows the ΔE values obtained using the weighting functions of D65 CIE illuminant (left) and real source (right) for the CIEL*a*b*, CMC(1:1), CIE94 and BFD(1:1) (from top to

bottom) plotted against the ΔV values. It shows that the scatters on the left diagrams are larger than those on the right for each formula. This implied that in order to get closer instrumental and visual agreement for assessing metamers, the weighting functions corresponding to the real light source should be used at least for D65 source, which is frequently used as the reference source.

3.4.4 Testing Illuminant Metamerism indices

As mentioned in Section 1.4.3, three types of illuminant metamerism indices (abbreviated as **IMI**) in terms of colour difference for each metamer were tested using the author's experimental results. The results are given in the following Sections.

3.4.4.1 Type I IMI

Four colour difference formulae, CIEL*a*b*, CMC(1:1) , BFD(1:1) and CIE94, were used to test their performance in predicting visual results. The latter three are the modified versions of CIEL*a*b* which imbed the capability of chromatic adaptation by specifying the tristimulus values (X_n Y_n Z_n) for a particular light source. The appropriate X_n Y_n Z_n values for each illuminant or source were used to calculate ΔE values. The PF/4 measure was again used to indicate the agreement between the ΔE and ΔV values. However, the magnitudes of the ΔE and ΔV values were on different scales. Thus a scaling factor was required to adjust ΔE values calculated from a particular colour difference formula onto the same scale as the ΔV values. (Similar to those mentioned in Sections 2.2.1 and 3.3.2, the PF/4 measure combines four statistical measures: correlation coefficient (r), coefficient of variation (CV), V_{AB} and γ. For calculating CV and V_{AB} , scaling factors are required, but not for r and γ.) For each light source studied, the predictive performance in terms of the PF/4 measure from four formulae is given in Table 3.4.7 together with results of observer precision.

It was obvious that the three formulae CMC, BFD and CIE94 gave very similar performance (with mean PF/4 values ranging from 28 to 30) and outperformed the CIEL*a*b* formula (see Table 3.4.7). It was also found that the CIE94 formula gave the most precise prediction to the source A results. It was encouraging that the precision from these three formulae was even higher than the typical observer precision except for D65 source.

As mentioned above, to adjust the ΔE values onto the same scale as the ΔV values of Experiments I and II, scaling factors were calculated using Eq. 2.4.1 for the four colour difference formulae investigated. These scaling factors are listed in Table 3.4.8. A mean scaling factor (abbreviated as MSF) was computed for a particular colour difference formula. Again, the same testing procedure was made for evaluating the four colour difference formulae by comparing the adjusted ΔE values (by MSF) with the visual results from both Experiments respectively. As shown in Table 3.4.9, each colour difference formula gave a very similar performance to that by using original ΔE values. The three formulae CMC, BFD and CIE94 gave very similar performance, and outperformed the CIEL*a*b* formula. They all gave a satisfactory prediction of the visual results under all sources except for D65.

Fig. 3.4.7 shows the ΔE values calculated using the CIEL*a*b*, CMC(1:1), CIE94 and BFD(1:1) (from top to bottom), and plotted against the ΔV results for sources A, TL84, TL83, W, WW and P27 (from left to right) respectively. (For each formula, its ΔE values were adjusted using MSF in Table 3.4.8 for all light sources.) It can be seen that the scatters from the CIEL*a*b* formula are much larger than those of the other three formulae under all these light sources. The scatters for the other three formulae are all very similar lying around the 45^{o} line. This suggests that these three formulae should be confidently used to quantify the degree of metamerism in industrial applications. All formulae badly predicted the D65 experimental results (see Fig. 3.4.6, with an average of PF/4 of 41) in comparison with those of the other sources (see Fig. 3.4.7, with an

average of 25). This discrepancy is caused by a larger degree of observer metamerism under the D65 source than the other sources. (The metamers in the author's study were prepared to give a close match under the D65 light source.)

The results obtained from Experiments I and II shows a very good agreement. As it can be seen in Tables 3.4.7 and 3.4.9, the PF/4 values for both experiments are very similar. This further confirms that the author's results are highly reliable.

3.4.4.2 Type II IMI

Metamerism is defined as a property of a pair of spectrally different colours having the same tristimulus values under a set of viewing conditions in the CIE International Lighting Vocabulary (CIE 1987). In practice, this limitation on equal tristimulus values never occurs. The CIE (1986) recommends that a suitable correction should be made to calculate illuminant metamerism index with the pair considered exactly matching under reference source. The type II IMI applies an additive correction where the colour difference existent in the reference source is subtracted from the difference in the test source. For example, the lightness, chroma and hue differences between a pair of samples under the test and reference sources expressed as ΔL, ΔC and ΔH. (These differences could be either calculated from a particular colour difference formula or the visual results in Experiment II.) The Type II IMI can be computed by using Eq. 3.4.1:

$$\text{Type II IMI} = (\Delta L^2 + \Delta C^2 + \Delta H^2)^{1/2}, \qquad (3.4.1)$$

where

$$\Delta L = \Delta L_2 - \Delta L_1,$$
$$\Delta C = \Delta C_2 - \Delta C_1,$$
$$\Delta H = \Delta H_2 - \Delta H_1,$$

where

ΔL_1: the visual or measured ΔL values under reference source.

$\Delta L2$: the visual or measured ΔL values under test source.

$\Delta C1$: the visual or measured ΔC values under reference source

$\Delta C2$: the visual or measured ΔC values under test source.

$\Delta H1$: the visual or measured ΔH values under reference source.

$\Delta H2$: the visual or measured ΔH values under test source.

An example for computation is given below:

	ΔL	ΔC	ΔH
Reference	1.0	1.5	2.0
Test	-1.0	1.5	-2.0
Difference	-2.0	0.0	-4.0

Type II IMI: $\sqrt{2^2 + 0^2 + 4^2} = 4.5$

For lightness difference, the sample is judged lighter than standard by 1 unit under the reference source, but darker by the same amount under the test source. Thus the corrected lightness difference between the two sources is doubled. Similar corrections apply to chroma and hue differences. The resultant metamerism index in this case is 4.5, which is much larger than the total colour difference of 2.7 under each source.

Only Experiment II results were used to test Type II IMI. Experiment I does not include the results of the three individual colour-difference components (ΔL_V, ΔC_V and ΔH_V). Again, four colour difference formulae were employed. The additive correction method was used to make zero colour difference under D65 source for both the instrumental and visual results. The results are given in Tables 3.4.10a to 3.4.10c. In general, Type II IMI gave a similar performance in predicting results under source A, but worse for those under source TL84 in comparison with those of Type I IMI.

This indicates that Type I IMI is sufficient in predicting visual results, or the additive correction is unnecessary.

3.4.4.3 Type III IMI

Colour difference formulae have been developed almost entirely on work carried out under daylight sources and may be inaccurate when used under the other light sources. The concept of corresponding chromaticities, required to maintain the same colour appearance when changing from one adapting light source to another, was used here. Type III IMI involves two stages: it initially employs a chromatic adaptation transform to obtain the corresponding tristimulus values of metamers under test source to those under reference source, and then to calculate the ΔE value for the metamers using the corresponding tristimulus values under reference source as an indicator of the degree of illuminant metamerism.

Eight chromatic adaptation transforms were tested, von Kries, Bartleson, CIE, BFD, Hunt, CIEL*a*b*, RLAB, and the KUO type transform developed in the last Chapter. The PF/4 measure was calculated between the ΔE values calculated from one of the four colour difference formulae under D65 source and the ΔV values for the test source in question. The ΔE values for each formula under each source were adjusted by single SF, not MSF. These PF/4 values are summarised in Table 3.4.11.

Table 3.4.11 summarises the results in terms of PF/4 values for all the sources investigated. The results showed that in general, there was not much performance difference between all the transforms tested. In most of the cases, no matter what colour difference formula used, the CIEL*a*b* chromatic adaptation transform gave a more accurate prediction of the visual results. It must be noted that for each colour difference formula, the ΔE value calculated from Type III IMI applying the CIEL*a*b* chromatic adaptation transform is equivalent to that from Type I IMI. This is because the colour

difference formulae tested are either the original or the modified version of the CIEL*a*b*, i.e. the same chromatic adaptation mechanism is applied to all formulae. It was surprised that the Bartleson transform, which gave the worst prediction to the author's data obtained from the Colour Constancy Study, fitted the best to the visual results under sources W and WW in the Metamerism Study. The KUO type transform did not perform as well as the CIEL*a*b* and Bartleson transforms. The KUO1 transform gave a slightly better fit to the visual results than KUO2 and KUO3, and had the same performance as BFD transform. In Luo and Rigg's (1987c) study, they tested the performance of various combined chromatic adaptation transform/colour difference formula such as that of Type III IMI using their combined illuminant A colour difference data set (over 1000 pairs). Their results clearly indicated that to include chromatic adaptation transform performed better than that only using colour difference formula. This was opposite to the author's results. This implied that chromatic adaptation transform was effective to predict change of colour difference under different light sources for pairs with high colour constancy (as included in the Luo and Rigg's combined illuminant A data), but not for metameric pairs (as produced in the author's study).

In conclusion, the Type I IMI outperformed the other IMIs, and can give reliable results in predicting the degree of metamerism.

3.5 Observer Metamerism

Observer metamerism is one of the four types of metamerism as mentioned in Section 1.4. It is related to the variation of assessment on colour matches perceived by different actual observers for a metamer that match under specific conditions such as a reference observer and a particular illuminant. Hence, observer metamerism is defined by the CIE (1987) as 'Variations of colour matches (of spectrally different stimuli) amongst different observers'.

In the last section, illuminant metamerism and three types of IMI in terms of colour difference were discussed. The results showed that according to the mean values of PF/4 measure under all the illuminants and sources used, the three colour difference formulae (CIE94, CMC(1:1) and BFD(1:1)) had a similar performance. Each of the formulae can be used as a reliable illuminant metamerism index, and gives lower predictive variation than the typical observer precision (say 29 in PF/4 measure) under all illuminants and sources except for D65. Under D65 illuminant or source, the three colour difference formulae produced a worse performance than those under the other sources. The reason, as mentioned in the last Section, may be because each metamer was prepared for the purpose of instrumental or visual matching under illuminant D65. For the 76 metamers used in the author's study, the mean ΔE under D65 source is 1.4 CMC(2:1) ΔE units (see Table 3.1.4), which is at least 250% smaller than that of the other sources. If observer metamerism is as marked as illuminant metamerism, the individual observer should have seen large difference across all the sources investigated. Hence, the individual grey scale ratings under D65 source should have been larger than those recorded. This was not found to be the case. This indicates that observer metamerism is much less than illuminant metamerism. The effect of observer metamerism is larger under D65 source than that under other illuminants and sources, and could have a significant impact in applications such as the matching work concerned with minimising the colour difference, or involved with a large amount of metamerism (image across different media). Therefore, there is a need to indicate the expected range of observer metamerism.

Although the CIE (1989) recommended a standard deviate observer (SDO) which was based on Nayatani et al.'s (1983, 1985) studies on observer metamerism, this has not been widely used in practice. The SDO was originated by Allen (1970), defined as an observer would have a set of colour-matching functions which differ from those of the standard observer by $\Delta\bar{x}_i(\lambda)$, $\Delta\bar{y}_i(\lambda)$, and $\Delta\bar{z}_i(\lambda)$,

where these quantities are the standard deviations of the colour matching values among a group of normal observers. In other words, the SDO represents a typical observer besides the CIE Standard Colorimetric Observer. The CIE (1989) recommended the calculation of colour differences based on a uniform colour space such as CIEL*a*b* for metamers using the CIE SDO to express the degree of observer metamerism.

The CIE SDO was derived by choosing 20 observers selected from Stiles' data of fifty three observers (Nayatani et al. 1983; Wyszecki 1969; Wyszecki and Stiles 1982). In addition, their experiment was to match coloured lights, not surface sample pairs. However, as elicited by North and Fairchild (1993a, 1993b) and Rich and Jalijali (1995), their results showed that the range of the observer differences was many times larger than that of the CIE SDO. They also suggested that the full set of fifty three Stiles observers should be used to derive a more general index of metamerism for change in observer. This implies that the CIE SDO derived by using the results obtained from part of the same group of observers is unlikely to represent the real observer. It was decided to derive a new set of colour-matching functions to represent the average observer used in the author's study. The new set of colour-matching functions can be considered as a new SDO.

3.5.1 Methods for Deriving SDO

Observer metamerism studies were reviewed by Nayatani et al. (1983). For the methods used to derive SDO, a brief survey is given below.

The studies on observer metamerism can be divided into two series. One included the studies based upon colour-matching functions of observers with normal vision (Wyszecki 1969; Allen 1970; Strocka 1978; Nayatani et al. 1983, 1985; Ohta 1985). Wyszecki (1969) proposed an index of observer metamerism using Stiles's 20 colour-matching functions (Wyszecki and Stiles 1982). His

index was given by an average of all the colour differences computed for a metameric pair by changing a reference observer (an average of the 20 colour-matching functions) to each of 20 observers. In practice, this method is inconvenient due to the large amount of data required and the number of laborious computations necessary. Allen (1970) also suggested a test observer called, 'standard deviate observer', derived using a statistical analysis based on variances and covariances of Stiles's twenty colour-matching functions. He replaced the twenty observers by one standard deviate observer. His observer metamerism index was calculated using a colour difference found only by changing the observer from the reference to the test for a pair of samples. Strocka (1978) suggested that using two selected colour-matching functions from Stiles's 20 observers to predict the average observer-metamerism index was better than using the SDO proposed by Allen.

Nayatani et al. (1983, 1985) also assumed that the Stiles's 20 observers were a representative of a population of observers with normal vision. They pointed out that the observer metamerism index using Allen's SDO did not give a good correlation with Wyszecki's average observer-metamerism index. Nayatani et al. then proposed a new SDO using the 'singular-value decomposition' technique. Ohta (1985) also developed an SDO using Stiles's 20 colour-matching functions in the CIEL*a*b* and CIEL*u*v* spaces. He concluded that his SDO and Nayatani et al.'s were much the same though the two SDO were derived via different methods. Both SDOs gave an equally good prediction of observer metamerism. At a later stage, the SDO derived by Nayatani et al. was recommended by the CIE (1989) for field trials.

The second series included the experiments conducted by Kaiser and Hemmendinger (1980), and Billmeyer and Saltzman (1980). In their studies, colour-matching experiments were conducted using the D-H Color Rule assessed by a panel of 59 observers. Their ages ranged from 17 to 60 (for Kaiser and Hemmendinger's study), and 72 observers (for Billmeyer and Saltzman's study). Nayatani et al.

(1985) found that there was a large difference between the two series of studies (using the Stiles's twenty observers and the D-H Color Rule respectively) in terms of the ratio between observer-metamerism index and illuminant-metamerism index between illuminants D65 and A. Using Stiles's 20 observer data, the observer metamerism index was relatively small compared to the illuminant metamerism index, i.e. the average observer-metamerism index was about 1/9 of the illuminant-metamerism index in CIEL*a*b* unit when 12 metamers were used. (Each of the 12 metameric pairs consists of a standard neutral grey with a reflectance of 30% for all wavelengths across spectrum and one of the 12 metameric greys derived by Wyszecki (1962) and modified by Takahama and Nayatani (1972) to provide colour matches under illuminant D65 and the CIE 1931 Standard Colorimetric Observer.) On the contrary, the observer-metamerism index was almost equal to the illuminant-metamerism index when the experiments were conducted using the D-H Color Rule. Nayatani et al. (1985) reanalysed Kaiser and Hemmendinger's (1980) results, and found that there was a significant observer variation within the data. Nayatani et al. (1985) then concluded that the results from the Color Rule experiments are not representative for determining the relation between observer-metamerism and illuminant-metamerism indices. The relation changes according to what metamer being used.

In order to verify the CIE SDO, it was decided to derive an SDO using the average results conducted from the author's experimental results, in which scaling method, mode of colour and groups of observers were largely different from those in Stiles's experiment. The fact that the similarity between the Ohta's results and the Nayatani et al.'s (1983) is expected because both used the Stiles's 20 observers' colour-matching data, and the majority of difference in their studies lies only in the computation methods. This has been confirmed with those of North and Fairchild's (1993a, 1993b), and Rich and Jalijali's (1995) studies. They used different experimental methods and different groups of observers, but found significant inter-observer variations, which was much larger than those

obtained from Nayatani et al.'s (1983, 1985) and Ohta's (1985) studies.

3.5.2 Deriving a New SDO

In this section, the author used a non-linear optimisation technique to derive a new SDO. The method is similar to that employed by Ohta (1985).

Ohta derived his SDO by minimising the difference between the colour difference calculated using the optimised SDO and the mean colour difference calculated from each of the 20 colour-matching functions from Stiles's observers. Two colour difference formulae were used, CIEL*a*b* and CIEL*u*v*. The minimised objective function (F) is given in Eq. 3.5.1:

$$F = F_{uv} + F_{ab}, \tag{3.5.1}$$

with

$$F_{uv} = 1/N \sum_{j=1}^{N} (\Delta E_{uvj} - \Delta \bar{E}_{uv\,j})^2, \tag{3.5.2}$$

$$F_{ab} = 1/N \sum_{j=1}^{N} (\Delta E_{ab\,j} - \Delta \bar{E}_{ab\,j})^2, \tag{3.5.3}$$

where

$$\Delta \bar{E}_{uv\,j} = 1/20 \sum_{i=1}^{20} \Delta E_{uv\,i}\ ,\quad \Delta \bar{E}_{ab\,j} = 1/20 \sum_{i=1}^{20} \Delta E_{ab\,i}\ ,$$

where N is the number of metamers. The ΔE_{uvj} and $\Delta E_{ab\,j}$ values are the colour differences for the jth metamer predicted by the optimised SDO. The $\Delta E_{uv\,i}$ and $\Delta E_{ab\,i}$ values are the colour differences for the metamer calculated using the ith colour-matching functions, and the $\Delta \bar{E}_{uv\,j}$ and $\Delta \bar{E}_{ab\,j}$ values are the mean colour difference for the metamer obtained from the twenty colour-matching functions. The metamers were obtained using a linear-programming technique (Ohta 1982). Ohta, firstly, defined 89 target colours in terms of chromaticity co-ordinate x, y, Y values. For each colour, he then

generated 15 different reflectance functions. The 15 reflectance functions represented 15 colours having the same chromaticity co-ordinate x, y, Y but different reflectance curves. These 15 colours formed a set of colours. For each target colour, 105 (= $_{15}C_2$) metameric pairs were obtained. In total, 9345 (105 x 89) metamers were used in the optimisation

Ohta used the same group of 20 observers selected from Stiles's 53 observers as those used by Nayatani et al. It was expected that Ohta's SDO was much the same as Nayatani et al.'s, and was little different from the CIE 1964 Standard Colorimetric Observer which was based on Stiles's 53 observers.

As mentioned earlier, it was necessary to verify this by deriving a new SDO based on the results from different groups of observers and different experimental methods. The work carried out here used a non-linear optimisation technique similar to that used by Ohta, but was based on CMC(1:1) ΔE unit and the author's visual results. The objective function F used is given in Eq. 3.5.4:

$$F = 1/N \sum_{i=1}^{N} (\Delta E_{CMC(1:1),\, i} - f \Delta V_{I,\, i})^2, \qquad (3.5.4)$$

where N is the number of the 76 metamers used in this work. $\Delta E_{CMC(1:1),\, i}$ is the colour difference computed for the ith metamer using the CMC(1:1) colour-difference formula with the new SDO. By assuming CMC formula gives a close agreement to visual difference perception, these ΔE values can be treated as a set of the mean visual results from one group of observers, while ΔV_I are those from the author's study. There is no particular reason to select ΔV_I, not ΔV_T due to a good agreement between these two data sets as mentioned in Section 3.4.2. The f value is a scaling factor, and equals 1.0 in this case because the total average of scaling factor for CMC(1:1) under the illuminants and sources studied is about 1.0 (see Table 3.4.8). A similar procedure could be used with the other colour difference formulae together with different scaling factors respectively. The ΔV_I

results are those obtained from Experiment II D65 results as described in Sections 3.3.1. (The D65 results were used due to these metamers given a close match under this source. Hence, observer metamerism is mainly responsible for the visual colour difference. The visual colour differences obtained from the other sources were mainly due to illuminant metamerism.)

The values of the CIE 1964 colour-matching functions were used as the initial values in the non-linear optimisation which was implemented by using the 'E04JAF' routine in the NAG Library supported by the Computer Centre, Loughborough University of Technology. As mentioned in Section 2.3.4, this routine applies the quasi-Newton algorithm (Gill and Murray 1976). Finally, a set of colour-matching functions $\bar{x}'(\lambda)$, $\bar{y}'(\lambda)$, $\bar{z}'(\lambda)$ were derived and can be considered as a new SDO. The differences between the CIE 1964 colour-matching functions and the new SDO are given in Table 3.5.1 and calculated as follows:

$$\begin{aligned} \Delta\bar{x}'(\lambda) &= \bar{x}'(\lambda) - \bar{x}_{10}(\lambda), \\ \Delta\bar{y}'(\lambda) &= \bar{y}'(\lambda) - \bar{y}_{10}(\lambda), \\ \Delta\bar{z}'(\lambda) &= \bar{z}'(\lambda) - \bar{z}_{10}(\lambda). \end{aligned} \qquad (3.5.5)$$

These can be used to test the illuminant metamerism indices employed in this work, and compared with those calculated using the CIE SDO. These are discussed in the following two Sections.

3.5.3 Comparing the New SDO with the CIE SDO

As described in the last section, a new SDO was derived using a non-linear optimisation method. In Fig. 3.5.1, the new SDO is plotted using a 'o' symbol together with the CIE 1964 Standard Colorimetric Observer using a 'Δ' symbol. It can be seen that the main difference between both observers is on the red and green responses, i.e. between the $\bar{x}'(\lambda)$ and $\bar{x}_{10}(\lambda)$, and $\bar{y}'(\lambda)$ and $\bar{y}_{10}(\lambda)$ functions. These results could be associated with the property of one of the samples in

each metamer (non-colour-constant sample) which always exhibits some trace of red or green when viewed under D65 source. The differences between the newly derived SDO and the CIE 1964 Observer are plotted in Fig. 3.5.2 using 'o' symbols. Similarly, those between the CIE SDO and the CIE 1964 Observer are also plotted in Fig. 3.5.2 using 'Δ' symbols. It is obvious that the new SDO has a much larger deviation to the CIE 1964 than that of the CIE SDO.

3.5.4 Effect of the New SDO and the CIE SDO on IMI

As mentioned in Section 3.4.4, Illuminants Metamerism Indices (IMIs) were unable to give satisfactory performance in predicting the visual results under D65 source. A new SDO was derived from this particular set of data. Here, the same testing procedure as that for evaluating Type I IMI was carried out except for calculating tristimulus values using the new SDO or the CIE SDO instead of the CIE 1964 colour-matching functions. The results in terms of PF/4 measure are summarised in Table 3.5.2.

It clearly showed that the new SDO gave an overall better agreement between the ΔE values calculated from all colour difference formulae and the visual results from all sources studied than that by the CIE 1964 colour-matching functions. The largest improvement (about 160% smaller in PF/4 values) was for the D65 data as expected, and about 20% improvement for the results from the other sources. In addition, all indices except CIEL*a*b* gave the predictive variation under each light source lower than the typical observer precision (the PF/4 value of 29) found in this work. Fig. 3.5.3 shows the ΔE values calculated using the new SDO for the CIEL*a*b*, CMC(1:1), CIE94 and BFD(1:1) (from top to bottom) plotted against the visual results ΔV_T under D65 source. It showed that the scatter for each formula was much less than that in Fig. 3.4.6. These results indicated that the new SDO fitted the visual results better than the CIE 1964 standard colorimetric observer no matter what colour difference formula or light source was used.

In addition, all indices computed using the new SDO gave a better performance to fit the visual results than that using the CIE SDO. This was the most marked for D65 results. The new SDO had larger deviation from the CIE 1964 colour-matching functions than the CIE SDO. It is quite encouraging that the new SDO developed here gave an overall improvement in predicting the author's data from that of the CIE 1964 colour-matching functions, and performed much better than that from the CIE SDO. This seems to imply that the new SDO may be more reliable than the CIE SDO for predicting observer metamerism of surface colours.

3.5.5 Testing the Performance of Type I IMI using the New SDO and CIE SDO with Obande Data

To further confirm the results as described in the last section, another set of experimental data produced by Obande (1981) at the University of Bradford were accumulated. Obande prepared 71 metamers surrounding 14 colour centres. Each metamer was intended to have a close match under the CIE D65 illuminant, but to show large difference under the other light sources. Obande's experiment was similar to the author's study: each metamer was prepared using wool serge and assessed by 20 observers against a grey scale. Five sources were used: D65, TL84, WW, W, and A. Only the results obtained from the sources D65, TL84 and A were accumulated here.

The grey scale method used in Obande's experiment was somewhat different from that used in this work in numbering each grade of the grey scale, i.e. the larger the number, the greater the colour difference between the grade and the standard. This is opposite to that used in this work as described in Section 3.1. Obande's method has a drawback in that a large computation error occurs for sample pairs having a small colour difference. The experimental data was transformed to visual colour difference using a third-order-polynomial equation in Eq. 3.5.5, while Eq. 3.5.6 was used for the raw data smaller than the '1.0' grey scale rating.

$$\Delta E = -1.650 + 2.0398\ GS - 0.17143\ GS^2 + 0.051667\ GS^3, \quad GS \geq 1 \quad (3.5.5)$$

and

$$\Delta E = 0.22\ GS, \quad GS < 1 \quad (3.5.6)$$

where GS represents the experimental raw data in terms of grade as described in Section 3.3.1. Table 3.5.3 summarises the performance of observer precision for the Obande data and the author's data. The results showed that the mean CIEL*a*b* colour differences for both data were similar for the D65 and TL84 sources, but the Obande data had a much smaller colour difference under source A than that of the author's study. As far as observer precision was concerned, the author's visual data are much more precise than the Obande data by at least 150% PF/4 unit.

The Obande data was also used to test the performance of Type I IMI, and the effect of the new SDO and the CIE SDO. The ΔE values were computed using the CIE 1964 Standard Colorimetric Observer, the new SDO and the CIE SDO respectively. Again, the PF/4 measure was used to indicate the agreement between each index's prediction and mean visual results. The results are given in Table 3.5.4. It showed that all indices gave a less precise prediction to the Obande data than the author's data (see Table 3.5.2). This could be due to large observer variations occurring in the Obande data as shown in Table 3.5.3. However, the predictive precision from all formulae was still much lower than the typical observer precision for all three light sources investigated. This strongly supported the previous findings that the Type I IMI based on the advanced formulae, CMC(1:1), CIE94 and BFD, was able to precisely quantify degree of illuminant metamerism. In comparing the Obande visual results with the Type I IMIs calculated using the CIE 1964 Standard Colorimetric Observer, the new SDO and the CIE SDO, all indices performed similarly, unlike that the new SDO gave a much more precise prediction of the author's visual results than those from both CIE 1964 Observer and CIE SDO. This implies that colour-matching functions could largely

vary between different groups of observers used, and between different parameters used in the experiment such as scaling techniques and colour stimuli. Further work is required in this area. However, the new SDO derived here showed a better agreement to the author's and Obande's D65 results than those of the CIE 1964 and the CIE SDO. Further industrial tests should be carried out.

3.5.6 Observer Metamerism Index

As mentioned earlier, the CIE (1989) suggested that for a pair of metameric samples which have identical tristimulus values under a reference illuminant and observer, the Observer Metamerism Index (**OMI**) can be evaluated by the CIE SDO based on the uniform colour space CIEL*a*b* or CIEL*u*v* under the reference illuminant and observer. When the samples are not exactly metameric (i.e. with close but different tristimulus values), further correction of OMI is needed. In the author's study, each of the 76 metamers used show a close match under reference source D65. The standard and the sample in each metamer do not have the same tristimulus values. Therefore, some correction is necessary to make a zero difference under the reference observer condition. Two methods are commonly used, multiplicative and additive corrections (Hunt 1991). If the difference between two sets of data is small, the results from these two methods would be very similar. The author used the additive in this work similar to that used in calculating the Type II IMI (mentioned in Section 3.4.4.2). The computation of OMI is given below:

$$OMI = 1/N \sum_{j=1}^{N} (\Delta L^2_j + \Delta C^2_j + \Delta H^2_j)^{1/2}, \qquad (3.5.7)$$

where

$$\Delta L_j = \Delta L_{2j} - \Delta L_{1j}, \qquad (3.5.8)$$

$$\Delta C_j = \Delta C_{2j} - \Delta C_{1j}, \qquad (3.5.9)$$

$$\Delta H_j = \Delta H_{2j} - \Delta H_{1j}, \qquad (3.5.10)$$

where ΔL_{1j}, ΔC_{1j}, and ΔH_{1j} are calculated for the jth pair using one of the four colour difference formulae studied with the CIE 1964 Standard Colorimetric Observer, and ΔL_{2j}, ΔC_{2j}, and ΔH_{2j} calculated using the same formula with one of the two SDOs tested (i.e. the CIE SDO and the new SDO derived here). Hence, this OMI provided that each metamer was exact match under the CIE 1964 Observer.

The OMI was calculated using the colorimetric data of the author's and the Obande's metamers under D65 reference source. The OMI was again computed using the four colour difference formulae for each SDO. The results are summarised in Table 3.5.5. The maximum and minimum values of the OMI for a particular test are also given in Table 3.5.5 to indicate the range of degree of observer metamerism. The results showed that the OMI gave quite similar results for both sets of metamers used no matter which SDO was used. However, the OMI obtained from the new SDO was larger than that from the CIE SDO by about 150%, i.e. the average 0.6 OMI unit from the CIE SDO, and 0.9 from the new SDO. This was expected because the author's SDO has a much larger difference from the CIE 1964 Observer than that of the CIE SDO as described in Section 3.5.3. It seemed to imply that the new SDO was more valid to indicate the observer metamerism than the CIE SDO.

3.6 Conclusions

In this study, 76 metamers were prepared, and covered a wide range of colour space. Two psychophysical experiments, Experiment I and Experiment II, were conducted to quantify the degree of metamerism for these metamers. From these experiments, two sets of mean visual results were obtained, ΔV_T and ΔV_I. The typical observer precision of 29 PF/4 was from both experiments. This magnitude indicated that the visual results were highly reliable. These were used to evaluate three types of Illuminant Metamerism Indices (IMI), in which each was calculated using four colour difference formulae: CIEL*a*b*, CMC(1:1), CIE94 and BFD(1:1). These were tested using the experimental results. The Type I IMI based on

the CMC(1:1), CIE94 and BFD(1:1) colour difference formulae achieved quite satisfactory predictions. The predictive precision was even better than the typical observer precision. This implied that the Type I IMI based on these three colour difference formulae should be confidently used for predicting the degree of illuminant metamerism. The results also indicated that it is unnecessary to apply additive correction (Type II IMI) or to use chromatic adaptation transforms (Type III IMI) in predicting the degree of illuminant metamerism.

Furthermore, a new SDO was derived. This new SDO gave a much improved fit to the D65 visual results, and a slightly more precise prediction to those under the other sources than the CIE 1964 Observer and the CIE SDO using the Type I IMI. The results implied that the new SDO was more valid than the CIE SDO in indicating the degree of observer metamerism, especially for evaluating surface colours.

Another set of experimental data, produced by Obande at the University of Bradford, was also accumulated. Similar tests were conducted as those for the author's data. The results confirmed that the Type I IMI gave reliable prediction of the visual results. However, in comparing the Obande visual results with the illuminant metamerism indices calculated using the CIE 1964 Observer, the CIE SDO and the new SDO derived here, the Type I IMIs gave a very similar performance, unlike the large improvement from the CIE 1964 Observer to the new SDO found when using the author's data. This implies that different colour-matching functions could largely vary between different groups of observers used, and between different parameters used in the experiments.

An OMI was derived and calculated using the author's and the Obande's metamers and the four colour difference formulae (CIEL*a*b*, CMC(1:1), CIE94 and BFD(1:1)) for the CIE SDO and the new SDO derived here. The results showed that the OMI obtained from the new SDO was larger than that from the CIE SDO by about

150%, i.e. the average 0.6 OMI unit from the CIE SDO, and 0.9 from the new SDO. It seemed to imply that the new SDO was more valid to indicate the observer metamerism than the CIE SDO.

CHAPTER 4

CHAPTER 4

RECOMMENDATIONS FOR FUTURE WORK

In this thesis, two studies have been accomplished: Colour Constancy and Metamerism Studies.

In the Colour Constancy Study, various chromatic adaptation transforms were tested. A general chromatic adaptation transform (KUO) was developed by modifying the CIE chromatic adaptation transform. The new transform (KUO) gave a more precise prediction to both Type I (coloured lights) and Type II (object colours) experimental data accumulated than the other transforms investigated. In the future work, three tasks for further study are defined below:

(1) to reproduce physical samples for the experimental grids under the D65 and A sources derived from the author's and the Luo et al.'s studies. These samples can be used to conduct further experiments to verify the large difference between the two sets of experimental grids as mentioned in Section 2.3.2.

(2) to develop new equations for improving the reversibility of the new chromatic adaptation transform (KUO). As mentioned in Section 2.3.4, the reversibility of the KUO type transform was good enough for surface colour applications, but may be not for cross-media colour reproduction for imaging industry.

(3) to verify the best z value of 1.0 found from this work for the Hunt94 model in predicting the lightness for surface colours. As mentioned in Section 1.5.6 (4), the z value was used to determine the lightness J, and associated with the background contrast effect. Further experiments should be conducted using large size samples against different achromatic backgrounds.

In the Metamerism Study, the Type I Illuminant Metamerism Index (IMI) based on the three colour difference formulae, CMC(1:1), CIE94 and BFD(1:1), was found to be a reliable metamerism index. It gave more precise prediction of the experimental data obtained from this work than the other two Type IMIs. The Type I IMI can be applied to the colour industry where illuminant metamerism is taken into account. In addition, a new SDO was also developed to indicate the observer metamerism. The Type I IMI using the new SDO had a better agreement with the visual results under D65 source than those using the CIE 1964 Observer and the CIE SDO. Three tasks should be carried out in future studies:

(1) to verify the relationship between the total score on the D-H Color Rule and the reciprocal colour temperature of illuminant. As mentioned in Section 3.2.2, the results from other researchers showed the relationship should be linear. However, their results were obtained from two illuminants (the series of daylight simulators and the tungsten lamp A). In the author's study, a non-linear relationship was found. This can be verified by conducting further experiments using various illuminants with a wide range of colour temperature.

(2) to verify the barocentric wavelengths for the metamers with large metamerism. As mentioned in Section 3.4.1, the cross-overs of metamers slightly moved away from the barocentric wavelengths (450 nm, 540 nm, 610 nm) to around 454 nm, 530 nm, 600 nm respectively. However, the number of the metamers with the largest metamerism (an average of 13.5 CMC(2:1) ΔE units) was limited, i.e. only 5 metamers obtained in the author's study. Further work using more metamers showing larger degree of metamerism than those of the author's metamers is required to confirm this finding.

(3) to smooth the new SDO functions derived from the author's study. As described in Sections 3.5.4 and 3.5.5, the new SDO performed significantly better in predicting the author's data than the CIE 1964 Observer and the CIE SDO, but not for the Obande's data. As shown in Fig. 3.5.1, the new SDO functions

were not smooth, in comparison with the CIE 1964 Observer, especially for $\bar{x}'(\lambda)$ function. These new functions can be further smoothed to verify whether the irregularity in these functions resulted from experimental errors (i.e. over-fitting the experimental errors), and to see if these lobs will significantly affect the performance in fitting the experimental results.

REFERENCES

REFERENCES

Adams, E. Q., 1942. X-Z planes in the 1931 ICI system of colorimetry, *J. Opt. Soc. Am.* **32**, p. 168.

Allen, E., 1970. An index of metamerism for observer differences, in *Color 69*, The First Congress of Int. Colour Assoc., Stockholm, 1969, Vol. **2**, Musterschmidt-Verlag, Gottingen, p.771.

Badcock, T., 1992. Precision of metameric indices in relation to visual assessments, *J. Soc. Dyers Col.* **108**, p. 31.

Bartleson, C. J., 1977. A review of chromatic adaptation, Proceedings of the Third AIC Congress, Color 77, Bristol: Adam & Hilger, Bristal, p. 63.

Bartleson, C. J., 1979a. Changes in colour appearance with variations in in chromatic adaptation, *Color Res. Appl.* **4**, p.119.

Bartleson, C. J., 1979b. Predicting corresponding colours with changes in adaptation, *Color Res. Appl.* **4**, p.143.

Bartleson, C. J.,1978. Comparison of chromatic-adaptation transforms, *Color Res. Appl.* **3**, p.129.

Berns, R. S., Alman, D. H., Reniff, L., Synder, G. D. S. and Balonon-Rosen, 1991. Visual Determination of Suprathreshold color-difference tolerances using probit analysis, *Color Res. Appl.* **16**, p. 297.

Berns, R. S., Fairchild, M. D. and Beering, M. M., 1988. Quantification of illuminant metamerism for four coloration systems via metameric mismatch gamuts, *Color Res. Appl.* **13**, p. 346.

Berns, Roy S. and Kuehni, Rolf G., 1990. What Determines Crossover Wavelengths of Metameric Pairs with Three Crossovers?, *Colour Res. Appl.*, **15**, p. 23.

Billmeyer, F. W. JR. and Saltzman, M., 1981. *Principle of Color Technology*, Second Edition, New York, John Wiley & Sons.

Billmeyer, F. W., Jr. and Saltzman, M., 1980. Observer Metamerism, *Color Res. Appl.* **5**, p.72.

Billmeyer,F. W. Jr., 1967. Metamerism - An Introduction, *Colour Eng.*, **5**, p. 42.

Breneman, E. J., 1977. Perceived saturation in complex stimuli viewed in light and dark surrounds, *J. Opt. Soc. Am.* **67**, p. 657.

Breneman, E. J., 1987. Corresponding chromaticities for different states of adaptation to complex visual fields, *J. Opt. Soc. Am.* A **4**, p. 1115.

Brockes, A., 1968. The problems of colour metamerism from an industrial viewpoint, *Color Eng.* **6**, p. 48.

Burnham, R. W., Evans, R. M. and Newhall, S. M., 1952. Influence on colour perception of adaptation to illumination., J. Opt. Soc. Am. **42**, p. 597.

Burnham, R. W., Evans, R. M. and Newhall, S. M., 1957. Prediction of color appearance with different adaptation illuminations, *J. Opt. Soc. Am.* **47**, p. 34.

CIE, 1974. *Method of specifying and measuring colour rendering properties of light sources*, Second Edition, Publication No. 13.2, Bureau Central de la CIE, Paris.

CIE, 1978. *Recommendations on Uniform Color Spaces, Color Difference Equations, and Psychometric Color Terms*, Suppl. No. 2 to Publication No. 15, *Colorimetry*, Bureau Central de la CIE, Pareis.

CIE, 1986. *Colorimetry*, Publication No. 15.2, Bureau Central de la CIE, Paris.

CIE, 1987. *International lighting vocabulary*, Publication No.17.4, Bureau Central de la CIE, Paris.

CIE, 1989. *Special Metamerism Index: Change in Observer*, First Edition, Publication. No. 80, Central Bureau de la CIE, Paris.

CIE, 1995. CIE Publication. No. 116, *Technical Report on Industrial Colour Difference Evaluations*, Central Bureau de la CIE, Vienna.

Clarke, F. J. J., McDonald, R. and Rigg, B., 1984. Modification to the JPC79 Colour-difference Formula, *J. Soc. Dyers Col.* **100**, p. 128.

Coates, E., Kriszka R. C., Provost, J. R. and Rigg, B., 1973. The precision of colour-difference equations in relation to perceived colour differences, *Colour 73*, The Second Congress of the International Colour Association, London, Adam Hilger, p.300.

Coates, E., Day S., Provost, J. R. and Rigg, B., 1972. The measurement and assessment of colour difference for industrial use III-Methods of scaling visual assessments, *J. Soc. Dyers Col.* **88**, p.186.

Coblentz, W. W. and Emerson, W. B., 1918. Relative sensitivity of the average eye to light of different colors and some pratical applications of radiation problems, *U.S. Bureau of Standards Bulletin* **14**, p. 167.

de Mattiello, M. L. F.,1987. On the exponents of Saturation functions, *Color Res. Appl.* **12**, p.327.

Fairchild, M. D. and Berns, R. S.,1993. Image color-appearance specification through extension of CIEL*a*b*, *Color Res. Appl.* **18**, p.178.

Fairchild, M. D., 1994. Visual evaluation and evolution of the RLAB color space, *Final Program and Proceedings of The Second IS&T/SID Color Imaging Conference: Color Science, Systems and Applications*, p. 9.

Foss, C. E., 1978. Space lattice used to sample the color space of the Committee of Uniform Color Scales of the Optical Society of America, *J. Opt. Soc. Am.* **68**, p.1616.

Gibson, K. S. and Tyndall, E. P. T., 1923. Visibility of radiant energy, *Bureau of Standards Bulletin* **19**, p. 131.

Gill, P. E. and Murray, W., 1976. Minimization subject to bounds on the variables, National Physical Laboratory report NAC 72.

Guild, J., 1931. The colorimetric properties of the spectrum, *Phil. Trans. Roy. Soc. A* **230**, p. 149.

Hård, A. and Sivik, L., 1981. NCS- Natural Color System: a Swedish standard for color notation, *Color Res. Appl.* **6**, p. 128.

Helson, H., Judd, D. B. and Warren, M. H., 1952. Object-color changes from daylight to incandescent filament illumination, *Illum. Eng.* **47**, p. 221.

Hering, E., 1964. *Outlines of a theory of the the light sense*, translated by Hurvich L. and Jameson D., Harvard University Press, Cambridge, Massachusetts.

Hesselgren, S., 1952. *Hesselgren's Colour Atlas*, Palmer, Stockholm.

Hesselgren, S., 1954. *Subjective Color Standardization*, Almqvist and Wiksell, Stockholm.

Hunt, R. G. W., 1987. A model of colour vision for predicting colour appearance under various viewing conditions., *Color Res. Appl.* **12**, p. 297.

Hunt, R. W. G. and Pointer, M. R., 1985. A colour-appearance transform for the CIE 1931 standard colorimetric observer, *Color Res. Appl.* **10**, p. 165.

Hunt, R. W. G., 1952. Light and dark adaptation and the perception of colour, *J. Opt. Soc. Am.* **42**, p. 190.

Hunt, R. W. G., 1953. The perception of colour in 1^0 fields for different states of adaptation, *J. Opt. Soc. Am.* **43**, p. 479.

Hunt, R. W. G., 1991. *Measuring Colour*, Second Edition, ELLIS HORWOOD, London.

Hunt, R. W. G., 1994. An Improved Predictor of Colourfulness in a Model of Colour Vision, *Color Res. Appl.* **19,** p. 23.

Johansson, T., 1937, 1952. *Farg*, Natur och Kultur, Stockholm.

Judd, D. B. and Wyszecki, G., 1975. *Color in Business, Science and Industry*, Third Edition, London, John Wiley & Sons.

Judd, D. B., 1940. Hue saturation and lightness of object colours with chromatic illumination , *J. Opt. Soc. Am.* **30,** p. 2.

Kaiser, P. K. and Hemmendinger, H., 1980. The Color Rule: A Device for Color-Vision Testing, *Color Res. Appl.* **5**, p. 65.

Kuehni, R. G., 1980. Three Unsolved Problems of Applied Colour Science, *Amer. Dyestuff Reporter* **69**, p. 28.

Lam, K. M., 1985. *Metamerism and colour constancy*, Ph. D. Thesis, The Bradford University, Bradford.

Luo, M. R. and Lo, M. C., 1992., private communication, unpublished.

Luo, M. R. and Rigg, B., 1986a. Chromaticity-discrimination ellipses for object colours, *Color Res. Appl.* **11**, p. 25.

Luo, M. R. and Rigg, B., 1986b. Uniform colour space based on the CMC(l : c) colour-difference formula, *J. Opt. Soc. Am.* **102**, p. 164.

Luo, M. R. and Rigg, B., 1987a. BFD(*l* : c) Colour-Difference Formula Part 1 - Development of the Formula, *J. Soc. Dyers Col.* **103**, p. 86.

Luo, M. R. and Rigg, B., 1987b. BFD(*l* : c) Colour-Difference Formula Part 2 - Performance of the Formula, *J. Soc. Dyers Col.* **103**, p. 126.

Luo, M. R. and Rigg, B., 1987c. A colour-difference formula for surface colours under illuminant A, *J. Soc. Dyers Col.* **103**, p. 161.

Luo, M. R., Clarke, A. A., Rhodes, P. A., Schappo, A., Scrivener, S. A. R. and Tait, C. J., 1991a. Quantifying colour appearance. Part I. LUTCHI Colour Appearance Data, *Color Res. Appl.* **16**, p. 166.

Luo, M. R., Clarke, A. A., Rhodes, P. A., Schappo, A., Scrivener, S. A. R. and Tait, C. J., 1991b. Quantifying Colour Appearance. Part II. Testing Colour Models Performance Using LUTCHI Colour Appearance Data, *Color Res. Appl.* **16**, p. 181.

MacAdam, D. L., 1956. Chromatic adaptation, *J. Opc. Soc. Am.* **46**, p. 500.

MacAdam, D. L., 1974. Uniform color scales, *J. Opt. Soc. Am.* **64**, p. 1691.

McDonald, R., 1987. *Colour physics for industry*, Second Edition, Soc. Dyers Col, Bradford.

McLaren, K. and Rigg, B., 1976. The SDC Recommended Colour Difference Formula: Change to CIEL*a*b*, *J. Soc. Dyers Col.*, **92** p. 337.

McLaren, K., 1970. Colour passing-visual or instrumental, *J. Soc. Dyers Col.* **86**, p. 389.

Moradian, S. and Rigg, B., 1987. The guantification of metamerism, *J. Soc. Dyers Col.* **103**, p. 209.

Nayatani, Y., 1995. Revision of the chroma and hue scales of a nonlinear color-appearance model, *Color Res. Appl.* **20**, p. 143.

Nayatani, Y., Hashimoto, K., Takahama, K. and Sobagaki, H., 1985. Comparison of Methods for Assessing Observer Metamerism, *Color Res. Appl.* **10**, p. 147.

Nayatani, Y., Hashimoto, K., Takahama, K. and Sobagaki, H.,1987. A nonlinear color-appearance model using Estevez-Hunt-Pointer primaries, *Color Res. Appl.* **12**, p. 231.

Nayatani, Y., Hashimoto, K., Takahama, K. and Sobagaki, H.,1990. Colour-appearance model and chromatic-adaptation transform, *Color Res. Appl.* **15**, p. 210.

Nayatani, Y., K. Takahama, K. and H. Sobagaki, H., 1986. Prediction of color appearance under various adapting condition, *Color Res. Appl.* **11**, p. 62.

Nayatani, Y., Takahama, K. and Sobagaki, H., 1972. Subjective estimation of color attributes for surface colors. Part 1. Reproduction of estimation, *Acta Chromatica* **2**, p. 129.

Nayatani, Y., Takahama, K. and Sobagaki, H., 1983. A Proposal of New Standard Deviate Observers, *Color. Res. Appl.* **8**, p. 47.

Nayatani, Y., Takahama, K. and Sobagaki, H., 1981. Formulation of a nonlinear model of chromatic adaptation, *Color Res. Appl.* **6**, p. 161.

Newhall, S. M., Nickerson, D. and Judd, D. B., 1943. Final report of the O.S.A. subcommittee on the spacing of the Munsell colors, *J. Opt. Soc. Am.* **33**, p. 385.

Nickerson, D., 1936. The specification of color tolerances, *Text. Res.* **6**, p. 505.

Nimeroff, I. and Yurow, J. A., 1965. Degree of Metamerism, *J. Opt. Soc. Am.* **55**, p. 185.

North, A. D. and Fairchild, M. D.,1993a. Measuring Color-Matching Functions.Part I, *Color Res. Appl.* **18**, p. 155.

North, A. D. and Fairchild, M. D.,1993b. Measuring Color-Matching Functions.Part II. New Data for Assessing Observer Metamerism, *Color Res. Appl.* **18**, p. 163.

Obande, O. D., 1981. *Measurement of Metamerism*, Ph. D. Thesis, The University of Bradford, Bradford.

Ohta, N., 1982. A simplified method for formulating pseudo-object colors, *Color Res. Appl.* **7**, p. 79.

Ohta, N., 1985. Formulation of a Standard Deviate Observer by a Nonlinear Optimization Technique, *Color Res. Appl.* **10**, p. 156.

Ohta, N., 1987. Intersections of Spectral Curves of Metameric Colors, *Color Res. Appl.* **12**, p. 85.

Pitt, I. T. and Winter, L. M., 1974. Effect of surround on perceived saturation, *J. Opt. Soc. Am.* **64**, p. 1328.

Pointer, M. R., 1980. The concept of colourfulness and its use for deriving grids for assessing colour appearance, *Color Res. Appl.* **5**, p. 99.

Pointer, M. R., 1982. Analysis of colour-appearance grids and chromatic-adaptation transforms, *Color Res. Appl.* **7**, p. 113.

Pointer, M. R., Ensell, J. S. and Bullock, L. M., 1977. Grids for assessing colour appearance, *Color Res. Appl.* **2**, p. 131.

Rich, D. C. and Jalijali, J., 1995. Effects of Observer Metamerism in the Determination of Human Color-Matching Functions, *Color Res. Appl.* **20**, p. 29.

Schultze, W. and Gall, L., 1971. Application of Color Difference Formulae to Highly Saturated Colors Differing only in Lightness and Saturation, *J. Color Appear.* **1:1**, p. 17.

Schultze, W., 1972. The Usefulness of Color-Difference Formulae for Fixing Colour Tolerances, Color Metrics, Soesterberg, AIC/Holland, p. 254.

Speranskaya, N. I., 1959. Determination of spectrum color co-ordinates for twenty-seven normal observers, *Optics and Spectroscopy* **7**, p. 424.

Stiles, W. S. and Burch, J. M., 1959. N. P. L. colour-matching investigation: final report (1958), *Optica Acta* **6**, p. 1.

Stiles, W. S. and Wyszecki, G., 1968. Intersections of the spectral reflectance curves of metameric object colors, *J. Opt. Soc. Am.* **58**, p. 32.

Strocka, D., 1978. Possibilities for specifying an index of observer metamerism, *Proceedings of The Third AIC Congress of Color 77*, Bristol, Adam Hilger, p. 432.

Strocka, D., Brockes A. and Paffhausen, W., 1983. Influence of Experimental Parameters on the Evaluation of Color-Difference Ellipsoids, *Color Res. Appl.*, **8**, p. 169.

Takahama, K. and Nayatani, Y., 1972. Studies on color rendering and illuminant metamerism (part 7) (A new method for constituting metameric object colors), *J. Illum. Eng. Soc. Jpn.* **56**, p. 315.

Takahama, K., Sobagaki, H. and Nayatani, Y.,1984. Formulation of a nonlinear model of chromatic adaptation for a light grey background, *Color Res. Appl.* **9**, p. 106.

Terstiege, H., 1972. Chromatic Adaptation A State-of -the-Art Report, *J. Color Appearance* **1**, p. 19.

Thornton, W. A., 1986. Evidence for three spectral responses of the normal human visual system, *Color Res. Appl.* **11**, p. 160.

Troscianko, T. S., 1979. Analysis of Colour-Scaling Data, *Color Res. Appl.* **4**, p. 225.

Wang, X.,1994. *Modelling of Colour Appearance*, Ph. D. Thesis, The Loughborough University of Technology, Loughborough, England.

Wassef, E. G. T.,1965. Application of the binocular matching method to the study of surface colors, *Optica Acta* **2**, p. 144.

Wright, W. D., 1928-1929. A re-determination of the trichromatic coefficients of the spectral colours, *Trans. Opt. Soc.* **30**, p. 141.

Wright, W. D., 1964. *The Measurement of Colour*, Third Edition, Hilger &Watts Ltd., London.

Wright, W. D., 1981. Why and how chromatic adaptation has been studied, *Color Res. Appl.* **6**, p. 147.

Wyszecki, G. and W. S. Stiles, W. S., 1982. *Color Science: Concepts and methods, quantitative data and formulae*, Second Edition, John Wiley & Sons, New York.

Wyszecki, G., 1962. Metameric object colors, *Acta Chromatica* **1**, p. 1.

Wyszecki, G., 1969. The Degree of Colour Metamerism and Its Specification, *Text. Chem. Col.* **1**, p. 46.

TABLES

Table 2.1.1 Colorimetric values for the three light sources used.

Light Source	X	Y	Z	x	y	L (cd/m^2)	CCT	Ra
D65	96.46	100	108.62	0.3162	0.3278	340	6461	95
A	115.19	100	23.75	0.4821	0.4185	340	2544	---
TL84	103.07	100	64.29	0.3855	0.3740	730	4019	85

Note: L: Luminance. CCT: Correlated colour temperature.
Ra: Colour rendering index.

Table 2.1.2. Summary of experimental phases of Colour Constancy Study.

Illuminant	Grey Background (Y%)	Luminance (cd/m^2)	No. of Colours	No. of observers	No. of Estimations
D65	16	250	240	5	3600
A	16	250	239	5	3585
TL84	16	540	239	5	3585
Total			718		10,770

Table 2.2.1 Individual observer's precision performance in terms of r and CV for Lightness, Colourfulness and Hue attributes under D65, A and TL84 sources.

Lightness

Light Source	Observer	M	K	J	R	X	mean
D65	r	0.96	0.97	0.96	0.98	0.96	
	CV	11	11	10	8	12	
A	r	0.98	0.97	0.98	0.98	0.97	
	CV	10	11	11	9	10	
TL84	r	0.98	0.98	0.98	0.98	0.98	
	CV	12	10	13	9	10	
Mean	r	0.97	0.97	0.97	0.98	0.97	0.97
	CV	11	11	11	9	11	11

Colourfulness

Light Source	Observer	M	K	J	R	X	mean
D65	r	0.92	0.94	0.94	0.96	0.96	
	CV	19	18	18	14	15	
A	r	0.94	0.94	0.93	0.95	0.96	
	CV	17	16	18	15	13	
TL84	r	0.91	0.95	0.92	0.94	0.96	
	CV	20	16	19	17	15	
Mean	r	0.92	0.94	0.93	0.95	0.96	0.94
	CV	19	17	18	15	14	17

Hue

Light Source	Observer	M	K	J	R	X	mean
D65	r	1.00	0.99	1.00	1.00	0.99	
	CV	6	7	6	5	6	
A	r	0.99	1.00	1.00	0.99	0.99	
	CV	7	7	7	7	7	
TL84	r	1.00	0.99	1.00	1.00	0.99	
	CV	6	7	7	5	7	
Mean	r	1.00	0.99	1.00	1.00	0.99	1.00
	CV	6	7	7	6	7	7

Table 2.2.2 Individual observer's repeatability performance in terms of r and CV for Lightness, Colourfulness and Hue attributes under D65, A and TL84 sources. Thirty samples were repeated assessed by the same observer with a one-month gap.

Lightness

Light Source	Observer	M	K	J	R	X	Mean
D65	r	0.95	0.97	0.98	0.99	0.97	
	CV	15	19	16	6	14	
A	r	0.97	0.98	0.99	0.99	0.98	
	CV	12	7	8	9	10	
TL84	r	0.98	0.97	0.99	0.98	0.99	
	CV	12	15	7	9	8	
Mean	r	0.97	0.97	0.99	0.99	0.98	0.98
	CV	13	14	10	8	11	11

Colourfulness

Light Source	Observer	M	K	J	R	X	Mean
D65	r	0.96	0.86	0.86	0.93	0.90	
	CV	20	29	22	20	37	
A	r	0.96	0.94	0.92	0.96	0.97	
	CV	13	24	30	14	15	
TL84	r	0.94	0.85	0.95	0.93	0.85	
	CV	25	34	13	16	27	
Mean	r	0.95	0.88	0.91	0.94	0.91	0.92
	CV	19	29	22	17	26	23

Hue

Light Source	Observer	M	K	J	R	X	Mean
D65	r	0.99	0.99	0.99	0.99	1.00	
	CV	10	8	6	8	6	
A	r	1.00	1.00	1.00	1.00	0.99	
	CV	5	4	4	5	10	
TL84	r	0.99	1.00	1.00	1.00	0.99	
	CV	6	4	4	6	7	
Mean	r	0.99	1.00	1.00	1.00	0.99	1.00
	CV	7	5	5	6	8	6

Table 2.2.3 The exponent factors (b) for each individual observer's colourfulness results.

Light Source	Observer	M	K	J	R	X	Mean
D65		0.90	0.89	0.86	0.99	0.78	
A		0.97	0.82	0.90	0.96	0.83	
TL84		0.93	0.74	0.93	1.12	0.77	
Ratio	(Max./Min)	1.08	1.20	1.07	1.17	1.08	1.12

Table 2.2.4 Error of prediction from various chromatic adaptation transforms.

Transform to light source D65 Transform from light source A	D65 TL84	Mean	Rank	Average rank from 4 measures
(Mean CIE L*a*b* ΔE Units)				
von Kries	9.0	5.7	7.3	3	2.5
Bartleson	12.8	5.3	9.0	7	7.0
Bradford	6.2	4.1	5.2	1	1.0
CIE	9.9	5.4	7.7	3	3.0
Hunt	7.7	7.6	7.7	3	3.0
CIE L*a*b*	8.7	4.5	6.6	2	2.0
RLAB	9.4	5.7	7.5	3	4.5
(RMS CIE L*a*b* ΔE Units)					
von Kries	9.6	5.9	7.8	3	
Bartleson	13.9	6.0	9.9	7	
Bradford	6.7	4.4	5.6	1	
CIE	11.6	5.8	8.7	5	
Hunt	9.1	7.7	8.4	5	
CIE L*a*b*	8.9	4.9	6.9	2	
RLAB	9.8	5.9	7.9	3	
(Mean CMC (1:1) ΔE)					
von Kries	5.7	3.8	4.8	2	
Bartleson	8.4	3.7	6.1	7	
Bradford	4.2	3.1	3.6	1	
CIE	5.7	3.6	4.6	2	
Hunt	4.5	4.5	4.5	2	
CIE L*a*b*	5.6	3.3	4.5	2	
RLAB	6.4	4.0	5.2	6	
(RMS CMC (1:1) ΔE)					
von Kries	6.0	4.0	5.0	2	
Bartleson	8.9	4.4	6.7	7	
Bradford	4.5	3.3	3.9	1	
CIE	6.2	3.8	5.0	2	
Hunt	5.1	4.5	4.8	2	
CIE L*a*b*	5.7	3.7	4.7	2	
RLAB	6.5	4.1	5.3	6	

Table 2.3.1. Error of prediction from the KUO1 transform.

Model to light source Model from light source	D65 A	D65 TL84	Mean
Mean CIE L*a*b* ΔE Unit	5.2	4.3	4.8
RMS CIE L*a*b* ΔE Unit	5.6	4.5	5.1
Mean CMC(1:1) ΔE Unit	3.5	3.1	3.3
RMS CMC(1:1) ΔE Unit	3.7	3.3	3.5

Table 2.3.2. Error of prediction from various transforms using three sets of data: Lam and Rigg, Helson et al. and Breneman.

Data	Lam & Rigg	Helson et al.	Breneman	Mean	Rank	Average rank from 4 measures
(Mean CIE L*a*b* ΔE Unit)						
von Kries	6.7	7.0	17.0	10.2	4	4.0
Bartleson	8.6	10.4	12.2	10.4	4	6.5
BFD	4.1	5.3	12.7	7.4	1	1.0
CIE	5.9	6.4	18.4	10.2	4	4.0
Hunt	5.6	7.9	19.2	10.9	8	7.5
CIE L*a*b*	6.8	8.5	15.6	10.3	4	4.5
RLAB	6.1	6.7	12.0	8.3	3	3.0
Kuo1	4.4	5.6	12.6	7.5	1	1.3
(RMS CIE L*a*b* ΔE Unit)						
von Kries	8.8	8.4	9.3	8.8	4	
Bartleson	11.9	11.8	12.2	12.0	8	
BFD	5.2	6.0	8.3	6.5	1	
CIE	8.3	7.5	9.9	8.6	4	
Hunt	7.2	9.3	13.7	10.1	7	
CIE L*a*b*	8.7	9.6	9.5	9.3	6	
RLAB	8.1	8.1	8.1	8.1	3	
Kuo1	5.4	6.6	9.2	7.1	2	
(Mean CMC(1:1) ΔE Unit)						
von Kries	4.9	5.0	11.0	7.0	4	
Bartleson	6.5	7.5	9.0	7.7	7	
BFD	3.5	4.0	8.5	5.3	1	
CIE	5.0	5.0	11.4	7.1	4	
Hunt	5.1	6.6	12.2	8.0	8	
CIE L*a*b*	4.9	6.2	9.6	6.9	4	
RLAB	4.8	5.2	7.9	6.0	3	
Kuo1	3.6	4.2	8.2	5.3	1	
(RMS CMC(1:1) ΔE Unit)						
von Kries	5.8	5.9	7.7	6.5	4	
Bartleson	8.0	8.4	10.7	9.0	7	
BFD	4.3	4.7	7.3	5.4	1	
CIE	5.9	6.0	7.9	6.6	4	
Hunt	5.5	8.8	13.0	9.1	7	
CIE L*a*b*	5.9	7.0	7.3	6.7	4	
RLAB	6.1	6.2	6.1	6.1	3	
Kuo1	4.4	5.0	7.2	5.5	1	

Table 2.3.3. Error of prediction from four new transforms, KUO2, KUO3, BFD2 and BFD3, for the four data sets: the author's, Lam and Rigg, Helson et al. and Breneman.

Data	the Author's	Lam & Rigg	Helson et al.	Breneman	Mean	Average of four measures
(Mean CIE L*a*b* ΔE Unit)						
KUO2	5.8	6.2	6.3	11.3	7.4	6.3
KUO3	6.0	5.6	6.2	11.9	7.4	6.5
BFD1	7.9	6.5	7.0	14.2	8.9	7.4
BFD2	8.9	6.1	6.7	16.0	9.4	7.9
(RMS CIE L*a*b* ΔE Unit)						
KUO2	6.1	7.1	7.4	8.4	7.3	
KUO3	6.4	6.6	7.2	8.8	7.3	
BFD1	8.1	8.4	8.2	10.1	8.7	
BFD2	9.3	7.9	8.0	10.6	9.0	
(Mean CMC(1:1) ΔE Unit)						
KUO2	3.8	4.9	4.6	7.4	5.2	
KUO3	4.2	4.8	4.8	7.8	5.7	
BFD1	4.8	4.7	5.1	8.9	5.9	
BFD2	6.2	5.0	5.2	10.3	6.7	
(RMS CMC(1:1) ΔE Unit)						
KUO2	4.0	5.2	5.5	6.9	5.4	
KUO3	4.5	5.3	5.7	6.9	5.6	
BFD1	4.9	5.5	6.0	7.7	6.0	
BFD2	6.3	6.1	6.3	7.8	6.6	

Table 2.3.4. Summary of the mean error of prediction from various transforms for the four data sets: the author's, Lam and Rigg, Helson et al. and Breneman.

Mean Units	CIE L*a*b*		CMC(1:1)				
Transforms	ΔE	RMS	ΔE	RMS	Mean	Average	Rank
von Kries	9.9	9.0	6.7	6.4	8.0	-----	4
Bartleson	11.0	12.5	7.9	9.0	10.1	-----	8
CIE	10.2	9.3	6.8	6.5	8.2	-----	4
Hunt94	10.1	9.8	7.1	8.1	8.8	-----	7
CIE L*a*b*	9.9	9.2	6.6	6.5	8.1	-----	4
RLAB	8.6	8.5	6.1	6.2	7.4	-----	2
BFD	7.1	6.6	5.1	5.2	6.0		
BFD1	8.9	8.7	5.9	6.0	7.4	7.1	2
BFD2	9.4	9.0	6.7	6.6	7.9		
KUO1	7.0	6.7	4.9	5.1	5.9		
KUO2	7.4	7.3	5.2	5.4	6.3	6.2	1
KUO3	7.4	7.3	5.7	5.6	6.5		

Table 2.4.1 Colour models' lightness scales performance in terms of r and CV under three sources D65, A and TL84.

Models		CMC(1:1)	CIE L*a*b*	Nayatani	Hunt94	RLAB	Modified Hunt94
Light source							
D65	r	0.98	0.98	0.98	0.97	0.98	0.98
	CV	28	7	9	17	7	8
A	r	0.99	0.98	0.98	0.97	0.98	0.98
	CV	26	7	8	18	7	8
TL84	r	0.99	0.99	0.98	0.98	0.98	0.98
	CV	29	7	8	14	7	7
Mean	r	0.99	0.98	0.98	0.97	0.98	0.98
	CV	28	7	8	16	7	8

Table 2.4.2 Colour models' chroma performance in terms of r and CV under three sources: D65, A and TL84.

Model Light	source	CMC(1:1)	CIE L*a*b*	Nayatani	Hunt94	RLAB
D65	r	0.85	0.81	0.94	0.95	0.79
	CV	27	33	18	16	36
	SFi	1.45	0.80	0.83	0.66	0.70
	r	0.85	0.81	0.94	0.95	0.79
	CV	27	33	19	17	37
	SFm	1.47	0.80	0.80	0.66	0.65
A	r	0.84	0.80	0.67	0.92	0.78
	CV	27	35	39	20	37
	SFi	1.52	0.82	0.83	0.69	0.71
	r	0.84	0.80	0.67	0.92	0.78
	CV	27	35	39	21	38
	SFm	1.47	0.80	0.80	0.66	0.65
TL84	r	0.80	0.76	0.88	0.93	0.68
	CV	30	38	24	19	47
	SFi	1.43	0.77	0.73	0.64	0.55
	r	0.80	0.75	0.88	0.93	0.68
	CV	30	38	27	19	51
	SFm	1.47	0.80	0.80	0.66	0.65
Mean	r	0.83	0.79	0.83	0.93	0.75
	CV	28	35	28	19	42
	SFm	1.47	0.80	0.80	0.66	0.65

Note: SFi: the scaling factor for each model/phase.
SFm: the mean scaling factor for all phases.

Table 2.4.3 Colour models' colourfulness performance in terms of r and CV under three light sources: D65, A and TL84.

Model / Light source		Nayatani	Hunt94
D65	r	0.94	0.95
	CV	18	16
	SFi	0.86	0.71
	r	0.94	0.95
	CV	20	17
	SFm	0.79	0.71
A	r	0.67	0.92
	CV	39	20
	SFi	0.85	0.74
	r	0.67	0.92
	CV	39	21
	SFm	0.79	0.71
TL84	r	0.88	0.93
	CV	24	19
	SFi	0.66	0.67
	r	0.88	0.93
	CV	32	20
	SFm	0.79	0.71
Mean (SFm)			
	r	0.83	0.93
	CV	30	19

Note: SFi: the scaling factor for each model/phase.
SFm: the mean scaling factor for all phases.

Table 2.4.4 Colour models' hue performance in terms of r and CV under three light sources: D65, A and TL84.

Model Light	source	Nayatani	Hunt94
D65	r	0.98	0.99
	CV	11	9
A	r	0.96	0.99
	CV	19	11
TL84	r	0.98	0.99
	CV	12	7
Mean	r	0.97	0.99
	CV	14	9

Table 3.1.1 Instrument performance from the 76 metamers measured using a Macbeth MS2020 spectrophotometer.

	Short term	Long term
Mean ΔE(CMC(1:1))	0.06	0.09
Max.	0.23	0.25
Min.	0.02	0.01

Note: Long term means a two-month gap.

Table 3.1.2 CIE L*a*b* co-ordinates for grey scale samples.

	Grades	L*	a*	b*	ΔL*	ΔE(CIE L*a*b*)
CIE D65						
	1	66.70	-0.33	0.11	24.63	24.63
	2	53.29	-0.35	-0.35	11.22	11.24
	3	47.36	-0.30	0.13	5.29	5.17
	4	43.35	-0.22	0.25	1.28	1.17
	5	41.68	-0.57	-0.01	-0.39	0.39
	SD	42.07	-0.49	-0.05		
CIE A						
	1	66.69	0.59	-0.58	24.66	24.68
	2	53.25	0.86	-1.29	11.22	11.23
	3	47.36	1.17	-0.86	5.33	5.15
	4	43.37	1.32	-0.73	1.34	1.24
	5	41.64	0.91	-1.08	-0.39	0.39
	SD	42.03	1.00	-1.12		
Philips TL84						
	1	66.26	0.53	-0.25	24.87	24.88
	2	52.68	0.91	-0.69	11.29	11.30
	3	46.71	1.18	-0.14	5.32	5.16
	4	42.70	1.29	0.00	1.31	1.20
	5	41.00	0.88	-0.29	-0.39	0.41
	SD	41.39	1.04	-0.34		

Table 3.1.3 Engineering information for the 11 light sources investigated.

	X_{10}	Y_{10}	Z_{10}	x_{10} x 10^4	y_{10} x10^4	L (cd/m^2)	CCT	Type	Ra	Group
Illuminant										
CIE D65	94.81	100	107.32	3138	3310		6500			
CIE A	111.15	100	35.20	4512	4059		2856			
Source										
Real A	115.19	100	23.75	4821	4185	340	2544			
Thorn D65+	96.46	100	108.62	3162	3278	340	6461	F7	95	B
Philips TL84	103.07	100	64.29	3855	3740	730	4019	F11	85	T
Philips TL83	112.49	100	39.54	4463	3968	680	2937	F12	85	T
Thorn p27	114.37	100	26.41	4749	4153	700	2684	F12	82	T
Thorn p30	112.85	100	34.49	4563	4043	590	2959	F4	51	N
Thorn W	107.91	100	49.31	4195	3888	760	3477	F3	54	N
Thorn WW	112.84	100	41.42	4437	3933	600	3056	F4	51	N
Thorn CW	101.56	100	63.05	3838	3779	650	4205	F6	58	N

Note: CCT: Correlated colour temperature.
Ra: CIE Colour rendering index.
Group: B: Broad-band, N: Normal-band, T: Three-band.
Type: N (F1-F6), B(F7-F9), and T(F10-F12).
+: Thorn artificial daylight.

Table 3.1.4 Mean CMC(2:1) ΔE values for the instrumental, visual and overall metamers.

		Illuminant		Source								
Metamers	pairs	D65	A	D65	A	TL84	TL83	P27	P30	W	WW	CW
Instrumental	55	0.9	6.0	1.4	7.2	3.5	4.5	5.0	4.4	3.3	4.0	2.5
Visual	21	2.2	5.0	2.0	6.3	3.7	4.0	4.3	4.8	4.0	4.5	4.0
Overall	76	1.3	5.7	1.5	7.0	3.5	4.4	4.8	4.5	3.5	4.1	2.9

Table 3.2.1 The match points on D-H Color Rule under sources (a) D65, (b) A, and (c) TL84.

(a) D65 Source

Observer	Numbered Scale	Lettered Scale	Conversion of Lettered Scale to Numbered Scale	Total Score
1	8.0	G	7.0	15.0
2	7.0	G	7.0	14.0
3	7.0	F	6.0	13.0
4	9.0	D	4.0	13.0
5	11.0	D	4.0	15.0
6	9.0	G	7.0	16.0
7	9-10 (9.5)	D	4.0	13.5
8	11.0	D	4.0	15.0
9	10.0	F	6.0	16.0
10	9.0	C	3.0	12.0
11	12.0	C	3.0	15.0
12	10-11 (10.5)	D-E	4.5	14.5
13	7.0	F	6.0	13.0
Mean				14.2

Table 3.2.1 Continued.

(b) A Source

Observer	Numbered Scale	Lettered Scale	Conversion of Lettered Scale to Numbered Scale	Total Score
1	18.0	O	15.0	33.0
2	20.0	J	10.0	30.0
3	19.0	K	11.0	30.0
4	20.0	K	11.0	31.0
5	21.0	K-L	11.5	32.5
6	18.0	P-Q	16.5	34.5
7	20-21 (20.5)	P-Q	16.5	37.0
8	21.0	M	13.0	34.0
9	20-21 (20.5)	M	13.0	33.5
10	19.0	L	12.0	31.0
11	21.0	L-M	12.5	33.5
12	19-20 (19.5)	L-M	12.5	32.0
13	19.0	K	11.0	30.0
Mean				32.5

(c) TL84 Source

Observer	Numbered Scale	Lettered Scale	Conversion of Lettered Scale to Numbered Scale	Total Score
1	11.0	B	2.0	13.0
2	13.0	C	3.0	16.0
3	11.0	D	4.0	15.0
4	11.0	B-C	2.5	13.5
5	13.0	B	2.0	15.0
6	13.0	D	4.0	17.0
7	13-14 (13.5)	A-B	1.5	15.0
8	13.0	C	3.0	16.0
9	11-12 (11.5)	D-E	4.5	16.0
10	12-13 (12.5)	C	3.0	15.5
11	13-14 (13.5)	D	4.0	17.5
12	10-11 (10.5)	C-D	3.5	14.0
13	11.0	C	3.0	14.0
Mean				15.2

Table 3.4.1 The cross-over wavelengths for 76 metamers.

Pair No.	Formula (dye codes)		Cross-over Wavelengths (nm)					
	STD	BATCH	450	540	610	Others		
1	(502,505,508)	(500,505,506)	455	525	605			
2	(502,503,508)	(500,505,506)	460	540	610			
3	(502,503,508)	(500,505,506)	455	520	605			
4	(500,504,505)	(503,509,510)	460	550	610	700		
5	(500,504,505)		450	560	620			
6	(502,504,506)	(500,504,505)	455	530	605			
7	(500,504,509)	(502,503,509)	450	540	595			
8	(500,504,506)	(502,503,509)	450	540	605			
9	(502,503,508)	(501,505,506)	450	540	605			
10	(502,505,509)	(500,504,505)	455	530	600			
11	(500,504,505)	(502,509,510)	455	535	610			
12	(502,504,506)	(502,503,509)	455	530	610			
13	(500,504,505)	(502,509,510)	455	545	605			
14	(502,509,510)	(500,503,504)	460	545	610			
15	(500,509,510)	(502,504,505)	455	520	620	570		
16	(500,503,509)	(502,505,510)	450	520	615	570		
17	(500,503,504)	(502,509,510)	455	545	610			
18	(502,509,510)	(500,504,505)	455	555	610			
19	(502,503,508)	(500,504,505)	460	540	600			
20	(500,502,505)	(500,504,505)	465	535	595	650		
21	(500,502,507)	(500,504,505)	465	535	595			
22	(500,502,509)	(500,505,506)	460	535	605			
23	(500,502,509)	(500,505,508)	460	530	605			
24	(500,502,507)	(500,504,506)	460	530	590			
25	(500,502,509)	(500,506)	460	535	600			
26	(500,502,509)	(500,505,509)	470	535	590			
27	(502,508,509)	(500,505,506)	450	530	590			
28	(500,502,509)	(500,506)	460	530	595			
29	(500,504,506)	(502,503,509)	455	530	595			
30	(502,506,508)		460	530	590	675		
31	(502,503,509)	(500,505,506)	455	530	600			
32	(502,504,509)	(500,503,505)	455	530	590			
33	(500,506,508)	(500,502,508)	460	520		585		
34	(500,506,508)	(500,505,506)	460	530	605			
35	(500,504,506)	(502,503,508)	455	525	590			
36	(500,505,507)	(502,503,508)	450	530	590	415	425	675
37	(502,503,508)	(500,505,506)	455	530	600			
38	(500,503,506)	(503,508)	455	535	600	410	430	
39	(502,503,508)	(502,504,507)	460	530		430	570	
40	(503,505,508)	(505,506)	440	550		410	570	

NOTES: 500----SANDOLAN YELLOW E-2GL
501----TECTILON YELLOW 4R200
502----SANDOLAN ORANGE E-GL
503----SANDOLAN RHODINE E-2GL172%
504----SANDOLAN RUBINOL E-3GPL
505----SANDOLAN VIOLET E-2R
506----SANDOLAN BLUE E-HRL
507----SANDOLAN BLUE E-2GL200
508----SANDOLAN TURQUOISE E-VR300
509----SANDOLAN BRILLIANT GREEN E-B400
510----LISS SCARLET 3B

.....to be continued

Table 3.4.1 Continued.

Pair No.	Formula (dye codes)		Cross-over Wavelengths (nm)				
	STD	BATCH	450	540	610	Others	
41	(503,505,508)	(500,505,506)	440	550		405	570
42	(503,505,508)	(503,506)	430			410	490
43	(503,508,510)	(504,507)	470	540	590	430	675
44	(502,503,508)	(500,505,506)	460	535	610		
45	(503,508,509)	(500,505,506)	460	535	610		
46	(503,505,508)	(500,505,506)	460	530	610		
47	(500,505,506)	(503,506)	450	535	605	420	
48	(502,503,508)	(500,505,508)	450	530	605		
49	(503,508,509)	(506,510)	460	550	600	410	430
50	(502,503,508)	(501,505,506)	465	535	610		
51	(500,504,505)	(503,508)	460	540	610		
52	(500,504,506)	(502,503,509)	450	550	605		
53	(503,507,509)	(506,510)	435		620	570	
54	(502,503,508)	(501,505,506)	460	540	610		
55	(500,506,508)	(500,502,509)	460	525	610		
56	(502,503,509)	(500,505,506)	450	530	600		
57	(500,502,509)	(500,506,508)	470	540	600		
58	(500,504,508)	(500,505,506)	460	540	620		
59	(502,504,507)	(500,505,506)	460	530	610		
60	(500,504,508)	(500,505,506)	440	540	610		
61	Missing	Missing	450	530	630	410	
62	(501,504,507)	(500,504,505)	430	550	620		
63	(501,503,508)	(502,503,509)	450	530	610		
64	(500,504,506)	(502,503,509)	450	540	610		
65	(500,504,509)	(502,503,509)	460	550	610		
66	(500,502,507)	(500,505,506)	460	530	610		
67	(500,502,509)	(500,506)	460	520	610		
68	(501,503,508)	(500,505,506)	450	540	610		
69	(500,502,509)	(500,506)	460	540	600		
70	(500,502,508)	(500,503,505)	460	530	600		
71	(501,503,507)	(502,503,508)	450	530		580	680
72	(501,506,508)	(502,503,508)	460	530	600		
73	(502,504,506)	(500,505,506)	450	540	610		
74	(501,504,509)	(500,505,506)	460	520	620		
75	(502,505,506)	(503,508)	470	550	620	400	420
76	(500,504,506)	(502,503,509)	450	550	610		
Mean			455	536	605		

Table 3.4.2a Individual observer precision performance (PF/4 measure) for Experiment I.

Observer	D65	A	TL84	TL83	W	WW	P27	Mean	Rank
RL	37	28	34	24	27	25	24	28	4
WD	41	40	32	41	38	37	40	38	11
MA	24	32	25	28	28	33	---	28	4
BN	---	---	---	---	---	---	40	40	12
WA	39	47	36	---	---	---	---	41	13
KE	---	---	---	39	35	30	29	33	10
YU	29	28	19	23	19	21	24	23	2
L I	31	29	---	---	---	---	---	30	7
GR	---	---	31	37	27	29	27	30	7
KN	29	26	25	26	30	34	36	29	6
TY	28	32	27	28	23	23	21	26	3
HN	38	38	30	31	33	23	29	32	9
WK	32	20	23	19	20	18	21	22	1

Note: The '-' represents no experiment conducted.

Table 3.4.2b Individual observer precision performance (PF/4 measure) for Experiment II.

Observer	D65	A	TL84	Mean	Rank
RL	29	21	24	25	4
WD	40	37	43	40	10
BN	38	33	42	38	9
KE	34	30	22	29	7
YU	21	24	19	21	1
GR	37	21	21	26	5
WA	---	37	42	40	10
KN	31	---	---	31	8
TY	24	22	22	23	3
HN	35	21	28	28	6
WK	26	19	18	21	1

Note: The '-' represents no experiment conducted.

Table 3.4.3a Individual observer's repeatability performance (PF/4 measure) for Experiment I.

Observer	D65	A	TL84	TL83	W	WW	P27	Mean	Rank
RL	40	30	35	26	33	25	23	30	3
WD	58	47	41	45	34	35	33	42	11
MA	28	38	22	26	30	28	---	29	2
BN	---	---	---	---	---	---	33	33	9
WA	44	40	46	---	---	---	---	43	12
KE	---	---	---	56	51	38	40	46	13
YU	41	31	27	28	29	28	30	31	5
L I	35	29	---	---	---	---	---	32	8
GR	---	---	28	34	35	30	30	31	5
KN	28	39	24	27	25	36	30	30	3
TY	32	27	29	36	36	31	27	31	5
HN	58	53	40	30	37	23	28	38	10
WK	27	25	17	23	22	24	20	23	1

Note: The '-' represents no experiment conducted.

Table 3.4.3b Individual observer's repeatability performance (PF/4 measure) for Experiment II.

Observer	D65	A	TL84	Mean	Rank
RL	34	22	29	28	6
WD	42	39	47	43	10
BN	39	35	33	36	9
KE	43	33	29	35	8
YU	19	29	22	23	2
GR	30	26	24	27	4
WA	---	52	53	53	11
KN	27	---	---	27	4
TY	20	34	22	25	3
HN	51	24	25	33	7
WK	21	17	15	18	1

Note: The '-' represents no experiment conducted.

Table 3.4.4a Individual observer's between-observer error (PF/4 measure) for Experiment I.

Observer	D65	A	TL84	TL83	W	WW	P27	Mean	Rank
RL	43	37	37	33	32	34	34	36	4
WD	44	47	36	46	45	43	49	44	11
MA	37	40	36	38	36	40	---	38	7
BN	---	---	---	---	---	---	44	44	11
WA	46	54	41	---	---	---	---	47	13
KE	---	---	---	42	37	36	36	38	7
YU	37	37	28	33	28	31	32	32	1
L I	41	38	---	---	---	---	---	40	10
GR	---	---	38	43	33	36	37	37	5
KN	39	34	34	35	39	41	45	38	7
TY	37	41	33	34	30	31	32	34	3
HN	42	41	34	37	38	32	37	37	5
WK	41	33	33	32	31	28	32	33	2

Note: The '-' represents no experiment conducted.

Table 3.4.4b Individual observer's between-observer error (PF/4 measure) for Experiment II.

Observer	D65	A	TL84	Mean	Rank
RL	39	29	32	33	3
WD	48	43	48	46	11
BN	45	36	44	42	9
KE	41	27	31	36	6
YU	34	31	29	31	1
GR	46	31	32	36	6
WA	---	39	45	42	9
KN	41	---	---	41	8
TY	37	28	32	32	2
HN	40	29	34	34	5
WK	37	31	31	33	3

Note: The '-' represents no experiment conducted.

Table 3.4.5 Observer variation performance (PF/4 measure).

Experiment	D65	A	TL84	TL83	P27	W	WW	Mean
			Observer Precision					
ΔV_T	33	32	28	29	28	27	29	29
ΔV_I	32	27	28	-	-	-	-	29
			Within-observer error					
ΔV_T	39	36	31	33	33	30	29	33
ΔV_I	33	31	30	-	-	-	-	31
			Between-observer error					
ΔV_T	41	40	35	37	35	35	38	37
ΔV_I	41	32	36	-	-	-	-	36

Note: The '-' represents no experiment conducted.

Table 3.4.6 Error analysis for three individual colour-difference components (ΔV_L, ΔV_C and ΔV_H) of Experiment II.

	D65		A		TL84		Mean	
	r	WD%	r	WD%	r	WD%	r	WD%
ΔV_L	0.71	24	0.57	37	0.77	28	0.68	30
ΔV_C	0.60	31	0.90	11	0.83	19	0.78	20
ΔV_H	0.74	18	0.95	3	0.93	7	0.87	9

Note: r: correlation coefficient, WD%: wrong decision.

Table 3.4.7 Type I IMIs' performance in terms of PF/4 measure.

Weighting Functions		CIE L*a*b*	CMC(1:1)	CIE94	BFD(1:1)	Observer Precision
			Experiment I			
D65	Real source	45	40	41	37	33
	CIE illuminant	65	62	63	62	
A	Real source	26	25	15	22	32
	CIE illuminant	28	27	19	24	
TL84	Real source	37	25	26	25	28
	ASTM	31	21	20	21	
TL83	Real source	31	21	22	20	29
W	Real source	36	28	31	24	28
WW	Real source	32	25	26	21	27
P27	Real source	32	20	22	21	29
Mean		37	30	29	28	29
			Experiment II			
D65	Real source	44	43	43	41	32
	CIE illuminant	61	62	62	62	
A	Real source	28	24	15	19	27
	CIE illuminant	28	25	18	21	
TL84	Real source	38	25	27	26	28
	ASTM	32	22	21	22	
Mean		39	34	31	32	29

Note: IMIs: Illuminant Metamerism Indices.

Table 3.4.8 Scaling factors for each formula in comparison Type I IMIs with ΔV_T and ΔV_I results under the illuminants and sources investigated.

	Weighting Functions	CIE L*a*b*	CMC(1:1)	CIE94	BFD(1:1)
			Experiment I		
D65	Real source	0.97	1.22	1.43	0.97
	CIE illuminant	1.01	1.22	1.43	0.96
A	Real source	0.83	0.87	1.24	0.69
	CIE illuminant	1.00	1.06	1.49	0.84
TL84	Real source	0.91	1.26	1.50	0.91
	ASTM source	0.82	1.11	1.33	0.79
TL83	Real source	0.86	1.14	1.36	0.81
W	Real source	0.86	1.02	1.14	0.83
WW	Real source	0.90	1.05	1.20	0.83
P27	Real source	0.83	1.13	1.34	0.78
MSF		0.90	1.11	1.35	0.84
			Experiment II		
D65	Real source	0.70	0.87	1.03	0.70
	CIE illuminant	0.74	0.88	1.03	0.69
A	Real source	0.72	0.76	1.08	0.60
	CIE illuminant	0.87	0.93	1.30	0.73
TL84	Real source	0.83	1.15	1.36	0.83
	ASTM	0.74	1.00	1.21	0.71
MSF		0.77	0.93	1.17	0.71

Note: MSF: Mean of scaling factor.
IMIs: Illuminant Metamerism Indices.

Table 3.4.9 Performance of Type I IMIs multiplied with the mean scaling factor for each formula in terms of PF/4 measure.

	Weighting Functions	CIE L*a*b*	CMC(1:1)	CIE94	BFD(1:1)	Observer Precision
			Experiment I			
D65	Real source	50	45	44	44	33
	CIE illuminant	76	73	72	75	--
RA	Real source	27	30	17	24	32
	CIE illuminant	30	31	23	27	--
TL84	Real source	40	29	29	30	28
	ASTM	33	23	21	24	--
TL83	Real source	31	22	22	21	29
W	Real source	37	29	33	25	28
WW	Real source	33	25	28	22	27
P27	Real source	33	22	23	23	29
Mean		39	33	31	32	29
MSF		0.90	1.11	1.35	0.84	
			Experiment II			
D65	Real source	46	46	45	43	32
	CIE illuminant	68	69	68	70	--
RA	Real source	29	28	17	22	27
	CIE illuminant	31	28	21	24	--
TL84	Real source	41	30	30	30	28
	ASTM	33	23	22	23	--
Mean		41	37	34	35	29
MSF		0.77	0.93	1.17	0.71	

Note: MSF: Mean of scaling factor.
IMIs: Illuminant Metamerism Indices.

Table 3.4.10a Type II IMIs' performance (PF/4 measure) using Experiment II results.

	Weighting Functions	CIE L*a*b*	CMC(1:1)	CIE94	BFD(1:1)	Observer Precision
			Experiment II			
A	Real source	27	26	18	22	26
	CIE illuminant	25	25	18	21	-
TL84	Real source	41	34	34	37	27
	ASTM	33	30	30	31	-
Mean		32	29	25	28	27

Note: IMIs: Illuminant Metamerism Indices.

Table 3.4.10b Scaling factors for each formula in comparison Type II IMIs with the Experiment II visual results.

	Weighting Functions	CIE L*a*b*	CMC(1:1)	CIE94	BFD(1:1)
A	Real source	0.66	0.69	0.98	0.55
	CIE illuminant	0.80	0.83	1.17	0.66
TL84	Real source	0.77	1.02	1.26	0.73
	ASTM	0.68	0.86	1.07	0.62
MSF		0.73	0.85	1.12	0.64

Note: MSF: Mean of scaling factor.
IMIs: Illuminant Metamerism Indices.

Table 3.4.10c Performance of Type II IMIs multiplied with MSF for each formula in terms of PF/4 measure.

	Weighting Functions	CIE L*a*b*	CMC(1:1)	CIE94	BFD(1:1)	Observer Precision
			Experiment II			
RA	Real source	35	39	28	25	26
	CIE illuminant	26	31	21	24	
TL84	Real	43	36	36	42	27
	ASTM	38	34	34	32	
Mean		36	35	30	31	27
MSF		0.73	0.87	1.13	0.65	

Note: MSF: Mean of scaling factor.
IMIs: Illuminant Metamerism Indices.

Table 3.4.11 Performance of Type III IMIs in predicting the visual results of Experiments I and II under all sources investigated in terms of PF/4 measure.

	Chromatic Adaptation Transform	CIE L*a*b*	CMC(1:1)	CIE94	BFD(1:1)	Observer Precision
			Experiment I			
A	von Kries	27	29	21	25	32
	Bartleson	25	24	17	22	
	CIE	28	28	23	27	
	BFD	30	29	21	25	
	Hunt	27	27	22	25	
	CIE L*a*b*	26	25	15	20	
	RLAB	28	31	22	27	
	KUO1	28	29	20	24	
	KUO2	26	27	21	26	
	KUO3	27	29	22	27	
TL84	von Kries	34	24	22	23	28
ASTM	Bartleson	32	24	21	23	
	CIE	33	23	22	23	
	BFD	33	23	21	22	
	Hunt	33	23	22	22	
	CIE L*a*b*	31	21	20	21	
	RLAB	34	24	22	23	
	KUO1	32	23	21	22	
	KUO2	33	24	22	24	
	KUO3	33	24	22	23	
TL83	von Kries	33	22	21	19	29
	Bartleson	32	22	18	19	
	CIE	32	24	23	21	
	BFD	31	21	20	18	
	Hunt	32	23	23	20	
	CIE L*a*b*	31	21	22	20	
	RLAB	33	24	22	19	
	KUO1	31	21	20	18	
	KUO2	32	23	21	19	
	KUO3	32	23	22	20	

Note: IMIs: Illuminant Metamerism Indices.

To be continued. .....

Table 3.4.11 Continued.

	Chromatic-Adaptation Transform	CIE L*a*b*	CMC(1:1)	CIE94	BFD(1:1)	Observer Precision
			Experiment I			
W	von Kries	33	27	27	22	28
	Bartleson	31	20	25	21	
	CIE	34	31	32	27	
	BFD	34	27	28	23	
	Hunt	35	31	32	26	
	CIE L*a*b*	36	28	31	24	
	RLAB	35	29	30	24	
	KUO1	34	28	29	23	
	KUO2	32	26	27	22	
	KUO3	34	28	29	24	
WW	von Kries	29	24	22	19	27
	Bartleson	26	18	18	17	
	CIE	30	30	29	24	
	BFD	30	25	23	20	
	Hunt	31	30	28	24	
	CIE L*a*b*	32	25	26	21	
	RLAB	31	27	26	22	
	KUO1	30	25	24	20	
	KUO2	28	24	22	20	
	KUO3	30	26	25	21	
P27	von Kries	36	23	22	21	29
	Bartleson	35	23	20	22	
	CIE	35	25	26	25	
	BFD	33	21	20	19	
	Hunt	35	24	24	23	
	CIE L*a*b*	32	20	21	21	
	RLAB	35	24	22	20	
	KUO1	32	20	20	19	
	KUO2	35	23	22	22	
	KUO3	34	23	22	21	

To be continued. .....

Table 3.4.11 Continued.

	Chromatic-Adaptation Transform	CIE L*a*b*	CMC(1:1)	CIE94	BFD(1:1)	Observer Precision
			Experiment II			
A	von Kries	29	28	20	24	26
	Bartleson	26	22	16	20	
	CIE	30	28	23	26	
	BFD	32	28	20	24	
	Hunt	29	26	21	24	
	CIE L*a*b*	28	24	15	19	
	RLAB	30	30	22	26	
	KUO1	30	27	19	22	
	KUO2	28	26	20	24	
	KUO3	29	28	21	26	
TL84	von Kries	34	23	22	23	27
	Bartleson	33	23	21	23	
	CIE	33	23	22	23	
	BFD	33	23	21	22	
	Hunt	34	23	22	23	
	CIE L*a*b*	32	22	21	22	
	RLAB	34	24	22	23	
	KUO1	33	23	21	22	
	KUO2	34	24	22	24	
	KUO3	34	24	23	23	

Table 3.5.1 Colour-matching functions of the CIE 1964 ($\bar{x}_{10}$, $\bar{y}_{10}$ and $\bar{z}_{10}$) and the new SDO ($\bar{x}'$, $\bar{y}'$ and $\bar{z}'$) together with their differences ($\Delta\bar{x}'$, $\Delta\bar{y}'$ and $\Delta\bar{z}'$).

Wavelength (nm)	$\bar{x}_{10}$	$\Delta\bar{x}'$	$\bar{x}'$	$\bar{y}_{10}$	$\Delta\bar{y}'$	$\bar{y}'$	$\bar{z}_{10}$	$\Delta\bar{z}'$	$\bar{z}'$
400	0.016	0.033	0.049	0.002	0.023	0.025	0.069	0.008	0.077
420	0.214	0.034	0.248	0.022	0.017	0.039	1.024	0.033	1.057
440	0.374	-0.029	0.345	0.061	0.012	0.073	1.920	-0.003	1.917
460	0.301	-0.152	0.149	0.130	0.008	0.138	1.751	0.006	1.757
480	0.088	0.051	0.139	0.255	-0.014	0.241	0.815	0.011	0.826
500	0.004	0.068	0.072	0.467	-0.027	0.440	0.218	-0.009	0.209
520	0.119	0.077	0.196	0.760	0.038	0.798	0.057	-0.017	0.040
540	0.377	-0.071	0.306	0.963	-0.013	0.950	0.013	0.003	0.016
560	0.711	0.050	0.761	1.000	-0.012	0.988	0.000	0.013	0.013
580	1.026	-0.006	1.020	0.880	0.040	0.920	0.000	0.099	0.099
600	1.124	0.100	1.224	0.661	0.064	0.725	0.000	0.014	0.014
620	0.861	-0.009	0.852	0.402	-0.027	0.375	0.000	0.035	0.035
640	0.442	0.025	0.467	0.184	0.012	0.196	0.000	0.024	0.024
660	0.154	-0.010	0.144	0.060	0.008	0.068	0.000	0.003	0.003
680	0.043	-0.002	0.041	0.017	0.009	0.026	0.000	0.015	0.015
700	0.010	0.020	0.030	0.004	0.014	0.018	0.000	0.002	0.002

Table 3.5.2 Performance of Type I IMIs calculated from the CIE 1964 Observer, the CIE SDO and the new SDO in terms of PF/4 measure using the author's data.

CMF	CIE L*a*b*			CMC(1:1)			CIE94			BFD(1:1)			Observer Precision
	New SDO	CIE 1964	CIE SDO	New SDO	CIE 1964	CIE SDO	New SDO	CIE 1964	CIE SDO	New SDO	CIE 1964	CIE SDO	
						Experiment I							
D65	37	45	48	27	40	40	28	41	41	25	37	36	33
A	22	26	26	22	25	25	15	15	15	20	20	20	32
TL84	32	36	33	24	26	25	24	27	24	24	26	25	28
TL83	28	30	28	23	22	22	22	23	22	20	21	21	29
P27	29	31	29	22	21	21	22	22	21	21	21	21	28
W	30	36	33	23	28	26	27	31	28	20	25	22	27
WW	27	32	30	21	25	24	23	26	24	18	21	20	29
Mean	29	34	32	23	27	26	23	26	25	21	24	24	29
						Experiment II							
D65	34	44	42	27	44	37	28	43	38	26	41	34	32
A	23	28	29	20	24	24	14	15	15	18	19	19	27
TL84	34	38	35	25	26	26	25	28	26	25	27	26	28
Mean	30	37	39	24	31	29	22	29	26	23	29	26	29

Note: CMF: colour-matching functions.

Table 3.5.3 Summary of the Obande data in comparison with the author's data

Light Source	D65	TL84	A
Size of colour difference (CIE L*a*b*)			
Obande data	2.5	5.3	3.9
the author's data	2.1	4.8	7.8
Observer Precision (PF/4)			
Obande data	76	45	42
the author's data	33	28	32

Table 3.5.4 Performance of Type I IMIs calculated from the CIE 1964 Observer, the CIE SDO and the new SDO in terms of PF/4 measure using Obande data.

	CIE L*a*b*			CMC(1:1)			CIE94			BFD(1:1)			Observer
CMF	New SDO	CIE 1964	CIE SDO	New SDO	CIE 1964	CIE SDO	New SDO	CIE 1964	CIE SDO	New SDO	CIE 1964	CIE SDO	Precision
D65	57	60	59	63	63	63	55	58	56	59	60	60	76
A	30	31	31	29	31	31	27	28	28	25	27	28	45
TL84	37	40	38	33	37	35	36	39	37	32	36	33	42
Mean	41	44	43	42	44	43	39	42	40	39	41	40	54

Note: CMF: colour-matching functions.

Table 3.5.5 In comparison the OMIs calculated from the new SDO with those from the CIE SDO using the author's and Obande's metamers.

	CIE L*a*b*		CMC(1:1)		CIE94		BFD(1:1)		Average	
SDO	New	CIE	New	CIE	New	CIE	New	CIE	New	CIE
				The author's metamers						
Mean	1.0	0.7	0.8	0.6	0.7	0.4	1.1	0.8	0.9	0.6
Max.	2.5	1.5	2.1	1.6	1.8	1.0	2.9	2.1	2.3	1.6
Min.	0.2	0.1	0.2	0.1	0.2	0.1	0.2	0.1	0.2	0.1
				Obande's metamers						
Mean	0.7	0.5	0.8	0.6	0.6	0.4	1.0	0.7	0.8	0.6
Max.	1.8	1.1	2.4	1.5	1.4	0.9	2.9	1.8	2.1	1.3
Min.	0.1	0.1	0.1	0.0	0.1	0.1	0.1	0.1	0.1	0.1

Note: Max.: the maximum degree of observer metamerism predicted by a particular SDO.

Min.: the minimum degree of observer metamerism predicted by a particular SDO.

SDO: standard deviate observer.

OMIs: Observer Metamerism Indices.

FIGURES

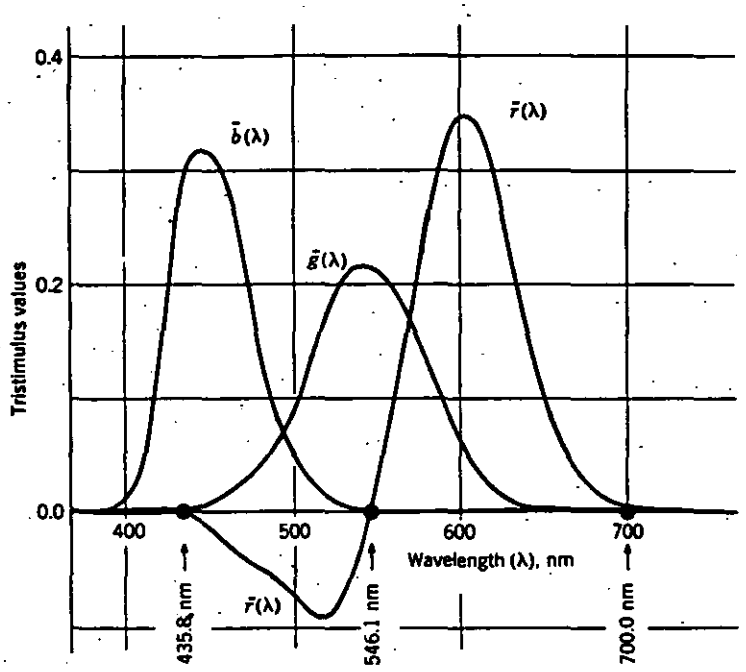

Fig. 1.2.1.1 The CIE 1931 $\bar{r}(\lambda)$, $\bar{g}(\lambda)$, $\bar{b}(\lambda)$ colour-matching functions.

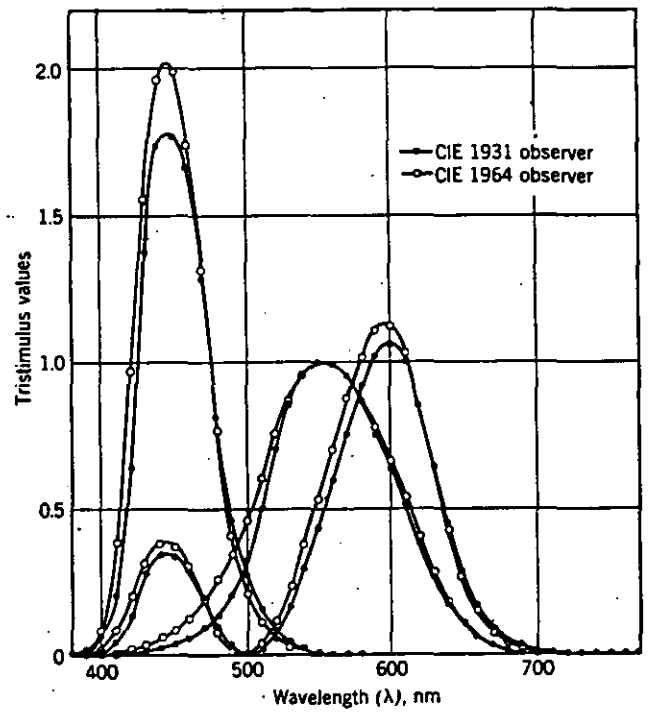

Fig. 1.2.1.2 The colour-matching functions of the CIE 1931 Standard Colorimetric Observer and the CIE 1964 Supplementary Standard Colorimetric Observer.

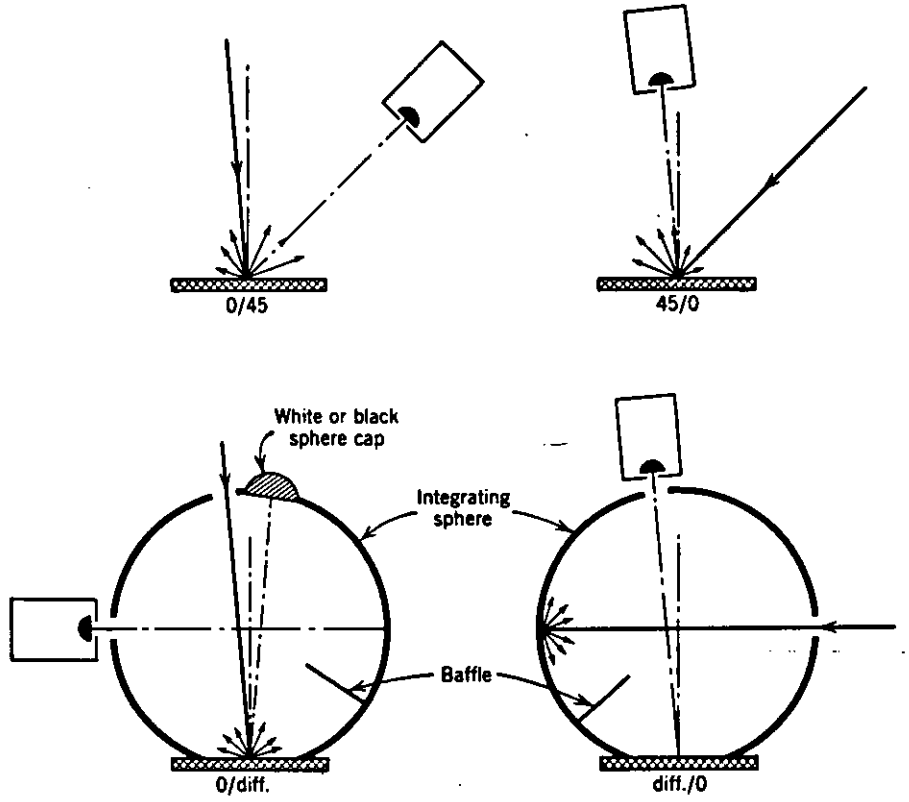

Fig. 1.2.1.3 The four CIE standard illuminating and viewing geometries for reflectance measurements.

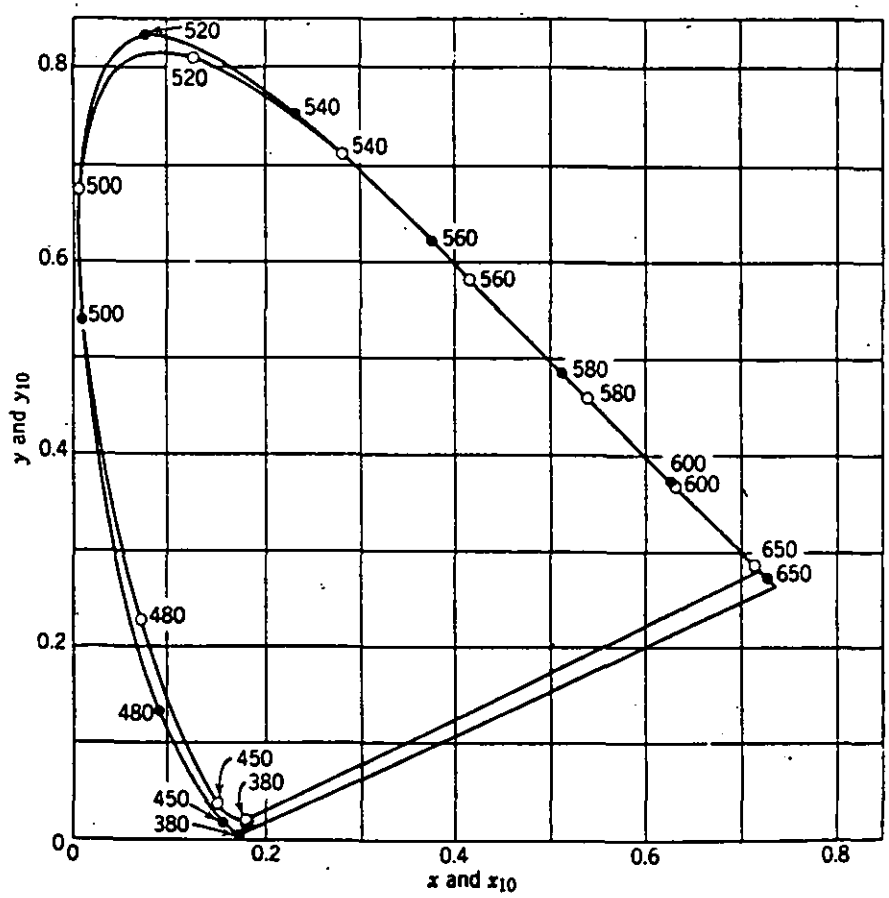

Fig. 1.2.1.4 CIE 1931 (x, y)-chromaticity diagram (•) and CIE 1964 (x_{10}, y_{10})-chromaticity diagram (o).

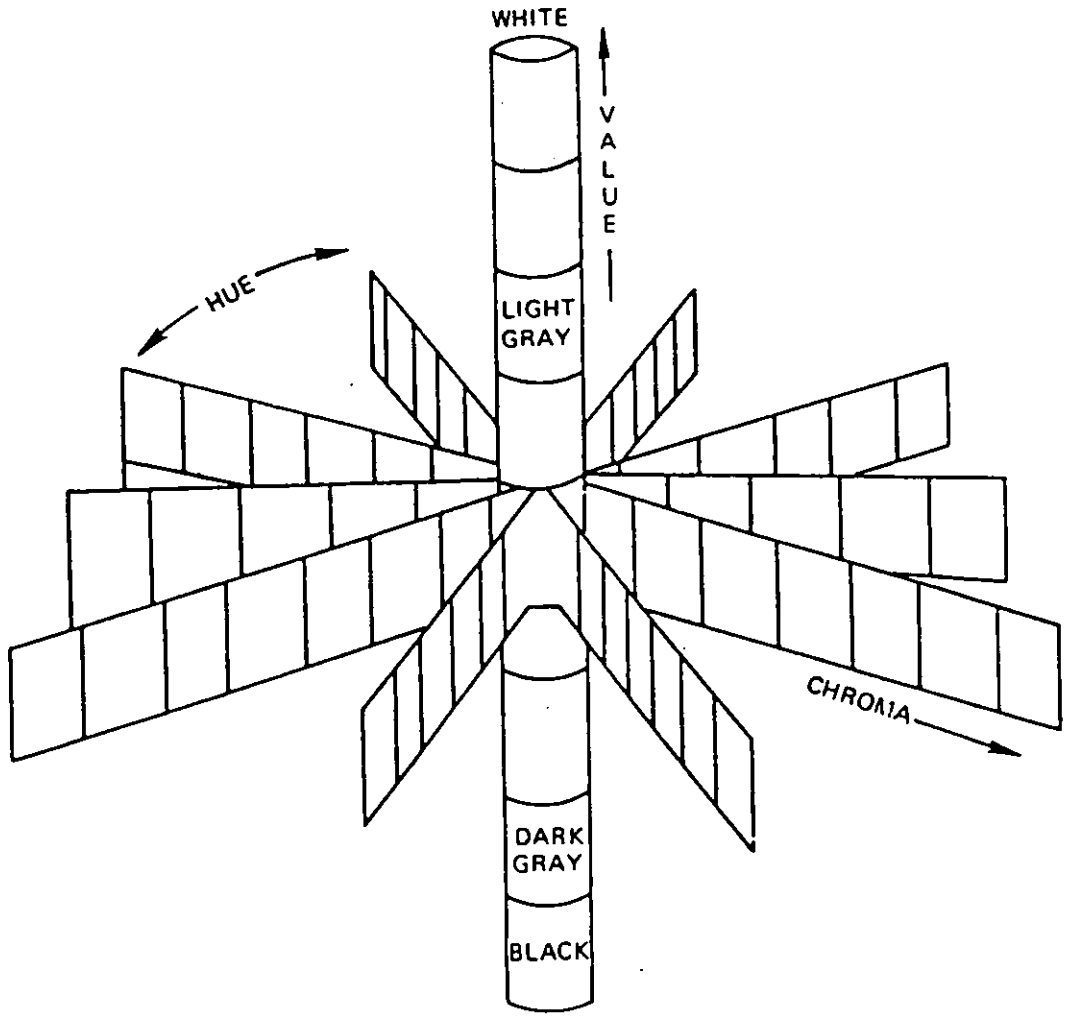

Fig. 1.2.2.1 The Munsell Colour System.

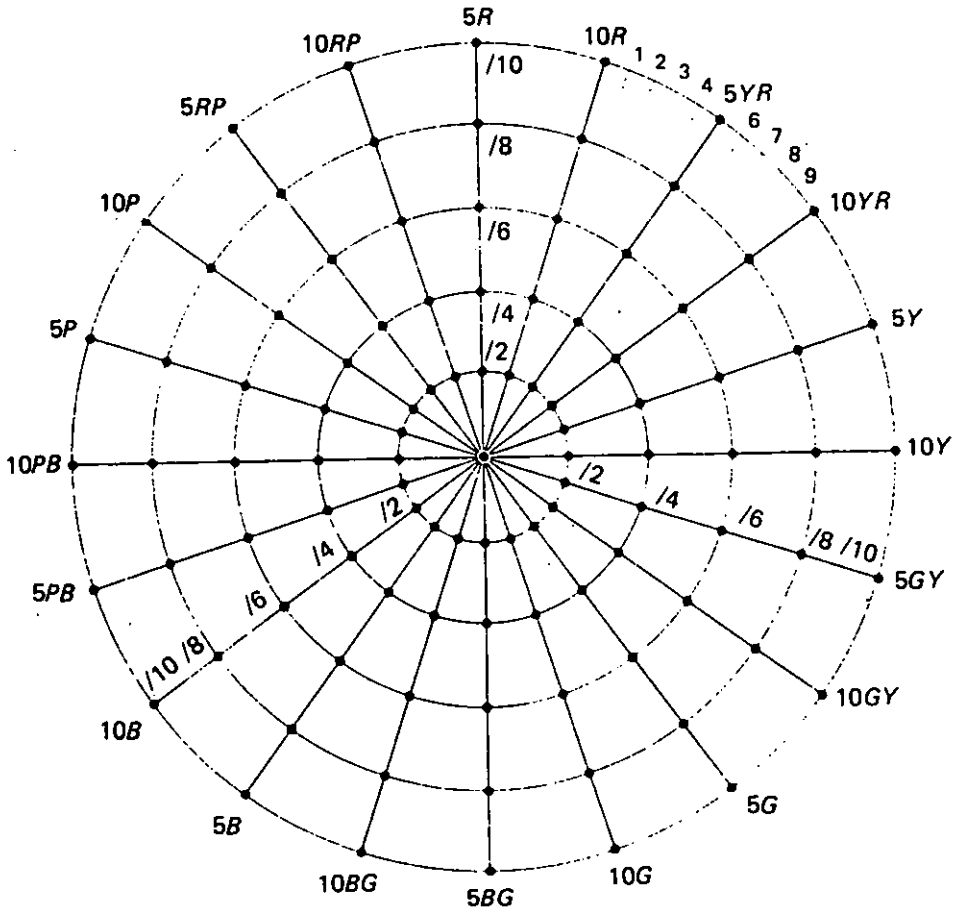

Fig. 1.2.2.2 Arrangement of Hue circle in Munsell Colour Order System.

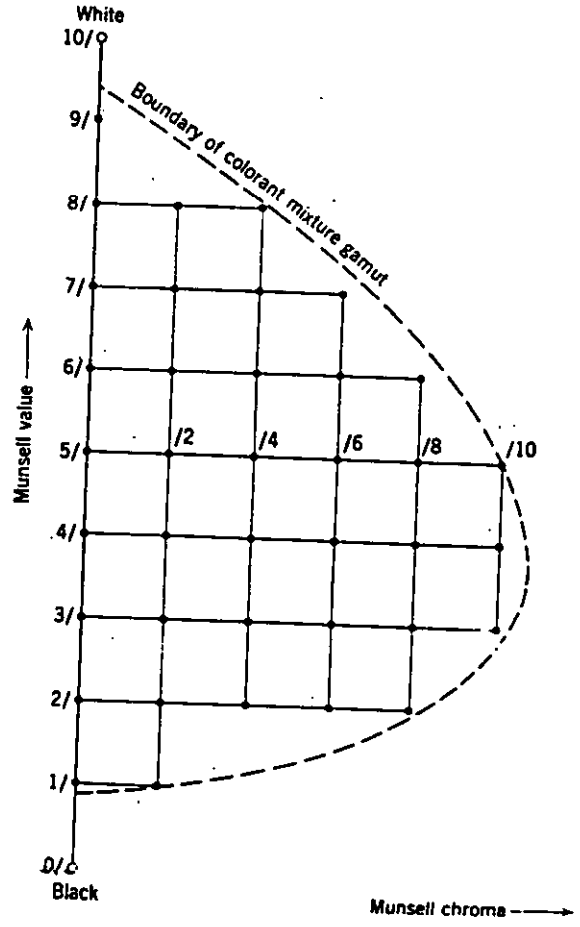

Fig. 1.2.2.3 Arrangement of colours with constant Hue in Munsell Colour Order System.

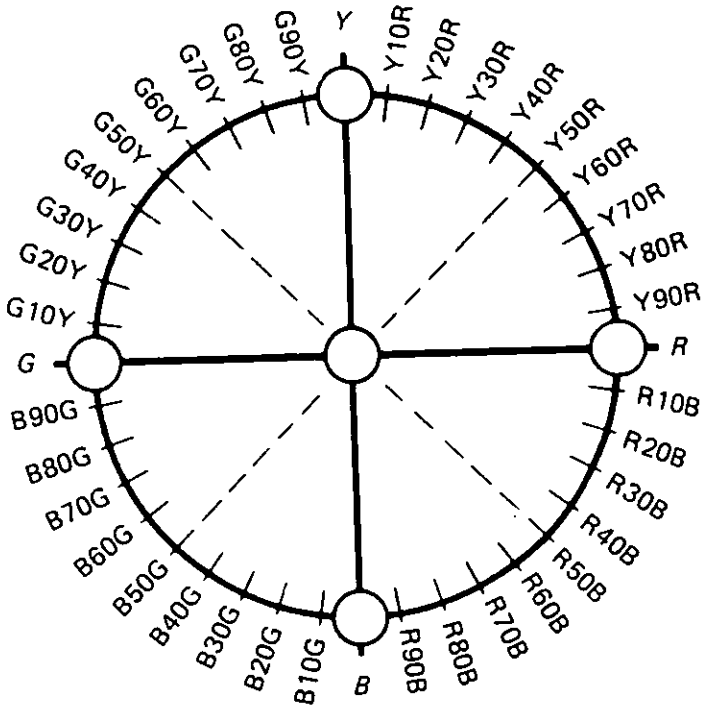

Fig. 1.2.3.1 Arrangement of hues in NCS.

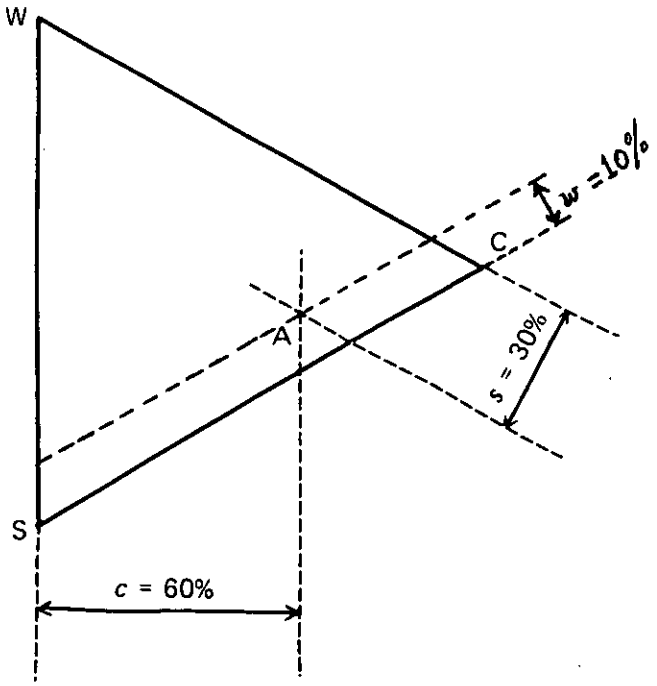

Fig. 1.2.3.2 Arrangement of colours on a NCS triangle.

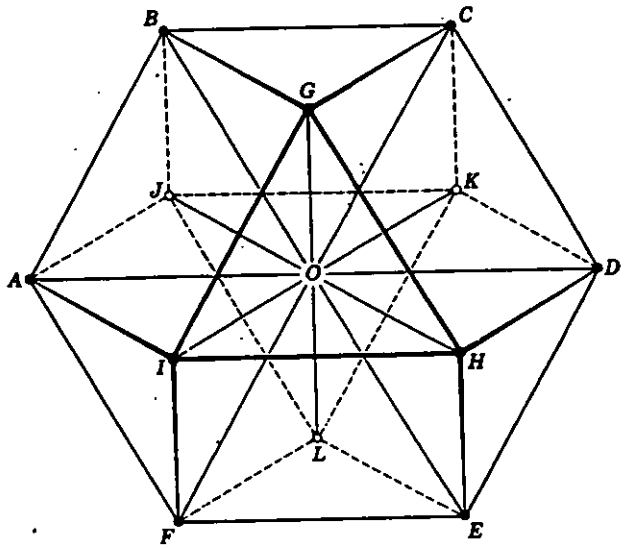

Fig. 1.2.4.1 The cubo-octahedral basis of the OSA colour system.

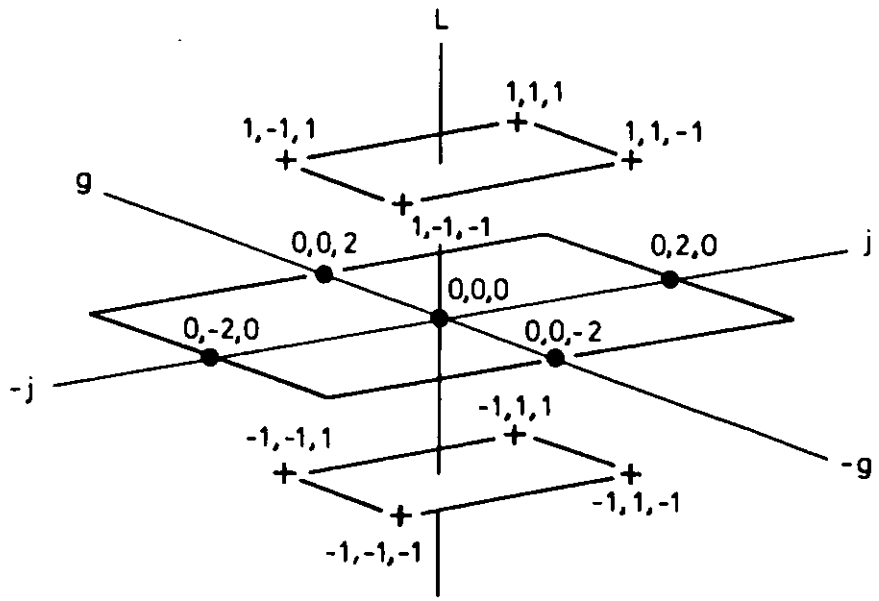

Fig. 1.2.4.2 The 13 points of a basic set in OSA colour space (corresponding to the corner points and central point of the cubo-octahedron in Fig. 1.2.4.1) and their notations (L, j, g).

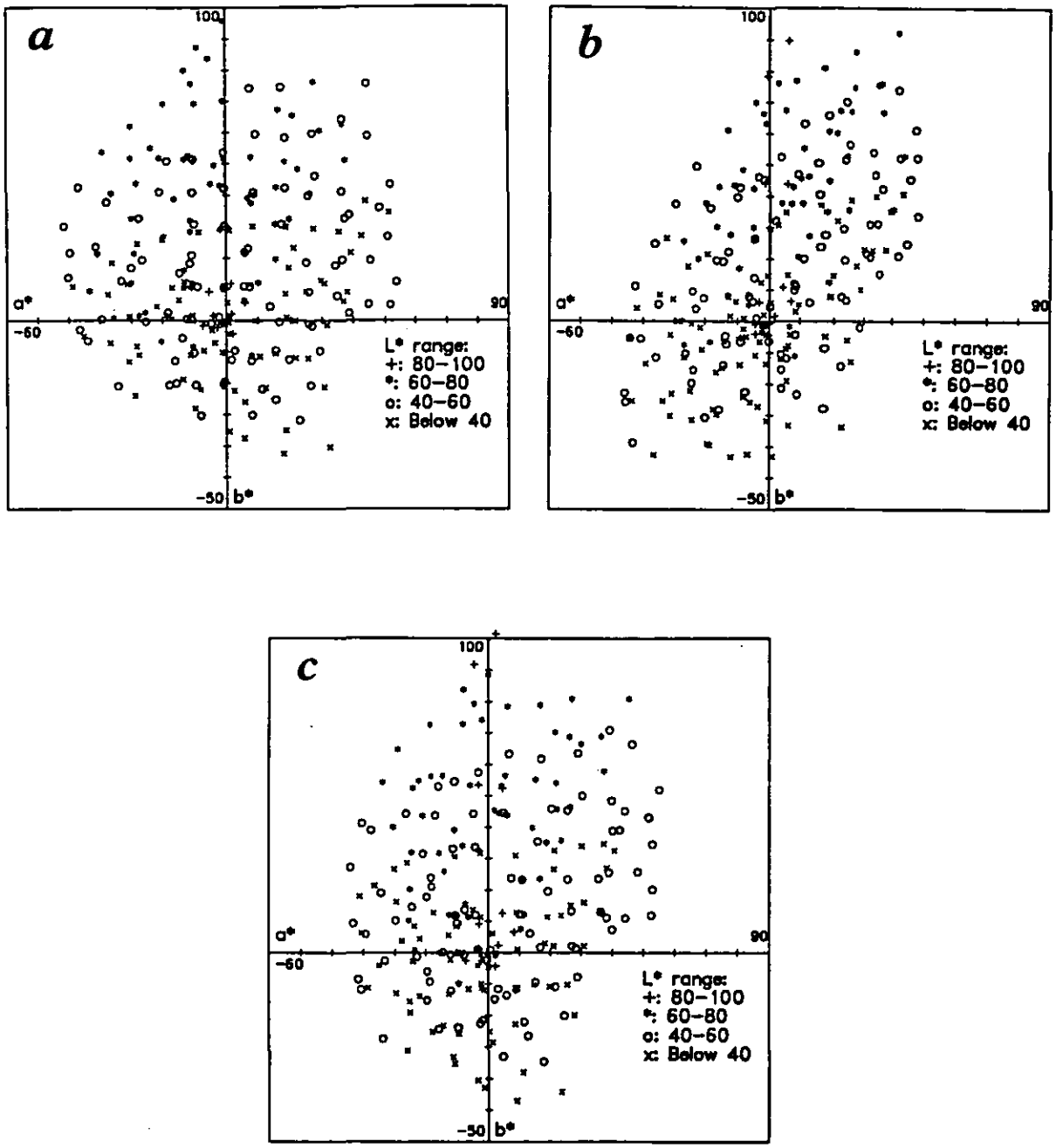

Fig. 2.1.1 240 test colours plotted in CIE a*b* diagram for three light sources, (a) D65, (b) A, (c) TL84. Different symbols represent colours within different L* ranges: '+' for 80-100, '*' for 60-80, 'o' for 40-60, and 'x': less than 40.

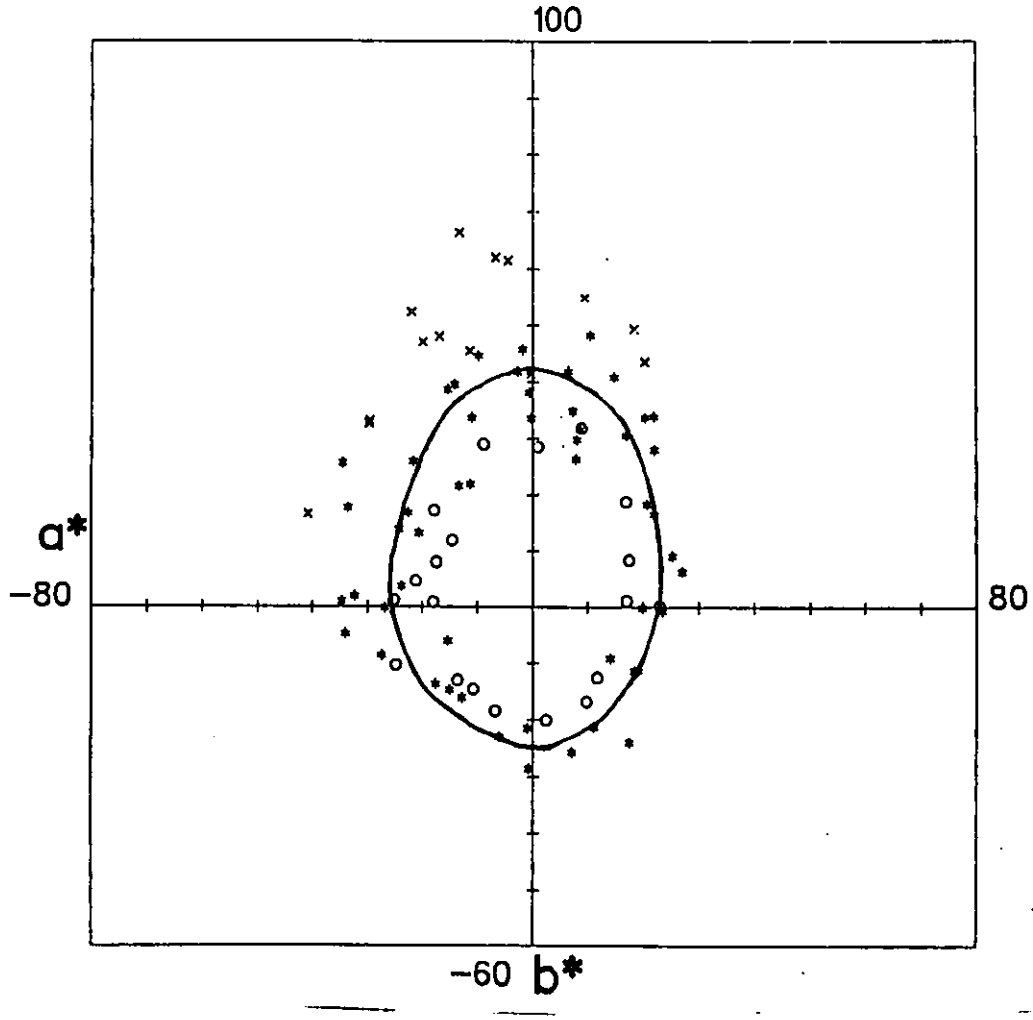

Fig. 2.2.1 The iso-colourfulness contour with a perceived colourfulness value 30 under D65 source plotted in CIE a*b* diagram. Symbols represent the colours within different L* ranges: '*' for 35-65, 'o' for 0-35, and 'x' for 65-100.

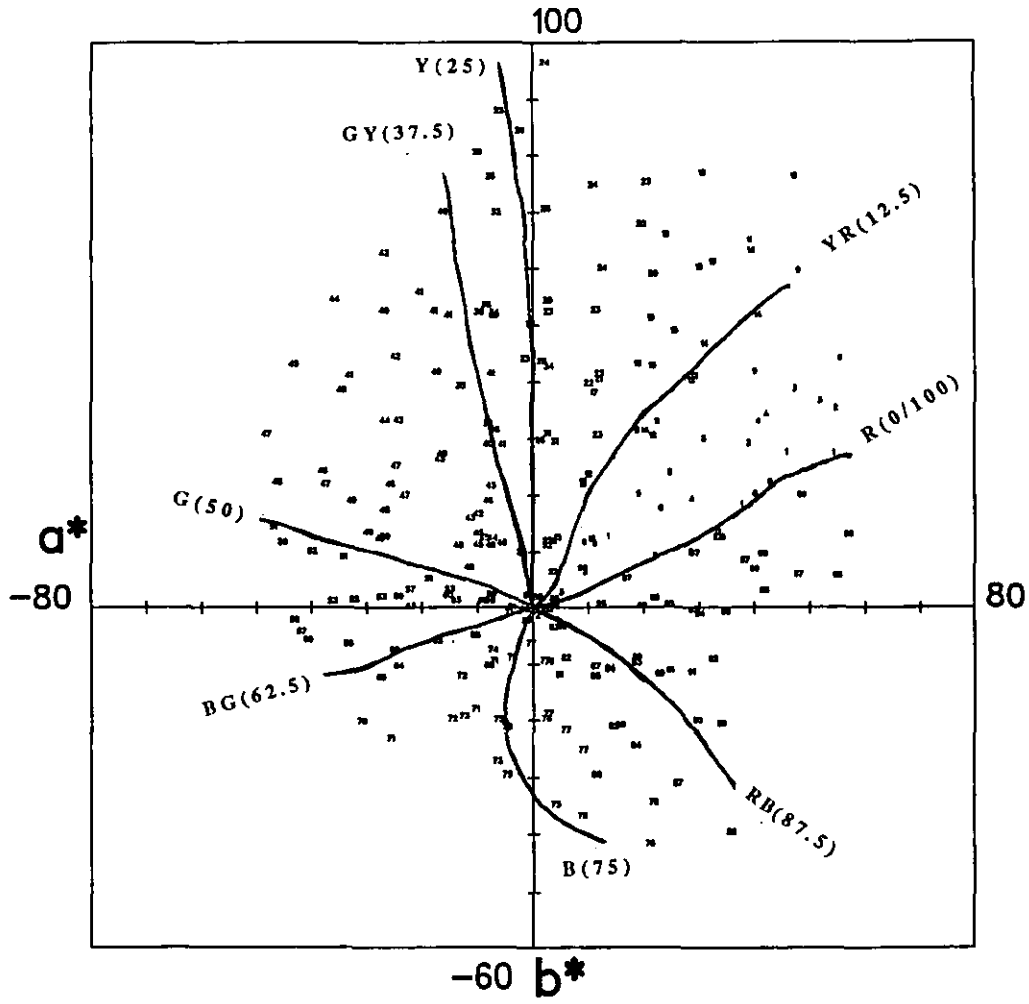

Fig. 2.2.2 The iso-hue loci plotted in CIE a*b* diagram under D65 source: 0/100 for R, 12.5 for YR, 25 for Y, 37.5 for GY, 50 for G, 65.6 for BG, 75 for B and 87.5 for RB.

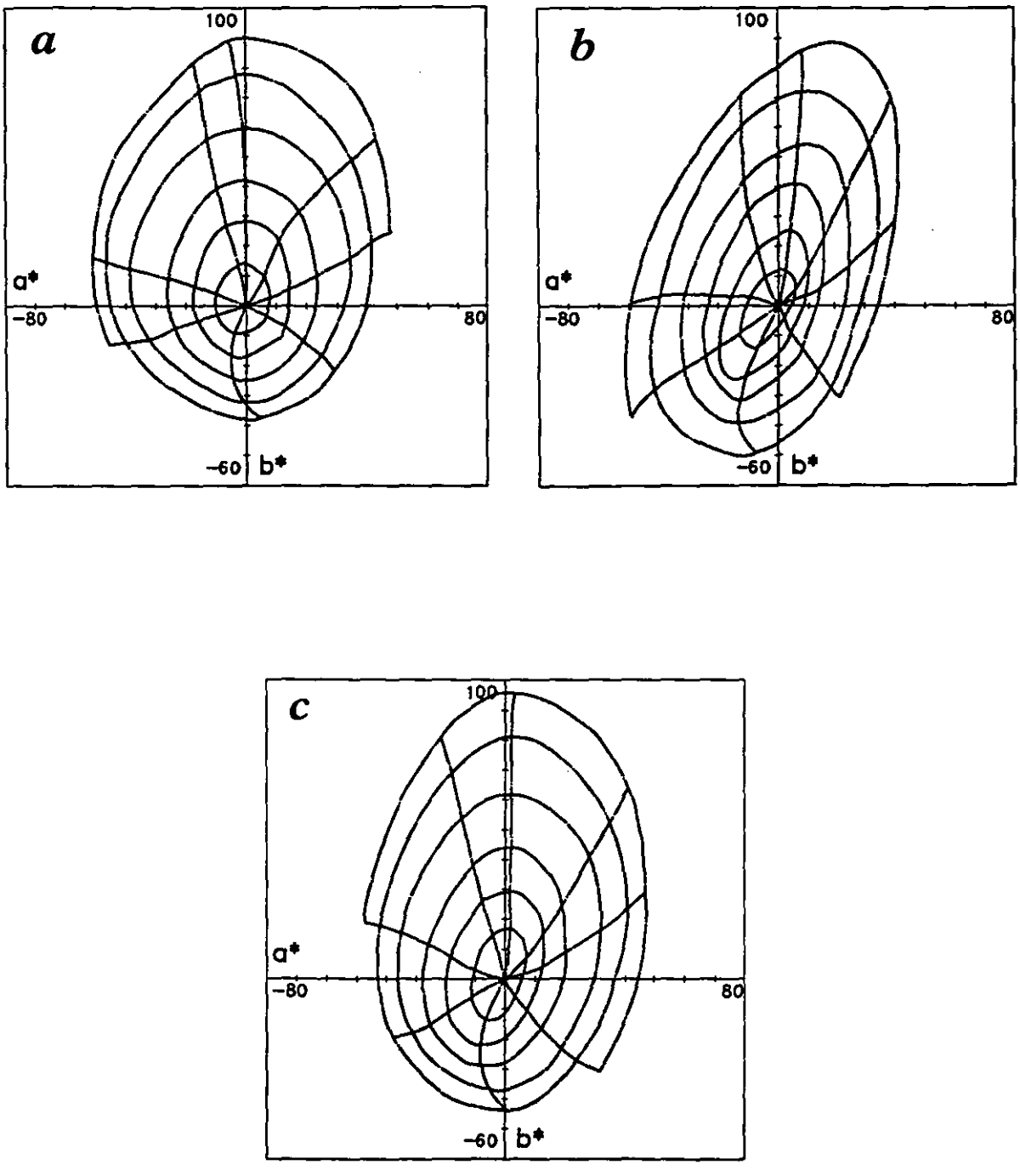

Fig. 2.2.3 Experimental grids derived from the visual results plotted in CIE a*b* diagram for three light sources, (a) D65, (b) A, (c) TL84.

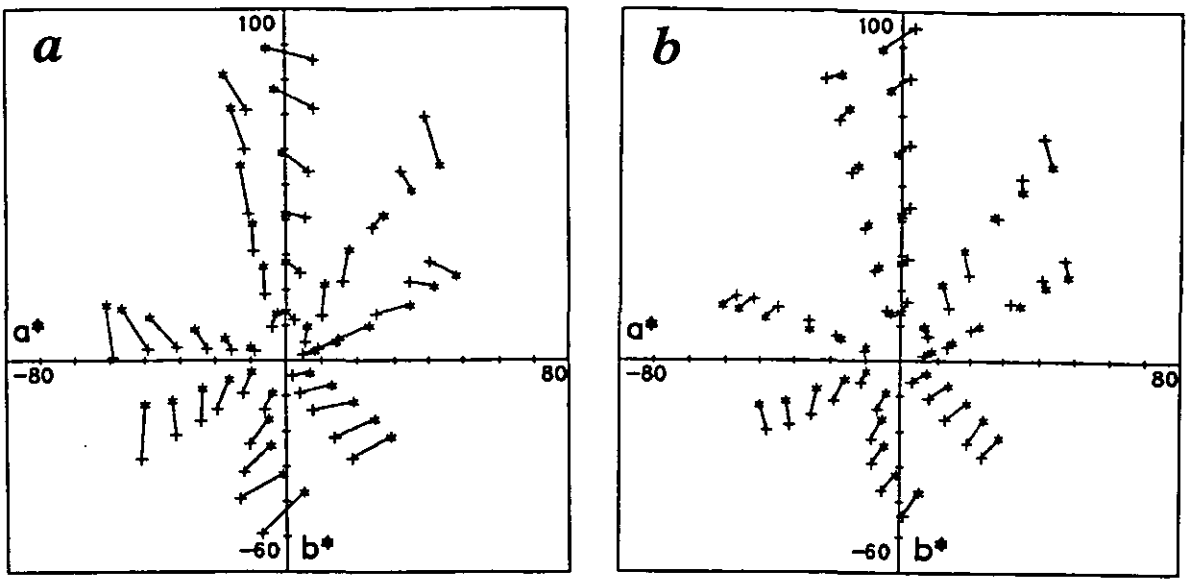

Fig. 2.2.4 Graphical representation of corresponding a*b* values showing direction and magnitude of the visual results for (a) A (+) and D65 (*) and (b) TL84 (+) and D65 (*).

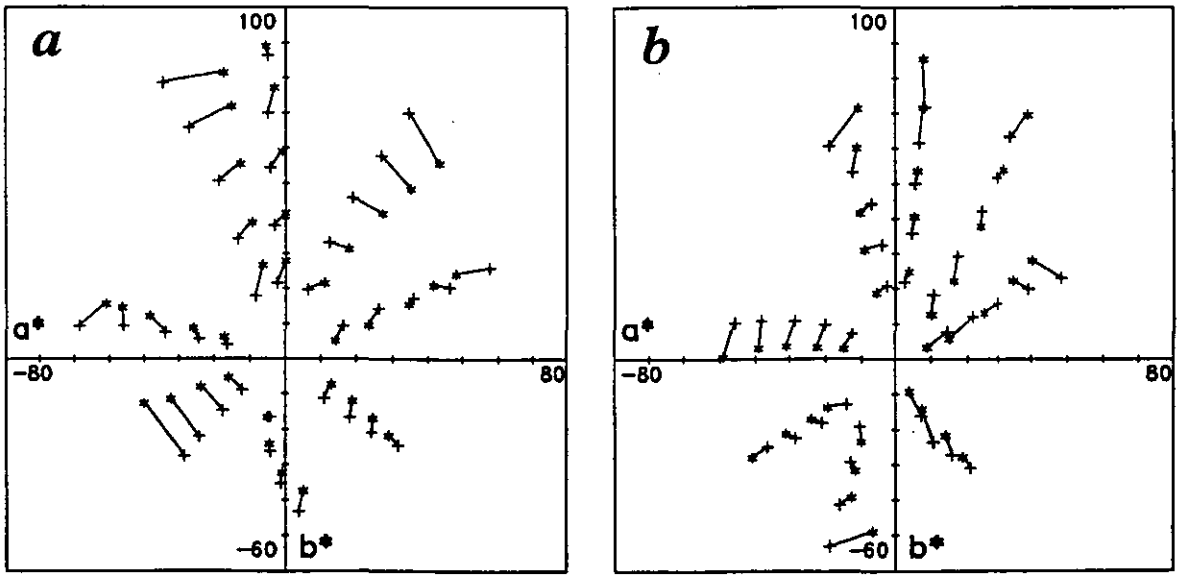

Fig. 2.2.5 Comparison with the visual results from the author's (*) and Luo's (+) studies plotted in CIE a*b* diagram for sources (a) D65, (b) A.

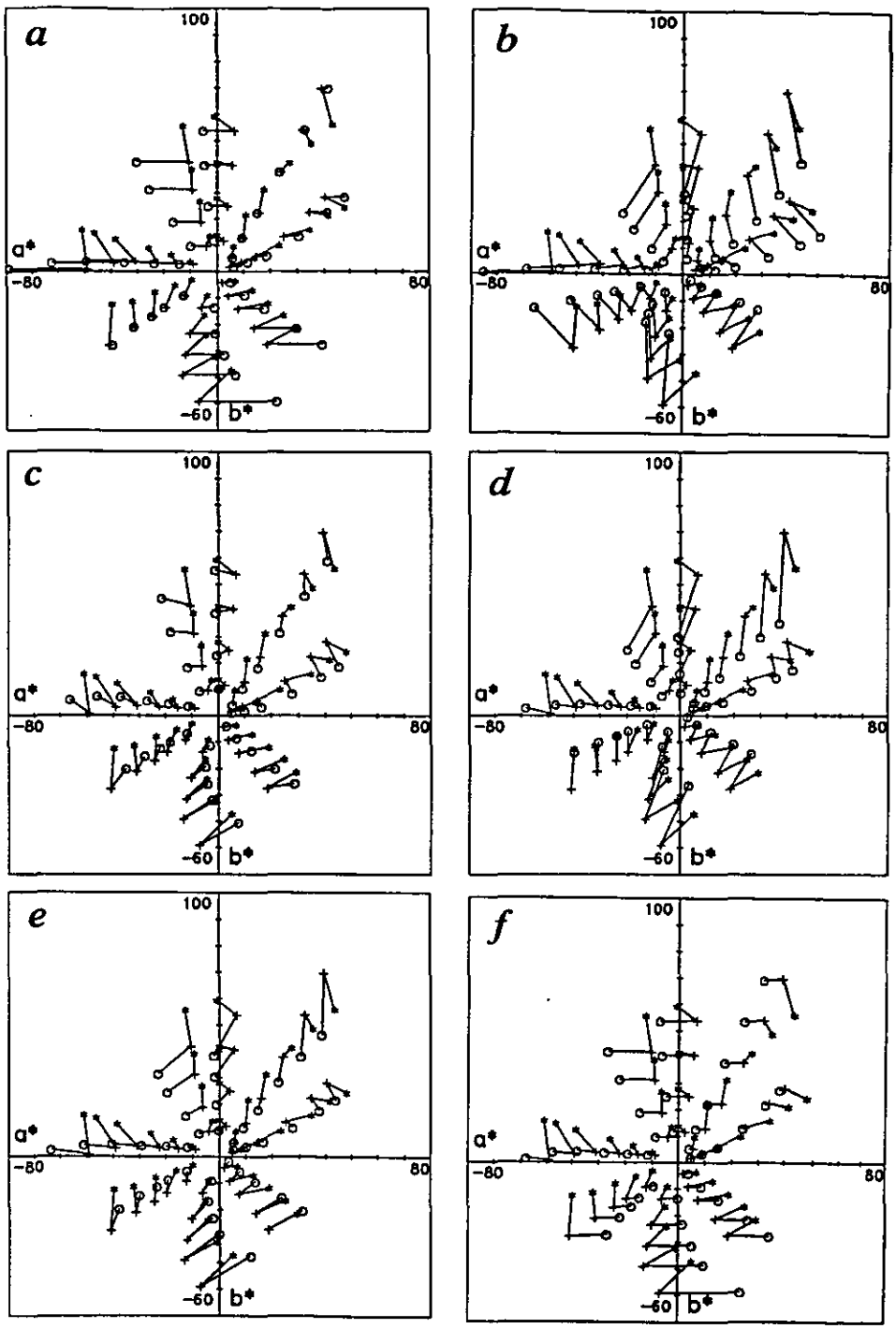

Fig. 2.2.6 Graphical representation of corresponding a*b* values showing direction and magnitude of the visual results for sources A (+) and D65 (∗) compared with those predicted by 7 chromatic adaptation transforms (o) respectively, (a) von Kries, (b) Bartleson, (c) Bradford, (d) CIE, (e) Hunt and (f) RLAB. For perfect agreement, the solid and dashed vectors should overlap each other.

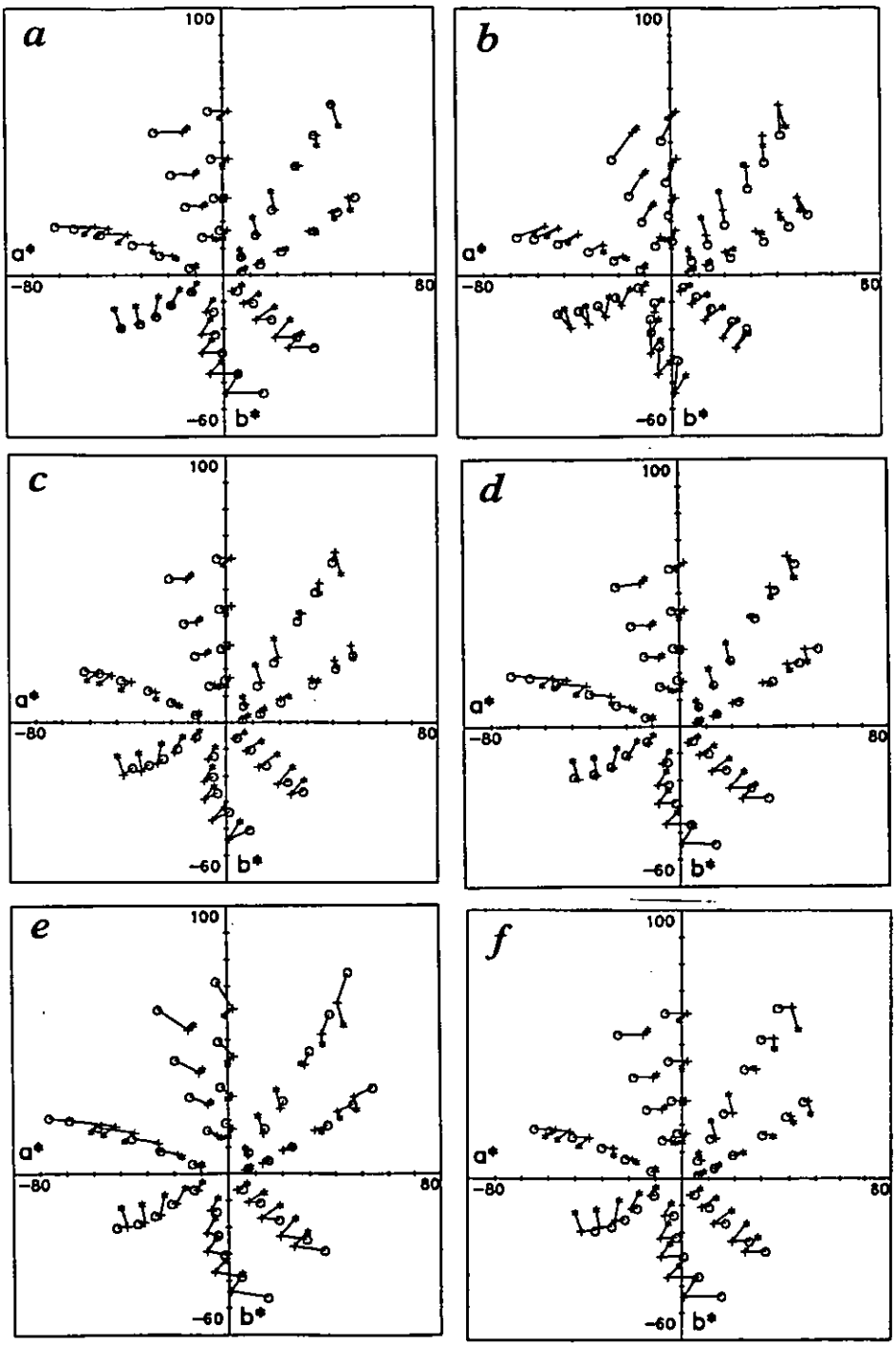

Fig. 2.2.7 Same as Figure 2.2.6, but except for sources TL84 (+) and D65 (∗).

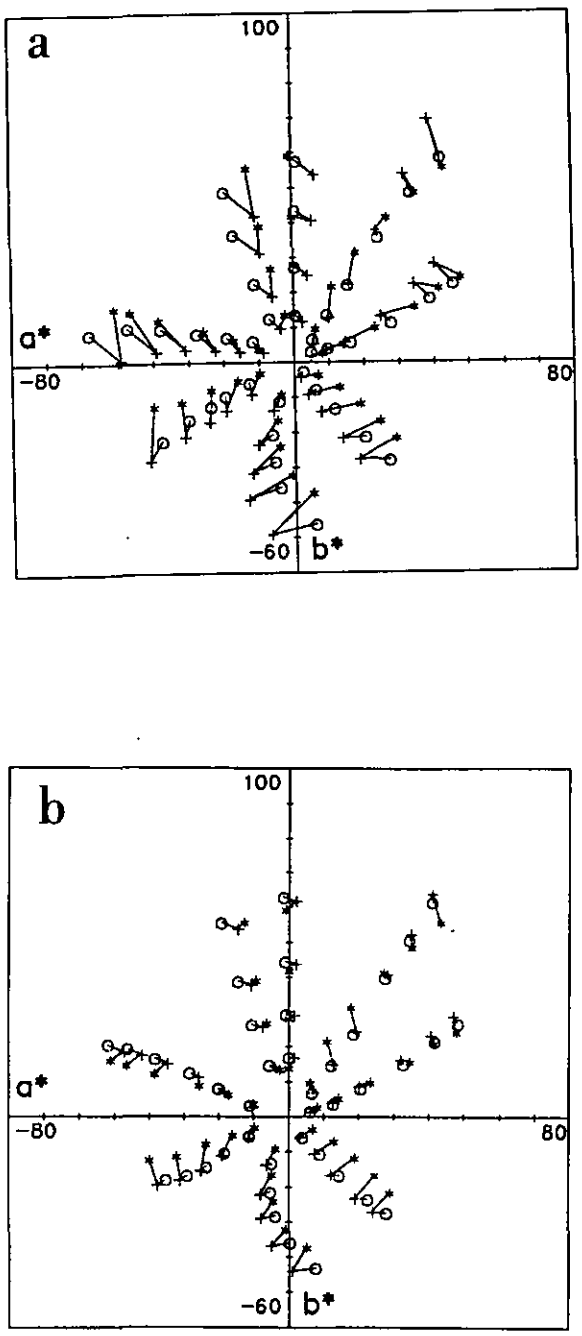

Fig. 2.3.1 Graphical representation of corresponding AB values showing direction and magnitude of the visual results for sources (a) A (+) and D65 (∗) and (b) TL84 (+) and D65 (∗) compared with those predicted by Kuo1 (o) chromatic adaptation transform. For perfect agreement, the solid and dashed vectors should overlap each other.

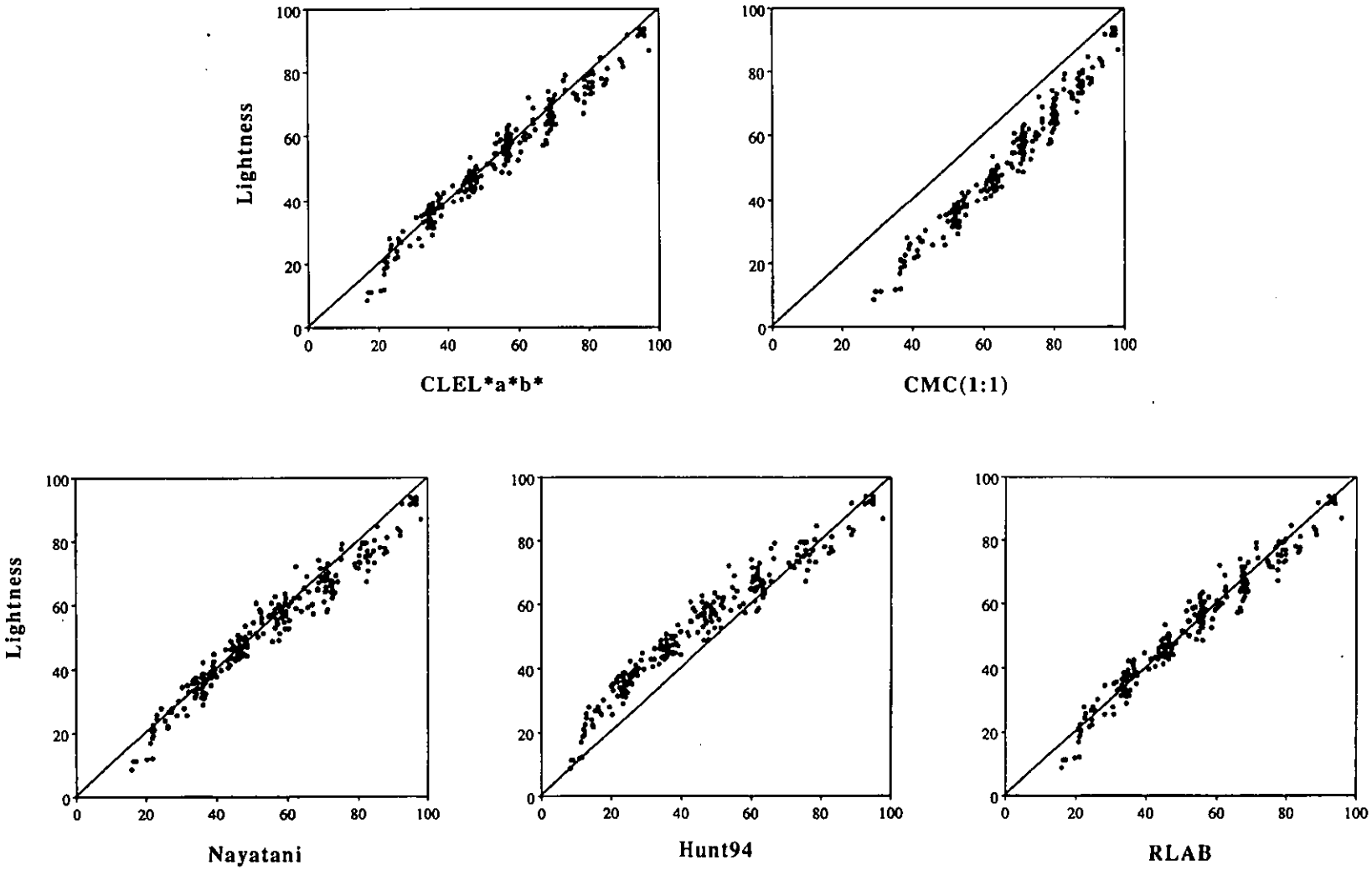

Fig. 2.4.1 Lightness visual data plotted against those predicted by CMC(1:1), CIE, Nayatani, Hunt94 and RLAB lightness scales under D65 source.

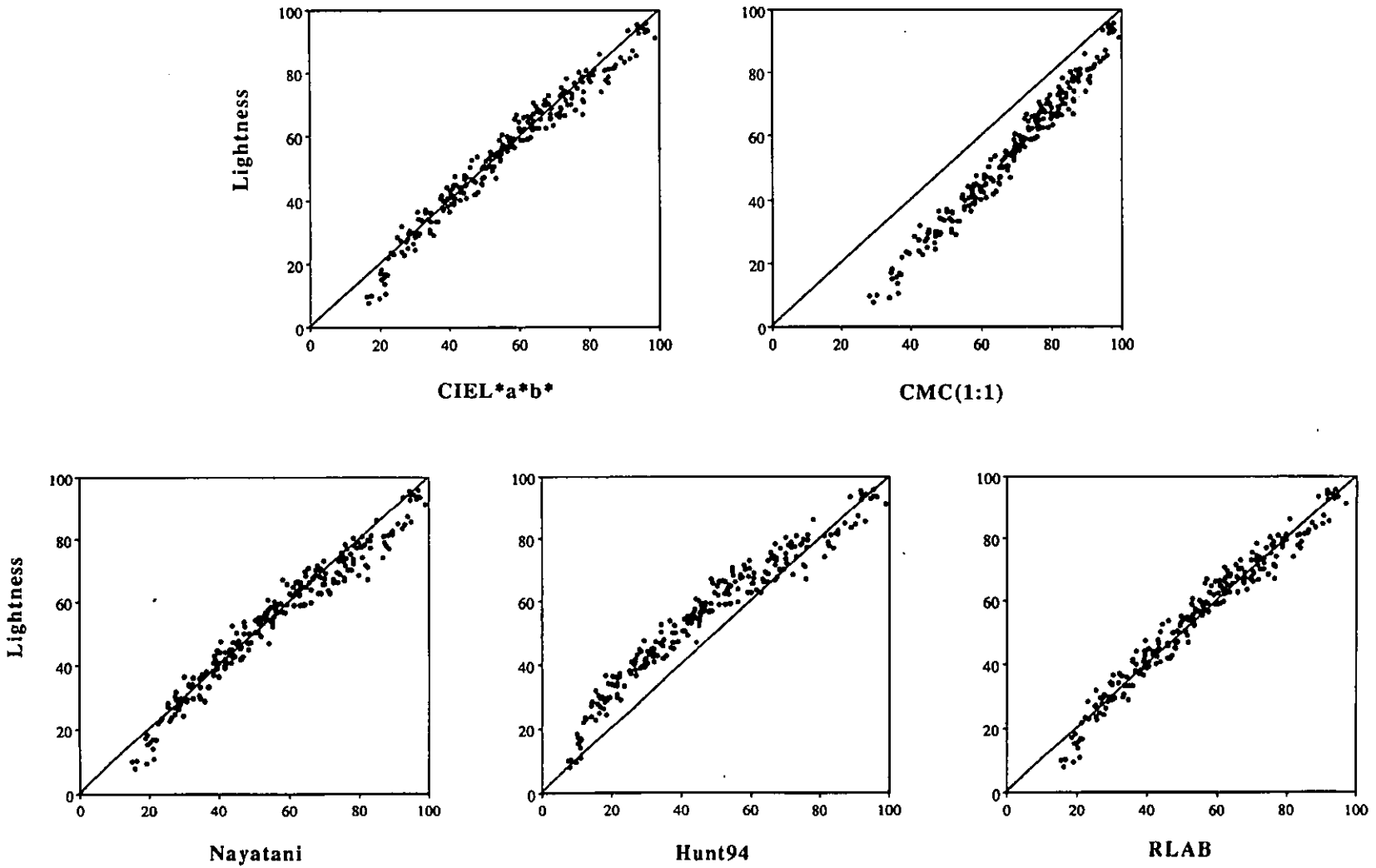

Fig. 2.4.2 Lightness visual data plotted against those predicted by CMC(1:1), CIE, Nayatani, Hunt94 and RLAB lightness scales under A source.

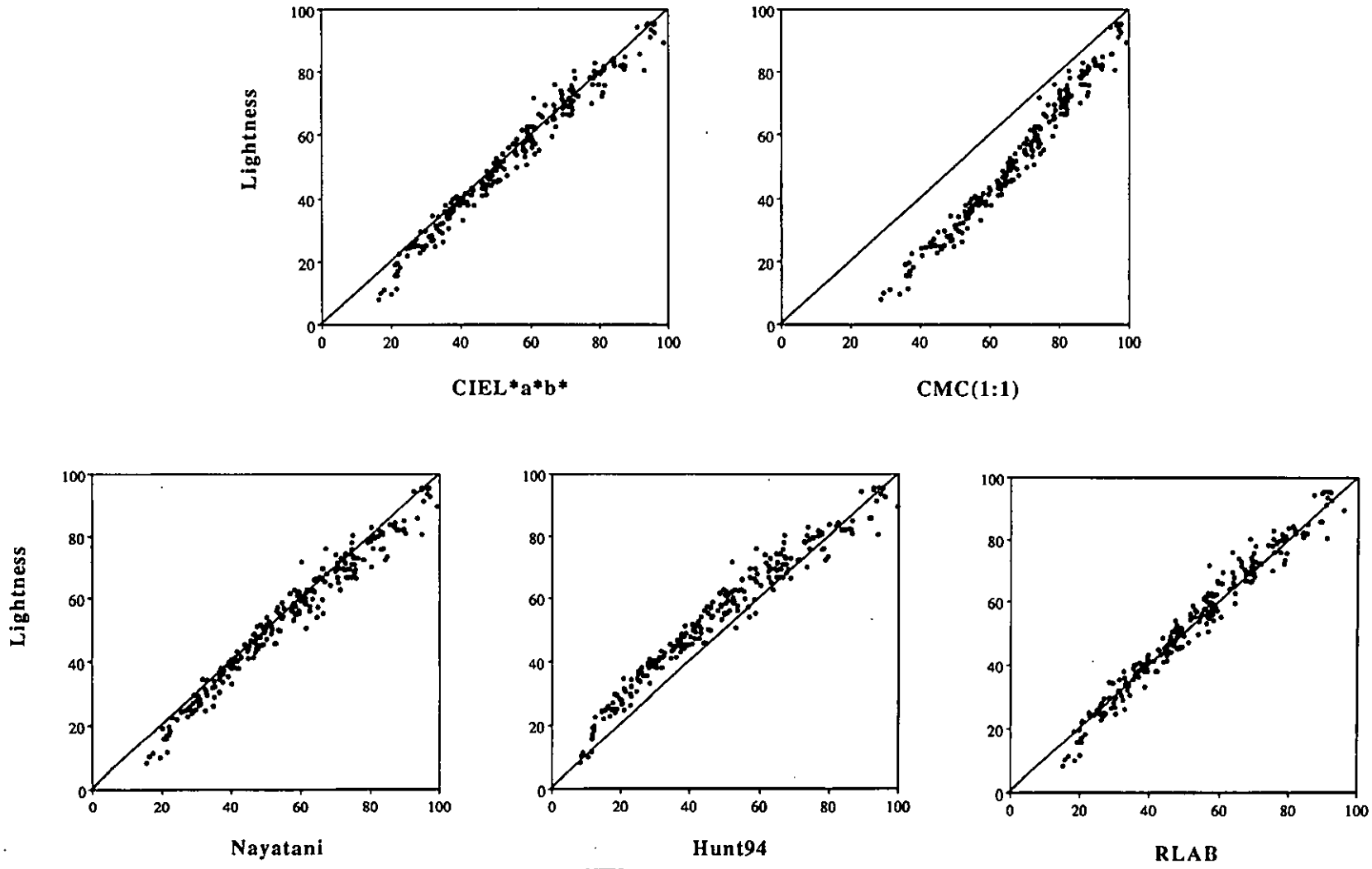

Fig. 2.4.3 Lightness visual data plotted against those predicted by CMC(1:1), CIE, Nayatani, Hunt94 and RLAB lightness scales under TL84 source.

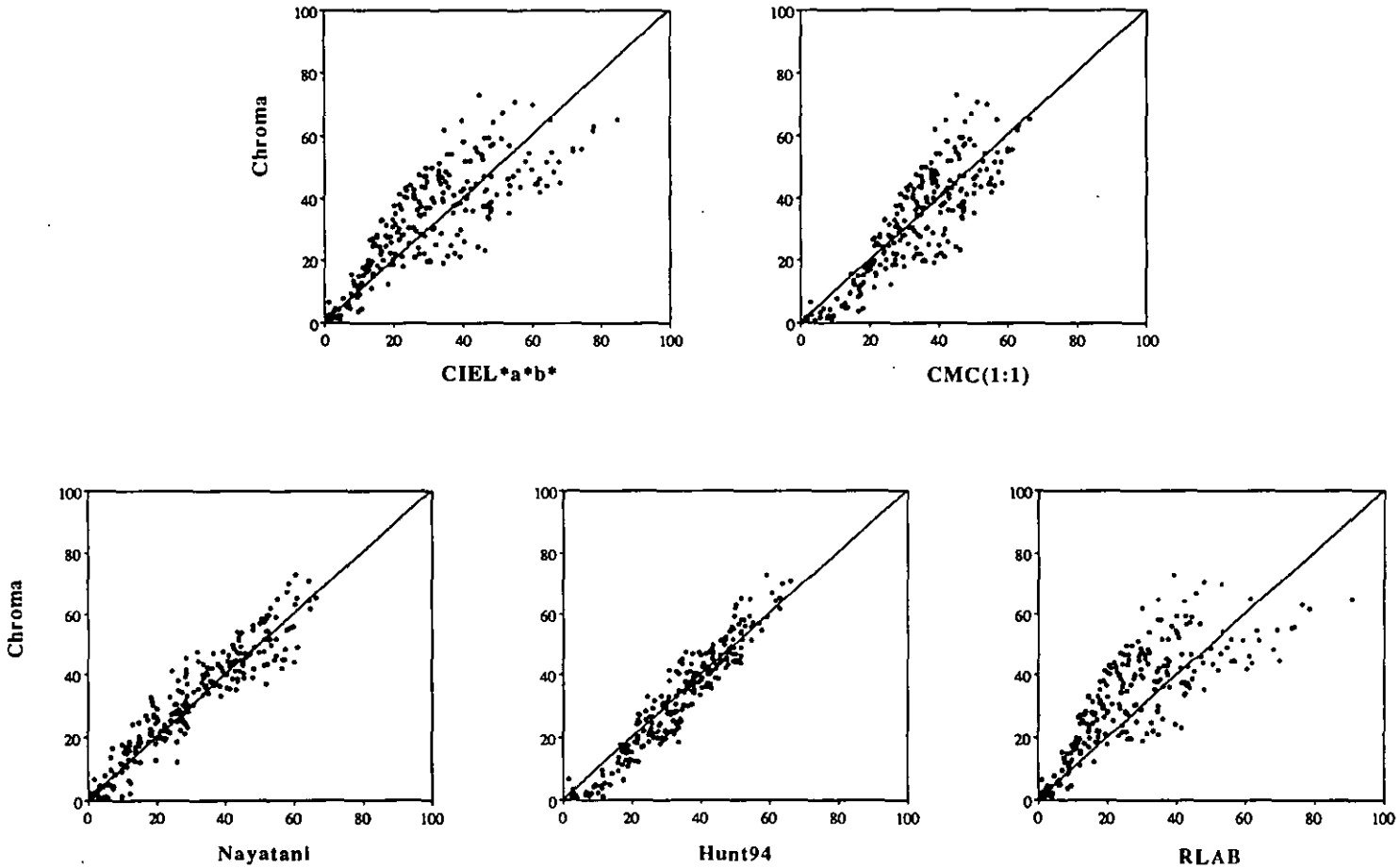

Fig. 2.4.4 Colourfulness visual data plotted against those predicted by CMC(1:1), CIE, Nayatani, Hunt94 and RLAB chroma scales under D65 source.

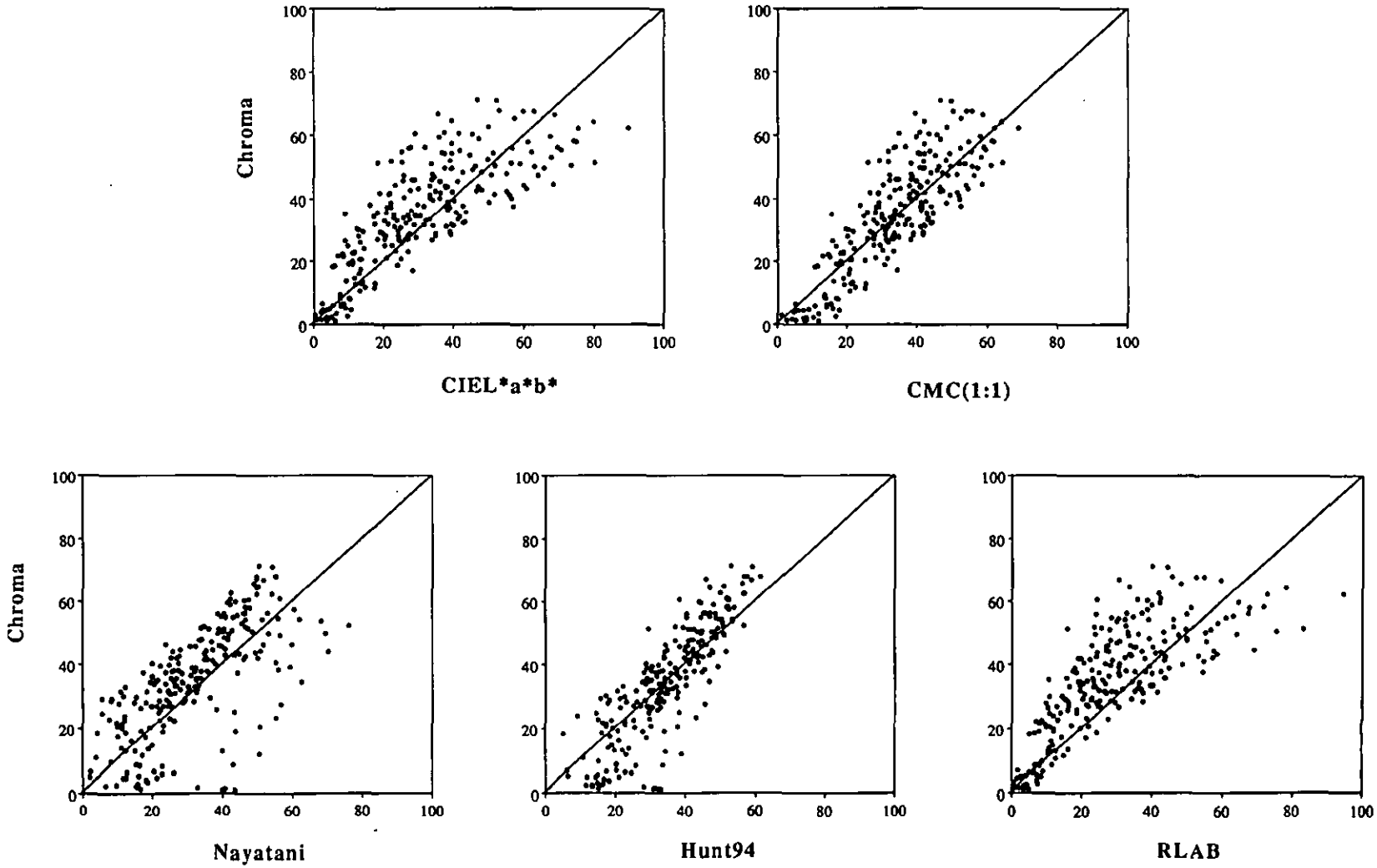

Fig. 2.4.5 Colourfulness visual data plotted against those predicted by CMC(1:1), CIE, Nayatani, Hunt94 and RLAB chroma scales under A source.

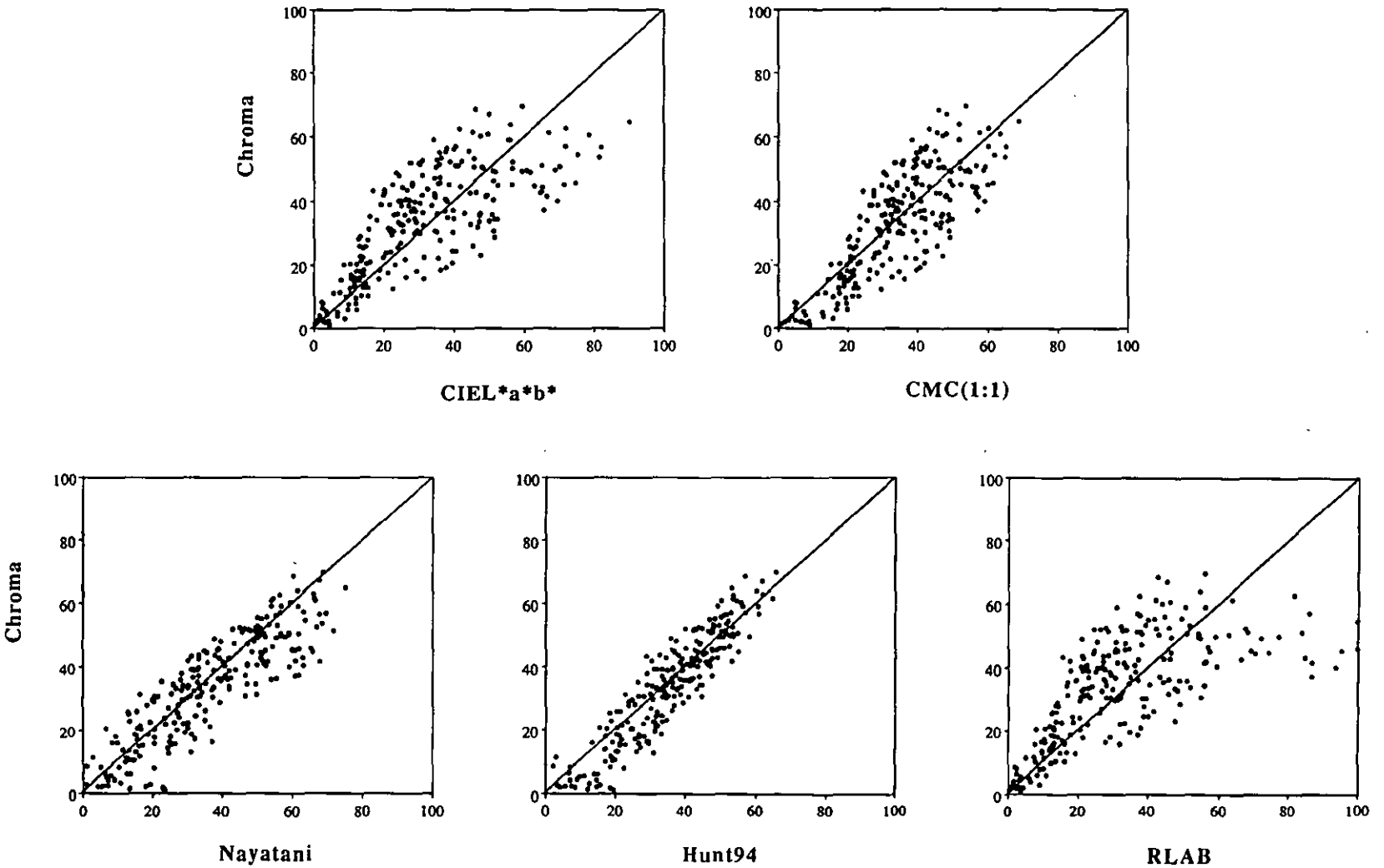

Fig. 2.4.6 Colourfulness visual data plotted against those predicted by CMC(1:1), CIE, Nayatani, Hunt94 and RLAB chroma scales under TL84 source.

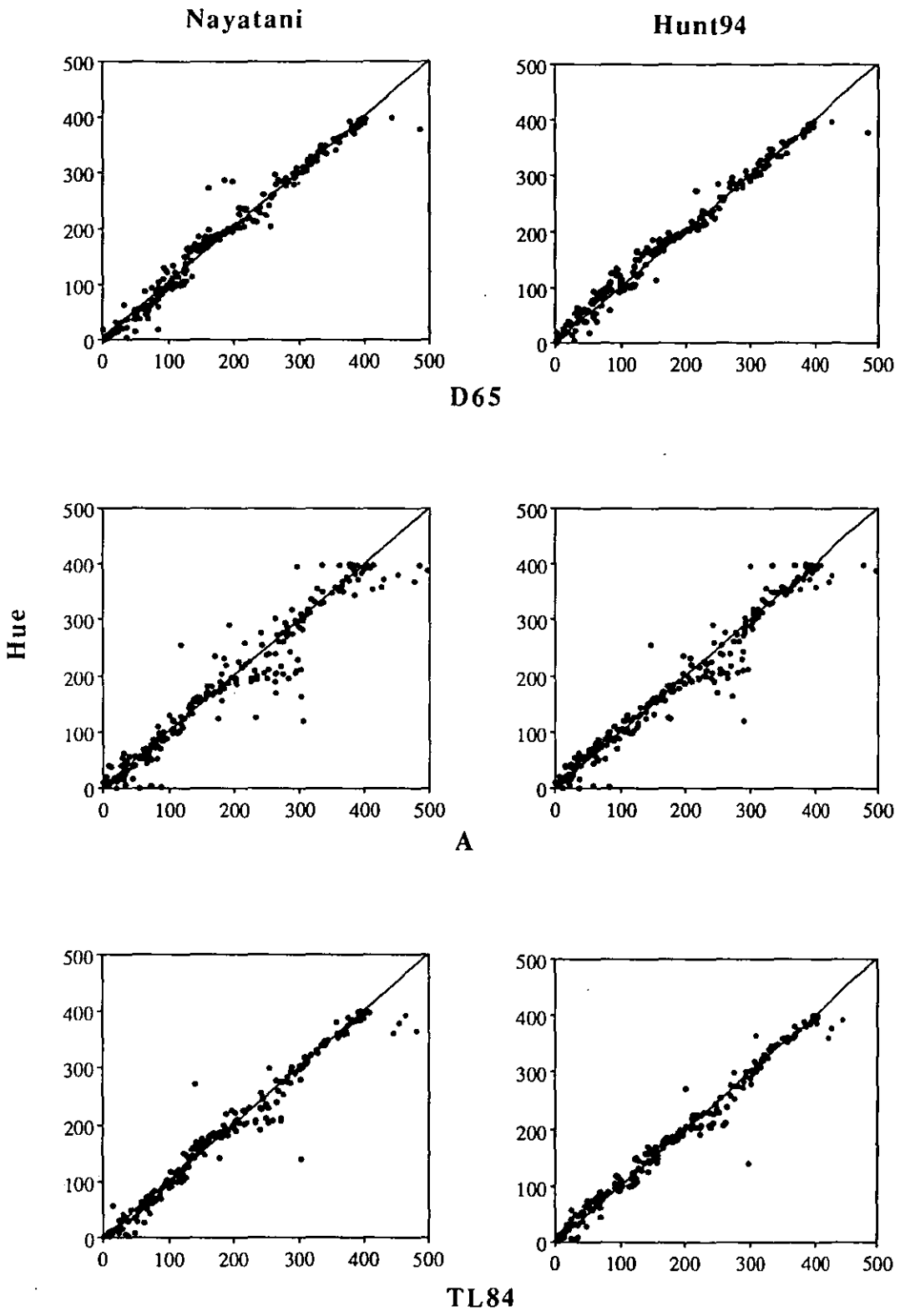

Fig. 2.4.7 Hue visual data plotted against those predicted by Nayatani (left) and Hunt94 (right) colour appearance models under D65, A and TL84 sources.

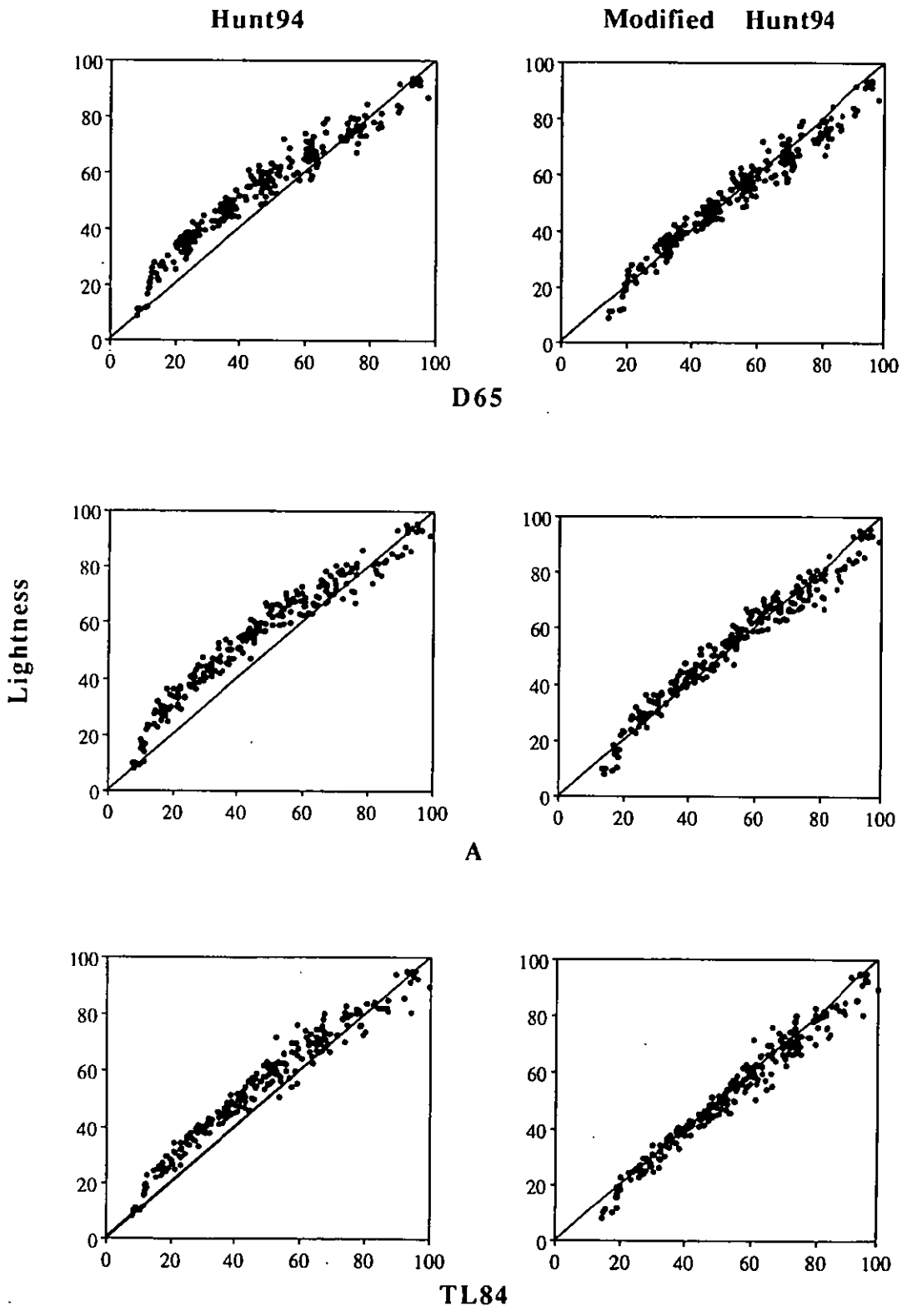

Fig. 2.4.8 Lightness visual data plotted against those predicted by Hunt94 (left) and modified Hunt94 (right) lightness scales under D65, A and TL84 sources.

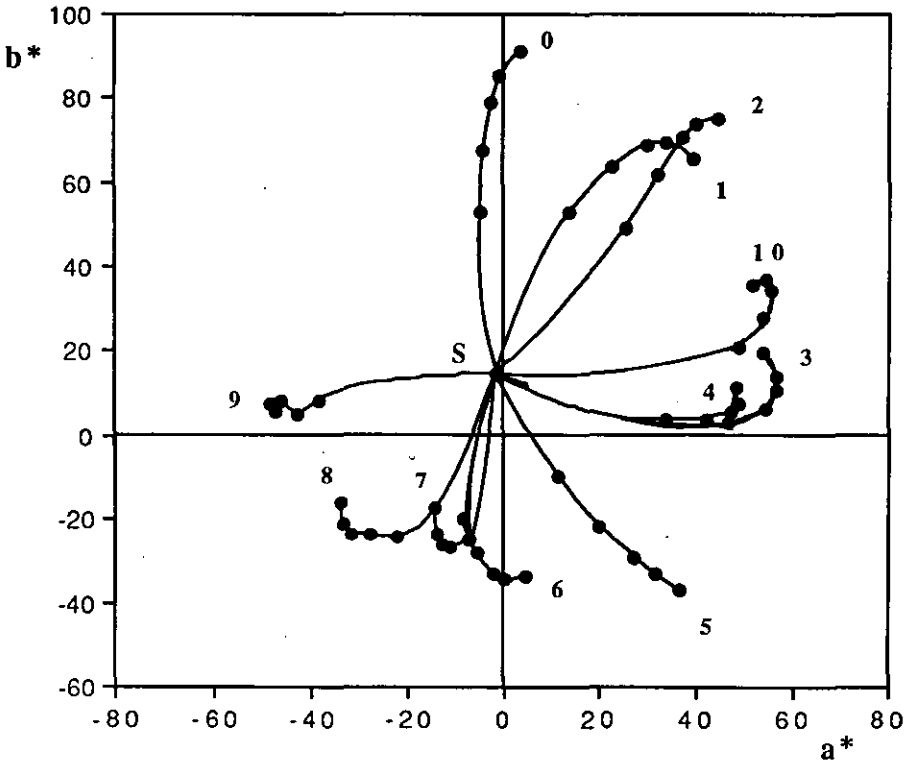

Fig. 3.1.1 Calibration samples for the 11 acid dyes employed plotted in CIE a*b* diagram.

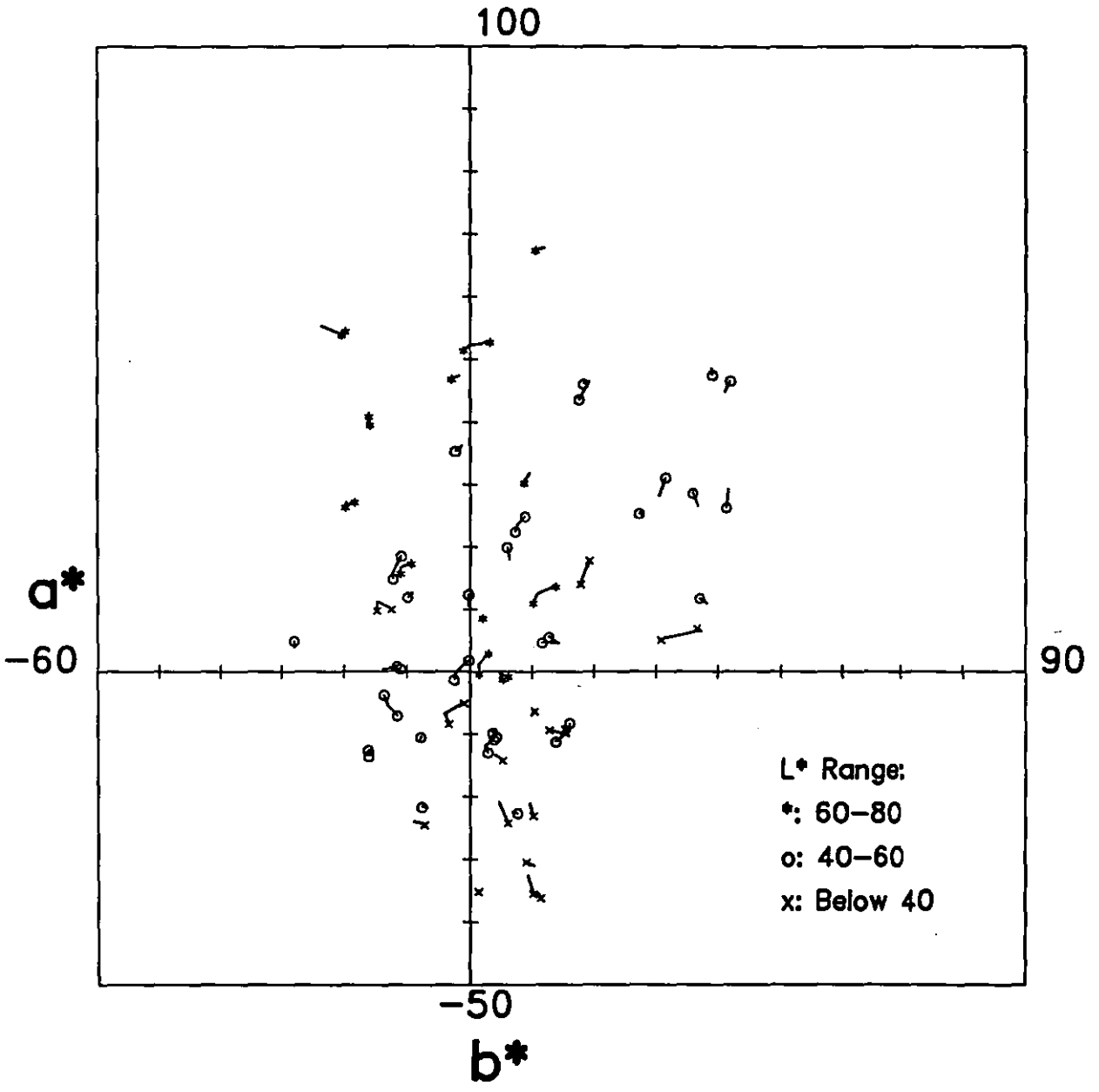

Fig. 3.1.2 76 metamers plotted using vectors in CIE a*b* diagram under D65 source. The symbols represent metamers' CIE L* range: '*' for 80 - 60, 'o' for 60 - 40, and 'x' for below 40.

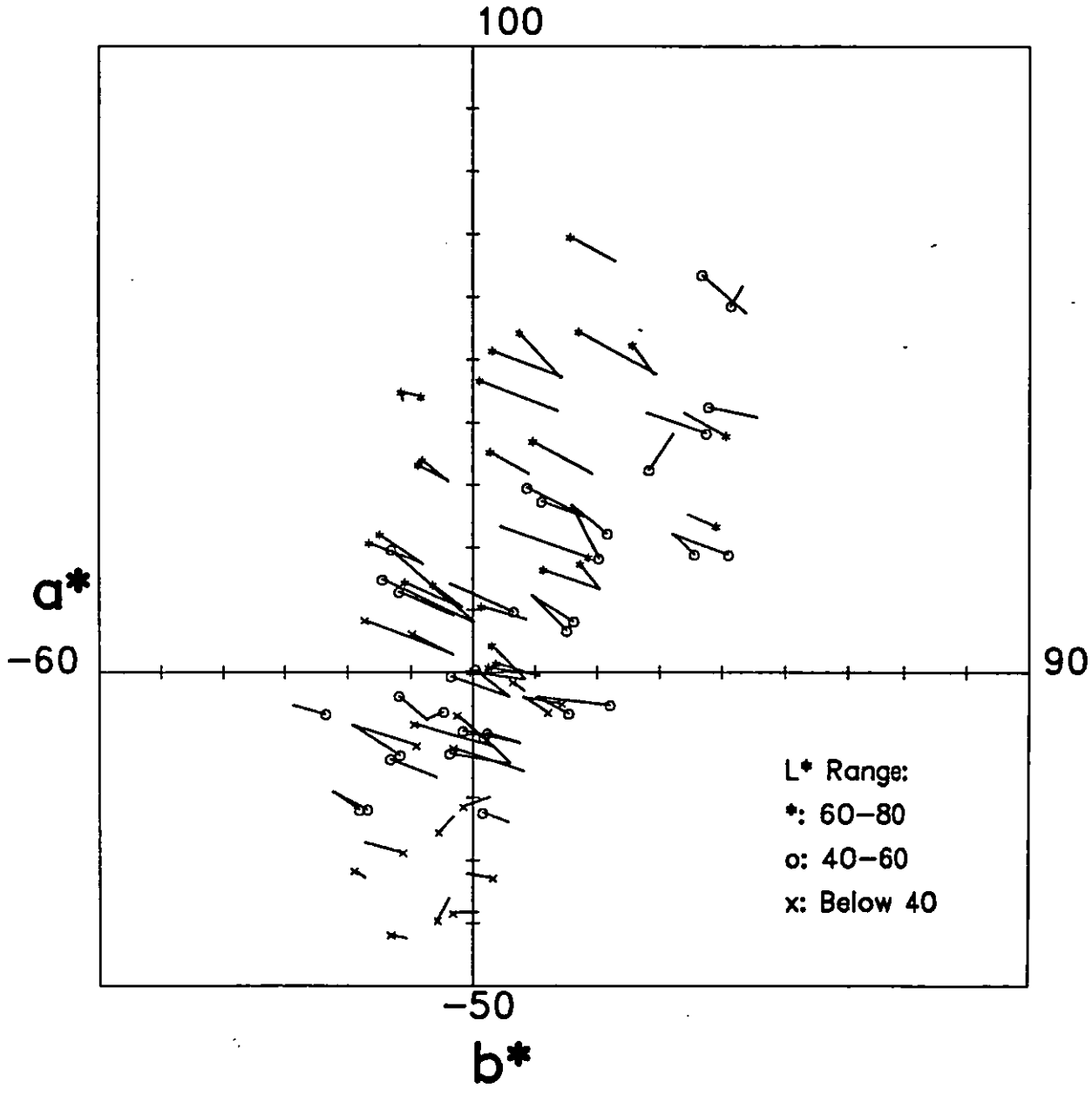

Fig. 3.1.3 Same as Figure 3.1.2, but under A source.

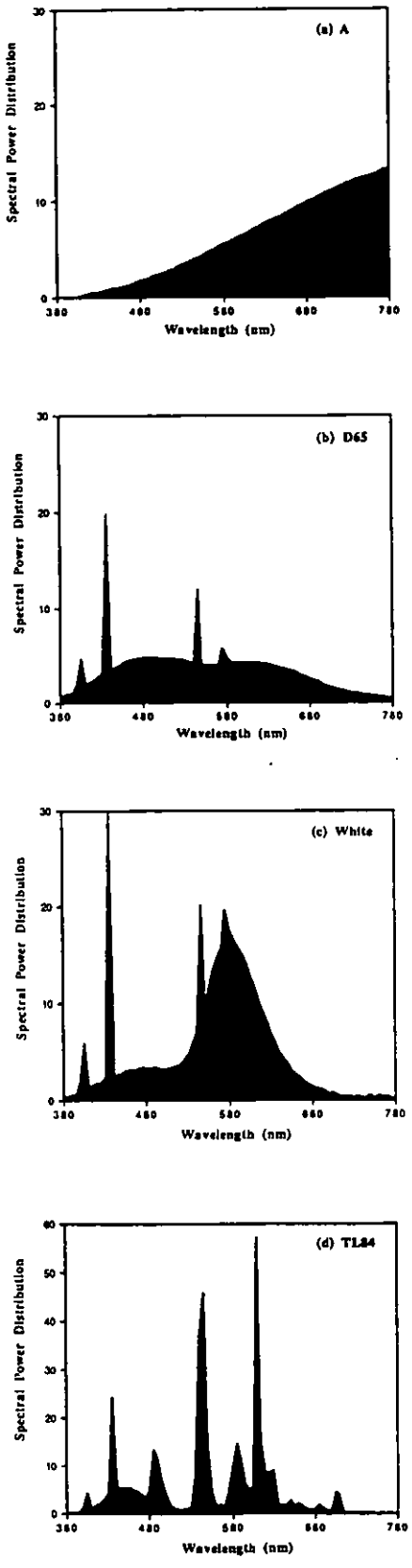

Fig. 3.1.4 The spectral power distribution curves plotted against wavelengths for (a) A, (b) D65, (c) White, and (d) TL84 sources.

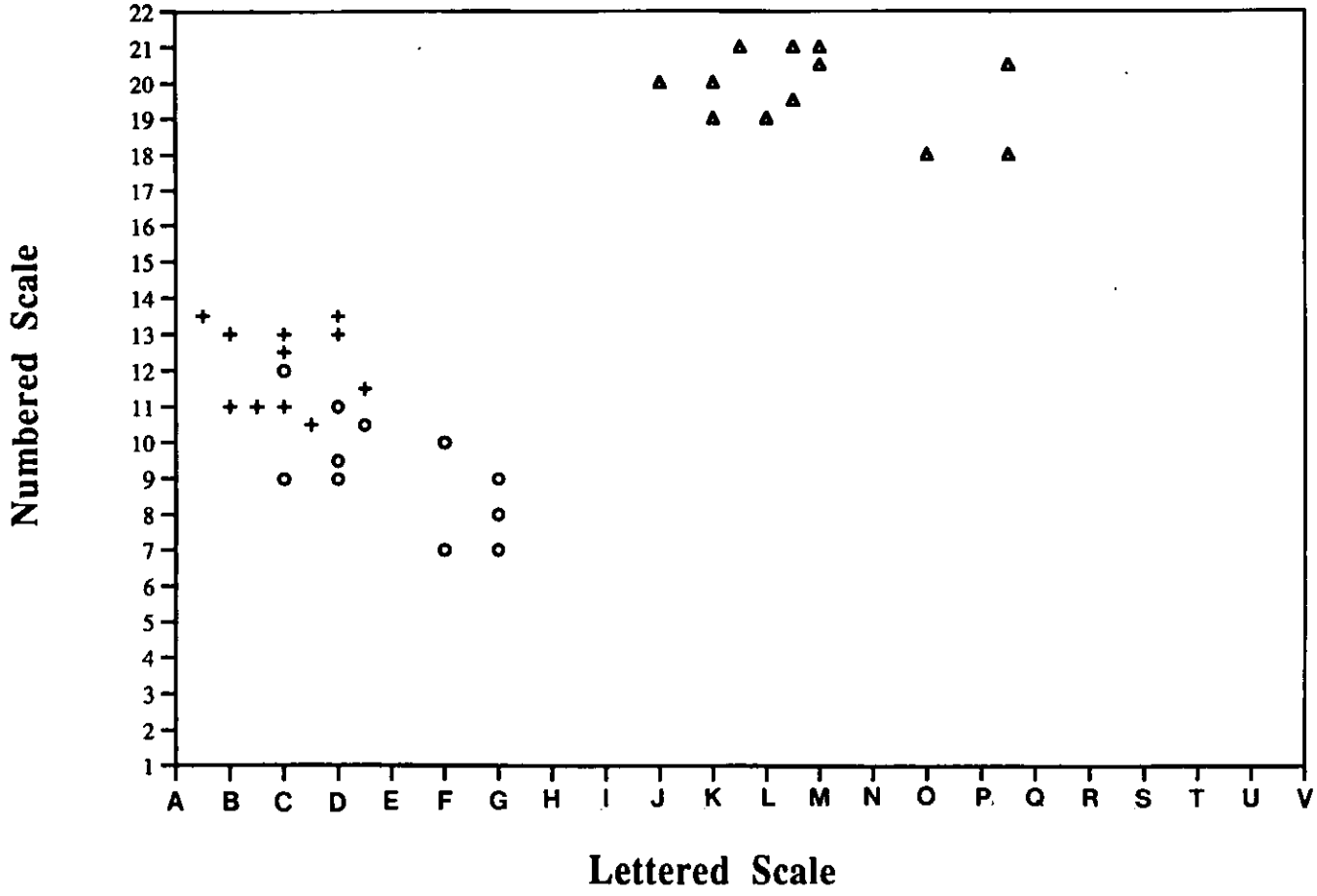

Fig. 3.2.1 Match points on D-H Color Rule for 13 observers under sources D65 (o), TL84 (+) and A (Δ).

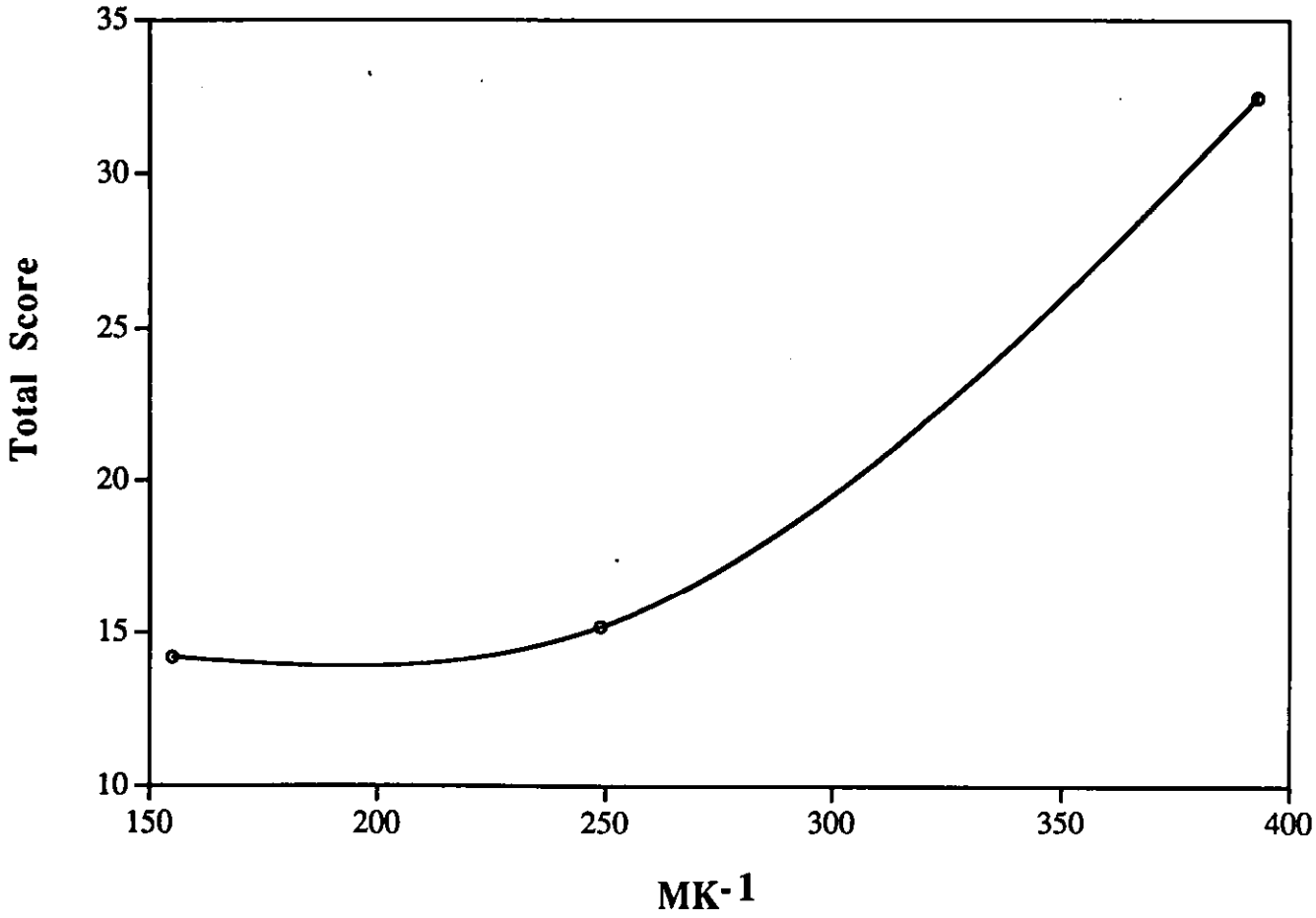

Fig. 3.2.2 Total score on the D-H Color Rule as function of reciprocal colour temperature of sources.

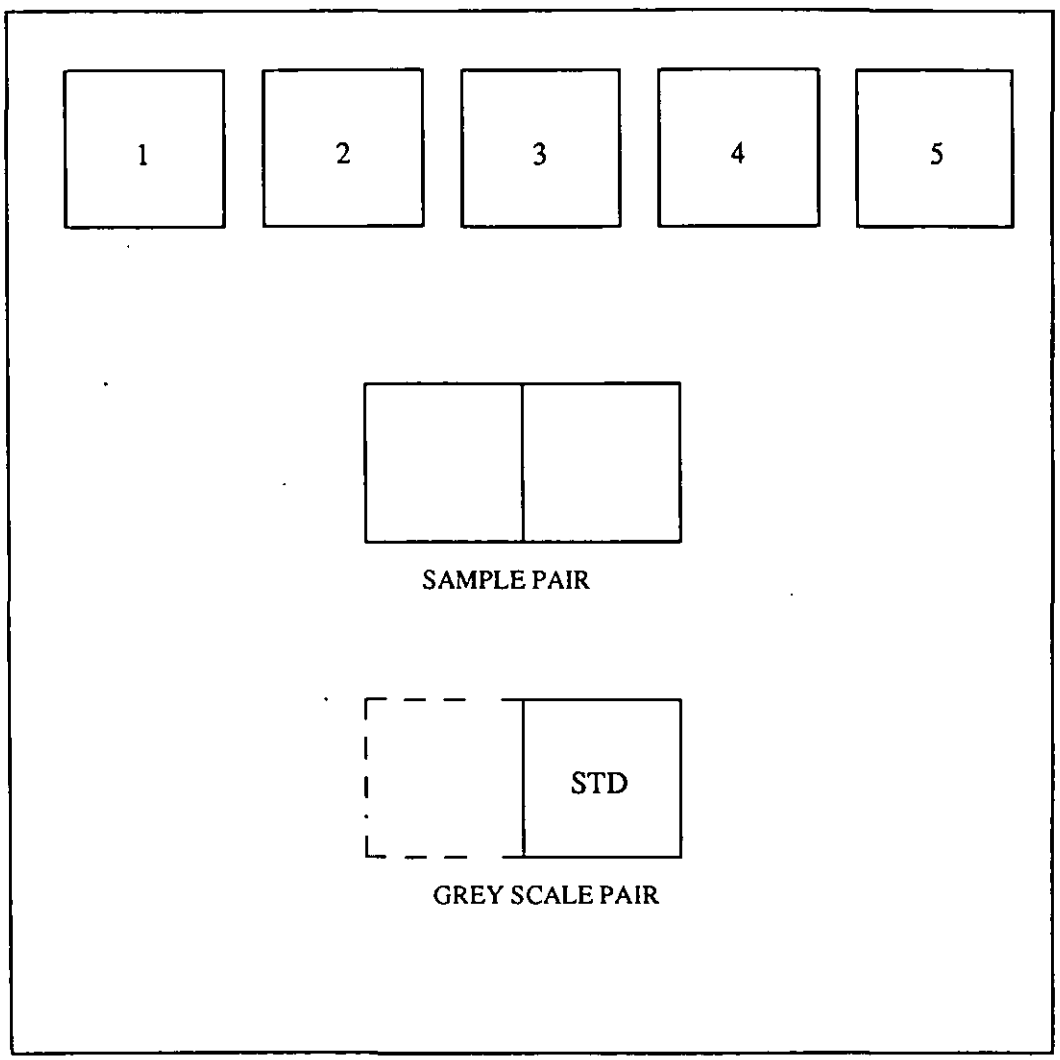

Fig. 3.2.3 Sample arrangement for visual assessment using the grey scale method.

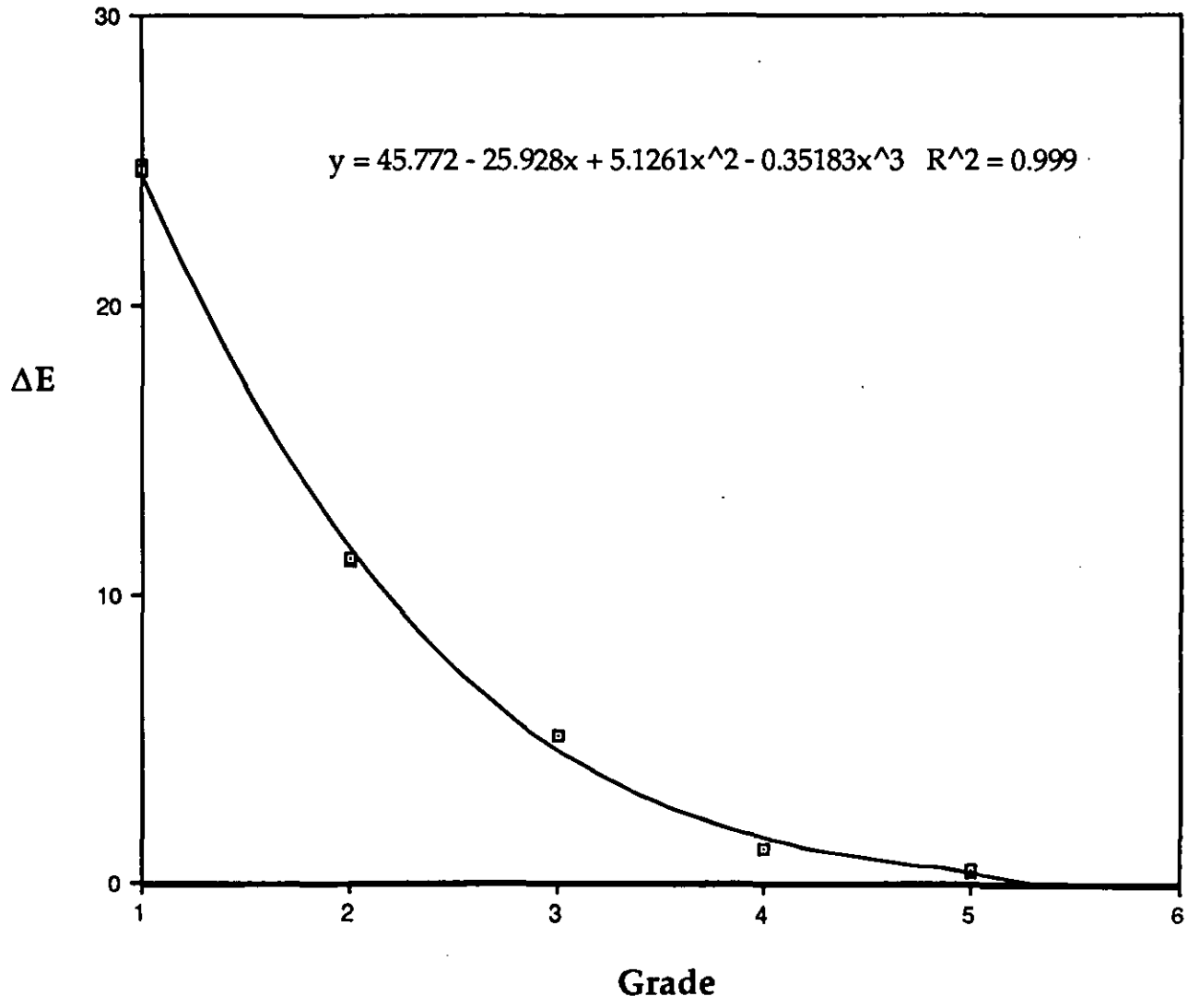

Fig. 3.3.1 Relation between grey scale ratings and CIEL*a*b* ΔE values.

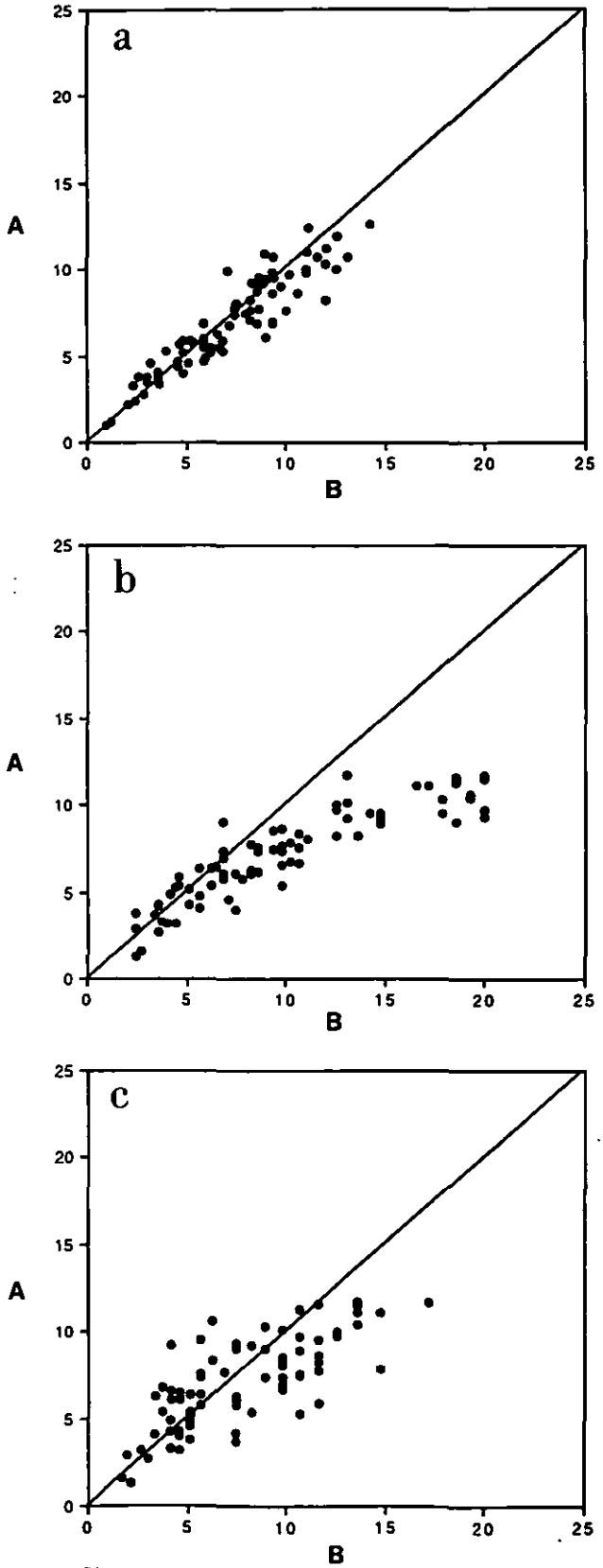

Fig. 3.3.2 The scatter diagrams illustrate the typical variations between two sets of data: (a) good agreement, (b) systematic discrepancy, and (c) random error.

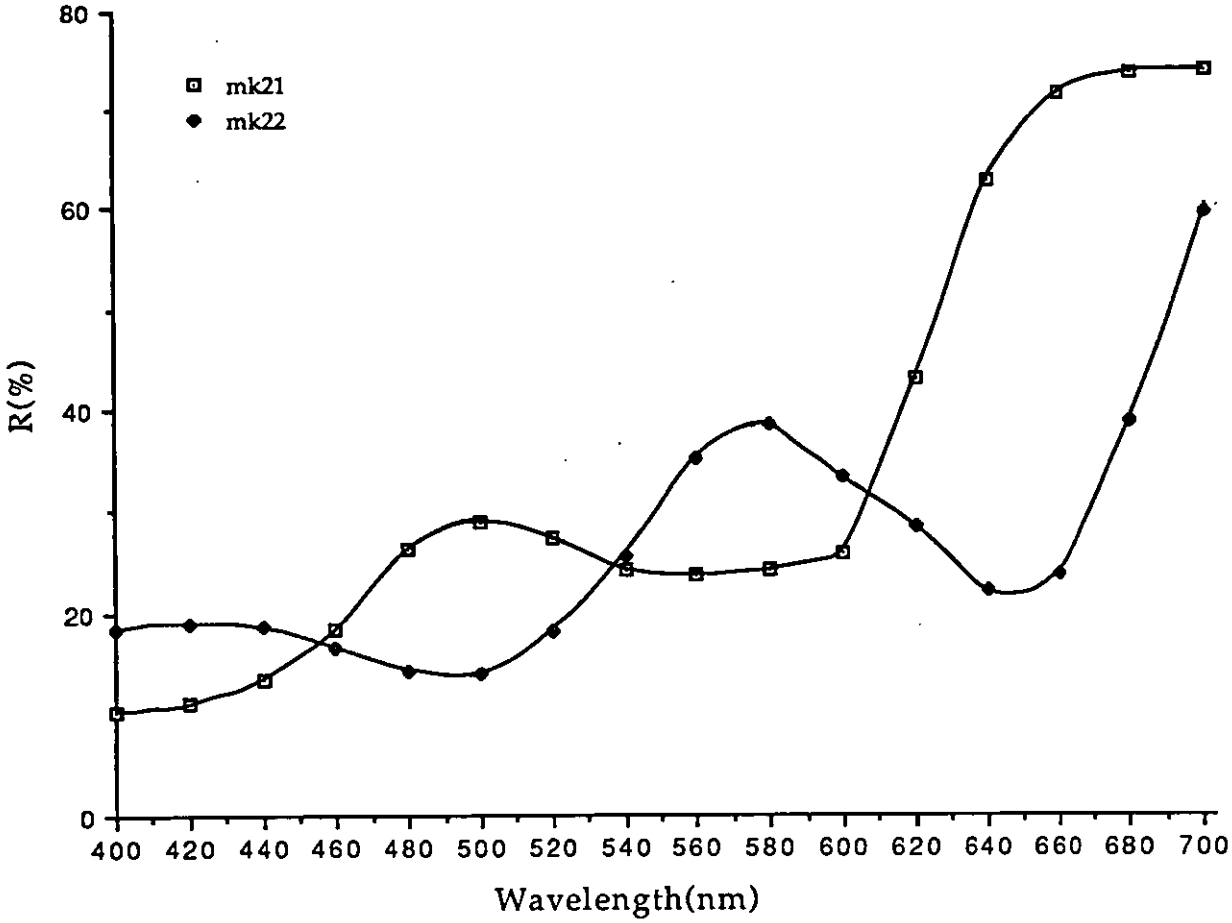

Fig. 3.4.1a A typical example of cross-over reflectance curves for a metamer in this study.

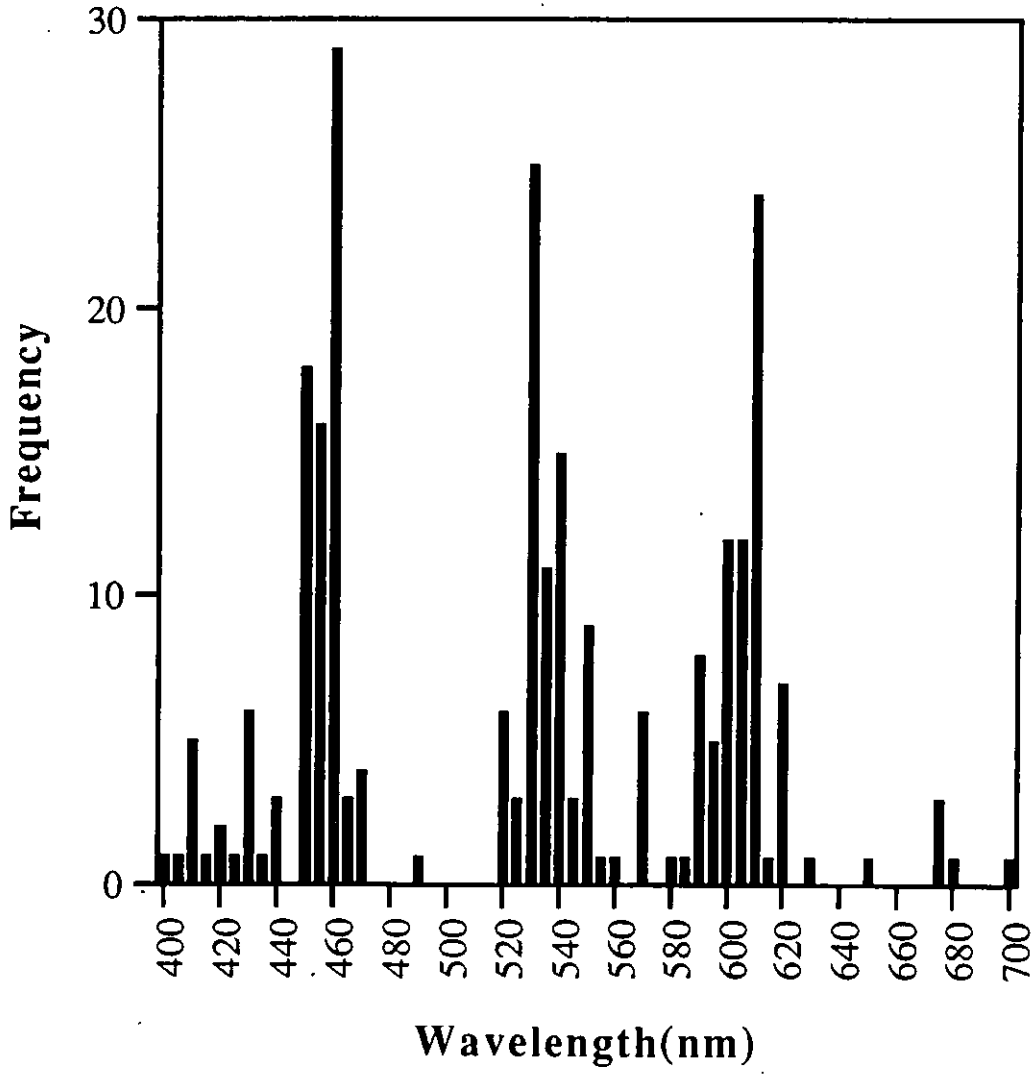

Fig. 3.4.1b The frequency of cross-overs at each wavelength for the 76 metamers studied.

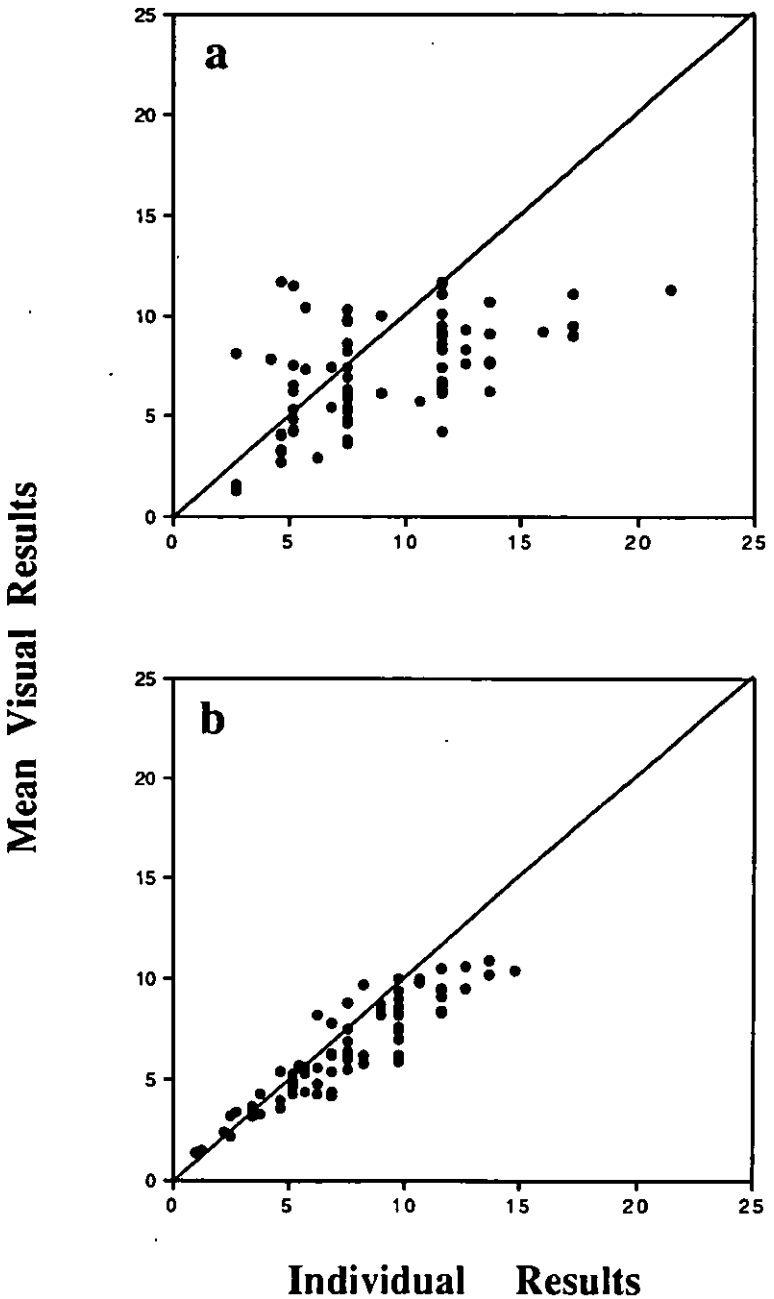

Fig. 3.4.2 The (a) worst and (b) best cases of individual observer precision in Experiments I and II under source A.

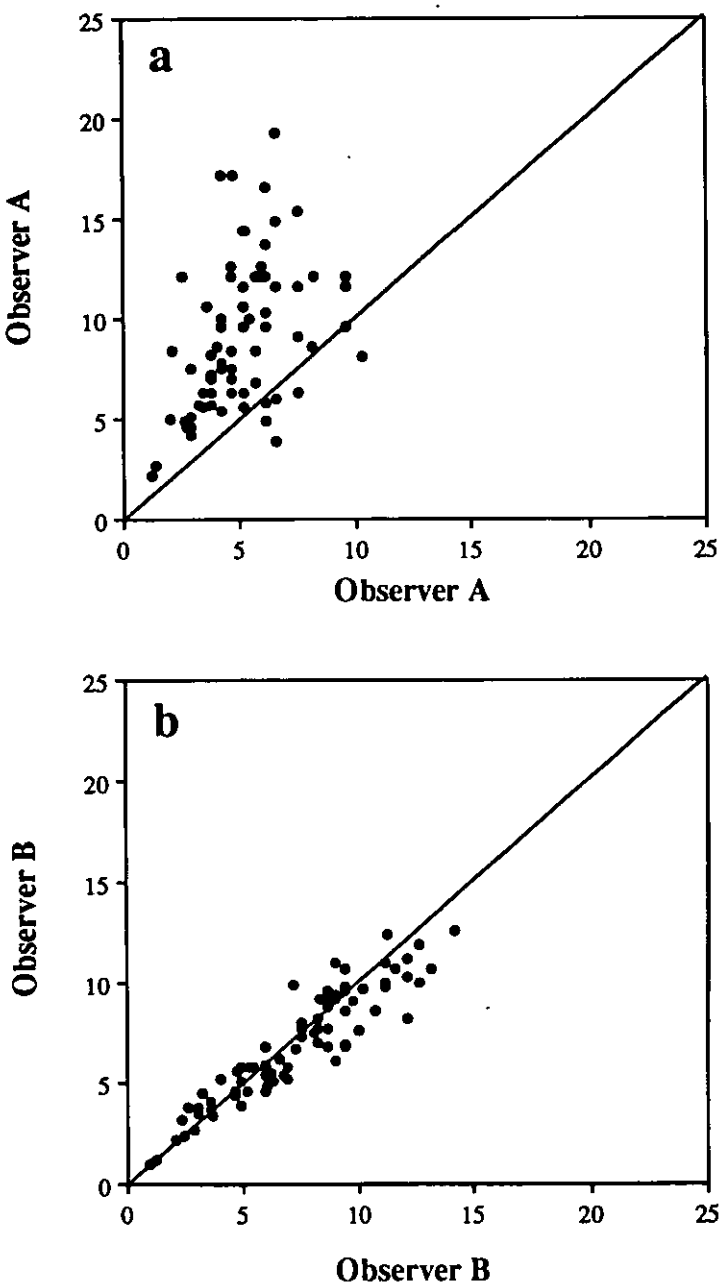

Fig. 3.4.3 The (a) worst and (b) best cases of individual observer's repeatability in Experiments I and II under source A.

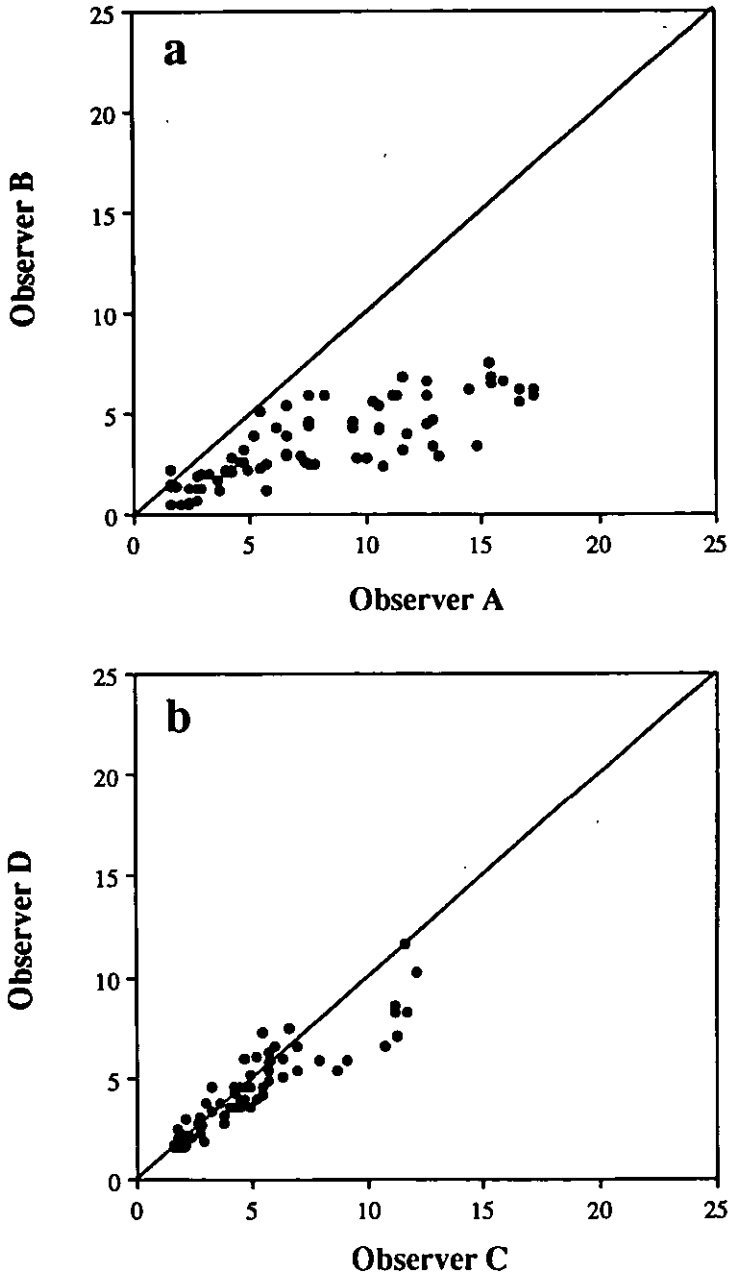

Fig. 3.4.4 The (a) worst and (b) best cases of individual observer's between-observer error in Experiments II under source TL84.

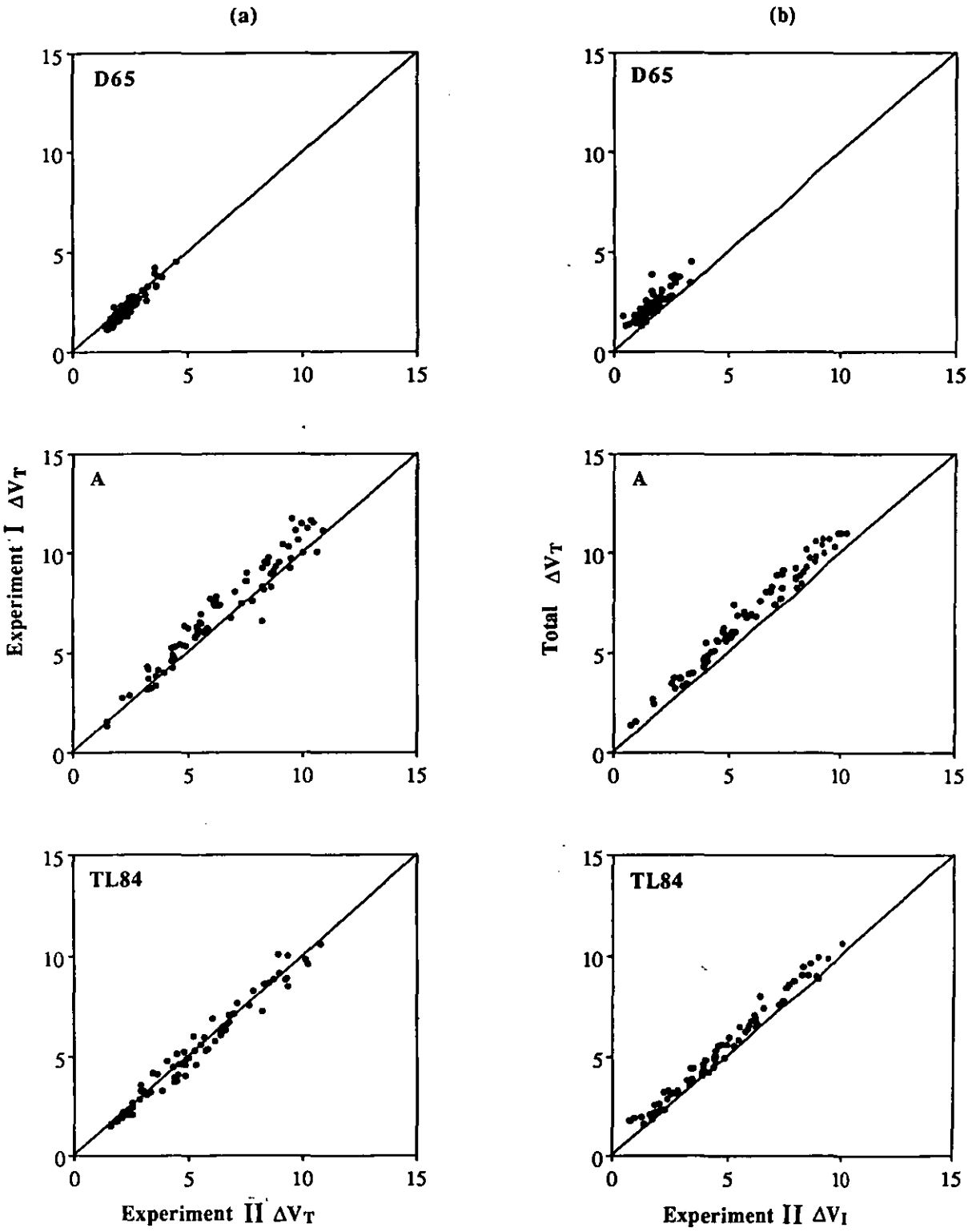

Fig. 3.4.5 The scatter diagrams plotted (a) between the ΔV_T results from Experiment I and II, and (b) between the overall mean ΔV_T and the ΔV_I results from Experiment II.

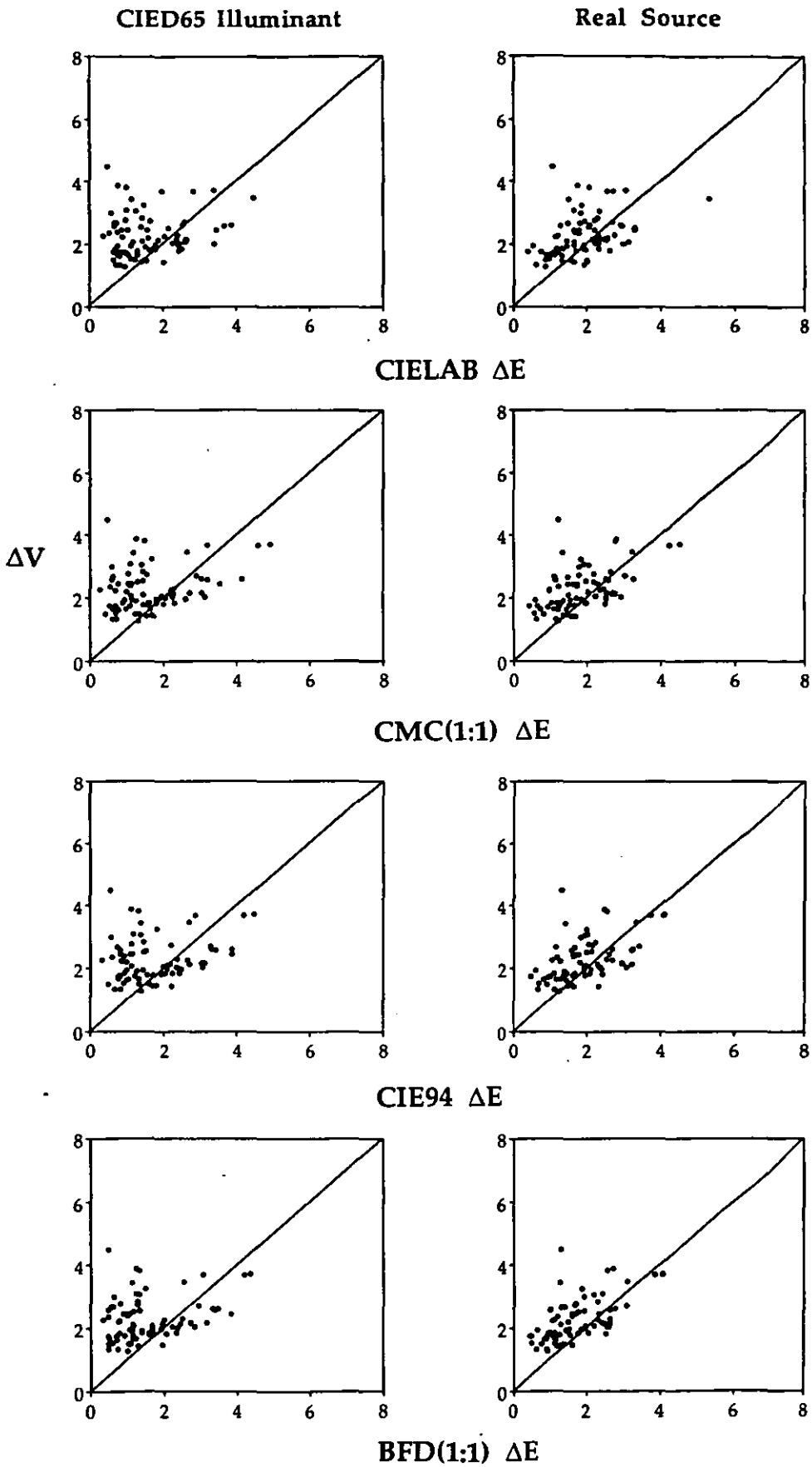

Fig. 3.4.6 The ΔE values calculated using the weighting functions of the CIE illuminant (left) and real source (right) for the CIEL*a*b*, CMC(1:1), CIE94 and BFD(1:1) formulae (from top to bottom) plotted against the ΔV results under D65 source.

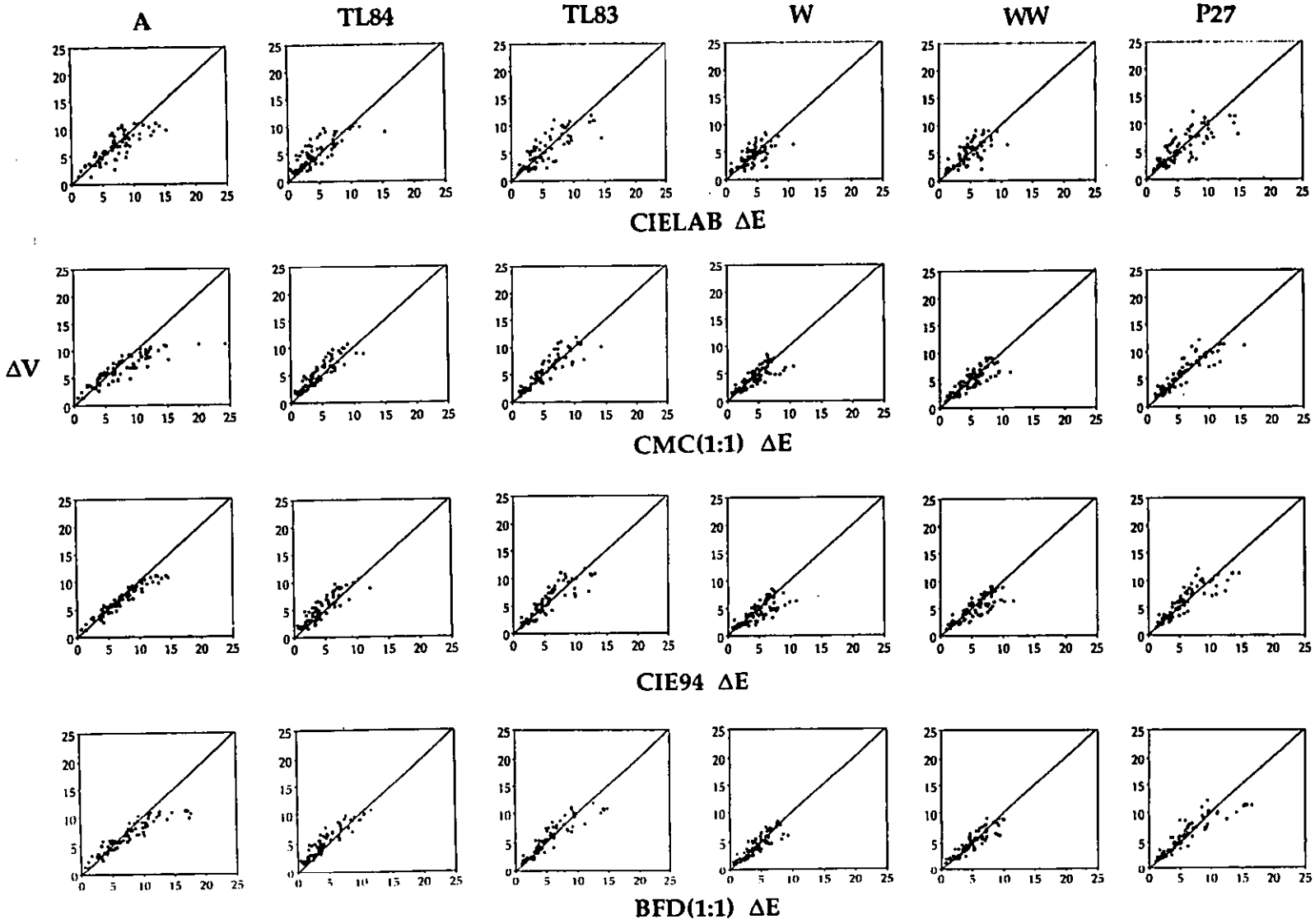

Fig. 3.4.7 The ΔE values calculated using the CIEL*a*b*, CMC(1:1), CIE94 and BFD(1:1) formulae (from top to bottom) plotted against the ΔV results under sources A, TL84, TL83, W, WW and P27 (from left to right).

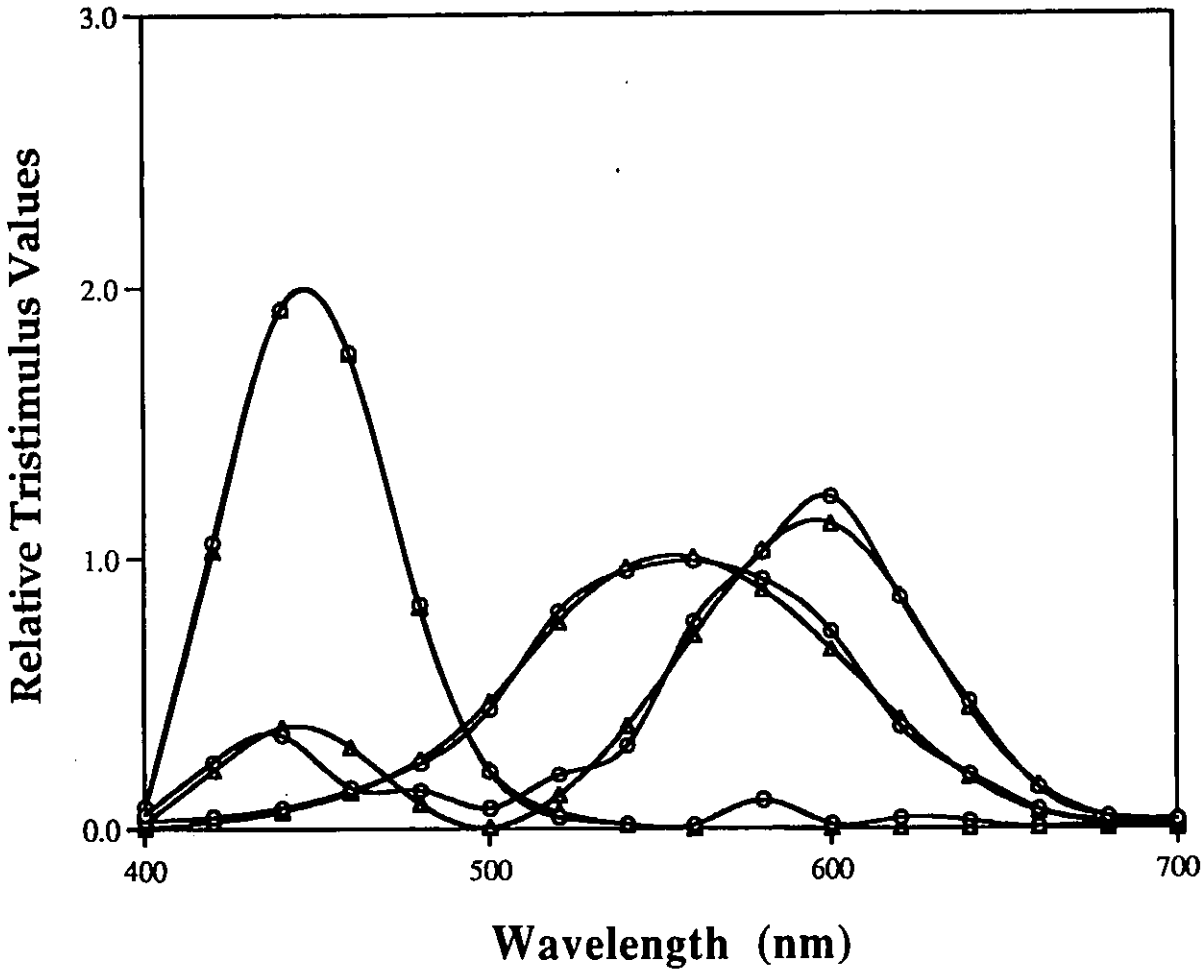

Fig. 3.5.1 Colour-matching functions of the new SDO (o) together with those of the CIE 1964 Observer (Δ).

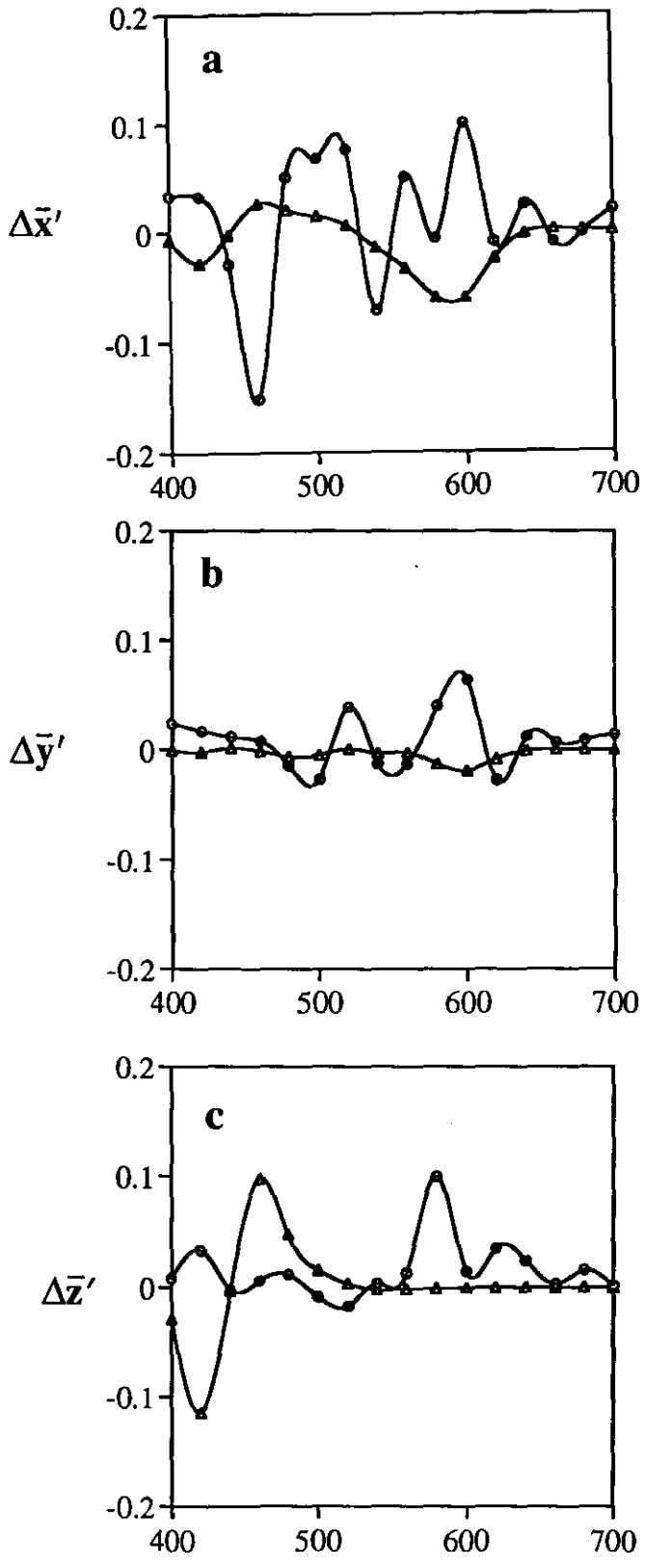

Fig. 3.5.2 Deviations of the CIE SDO (Δ) and new SDO (o) from the CIE 1964 colour-matching functions, (a) $\Delta\bar{x}'$, (b) $\Delta\bar{y}'$ and (c) $\Delta\bar{z}'$.

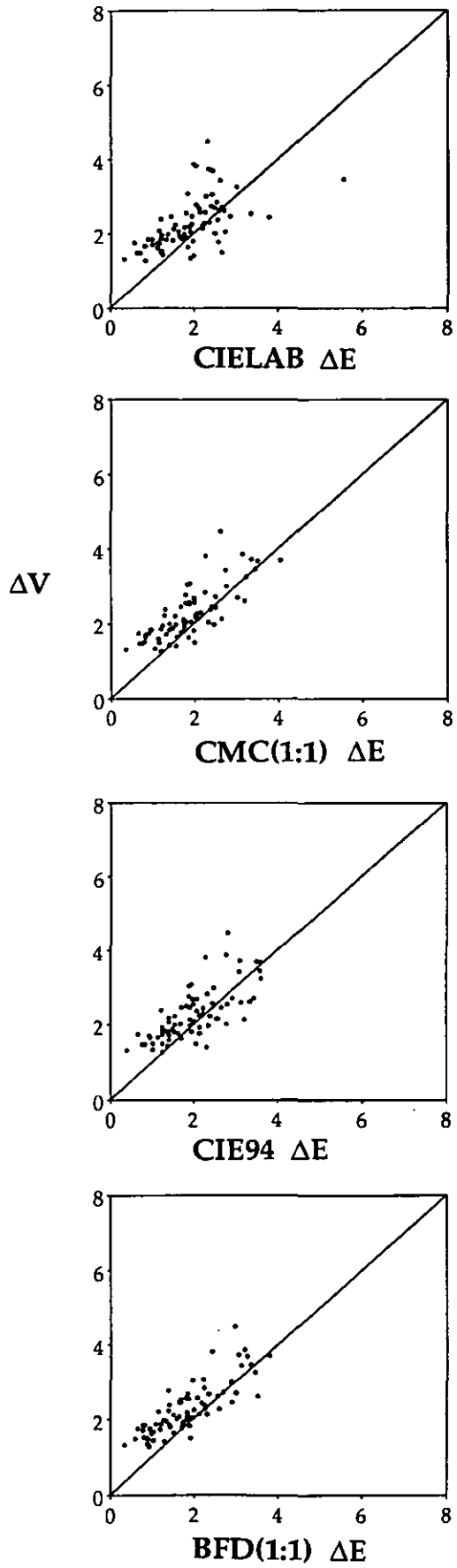

Fig. 3.5.3 The ΔE values calculated using the new SDO for the CIEL*a*b*, CMC(1:1), CIE94 and BFD(1:1) formulae (from top to bottom) plotted against the D65 ΔV results.

APPENDICES

Appendix A.1 List of the reflectance values of the 240 samples prepared in the Colour Constancy Study.

Sample No.	1	2	3	4	5	6	7	8	9	10	11	12
Wavelength (nm)												
400	60.99	50.28	34.19	14.96	17.85	6.75	7.49	2.03	2.22	2.11	2.07	1.95
420	65.34	53.67	40.61	16.95	19.65	7.84	7.66	1.97	2.20	1.96	2.07	1.84
440	67.95	57.01	46.56	20.29	19.96	10.34	7.33	2.25	2.38	1.89	2.10	1.78
460	69.13	60.33	50.84	25.72	17.48	13.88	5.78	3.10	2.77	1.85	2.07	1.75
480	66.86	60.79	51.16	31.20	14.61	15.47	4.38	3.83	2.94	1.81	1.91	1.71
500	64.62	59.52	49.68	30.32	14.04	14.09	4.16	3.35	2.67	1.81	1.77	1.70
520	61.66	56.88	46.62	25.58	17.12	12.00	5.65	2.50	2.34	1.94	1.66	1.70
540	61.08	56.34	45.05	21.21	21.01	11.18	7.86	2.20	2.30	2.06	1.61	1.73
560	61.49	56.87	45.06	19.12	20.41	11.40	7.57	2.06	2.57	1.82	1.59	1.71
580	65.92	61.65	45.87	18.39	18.57	12.32	6.49	1.97	2.96	1.69	1.56	1.68
600	64.90	60.75	50.15	18.46	17.32	12.72	5.81	1.98	2.69	1.65	1.55	1.65
620	63.47	59.24	49.84	27.08	17.23	12.69	5.75	1.84	2.19	1.64	1.54	1.65
640	62.60	58.43	44.59	34.19	17.47	12.87	5.92	1.69	1.78	1.63	1.54	1.64
660	54.00	50.00	5.00	4.00	2.00	1.00	7.00	1.84	1.00	1.00	1.00	1.00
680	.52	.36	.01	2.72	.82	4.97	.77	3.35	.93	.67	.56	.69
700	48.32	44.38	67.81	57.25	30.25	20.30	13.49	10.66	3.66	1.75	1.64	1.98

Sample No.	13	14	15	16	17	18	19	20	21	22	23	24
Wavelength (nm)												
400	51.43	56.87	12.79	15.00	46.00	11.05	2.22	14.68	3.00	2.51	47.92	56.68
420	53.03	59.91	13.41	15.87	47.01	11.50	2.02	15.51	2.89	2.35	49.70	59.17
440	56.10	62.83	15.86	18.62	50.19	13.98	2.08	18.57	3.57	2.71	53.18	62.34
460	60.40	65.95	20.70	23.89	55.92	19.98	2.78	25.58	5.99	4.34	59.01	66.49
480	62.30	66.71	27.45	31.13	61.87	33.50	7.35	40.69	14.49	11.38	65.37	68.74
500	61.57	66.00	30.27	34.27	63.78	46.30	18.84	55.28	28.42	25.13	67.73	68.69
520	59.12	64.10	32.16	36.41	62.89	54.76	45.31	68.00	48.38	50.81	67.25	66.98
540	58.91	63.88	35.05	39.38	62.76	55.94	61.46	72.14	55.14	62.79	66.96	66.41
560	60.67	64.86	51.90	54.99	64.15	57.51	68.75	75.19	57.47	67.11	66.87	65.92
580	69.23	69.98	69.09	67.58	70.76	60.44	70.98	76.49	57.49	66.88	69.63	67.83
600	74.95	70.65	75.79	69.35	74.44	69.05	72.07	77.41	57.69	65.02	66.82	64.25
620	75.40	70.10	77.49	66.88	74.65	75.70	72.57	77.33	55.10	62.15	64.58	61.76
640	75.31	69.50	78.43	62.39	74.54	78.98	72.03	77.31	49.51	57.93	63.54	60.72
660	70.00	61.00	8.00	6.00	69.00	8.00	7.00	8.00	5.00	6.00	55.00	53.00
680	.07	.88	.47	6.53	.78	1.55	4.60	.58	4.27	2.13	.82	.29
700	64.88	56.00	82.56	77.84	65.43	83.48	79.49	84.27	69.74	73.70	49.61	47.45

Appendix A.1 Continued.

Wavelength (nm)	Sample No. 25	26	27	28	29	30	31	32	33	34	35	36
400	57.99	58.83	23.60	15.85	15.80	9.61	3.63	14.37	3.28	6.92	5.44	2.36
420	62.65	62.30	26.03	17.76	15.63	8.87	3.58	15.62	3.19	7.12	5.07	2.18
440	66.22	65.21	30.08	20.86	14.57	7.82	4.47	17.50	3.94	8.87	6.36	2.41
460	69.61	68.04	35.78	23.80	11.86	5.87	7.14	18.31	6.37	13.32	10.19	3.68
480	71.09	68.24	40.31	25.03	9.64	4.50	13.87	17.94	13.26	23.26	20.48	9.86
500	71.02	67.11	39.54	25.63	9.71	4.51	19.57	18.68	20.08	31.50	31.26	22.40
520	69.50	64.69	35.56	30.27	16.03	8.58	23.65	26.99	25.62	36.44	38.59	44.67
540	68.48	63.90	33.40	37.35	33.97	23.24	26.40	44.12	28.76	37.02	37.43	53.58
560	66.23	63.36	33.10	44.29	56.13	47.97	42.15	55.46	43.81	39.07	38.13	56.57
580	64.94	65.40	35.22	53.94	65.05	61.60	60.92	56.38	59.19	41.59	39.87	57.86
600	58.99	61.72	44.79	65.01	68.71	67.23	68.37	55.96	64.14	43.76	41.15	60.85
620	56.17	59.39	52.80	70.47	70.49	69.45	70.11	56.29	65.10	47.42	55.63	60.42
640	55.11	58.33	62.82	73.69	72.56	71.60	71.16	57.23	65.77	52.66	68.05	56.06
660	47.00	50.00	7.00	7.00	7.00	7.00	73.00	6.00	68.00	5.00	73.00	6.00
680	.36	.37	5.29	6.59	5.28	4.53	.39	1.13	.44	9.54	22.00	.68
700	41.46	44.54	81.61	78.68	77.43	77.06	76.66	67.48	73.14	66.23	75.55	74.69

Wavelength (nm)	Sample No. 37	38	39	40	41	42	43	44	45	46	47	48
400	2.38	4.55	11.30	10.43	5.24	18.25	4.47	28.65	9.74	6.48	20.31	27.12
420	2.24	5.12	13.02	10.60	4.89	20.27	5.05	32.10	11.16	7.42	23.01	32.04
440	2.60	7.30	16.77	12.98	6.21	24.02	7.22	34.01	14.71	10.24	27.15	37.29
460	4.25	12.63	22.77	18.72	10.15	30.94	12.73	34.10	21.82	16.60	34.09	43.35
480	11.21	24.13	29.89	31.33	21.30	41.55	25.80	33.59	35.13	30.28	44.99	49.46
500	24.45	34.05	33.85	42.77	35.71	46.50	39.88	34.61	45.53	43.66	51.74	51.79
520	46.97	41.59	41.03	49.42	50.01	45.83	53.12	41.72	51.80	54.09	53.23	50.19
540	55.24	44.29	47.35	48.15	50.89	42.04	54.51	50.03	51.06	52.96	49.39	46.35
560	56.84	47.74	46.90	45.40	47.31	39.28	50.56	49.45	46.92	46.04	42.58	41.48
580	55.25	49.50	43.97	42.58	42.03	37.31	43.15	43.63	39.64	36.61	34.61	36.37
600	53.28	47.07	42.13	41.41	37.67	36.62	35.36	37.76	31.99	28.28	27.80	32.40
620	49.32	42.81	42.08	41.91	33.79	40.90	30.03	33.71	26.80	23.17	23.58	30.18
640	43.13	35.86	42.66	42.95	29.57	43.73	23.42	28.20	20.56	17.22	18.37	26.97
660	4.00	3.00	4.00	49.00	36.00	5.00	25.00	3.00	22.00	19.00	2.00	2.00
680	8.26	8.02	7.25	.39	63.00	.82	.53	.83	.61	.13	.47	9.97
700	65.73	53.84	57.09	61.08	55.74	63.38	40.89	46.04	37.45	33.46	34.61	43.61

Appendix A.1 Continued.

Sample No.	49	50	51	52	53	54	55	56	57	58	59	60
Wavelength (nm)												
400	28.53	29.96	23.36	15.18	8.07	15.67	20.20	8.84	12.48	7.38	4.30	2.71
420	31.41	37.37	26.07	15.85	8.07	16.62	20.34	8.21	11.72	8.28	4.28	2.34
440	37.57	42.64	30.14	15.41	8.36	19.36	19.55	7.51	10.59	10.77	4.59	2.10
460	46.07	45.07	35.74	13.53	7.76	24.22	17.28	5.95	8.31	15.05	4.38	1.89
480	51.86	43.35	40.49	9.86	6.06	29.36	14.69	4.66	6.47	18.96	3.88	1.77
500	53.50	39.71	39.73	7.98	5.12	29.42	14.29	4.63	6.40	19.58	3.98	1.78
520	53.55	34.64	35.70	7.30	5.03	26.92	18.09	7.98	10.62	19.85	7.22	2.28
540	51.43	30.17	31.30	8.06	5.91	24.78	25.09	17.26	21.17	21.46	17.26	8.12
560	46.67	28.68	29.42	15.65	14.70	25.34	32.79	29.25	32.89	26.72	31.15	29.69
580	38.16	28.62	28.93	34.58	34.17	27.43	41.19	43.21	43.18	36.86	45.32	51.14
600	29.96	29.63	29.31	56.07	56.65	29.96	45.80	60.69	52.07	49.29	61.28	63.50
620	24.12	46.95	41.69	65.74	70.33	46.91	43.30	68.90	55.24	54.46	68.50	67.74
640	18.40	66.93	51.99	70.42	76.66	64.88	36.72	72.15	56.77	56.38	71.55	70.59
660	2.00	7.00	60.00	7.00	8.00	73.00	3.00	74.00	6.00	60.00	73.00	73.70
680	2.83	6.25	.10	4.04	.43	.18	9.13	.36	.86	.47	.82	76.31
700	41.32	78.79	69.58	76.76	82.99	76.30	54.71	75.85	67.56	67.16	75.43	78.18

Sample No.	61	62	63	64	65	66	67	68	69	70	71	72
Wavelength (nm)												
400	11.24	7.94	2.12	9.36	2.11	4.41	2.05	10.95	3.67	2.08	2.11	3.26
420	12.74	7.71	1.96	9.80	1.96	4.77	1.91	12.05	4.09	1.95	1.97	3.51
440	15.99	7.45	1.94	10.56	1.93	5.90	1.88	14.02	5.81	1.95	1.96	4.64
460	21.00	6.18	2.02	10.15	2.01	7.07	1.97	15.37	10.12	2.26	2.16	6.84
480	24.98	5.00	2.34	9.15	2.47	7.69	2.79	15.56	18.62	4.70	4.70	9.73
500	25.39	5.07	2.77	9.43	3.31	8.37	4.65	16.25	24.16	9.56	12.79	11.73
520	25.32	9.60	5.67	15.55	7.33	14.40	10.99	23.01	26.99	20.09	29.52	19.52
540	26.52	24.17	17.42	30.26	20.63	29.06	26.07	34.49	28.12	32.46	35.48	35.67
560	30.51	41.21	38.26	40.46	41.17	39.98	42.93	37.82	30.83	37.57	34.85	42.96
580	36.40	44.63	48.80	39.88	47.90	39.75	44.35	35.20	34.23	35.99	32.57	35.97
600	41.19	44.07	51.76	38.30	45.29	38.24	39.24	33.26	36.46	34.11	30.72	27.91
620	42.83	44.19	52.90	38.18	41.30	38.16	34.66	33.11	37.27	33.59	30.17	22.87
640	43.70	44.86	54.12	38.64	34.73	38.65	28.07	33.59	37.89	33.92	30.45	16.97
660	4.00	49.00	57.00	43.00	36.00	43.00	29.00	3.00	42.00	37.00	33.00	18.00
680	8.18	.42	.96	.19	.59	.20	.74	8.05	.37	.18	.49	.76
700	57.76	58.73	64.63	53.43	51.84	53.40	44.99	48.64	52.50	44.25	40.31	32.83

Appendix A.1 Continued.

Wavelength (nm)	Sample No. 73	74	75	76	77	78	79	80	81	82	83	84
400	12.64	2.04	2.99	2.08	12.88	10.49	3.13	2.36	9.98	3.53	9.15	17.34
420	13.24	1.91	3.21	1.99	14.88	10.83	3.42	2.35	11.13	3.48	9.32	17.55
440	14.16	1.89	4.32	2.14	18.92	13.32	4.84	2.91	14.08	4.46	11.86	18.86
460	14.21	2.09	7.10	3.21	25.23	19.05	8.97	5.24	19.93	7.66	17.95	23.28
480	13.75	4.51	12.40	8.57	31.37	30.72	19.92	13.97	29.71	17.51	30.16	34.45
500	14.42	12.33	16.49	17.43	32.56	39.20	31.69	26.77	35.71	31.45	39.73	44.30
520	21.91	29.90	26.00	32.57	31.42	41.28	39.39	41.58	38.11	44.12	42.00	46.24
540	37.34	38.18	39.61	41.53	30.21	37.85	36.58	41.75	37.30	39.56	37.03	38.52
560	42.28	38.30	40.97	37.45	29.39	33.75	31.43	34.56	34.11	29.16	29.28	27.66
580	34.46	32.91	32.49	28.30	28.49	30.38	26.84	25.65	27.90	19.81	21.35	18.48
600	26.37	26.05	24.50	20.55	27.70	28.88	23.55	18.26	21.10	13.50	15.51	12.08
620	21.46	21.43	19.75	16.17	27.77	29.17	21.93	14.09	16.73	9.75	11.59	8.85
640	15.79	15.68	14.28	11.24	28.23	29.89	19.63	9.51	11.74	6.46	7.97	5.72
660	1.00	16.00	15.00	12.00	3.00	36.00	22.00	10.00	13.00	8.63	1.00	6.73
680	7.54	.91	.88	.52	2.49	.43	.25	.73	.29	20.16	.58	15.31
700	31.15	30.14	28.96	24.38	43.15	51.27	34.22	21.90	25.68	41.43	23.38	32.68

Wavelength (nm)	Sample No. 85	86	87	88	89	90	91	92	93	94	95	96
400	18.06	17.44	24.27	17.22	24.69	26.96	21.40	21.93	19.27	18.91	18.92	15.30
420	19.09	20.02	24.59	15.89	27.77	30.98	28.57	25.07	20.75	20.41	20.44	19.63
440	23.15	24.15	25.03	21.93	30.86	34.81	36.46	29.19	20.83	20.51	20.59	18.93
460	26.24	30.75	28.47	36.23	35.26	38.46	41.60	33.68	18.67	18.24	18.61	13.67
480	27.40	39.76	37.73	47.63	39.85	39.45	39.95	35.03	14.94	14.92	14.57	8.40
500	27.37	42.94	44.39	47.75	40.13	37.70	35.67	31.83	12.82	13.42	12.01	6.18
520	26.85	39.47	43.82	40.49	36.56	34.20	28.99	26.52	11.79	13.69	10.26	5.16
540	26.59	33.71	37.05	31.03	32.42	31.63	23.87	22.25	12.41	15.24	10.42	5.11
560	26.37	27.51	27.81	20.73	27.75	29.44	19.73	20.43	15.22	17.79	13.19	8.65
580	24.10	22.18	19.59	12.83	23.02	27.08	16.85	19.91	22.02	22.33	21.47	22.99
600	20.24	18.21	13.58	7.96	18.77	24.30	15.69	20.14	31.73	26.98	38.89	45.87
620	15.79	16.03	10.34	5.41	16.13	22.28	15.95	29.60	37.07	29.04	55.75	61.73
640	11.71	13.08	6.95	3.46	12.76	19.43	16.80	37.49	39.42	30.08	66.54	69.92
660	16.00	1.00	8.17	4.71	1.00	2.00	2.00	46.00	4.00	3.00	7.00	7.00
680	.84	5.07	17.70	12.53	4.37	1.50	2.38	.07	4.40	4.60	2.30	4.27
700	35.08	26.63	35.88	30.09	24.79	32.03	36.30	59.86	54.44	45.41	75.18	76.77

Appendix A.1 Continued.

Wavelength (nm)	Sample No. 97	98	99	100	101	102	103	104	105	106	107	108
400	16.45	16.27	13.57	8.91	13.19	5.66	4.68	7.98	2.24	6.82	10.06	2.02
420	17.07	16.82	13.41	8.88	13.05	5.64	4.57	9.19	2.06	6.16	9.49	1.88
440	16.53	16.24	12.51	8.29	12.11	6.07	4.70	11.93	1.98	5.32	8.45	1.88
460	14.14	13.74	10.16	6.84	9.71	6.03	4.33	15.93	1.86	3.93	6.38	1.98
480	10.92	10.82	7.79	4.58	7.48	5.00	3.36	18.28	1.77	2.99	4.83	2.28
500	9.42	9.78	7.08	3.61	7.01	4.29	2.88	17.29	1.76	2.95	4.74	3.04
520	9.22	10.73	8.29	3.28	9.18	4.24	2.87	15.53	2.19	5.14	8.08	5.57
540	10.40	13.13	10.92	3.62	13.41	4.98	3.35	15.30	5.74	12.03	16.52	10.04
560	13.56	16.72	14.74	8.14	17.87	12.83	9.34	17.13	14.52	20.00	23.75	19.81
580	21.83	23.97	23.17	23.36	25.11	29.86	27.00	21.06	26.05	27.36	27.91	32.33
600	36.95	33.72	38.07	46.61	33.93	42.50	52.60	24.55	44.55	34.20	30.51	46.90
620	48.26	38.82	48.66	60.68	37.86	45.34	67.44	25.61	59.20	36.72	31.61	57.14
640	53.84	40.99	53.76	68.03	39.48	46.01	72.33	26.20	67.64	37.85	32.28	63.91
660	5.00	4.00	5.00	7.00	4.00	4.00	7.00	2.00	7.00	4.00	3.00	6.00
680	9.00	5.80	8.00	2.69	3.08	8.90	5.65	9.28	2.48	1.36	6.70	8.71
700	66.12	55.64	63.19	75.48	50.04	55.49	79.28	36.29	75.15	48.55	47.35	72.22

Wavelength (nm)	Sample No.109	110	111	112	113	114	115	116	117	118	119	120
400	2.09	5.74	1.92	4.88	1.90	5.81	2.01	1.91	3.79	1.88	11.80	9.72
420	1.94	5.56	1.80	4.86	1.79	6.22	1.94	1.82	4.24	1.78	10.76	11.06
440	1.90	6.47	1.80	4.99	1.77	7.15	2.14	1.90	5.67	1.80	9.55	13.37
460	1.81	8.14	1.85	4.41	1.88	7.43	2.91	2.48	7.99	2.19	7.94	15.17
480	1.73	10.44	1.93	3.71	2.42	7.00	4.66	5.30	10.30	5.36	6.79	15.57
500	1.73	12.56	2.04	3.78	3.18	7.26	6.11	9.05	11.57	12.10	6.95	15.88
520	2.28	14.82	3.59	7.23	6.77	12.03	11.40	16.22	16.61	22.06	11.68	19.56
540	7.94	14.69	11.89	18.04	17.50	21.70	22.08	23.31	22.95	24.11	21.84	22.98
560	24.27	14.82	25.88	26.66	27.60	24.53	26.73	23.03	22.12	20.89	24.06	20.79
580	33.78	14.99	29.47	25.73	27.60	21.92	24.47	20.03	19.04	17.68	18.01	17.78
600	35.49	15.39	28.50	23.75	25.77	19.80	22.27	17.91	16.99	15.59	11.90	16.08
620	35.85	25.81	27.97	23.09	25.10	19.15	21.58	17.27	16.38	14.94	8.84	15.90
640	36.40	36.41	28.20	23.26	25.26	19.31	21.72	17.37	16.50	14.98	5.63	16.20
660	4.00	46.00	31.00	26.00	28.00	22.00	24.00	19.00	18.00	17.00	6.00	19.00
680	.66	11.00	.17	.19	.05	.05	.52	.80	.98	.11	.43	.64
700	50.52	59.93	38.05	33.01	34.67	28.58	31.18	25.80	25.04	22.57	14.76	29.04

Appendix A.1 Continued.

Wavelength (nm)	Sample No.121	122	123	124	125	126	127	128	129	130	131	132
400	4.59	2.40	6.55	6.20	4.12	5.74	8.42	10.13	7.72	10.21	20.61	10.78
420	4.85	2.55	6.64	6.22	4.04	5.45	10.11	11.97	9.31	9.10	22.41	11.23
440	6.23	3.50	8.53	8.06	5.31	7.51	13.84	15.71	13.07	13.14	31.28	23.99
460	9.83	6.61	13.23	12.73	9.21	13.17	20.10	21.24	20.08	23.76	33.13	35.98
480	17.40	15.11	22.37	21.82	19.90	24.70	26.80	25.02	28.38	35.75	29.71	38.30
500	20.78	22.64	27.60	26.92	32.78	33.01	27.26	23.98	28.93	37.36	27.70	35.19
520	18.50	25.60	26.64	25.68	39.37	31.71	23.36	20.84	23.57	30.39	27.50	26.94
540	14.78	22.59	23.97	22.47	31.82	24.00	19.70	18.74	18.49	22.06	26.77	18.84
560	12.60	18.12	21.30	18.95	21.44	15.45	16.58	17.33	14.13	13.74	23.68	11.16
580	11.62	14.92	18.22	15.08	13.38	9.11	14.37	16.47	11.31	7.85	18.17	6.08
600	11.31	13.00	15.81	11.98	8.37	5.37	13.09	15.68	9.70	4.56	13.01	3.62
620	15.53	12.44	12.67	9.11	5.72	3.62	13.00	15.38	9.24	3.12	9.31	2.51
640	18.79	12.52	8.84	6.10	3.63	2.42	13.25	15.61	9.32	2.20	6.43	2.03
660	2.00	14.00	1.00	8.17	4.87	3.14	16.00	1.00	11.00	2.78	10.00	2.93
680	5.12	.64	1.54	19.31	12.78	8.50	.31	8.15	.15	7.30	.13	8.49
700	39.54	20.02	25.12	40.10	30.34	22.99	25.16	24.21	15.89	20.64	24.86	23.34

Wavelength (nm)	Sample No.133	134	135	136	137	138	139	140	141	142	143	144
400	14.84	21.53	20.16	23.65	19.86	25.01	25.71	19.67	12.14	11.22	9.70	7.54
420	18.40	26.30	23.24	26.42	22.29	33.97	29.88	22.09	13.22	11.50	10.78	10.26
440	24.44	30.63	27.31	31.35	22.86	37.82	33.22	25.69	14.01	11.02	9.64	9.37
460	32.19	31.73	31.74	32.02	21.05	34.68	30.40	26.74	13.27	9.19	6.55	5.78
480	33.60	27.93	32.82	25.64	17.78	26.71	24.16	22.79	10.44	6.38	4.04	3.17
500	29.12	24.23	29.27	20.78	15.87	20.83	20.49	18.85	8.45	4.89	3.17	2.41
520	21.94	20.26	23.57	16.26	14.63	15.36	18.52	14.88	7.07	4.00	3.00	2.12
540	16.81	18.06	19.22	14.54	13.93	11.89	18.30	13.42	7.12	4.07	3.19	2.10
560	12.62	16.72	17.13	14.20	14.22	10.68	23.58	13.47	9.04	5.50	5.67	3.34
580	9.95	15.90	16.43	15.20	15.10	10.66	32.63	15.44	14.39	10.80	16.02	11.60
600	8.42	15.21	16.45	20.09	14.87	11.36	32.69	24.71	22.78	24.96	26.24	31.00
620	7.99	15.17	24.56	21.55	16.76	25.42	27.79	34.37	27.73	43.19	26.18	50.34
640	8.01	15.40	31.24	17.98	24.11	51.39	22.49	35.97	29.90	58.38	20.67	63.18
660	9.58	1.00	39.00	2.00	3.00	7.00	29.00	4.00	3.00	6.00	22.00	6.00
680	13.85	8.39	.61	2.18	7.00	1.56	.20	2.27	4.57	7.46	8.00	9.86
700	21.72	26.70	54.53	39.90	52.61	78.19	50.01	59.85	44.92	72.02	36.62	73.43

Appendix A.1 Continued.

Wavelength (nm)	Sample No.145	146	147	148	149	150	151	152	153	154	155	156
400	12.49	5.83	3.59	2.55	2.32	8.36	5.62	2.96	2.21	2.95	3.13	2.25
420	12.55	5.69	3.39	2.56	2.20	7.95	6.16	2.56	2.03	2.58	3.46	2.16
440	11.38	5.93	3.08	3.00	2.21	6.87	7.71	2.29	1.94	2.32	4.74	2.21
460	8.95	6.09	2.57	3.91	2.11	5.01	10.00	2.02	1.86	2.03	7.52	2.17
480	6.71	5.08	2.00	4.28	1.96	3.66	10.70	1.87	1.80	1.89	11.24	2.06
500	5.97	4.35	1.84	4.00	1.93	3.38	9.92	1.86	1.80	1.88	11.87	2.10
520	6.92	4.10	1.79	3.85	2.23	4.57	9.30	2.18	1.96	2.44	10.89	3.53
540	8.67	4.58	1.82	4.34	3.26	6.91	9.75	4.07	4.62	6.77	10.62	11.81
560	12.95	6.76	3.05	6.50	5.29	11.56	11.68	8.44	14.50	16.16	11.77	22.52
580	19.39	13.17	11.28	13.10	10.81	19.49	14.79	16.78	22.70	22.75	15.28	19.07
600	17.70	26.92	31.21	28.02	24.98	19.69	17.05	31.23	26.78	23.39	19.35	12.98
620	14.31	36.91	49.51	39.56	42.25	16.50	17.45	36.83	27.92	20.06	19.82	9.65
640	9.79	40.71	61.45	44.02	55.65	11.60	17.71	32.25	28.57	14.54	23.68	6.16
660	10.00	4.00	6.00	4.00	6.00	12.00	2.00	3.00	3.00	1.00	3.00	6.94
680	.86	5.65	8.46	8.99	3.74	76.00	.16	4.07	2.66	5.74	8.29	15.57
700	21.94	55.20	72.36	58.09	69.19	24.81	26.20	49.47	42.48	28.63	56.71	33.20

Wavelength (nm)	Sample No.157	158	159	160	161	162	163	164	165	166	167	168
400	11.21	2.02	8.33	2.03	4.89	1.91	3.12	2.44	4.57	2.46	6.06	11.31
420	10.50	1.93	7.28	1.93	4.87	1.83	3.24	2.48	4.78	2.48	5.23	9.53
440	9.35	1.97	6.37	1.95	6.02	1.82	4.14	3.04	5.92	2.94	5.30	9.00
460	7.62	2.14	5.15	2.12	9.02	1.96	6.73	5.03	8.90	4.74	7.23	11.03
480	6.23	2.48	4.30	3.10	14.95	3.71	12.57	11.28	15.22	11.49	14.68	18.23
500	6.04	2.81	4.40	4.52	17.71	8.82	14.87	17.57	18.81	20.30	23.15	23.54
520	8.63	5.59	8.03	9.50	15.78	18.35	12.39	20.16	18.46	23.11	23.26	21.19
540	13.11	15.19	17.32	19.09	12.73	20.03	9.31	17.34	16.33	16.53	15.60	15.22
560	16.80	20.49	19.81	19.32	10.14	13.46	7.46	12.23	13.05	9.32	8.25	9.22
580	16.94	14.76	14.18	12.54	8.61	7.59	6.61	7.41	9.08	4.96	4.21	5.25
600	12.27	9.26	9.00	7.42	8.50	4.15	6.27	4.22	5.60	2.85	2.47	3.11
620	9.24	6.62	6.43	5.20	11.00	2.94	8.49	3.01	3.97	2.23	2.03	2.40
640	5.92	4.12	4.04	3.28	17.13	2.12	10.29	2.16	2.65	1.90	1.83	1.96
660	6.00	4.67	4.68	3.69	28.00	2.35	1.00	2.45	3.06	2.07	1.98	2.17
680	.71	11.16	11.27	8.93	38.00	5.05	4.89	5.45	7.31	3.70	3.16	4.27
700	15.18	26.59	26.72	23.08	43.64	14.98	27.13	15.87	19.73	11.25	9.53	12.76

Appendix A.1 Continued.

Wavelength (nm)	Sample No.169	170	171	172	173	174	175	176	177	178	179	180
400	5.55	11.79	11.36	15.59	4.54	12.86	7.71	14.23	16.42	22.68	20.15	14.57
420	4.54	12.10	11.53	15.41	4.59	14.93	8.49	18.77	18.82	26.38	23.24	15.64
440	7.27	15.92	12.57	15.62	14.20	18.31	10.76	25.70	21.49	29.40	26.49	14.66
460	16.27	14.74	15.74	16.80	26.90	23.11	14.74	31.12	22.98	28.74	25.64	12.07
480	26.71	11.99	21.04	17.01	28.26	25.46	18.32	27.78	20.05	23.31	20.08	8.84
500	26.62	11.34	21.63	15.85	23.44	22.53	16.56	22.30	16.95	18.60	15.78	7.03
520	19.39	13.97	16.94	14.18	14.91	16.35	12.18	15.65	13.68	13.59	11.70	6.24
540	12.40	16.74	12.30	13.22	8.62	11.90	9.04	11.39	11.78	11.08	9.98	6.27
560	6.49	14.89	8.18	12.18	4.16	8.35	7.48	8.18	10.37	9.31	9.21	9.34
580	3.32	10.47	5.41	10.40	2.24	6.12	6.92	6.28	9.53	8.76	9.66	14.97
600	2.06	6.79	3.70	8.05	1.70	4.77	6.81	5.27	9.05	10.11	13.24	13.65
620	1.74	4.54	2.97	6.47	1.58	4.21	11.00	5.07	9.34	10.73	15.95	10.76
640	1.63	3.11	2.31	4.61	1.57	3.60	14.55	5.13	10.08	16.91	24.00	7.04
660	1.75	5.00	2.57	5.28	1.73	4.18	20.00	6.47	1.00	3.00	4.00	7.00
680	2.92	.09	5.34	11.32	2.95	7.87	49.00	10.74	2.37	4.52	3.32	.93
700	9.66	14.90	13.21	23.60	10.17	15.65	34.58	19.00	17.54	56.21	63.02	17.43

Wavelength (nm)	Sample No.181	182	183	184	185	186	187	188	189	190	191	192
400	19.16	13.40	7.94	8.17	5.09	4.93	3.52	2.15	2.23	3.43	2.13	2.25
420	22.15	14.78	8.07	7.31	5.01	4.31	2.91	1.99	2.07	3.00	1.99	2.09
440	25.46	17.02	7.62	6.64	4.69	3.96	2.55	1.91	2.00	2.65	1.93	2.02
460	23.87	17.01	6.18	5.86	3.83	3.58	2.27	1.87	1.95	2.23	1.88	1.97
480	17.80	13.46	4.22	4.34	2.78	2.80	1.99	1.83	1.91	1.96	1.84	1.92
500	13.72	10.53	3.29	3.61	2.35	2.46	1.91	1.83	1.90	1.95	1.83	1.92
520	10.17	8.00	2.79	3.34	2.15	2.35	1.91	1.84	1.94	2.38	1.89	2.01
540	8.91	7.24	2.82	3.62	2.15	2.54	2.01	1.90	2.26	4.09	2.60	3.35
560	8.84	7.69	3.62	4.88	2.56	3.49	2.54	2.26	3.67	6.82	5.64	8.82
580	10.20	9.33	6.76	7.77	4.78	6.81	5.19	4.33	8.04	10.20	11.36	14.30
600	17.37	17.38	13.73	11.21	12.86	13.98	14.89	14.23	19.08	13.38	18.43	15.70
620	26.85	30.81	18.50	12.33	23.16	18.55	25.99	30.08	25.97	14.52	18.65	13.24
640	38.82	44.67	19.23	12.77	30.26	20.23	31.70	38.59	23.06	15.03	14.03	9.05
660	5.00	5.00	22.00	14.00	36.00	24.00	36.00	43.00	24.00	18.00	15.00	9.00
680	5.90	8.43	.45	.96	.65	.05	.98	.47	.47	.20	.03	.84
700	69.50	70.52	33.36	20.30	46.45	33.27	46.38	56.16	38.40	26.75	27.04	19.75

Appendix A.1 Continued.

Wavelength (nm)	Sample No.193	194	195	196	197	198	199	200	201	202	203	204
400	2.24	5.40	2.06	1.99	2.03	2.34	1.98	2.02	2.08	4.03	3.15	2.90
420	2.08	5.16	1.98	1.91	1.96	2.38	1.90	1.94	2.06	2.94	3.55	3.10
440	2.00	4.69	1.97	1.90	1.94	2.85	1.89	1.96	2.33	2.64	4.84	3.88
460	1.94	3.57	2.02	1.97	1.98	4.23	1.93	2.21	3.61	3.22	7.36	5.99
480	1.90	2.80	2.14	2.57	2.29	6.80	2.49	4.42	8.24	6.91	9.56	10.89
500	1.89	2.76	2.30	3.78	2.95	7.59	4.35	9.31	11.92	12.35	9.19	13.13
520	2.03	4.42	3.72	6.88	5.91	7.12	9.23	12.65	10.77	12.19	7.76	10.32
540	4.47	8.42	8.49	10.15	11.65	6.89	12.11	9.27	7.61	7.00	6.75	6.86
560	12.55	8.99	10.82	9.41	10.29	7.20	7.91	4.96	5.02	3.22	5.99	4.25
580	14.45	7.38	9.37	7.62	5.78	7.02	4.13	2.73	3.51	1.92	5.39	2.83
600	11.09	6.38	8.19	6.55	3.23	5.38	2.44	1.96	2.71	1.60	4.96	2.16
620	8.31	6.28	8.03	6.41	2.44	3.96	2.01	1.81	2.42	1.55	4.94	1.94
640	5.29	6.42	8.14	6.52	2.01	2.65	1.83	1.77	2.12	1.54	5.05	1.79
660	5.00	8.00	10.00	8.00	2.00	3.00	1.00	1.00	2.00	1.58	6.00	1.00
680	.90	.41	.17	.26	.17	.03	.94	.85	.36	1.77	.59	.91
700	13.31	14.94	16.51	13.86	3.86	7.15	2.89	2.28	4.77	3.44	12.06	3.19

Wavelength (nm)	Sample No.205	206	207	208	209	210	211	212	213	214	215	216
400	3.31	2.61	4.76	9.55	4.42	7.05	7.75	11.40	8.17	10.48	10.14	16.91
420	2.80	3.08	4.09	8.73	6.10	8.48	10.26	10.05	13.18	15.34	12.60	20.36
440	4.64	4.86	6.44	8.34	9.39	10.92	15.36	9.19	21.00	21.05	14.71	21.76
460	11.74	8.41	14.07	8.89	12.38	13.62	22.18	9.02	25.28	20.90	14.05	18.55
480	19.07	13.81	19.81	9.80	13.61	13.13	20.60	8.29	19.49	16.26	10.53	12.30
500	17.59	13.95	17.27	9.24	11.53	10.56	15.37	7.38	14.10	12.01	8.18	8.49
520	11.79	8.82	10.89	7.62	7.70	7.17	9.65	6.48	8.88	7.48	6.15	5.17
540	6.94	5.03	6.27	6.58	5.30	5.20	6.47	6.27	6.07	5.13	5.17	3.70
560	3.41	2.59	3.28	5.65	3.35	3.78	4.34	6.43	4.29	3.43	4.55	2.81
580	2.00	1.83	2.15	4.48	2.42	2.96	3.26	6.36	3.35	2.65	4.17	2.46
600	1.60	1.63	1.73	3.22	1.95	2.48	2.72	5.52	3.00	2.29	3.90	2.53
620	1.52	1.59	1.61	2.56	1.79	2.30	2.59	4.69	3.06	2.05	3.91	2.50
640	1.49	1.65	1.55	2.04	2.27	2.12	2.59	3.40	3.29	3.05	4.04	3.74
660	1.53	2.07	1.00	2.00	6.00	2.00	3.06	4.08	5.17	9.71	5.34	8.74
680	1.80	5.33	.61	.27	.27	.37	4.70	9.87	12.18	26.04	9.91	20.66
700	4.71	16.62	2.28	4.70	19.62	4.05	8.68	24.00	27.25	46.32	19.03	38.40

Appendix A.1 Continued.

Wavelength (nm)	Sample No.217	218	219	220	221	222	223	224	225	226	227	228
400	11.19	10.48	17.28	9.83	10.70	8.56	2.67	3.24	2.51	2.24	2.36	2.13
420	13.04	10.47	26.55	10.44	12.37	9.48	2.55	3.10	2.30	2.05	2.14	2.00
440	14.03	10.41	28.97	10.45	14.57	11.54	2.56	2.87	2.16	1.97	2.04	1.94
460	12.62	9.81	23.08	9.06	12.66	12.03	2.54	2.41	2.03	1.93	1.96	1.89
480	9.25	7.51	14.84	6.43	8.01	9.30	2.17	1.95	1.90	1.86	1.89	1.86
500	7.15	6.13	10.19	4.93	5.51	6.87	1.96	1.80	1.87	1.84	1.87	1.85
520	5.53	5.33	6.53	3.96	3.78	4.82	1.87	1.73	1.84	1.82	1.87	1.90
540	5.00	5.32	4.66	3.87	3.32	4.22	1.92	1.72	1.84	1.82	1.91	2.41
560	5.10	6.00	4.05	4.61	3.38	4.27	2.19	1.83	1.88	1.85	2.08	4.07
580	5.65	7.06	4.07	6.71	4.07	5.17	2.88	2.53	2.32	2.12	3.03	5.70
600	6.16	7.81	4.47	9.53	8.54	10.60	3.70	4.95	5.64	5.40	6.07	5.67
620	6.58	8.25	13.20	11.39	16.97	19.47	3.94	7.14	11.47	14.28	8.32	4.48
640	7.06	8.88	35.24	13.05	23.83	24.87	4.07	8.20	15.56	22.77	9.12	2.95
660	9.29	1.00	5.00	16.00	3.00	3.00	4.00	10.00	19.00	29.00	10.00	3.00
680	15.69	1.04	9.88	.22	2.29	2.40	.98	.60	.74	.27	.84	.22
700	26.70	16.01	72.12	22.40	49.61	50.06	7.68	17.29	28.00	38.24	15.10	7.41

Wavelength (nm)	Sample No.229	230	231	232	233	234	235	236	237	238	239	240
400	1.83	2.03	1.94	1.83	4.27	2.85	2.70	3.96	2.74	4.89	10.99	4.67
420	1.75	1.92	1.87	1.75	3.39	2.66	2.34	3.82	3.02	6.06	12.86	4.86
440	1.73	1.86	1.85	1.75	3.07	2.58	2.26	3.85	3.83	7.29	15.10	4.78
460	1.81	1.82	1.87	1.87	3.30	2.47	2.62	4.33	5.07	7.67	12.91	4.03
480	2.04	1.79	1.96	2.75	4.32	2.35	4.39	5.04	5.28	6.46	7.85	2.84
500	2.13	1.78	2.11	4.01	5.23	2.36	5.90	4.70	4.25	4.81	5.22	2.32
520	2.14	1.85	3.30	4.27	6.94	2.97	4.95	3.53	2.94	3.08	3.36	2.05
540	2.26	2.94	5.72	3.62	6.84	3.43	3.15	2.70	2.34	2.31	2.70	2.01
560	2.71	5.60	4.19	2.78	3.88	2.54	2.02	2.11	2.06	1.93	2.38	2.18
580	3.30	4.97	2.40	2.07	2.22	1.93	1.70	1.81	1.96	1.78	2.30	2.62
600	3.05	3.23	1.82	1.70	1.67	1.68	1.62	1.68	2.00	1.72	2.67	3.09
620	2.42	2.45	1.73	1.62	1.56	1.62	1.60	1.64	2.30	1.72	2.84	3.33
640	1.88	1.96	1.70	1.60	1.54	1.59	1.59	1.63	3.05	1.72	3.90	3.47
660	2.00	2.00	1.00	1.00	1.00	1.00	1.00	1.00	4.00	1.00	7.78	4.00
680	.06	.12	.76	.66	.60	.62	.64	.68	.69	.87	18.52	.54
700	4.11	3.91	2.06	1.94	1.96	1.94	1.73	2.02	8.11	3.22	36.41	8.57

Appendix A.2 Mean visual lightness, colourfulness and hue results for the 240 samples studied.

Sample	Visual Results under D65			under A			under TL84		
No.	L	C	H	L	C	H	L	C	H
1*	91.40	1.00	999.00	94.20	1.00	999.00	95.40	1.00	999.00
2	91.80	1.00	999.00	95.40	1.00	999.00	95.40	1.00	999.00
3	84.60	1.00	999.00	94.20	1.00	999.00	94.80	1.00	999.00
4	59.00	1.00	999.00	57.60	1.00	999.00	57.00	1.00	999.00
5	62.60	1.00	999.00	60.00	1.00	999.00	56.20	1.00	999.00
6	43.80	1.00	999.00	40.20	1.00	999.00	41.40	1.00	999.00
7	29.00	1.00	999.00	10.40	1.00	999.00	9.80	1.00	999.00
8	11.60	1.00	999.00	10.00	1.00	999.00	11.40	1.00	999.00
9	12.00	1.00	999.00	9.80	1.00	999.00	8.00	1.00	999.00
10	11.20	1.00	999.00	7.80	1.00	999.00	10.00	1.00	999.00
11	8.60	1.00	999.00	7.60	1.00	999.00	7.40	1.00	999.00
12	11.20	1.00	999.00	9.60	1.00	999.00	9.40	1.00	999.00
13	92.00	5.00	413.00	83.60	32.50	50.00	80.80	26.30	58.00
14	93.60	3.40	418.00	84.80	28.20	75.00	82.20	19.30	61.00
15	76.60	26.00	52.00	93.40	4.70	52.00	92.60	5.90	44.00
16	81.20	19.20	67.40	87.20	31.70	88.80	85.80	31.90	93.00
17	93.00	4.50	60.00	85.60	64.40	99.00	80.60	64.90	99.40
18	81.80	24.30	96.40	91.20	28.50	97.80	89.60	23.10	99.60
19	83.20	64.90	97.40	81.80	51.30	102.20	82.00	50.90	103.20
20	87.00	23.20	102.20	84.60	56.30	100.40	85.80	53.80	102.80
21	77.80	51.50	104.60	93.00	3.40	129.00	95.20	3.10	101.00
22	84.00	63.00	99.20	92.60	5.00	254.00	91.20	5.00	271.00
23	91.40	3.70	113.00	93.40	2.80	2.00	94.20	3.90	392.00
24	92.00	4.30	272.00	77.40	19.00	400.00	78.40	13.40	405.40
25	92.40	4.80	284.00	81.20	28.90	44.40	84.20	22.10	58.00
26	93.60	4.50	286.00	81.60	39.80	71.60	82.00	28.70	79.60
27	73.00	9.40	397.80	74.20	55.60	73.00	76.20	42.70	73.40
28	80.40	19.70	37.00	77.00	47.50	75.00	73.60	51.20	65.00
29	73.20	33.40	59.00	80.80	29.40	84.60	83.20	20.80	96.40
30	73.60	49.20	58.00	77.80	50.50	72.80	72.40	44.40	76.00
31	70.60	44.70	77.00	74.20	26.90	86.80	70.20	24.60	99.80
32	77.00	21.50	87.20	77.20	32.10	86.40	76.00	33.60	92.40
33	67.20	44.60	81.40	82.60	59.80	100.00	84.80	61.00	100.00
34	71.80	21.20	100.80	78.80	54.90	108.20	82.00	46.00	107.80
35	71.60	37.60	91.00	79.60	31.00	111.60	80.60	36.20	113.80
36	76.20	55.60	102.60	79.80	18.90	115.80	81.00	15.80	128.00
37	78.20	54.90	105.00	81.20	23.10	127.00	81.20	18.50	142.00
38	76.80	34.20	118.80	78.40	31.40	149.00	80.00	34.60	142.00
39	75.20	20.10	126.40	78.80	8.30	123.40	80.40	10.20	126.00
40	75.40	22.30	141.00	78.00	37.70	156.00	75.80	30.80	156.00
41	79.20	35.40	164.60	81.00	13.40	161.00	81.80	12.90	175.00
42	77.80	12.20	169.00	77.20	32.20	181.00	79.80	27.80	168.00
43	73.40	44.30	160.00	75.20	33.30	181.00	78.80	33.10	171.00
44	74.80	11.20	197.00	77.00	26.70	202.20	78.00	27.00	199.00
45	79.40	30.10	175.40	80.40	11.50	235.00	83.00	10.20	220.00

* Note: Samples from 1 to 12 are greys.

Appendix A.2 Continued.

Sample	Visual Results under **D65**			under A			under TL84		
No.	L	C	H	L	C	H	L	C	H
46	73.20	36.80	165.00	78.20	20.80	232.00	79.60	17.80	226.00
47	75.40	22.00	200.00	78.40	30.20	373.00	80.20	18.00	357.60
48	79.60	17.10	238.00	86.00	4.70	388.00	83.80	6.30	378.00
49	79.40	18.00	226.00	73.80	18.40	380.60	74.40	7.90	361.00
50	79.20	16.30	348.00	73.00	48.50	20.40	62.60	50.40	397.00
51	77.60	6.70	379.00	67.60	58.20	23.00	65.00	49.70	7.00
52	60.20	44.60	396.00	75.40	28.90	406.00	73.00	20.50	4.00
53	59.20	56.90	12.00	71.40	27.00	60.00	73.60	22.00	36.00
54	70.20	15.70	404.00	71.40	53.20	51.00	72.40	49.80	50.00
55	67.60	21.20	21.00	72.20	41.20	60.00	73.00	35.60	63.00
56	69.20	43.80	54.00	73.60	36.40	39.00	70.80	35.00	38.00
57	64.00	36.00	48.00	70.80	58.00	52.80	72.40	49.80	64.00
58	63.40	29.00	43.00	67.00	62.50	52.00	66.40	56.90	51.00
59	67.20	51.70	56.00	74.40	27.10	56.00	66.80	20.30	60.00
60	63.80	61.50	62.00	70.20	51.40	77.40	68.00	36.00	84.00
61	63.80	20.40	38.00	68.40	51.70	80.00	69.20	54.60	70.00
62	62.00	37.30	71.00	73.80	34.20	98.00	73.00	24.50	103.40
63	66.60	55.80	73.40	70.20	50.80	84.40	69.20	45.20	89.40
64	65.00	25.00	85.00	66.80	38.80	89.00	75.80	34.00	104.40
65	58.80	45.00	90.60	73.80	44.70	104.40	66.60	40.30	110.40
66	66.20	37.40	92.40	69.20	27.10	105.00	70.80	18.00	121.00
67	57.80	48.50	95.80	68.80	31.30	88.00	66.80	30.40	91.00
68	66.40	21.00	103.40	66.00	44.50	105.80	69.60	37.40	113.00
69	67.40	28.40	111.00	67.00	41.00	125.40	71.20	42.90	132.00
70	64.80	46.40	112.60	63.40	35.50	136.00	69.00	34.50	157.60
71	68.80	42.00	128.00	69.00	28.10	161.00	74.40	22.60	160.00
72	64.00	35.70	150.00	67.20	42.10	154.00	69.60	41.50	146.00
73	65.20	22.20	159.60	65.60	35.70	153.00	71.80	44.90	153.00
74	61.00	44.00	158.00	70.20	42.80	171.00	69.60	44.70	154.00
75	69.40	41.40	164.00	73.00	6.40	132.00	71.60	9.60	146.00
76	68.60	44.90	166.00	73.00	20.30	157.00	78.20	16.10	161.00
77	67.40	14.90	175.00	70.40	34.40	157.00	66.60	36.60	161.00
78	74.40	19.70	160.40	67.40	48.30	172.00	68.80	50.40	172.00
79	65.60	42.40	169.00	70.20	31.10	190.00	70.40	30.20	183.00
80	67.80	54.30	176.40	63.40	49.50	176.80	59.60	46.40	179.40
81	73.00	25.20	184.00	65.00	37.60	197.40	65.20	30.60	190.00
82	57.20	49.10	181.00	63.00	45.70	216.00	66.20	36.20	208.20
83	64.80	36.40	188.60	66.40	15.90	220.00	65.80	11.10	222.00
84	65.00	42.30	208.00	68.00	30.90	225.40	67.80	23.90	225.00
85	65.20	13.00	236.00	62.20	41.40	220.20	69.60	30.80	229.60
86	71.40	25.40	235.00	58.40	50.40	254.00	62.20	37.10	246.00
87	67.00	30.70	220.00	69.60	26.00	259.00	76.00	15.80	254.00
88	62.00	38.70	238.00	71.40	12.90	291.00	74.20	7.90	299.00
89	74.00	22.30	261.00	67.00	17.20	301.80	71.80	12.40	302.60
90	71.40	17.00	296.00	70.60	22.90	354.00	66.20	20.50	340.00

Appendix A.2 Continued.

Sample	Visual Results under **D65**			under A			under TL84		
No.	L	C	H	L	C	H	L	C	H
91	72.20	18.70	299.00	66.20	18.10	369.00	61.80	8.20	365.00
92	69.00	13.60	329.00	66.00	37.30	395.00	60.00	33.50	384.40
93	58.20	32.90	379.80	64.60	29.80	400.00	60.60	28.00	384.60
94	59.60	25.00	371.00	67.80	46.90	393.20	66.60	47.70	385.00
95	62.20	42.20	379.60	62.60	60.30	393.60	54.20	60.30	386.80
96	62.00	59.30	382.40	63.80	48.00	398.20	62.60	41.70	394.40
97	63.40	38.90	387.00	64.60	34.80	14.00	57.60	34.30	398.00
98	60.60	30.80	388.40	67.20	42.20	15.60	62.00	40.20	6.00
99	56.80	40.00	405.20	62.80	65.40	11.80	59.80	59.30	4.00
100	59.00	58.90	402.40	59.40	40.20	31.40	56.00	36.50	22.00
101	54.60	34.30	15.00	59.80	50.50	37.00	50.60	49.70	17.00
102	49.00	53.80	17.40	62.80	66.60	24.00	55.40	61.50	16.00
103	52.60	69.90	23.60	59.40	22.40	16.60	57.60	18.60	30.00
104	59.40	17.70	37.00	65.60	62.30	37.00	57.20	62.90	30.00
105	57.40	64.90	36.00	59.20	47.70	56.60	62.80	42.60	54.00
106	51.20	43.30	47.00	64.80	37.80	70.60	62.40	30.80	72.00
107	58.20	30.50	56.00	66.20	58.40	53.00	64.20	57.40	53.00
108	58.00	54.80	45.40	66.00	49.80	66.60	59.00	49.30	66.00
109	57.20	51.90	61.00	56.80	33.80	48.00	56.20	29.70	70.00
110	54.80	26.60	46.00	59.00	43.30	86.20	55.40	52.50	89.40
111	54.60	47.40	78.00	61.80	37.70	94.00	59.20	34.70	117.00
112	60.20	35.40	93.40	62.40	37.60	99.80	59.40	45.30	115.40
113	56.00	41.90	97.00	56.60	31.50	119.00	62.20	29.80	150.00
114	55.60	24.00	122.40	59.00	42.50	118.80	58.40	40.40	123.00
115	57.80	38.60	120.80	59.60	33.40	132.00	55.00	42.00	158.00
116	58.60	42.90	137.00	59.40	28.30	143.00	53.40	32.50	162.00
117	53.00	27.70	150.00	55.60	36.90	159.00	61.60	41.60	157.00
118	56.60	39.00	164.00	54.40	31.90	182.00	57.40	32.80	184.60
119	50.20	25.70	185.00	58.60	13.80	168.00	57.80	16.80	180.40
120	54.20	16.90	185.00	50.00	9.40	123.00	45.20	12.90	147.00
121	51.60	18.60	172.40	Missing			Missing		
122	57.00	38.00	173.00	56.80	33.90	172.00	53.80	38.80	174.00
123	52.80	34.90	189.00	57.80	29.10	188.00	62.80	25.50	179.00
124	48.60	37.10	191.00	53.20	35.60	192.00	49.80	30.90	193.40
125	59.80	46.40	188.40	56.40	52.00	196.00	58.40	50.70	183.00
126	51.40	47.10	202.60	52.40	54.40	209.00	47.20	52.30	202.40
127	60.60	23.00	212.60	55.60	12.70	224.40	55.20	15.00	225.00
128	57.00	10.60	234.00	45.40	49.30	237.00	49.40	40.80	228.00
129	58.80	28.20	213.00	57.00	33.40	276.00	56.00	24.30	277.00
130	56.20	45.70	233.00	52.60	54.50	273.00	49.00	45.40	274.00
131	61.00	27.40	286.40	50.20	33.10	295.00	51.80	32.80	300.00
132	54.80	54.10	279.00	54.60	21.00	319.00	58.80	18.50	313.40
133	60.80	36.70	290.40	62.80	29.30	344.00	61.00	16.00	330.00
134	57.40	20.10	308.60	60.80	29.30	349.00	54.40	30.80	344.00
135	55.40	15.10	322.00	50.60	24.90	351.00	51.80	26.00	338.00

Appendix A.2 Continued.

Sample	Visual Results under D65			under A			under TL84		
No.	L	C	H	L	C	H	L	C	H
136	56.60	30.30	329.00	55.00	46.10	354.40	54.00	42.50	346.00
137	51.40	18.50	339.40	68.40	21.50	359.00	69.60	31.20	361.40
138	57.80	39.20	349.00	65.60	34.40	373.00	55.20	31.70	366.00
139	64.20	24.40	355.40	54.40	41.80	385.00	50.80	44.40	382.20
140	54.60	31.90	357.00	59.00	60.70	390.40	49.00	57.40	386.60
141	50.20	40.30	375.00	50.60	44.30	9.20	44.40	52.90	391.40
142	44.80	58.20	387.00	57.00	71.00	398.40	50.20	67.20	392.00
143	43.20	51.40	382.40	47.00	20.50	39.00	44.40	21.30	387.00
144	53.60	64.30	394.00	47.00	55.20	9.60	52.60	51.30	401.60
145	43.80	19.80	389.00	57.00	67.70	11.80	46.00	69.90	13.60
146	49.20	54.10	401.40	54.80	62.80	17.00	50.40	61.00	21.40
147	47.20	70.90	8.60	54.00	67.90	14.40	47.40	64.20	18.80
148	45.00	56.20	16.00	47.20	34.80	54.00	43.00	33.20	32.80
149	45.00	67.00	13.00	45.00	27.90	21.00	44.20	26.00	31.00
150	43.60	28.30	32.00	53.80	56.20	41.00	46.00	59.30	32.00
151	46.60	17.40	36.00	52.40	47.90	55.00	51.40	49.20	47.00
152	47.20	57.40	37.00	49.20	44.00	68.40	49.80	42.60	73.00
153	47.00	47.00	55.40	50.80	28.30	55.60	45.60	30.90	62.00
154	44.40	40.10	59.00	47.00	39.20	144.00	47.80	37.20	145.00
155	47.80	22.20	53.00	42.80	17.50	166.00	47.20	13.80	170.00
156	47.00	37.90	134.00	46.40	42.00	167.00	46.20	44.60	169.00
157	44.20	8.20	129.00	42.00	35.10	182.40	45.20	38.70	183.40
158	46.00	41.40	163.40	46.60	45.50	178.00	51.40	53.20	179.60
159	47.60	29.10	172.00	42.00	4.90	97.40	41.00	18.30	177.40
160	49.00	41.20	159.00	40.20	54.40	185.80	44.40	50.80	183.60
161	43.40	18.30	179.00	36.40	8.60	169.00	33.00	14.80	181.00
162	47.40	59.30	184.80	44.20	56.30	196.00	45.60	55.50	188.60
163	39.60	24.50	192.20	44.80	45.90	199.60	44.00	46.00	204.60
164	42.80	51.90	193.40	44.60	60.90	199.00	37.80	56.30	199.00
165	45.80	40.00	196.60	43.00	57.50	205.00	41.40	53.60	203.60
166	46.20	56.70	193.80	38.80	54.80	211.40	38.00	48.10	229.60
167	41.20	54.70	201.60	38.00	53.90	239.00	38.80	45.50	230.00
168	43.40	48.60	210.60	40.80	33.00	239.00	46.60	34.20	235.00
169	46.20	43.20	228.00	38.20	46.10	261.00	39.00	40.60	259.00
170	50.80	26.70	258.00	45.00	27.20	277.00	43.40	14.30	275.00
171	42.60	40.20	255.00	34.20	52.40	289.60	34.00	51.50	282.00
172	46.40	20.20	282.00	44.20	42.50	280.00	43.20	40.50	292.00
173	44.80	49.00	285.00	43.20	20.00	330.00	37.80	9.90	319.60
174	48.60	42.60	286.60	47.60	37.20	299.00	42.80	44.00	299.80
175	40.40	6.40	309.00	47.20	25.10	311.00	44.60	22.50	309.00
176	46.60	39.00	298.80	50.40	36.20	336.00	45.00	33.20	323.00
177	44.20	28.00	311.40	53.80	37.40	349.00	48.80	36.00	342.00
178	50.20	34.80	320.00	42.40	21.60	352.00	41.20	35.40	352.00
179	47.40	41.30	337.00	55.20	44.40	371.40	50.60	45.00	359.00
180	42.60	33.00	341.40	53.40	51.80	383.00	47.80	43.50	374.40

Appendix A.2 Continued.

Sample	Visual Results under **D65**			under A			under TL84		
No.	L	C	H	L	C	H	L	C	H
181	44.20	45.40	361.00	45.80	6.60	396.00	40.00	52.20	385.40
182	49.40	47.50	368.00	41.80	56.00	390.60	33.60	39.00	381.40
183	37.00	43.80	382.80	40.00	35.70	396.00	38.80	59.30	391.40
184	38.60	27.90	378.40	45.00	64.60	397.80	35.20	52.80	401.00
185	35.80	62.00	393.20	39.00	51.20	4.00	38.20	62.70	6.60
186	32.40	50.00	399.00	42.60	71.20	8.80	40.20	68.60	11.80
187	38.60	64.80	401.00	48.00	67.90	9.00	41.60	61.50	16.40
188	39.20	72.70	2.20	46.80	58.90	19.00	40.80	39.50	41.00
189	39.80	58.10	12.40	40.80	39.50	40.60	40.20	51.40	29.00
190	37.20	37.60	32.00	43.40	45.60	38.00	40.20	41.30	49.00
191	38.40	43.70	20.40	44.20	40.30	61.00	38.60	34.40	83.20
192	37.60	40.40	48.00	39.40	31.60	109.00	37.20	22.70	166.00
193	38.40	28.50	93.40	33.40	10.60	125.00	38.00	37.80	148.00
194	31.40	11.70	103.00	40.80	28.90	122.00	39.40	37.00	161.00
195	38.60	30.60	125.00	37.00	33.00	155.60	36.20	47.30	186.40
196	35.00	29.50	165.60	35.80	47.50	188.80	32.20	22.50	185.00
197	33.00	43.60	179.00	33.20	22.40	190.20	36.80	55.40	185.40
198	38.40	22.20	181.00	36.20	42.80	193.00	30.60	51.80	194.40
199	37.40	47.70	187.20	36.40	56.30	195.40	31.20	45.30	200.40
200	37.20	47.60	194.40	29.60	41.50	203.00	29.60	40.20	206.40
201	33.80	47.00	195.80	30.40	46.10	204.80	26.20	11.50	203.00
202	33.00	47.10	202.00	30.80	5.70	230.00	28.20	39.10	212.00
203	32.80	15.00	218.00	30.00	40.40	216.40	26.80	39.80	239.60
204	36.60	36.30	212.00	28.40	49.90	261.00	22.80	35.90	252.60
205	35.80	47.50	223.00	22.80	34.50	243.00	26.60	37.10	275.00
206	27.80	40.30	241.00	26.60	43.80	270.00	24.80	21.20	273.00
207	32.40	37.00	261.00	29.20	25.20	274.00	23.80	36.20	289.00
208	31.40	24.70	277.00	25.00	27.70	291.60	25.20	40.30	299.00
209	25.60	37.80	285.60	29.60	38.20	287.40	29.60	41.90	297.20
210	35.00	35.30	293.40	34.00	39.00	296.60	29.00	7.70	316.00
211	37.60	43.10	291.40	30.00	8.00	298.00	34.20	45.90	301.40
212	31.20	12.10	305.00	33.60	49.90	301.80	27.80	56.70	304.80
213	42.20	49.80	301.40	24.60	44.20	305.60	34.40	38.80	313.40
214	33.40	45.10	300.80	34.20	29.50	309.40	25.20	52.80	309.00
215	35.60	40.80	306.80	27.00	43.60	313.00	31.80	38.90	325.00
216	34.40	51.80	303.00	36.20	31.90	328.00	34.40	29.10	348.80
217	34.20	38.00	320.80	33.20	26.60	351.00	35.40	55.70	339.00
218	31.00	27.10	334.00	44.20	59.60	359.00	36.00	43.50	359.00
219	42.40	52.50	344.00	40.80	38.00	368.20	37.80	51.70	361.00
220	35.80	41.60	362.00	41.60	55.00	362.00	40.20	48.20	364.00
221	34.80	46.30	357.00	41.00	52.20	377.00	30.40	5.30	208.00
222	41.00	44.40	364.40	29.20	4.50	120.00	22.60	20.10	380.00
223	21.20	15.40	391.60	23.60	22.10	-1.00	24.20	43.20	388.40
224	28.00	33.10	381.80	31.80	51.60	398.00	27.00	49.10	398.60
225	28.00	43.50	401.60	29.80	60.80	400.00	29.40	52.10	400.00

Appendix A.2 Continued.

Sample	Visual Results under **D65**			under A			under TL84		
No.	L	C	H	L	C	H	L	C	H
226	30.20	46.90	400.40	37.00	66.90	398.80	26.00	41.80	9.60
227	21.60	31.60	18.00	29.60	38.80	16.00	25.40	25.40	57.00
228	26.80	18.60	63.00	27.80	23.90	68.00	17.00	11.20	72.00
229	18.60	7.60	88.00	16.60	6.00	69.00	24.40	15.90	142.00
230	22.20	9.30	108.60	23.80	14.40	164.00	24.80	38.90	189.60
231	24.00	27.40	179.80	23.20	26.00	196.00	18.20	20.30	192.20
232	24.40	25.50	192.80	16.80	19.20	205.40	24.80	42.80	203.40
233	25.60	30.90	202.60	27.40	42.00	203.00	15.80	15.50	206.40
234	16.80	5.40	204.00	18.20	8.40	212.00	16.80	17.00	212.00
235	26.00	28.50	210.40	15.60	20.50	208.60	15.60	16.20	279.00
236	20.40	11.90	278.00	15.00	11.80	282.40	15.60	12.70	303.80
237	19.20	12.70	306.00	13.80	12.40	318.00	19.20	31.20	307.00
238	22.40	33.10	308.00	17.20	23.30	306.00	22.00	50.80	321.00
239	26.80	45.60	314.80	28.60	43.30	333.00	19.60	28.10	341.00
240	20.80	19.70	334.60	21.80	35.00	355.60	21.00	22.70	339.00

Appendix A.3 The corresponding colours under D65, A, and TL84.

Sample	Corr. Colour under D65			under A			under TL84		
No.	L*	a*	b*	L*	a*	b*	L*	a*	b*
1	50.00	6.80	-3.40	50.00	1.90	-4.00	50.00	3.20	-5.80
2	50.00	8.00	2.80	50.00	4.80	2.00	50.00	6.10	1.60
3	50.00	6.00	9.90	50.00	5.50	5.50	50.00	7.00	7.00
4	50.00	.00	14.10	50.00	2.40	11.80	50.00	1.60	17.00
5	50.00	-2.60	13.80	50.00	-3.90	9.80	50.00	-4.00	14.50
6	50.00	-9.90	4.00	50.00	-8.80	3.00	50.00	-10.20	2.90
7	50.00	-9.80	-2.90	50.00	-12.20	-9.00	50.00	-11.40	-6.00
8	50.00	-3.80	-9.00	50.00	-6.00	-13.50	50.00	-6.40	-13.60
9	50.00	12.90	-6.90	50.00	4.00	-9.00	50.00	7.40	-10.50
10	50.00	14.20	5.50	50.00	9.00	3.50	50.00	12.50	4.20
11	50.00	10.90	21.90	50.00	10.00	13.00	50.00	12.80	15.20
12	50.00	.00	28.20	50.00	3.90	25.20	50.00	1.50	29.20
13	50.00	-6.40	26.90	50.00	-6.00	19.00	50.00	-7.60	25.90
14	50.00	-17.20	6.50	50.00	-15.20	3.20	50.00	-18.50	7.40
15	50.00	-16.10	-5.00	50.00	-19.50	-13.50	50.00	-19.20	-11.00
16	50.00	-5.00	-16.40	50.00	-10.20	-23.40	50.00	-8.10	-22.00
17	50.00	18.80	-11.70	50.00	7.60	-14.00	50.00	12.00	-16.50
18	50.00	23.20	10.10	50.00	14.80	6.00	50.00	20.20	9.00
19	50.00	17.60	31.60	50.00	15.90	22.50	50.00	19.20	24.60
20	50.00	.00	42.00	50.00	5.50	40.80	50.00	2.00	44.00
21	50.00	-9.50	39.20	50.00	-9.20	31.50	50.00	-10.60	37.90
22	50.00	-25.90	9.20	50.00	-22.40	3.50	50.00	-25.90	11.60
23	50.00	-23.80	-7.60	50.00	-24.20	-16.80	50.00	-25.20	-15.20
24	50.00	-4.50	-23.90	50.00	-12.00	-31.40	50.00	-7.90	-28.90
25	50.00	24.50	-16.50	50.00	13.60	-21.50	50.00	19.00	-23.20
26	50.00	34.50	16.00	50.00	25.00	13.40	50.00	32.00	16.50
27	50.00	27.00	41.50	50.00	24.00	38.00	50.00	28.20	41.00
28	50.00	-1.00	59.50	50.00	6.50	53.80	50.00	2.00	61.80
29	50.00	-12.80	55.80	50.00	-10.50	42.00	50.00	-14.50	53.80
30	50.00	-38.60	12.40	50.00	-31.00	4.00	50.00	-34.80	15.40
31	50.00	-32.20	-11.20	50.00	-31.20	-21.00	50.00	-31.20	-17.90
32	50.00	-1.00	-32.00	50.00	-13.10	-38.90	50.00	-5.20	-36.60
33	50.00	29.00	-21.50	50.00	18.50	-27.50	50.00	24.00	-27.00
34	50.00	41.50	21.20	50.00	34.40	22.50	50.00	40.60	23.50
35	50.00	35.00	48.80	50.00	31.90	54.00	50.00	34.80	52.40
36	50.00	-3.20	77.50	50.00	7.90	72.00	50.00	2.10	81.00
37	50.00	-15.40	72.20	50.00	-11.50	60.40	50.00	-18.00	69.00
38	50.00	-46.50	14.80	50.00	-39.00	3.40	50.00	-42.00	17.80
39	50.00	-40.00	-12.20	50.00	-41.00	-27.80	50.00	-37.80	-19.40
40	50.00	5.00	-37.20	50.00	-7.00	-49.00	50.00	1.00	-43.80
41	50.00	47.90	24.50	50.00	40.20	28.20	50.00	47.00	29.00
42	50.00	43.20	55.90	50.00	39.00	69.80	50.00	40.90	64.00
43	50.00	-5.50	89.20	50.00	8.00	85.80	50.00	3.20	95.50
44	50.00	-17.50	81.80	50.00	-11.00	71.50	50.00	-21.80	80.80
45	50.00	-51.00	16.00	50.00	-49.00	1.00	50.00	-47.20	18.50

Appendix B List of the reflectance values of the 76 metamers prepared in Metamerism Study.

Pair No.	1		2		3		4		5		6	
Sample	mk1	mk2	mk3	mk4	mk5	mk6	mk7	mk8	mk9	mk10	mk11	mk12
Wavelength (nm)												
400	20.56	14.46	25.22	21.77	11.75	7.03	14.39	16.90	6.56	8.84	20.75	14.76
420	23.00	16.43	30.18	25.34	12.23	8.11	15.46	19.05	6.85	10.43	23.27	16.17
440	25.18	19.76	34.95	29.64	15.04	10.39	16.87	19.38	7.63	9.46	23.95	19.04
460	23.17	24.93	35.20	34.96	13.19	14.18	17.47	17.14	8.15	6.45	21.67	23.71
480	20.22	30.31	32.35	39.57	10.14	17.64	15.68	12.85	7.14	3.97	18.81	28.75
500	19.57	29.59	30.43	38.93	9.10	16.08	13.60	10.53	5.82	3.14	18.31	28.87
520	22.59	24.96	30.13	34.95	10.02	11.80	11.79	9.45	4.65	2.93	21.95	26.38
540	25.34	20.84	31.00	30.81	11.49	8.83	11.97	10.10	4.45	3.15	27.77	24.38
560	24.43	18.75	34.73	28.95	12.19	7.29	15.02	17.41	5.46	5.59	30.89	24.97
580	22.17	18.13	37.79	28.59	10.97	6.79	24.17	35.41	8.28	15.47	33.00	27.20
600	19.73	18.28	34.78	29.12	7.95	6.72	42.34	49.70	13.01	25.37	34.83	29.94
620	20.24	26.80	29.62	41.50	5.53	10.81	57.61	51.25	28.00	25.50	36.14	47.05
640	17.58	33.70	24.73	51.63	3.87	14.23	66.21	46.69	50.49	20.37	37.56	65.03
660	24.11	42.15	32.11	59.74	6.56	20.14	70.75	49.31	65.03	22.27	44.65	73.24
680	44.05	57.15	52.62	69.86	17.85	34.53	73.53	63.64	70.91	37.40	58.37	76.72
700	64.64	70.86	69.70	76.40	38.05	54.29	75.01	75.12	73.55	58.29	69.94	78.63

Pair No.	7		8		9		10		11		12	
Sample	mk13	mk14	mk15	mk16	mk17	mk18	mk19	mk20	mk21	mk22	mk23	mk24
Wavelength (nm)												
400	4.27	7.94	7.29	12.27	25.12	23.39	19.89	12.19	9.93	17.95	10.12	5.35
420	4.29	7.72	7.81	12.58	29.33	27.14	21.39	13.06	10.67	18.67	10.04	5.37
440	5.08	6.74	9.25	11.49	32.61	30.82	21.34	15.72	13.03	18.31	9.19	6.30
460	6.57	4.89	11.15	8.99	32.00	34.31	18.88	20.97	17.84	16.23	7.02	7.86
480	7.69	3.55	11.73	6.72	29.65	37.70	16.50	29.31	25.63	13.96	5.36	10.10
500	7.19	3.30	10.55	5.98	29.06	39.44	16.72	33.10	28.34	13.64	5.31	12.13
520	6.25	4.41	8.95	6.87	32.41	39.88	24.11	33.69	26.69	17.52	9.01	14.41
540	6.39	6.71	8.69	8.64	37.13	38.00	40.26	33.88	23.75	24.89	17.79	14.45
560	8.30	11.13	9.95	12.79	42.12	37.44	51.62	37.25	23.07	34.33	21.62	14.59
580	13.74	18.74	13.04	19.16	44.80	37.34	52.19	43.76	23.79	37.71	19.99	14.84
600	21.02	19.06	16.48	17.52	41.47	38.11	49.87	51.04	25.43	32.50	18.96	15.37
620	21.90	16.01	18.27	14.18	36.23	49.54	48.94	62.49	42.77	27.74	19.32	25.70
640	17.43	11.42	19.52	9.80	31.11	58.16	44.22	70.68	62.67	21.56	20.16	36.02
660	19.28	12.94	25.60	11.18	38.83	64.93	46.82	74.91	71.63	23.89	26.26	45.51
680	33.50	25.44	40.61	22.96	58.74	72.35	60.71	77.29	74.19	39.81	41.41	59.60
700	53.55	46.37	59.02	43.46	73.36	76.70	71.59	78.60	74.94	60.50	59.91	71.54

Appendix B Continued.

Pair No.	13		14		15		16		17		18	
Sample	mk25	mk26	mk27	mk28	mk29	mk30	mk31	mk32	mk33	mk34	mk36	mk35
Wavelength (nm)												
400	5.66	10.98	5.01	2.04	2.42	5.16	6.03	11.68	6.47	11.80	3.66	6.71
420	5.77	10.89	4.49	1.91	2.31	4.55	6.42	11.53	6.65	11.94	3.63	6.61
440	7.04	10.21	3.90	2.11	2.62	3.87	7.76	10.55	7.95	11.34	4.31	6.14
460	9.61	8.27	2.92	2.98	3.41	2.83	9.83	8.17	10.26	9.37	5.60	4.93
480	12.59	6.24	2.28	5.56	4.17	2.21	11.05	6.27	12.13	7.03	6.50	3.41
500	12.74	5.71	2.20	7.09	4.04	2.18	10.10	6.08	11.62	6.23	5.98	2.84
520	11.69	7.12	3.18	7.25	3.89	3.54	9.03	9.27	10.40	7.04	5.13	2.81
540	11.88	10.46	6.41	7.49	4.41	8.23	9.01	15.45	10.60	9.39	5.21	3.40
560	14.79	19.91	15.40	10.19	9.73	14.33	13.75	20.58	13.60	18.20	6.95	7.93
580	23.23	35.96	32.49	18.88	25.47	21.59	28.12	22.81	22.72	35.94	12.93	21.86
600	38.89	42.64	44.50	36.40	43.20	31.87	38.36	24.39	40.81	47.64	26.80	36.08
620	54.39	40.18	44.64	52.96	47.71	49.22	37.77	42.16	56.52	47.72	45.08	37.55
640	64.32	33.86	39.65	63.42	44.38	64.74	32.06	63.51	65.79	42.54	60.25	32.36
660	69.16	36.35	42.31	68.91	46.99	71.82	34.54	73.57	70.66	45.01	68.01	34.78
680	71.78	52.68	56.88	71.87	60.72	74.86	50.77	76.76	73.54	59.83	71.59	50.52
700	73.21	69.07	69.53	73.47	71.58	76.39	67.95	77.99	75.15	72.25	73.40	66.38

Pair No.	19		20		21		22		23		24	
Sample	mk37	mk39	mk38	mk39	mk40	mk41	mk42	mk43	mk44	mk45	mk46	mk47
Wavelength (nm)												
400	10.06	3.67	5.98	3.67	3.37	2.48	7.41	4.81	8.30	5.14	8.20	5.48
420	9.55	3.64	5.95	3.64	3.27	2.33	7.51	4.83	8.49	5.22	8.47	5.63
440	8.58	4.57	6.73	4.57	3.89	2.75	8.75	6.12	9.79	6.64	9.74	7.13
460	6.48	7.29	7.70	7.29	5.31	4.50	10.75	9.85	11.70	10.56	11.32	10.93
480	4.96	13.72	8.53	13.72	7.69	11.16	13.20	19.91	13.90	20.85	12.73	19.05
500	4.96	18.08	9.35	18.08	9.57	20.22	15.06	30.30	15.65	31.07	13.94	24.31
520	8.94	19.39	14.76	19.39	16.66	29.05	23.34	37.72	23.67	37.39	20.36	25.72
540	20.99	19.59	25.06	19.59	33.04	31.09	41.00	36.79	40.20	35.05	31.52	25.43
560	36.30	22.54	31.47	22.54	47.22	34.97	52.74	37.46	50.31	33.95	34.69	26.81
580	43.24	29.57	32.77	29.57	49.15	42.74	50.41	39.42	47.28	34.17	32.03	29.81
600	41.40	39.14	34.00	39.14	48.46	51.84	44.60	40.91	41.13	35.37	29.65	32.65
620	36.44	54.65	50.37	54.65	48.36	62.45	39.91	55.75	36.38	52.06	28.95	34.28
640	31.38	66.88	66.10	66.88	49.10	69.54	33.29	68.42	29.88	67.79	29.13	35.74
660	38.78	72.29	72.71	72.29	52.16	73.20	35.82	73.65	32.39	74.20	31.92	42.89
680	57.73	74.90	75.33	74.90	58.20	75.42	52.04	76.34	48.55	76.51	38.75	57.25
700	71.08	76.31	76.62	76.31	65.33	76.70	68.35	77.73	65.51	77.51	48.60	70.11

Appendix B Continued.

Pair No.	25		26		27		28		29		30	
Sample	mk48	mk49	mk51	mk50	mk52	mk53	mk54	mk55	mk56	mk57	mk58	mk59
Wavelength (nm)												
400	11.53	9.70	5.62	4.96	23.58	17.64	14.21	9.71	4.63	10.94	10.41	8.97
420	12.18	10.23	5.68	5.00	26.36	19.67	14.89	10.38	4.91	10.30	10.30	8.27
440	14.48	12.64	7.09	6.35	28.18	23.45	16.65	12.91	6.20	9.23	10.79	8.18
460	19.04	18.24	10.76	10.18	27.63	30.08	19.42	18.47	8.84	7.45	8.80	9.06
480	26.97	30.72	19.34	20.77	26.62	40.43	23.13	29.94	12.23	6.05	6.93	11.96
500	32.80	41.83	27.43	33.60	27.44	45.20	25.79	38.12	12.55	5.86	6.89	15.73
520	42.54	48.64	39.74	46.72	35.24	44.66	34.07	40.27	11.10	8.32	11.10	16.45
540	52.18	47.44	50.62	47.99	46.87	41.15	44.60	36.94	10.37	12.72	19.50	14.49
560	53.56	44.75	51.10	46.41	47.97	38.43	43.34	32.89	10.69	16.25	19.66	12.91
580	48.19	42.01	44.38	43.06	40.73	36.61	34.84	29.60	11.84	16.47	14.29	12.22
600	41.46	40.85	36.81	38.51	33.40	36.00	26.88	28.12	12.96	11.91	10.40	12.69
620	36.57	41.38	31.79	36.92	28.12	40.21	22.15	28.45	13.77	8.97	7.73	13.16
640	29.96	42.52	25.31	31.27	22.36	43.05	16.57	29.25	14.61	5.80	5.61	13.25
660	32.52	49.24	27.66	33.75	26.38	50.27	18.70	36.02	19.93	6.85	9.03	14.10
680	48.92	61.85	44.23	50.14	43.88	63.45	33.40	51.59	33.99	15.97	22.36	19.55
700	66.39	71.88	64.20	67.39	63.57	73.84	54.21	67.75	52.94	34.26	43.55	31.30

Pair No.	31		32		33		34		35		36	
Sample	mk60	mk61	mk62	mk63	mk64	mk65	mk66	mk67	mk68	mk69	mk70	mk71
Wavelength (nm)												
400	11.47	4.56	8.54	3.04	13.86	16.81	17.38	14.63	7.38	11.71	18.49	20.00
420	10.71	4.80	7.34	3.16	15.50	18.10	18.58	16.90	8.68	11.80	22.25	21.77
440	9.80	6.17	6.54	4.04	20.00	23.80	22.67	20.68	11.33	15.57	27.86	30.51
460	8.42	9.69	5.78	6.56	26.45	27.42	25.53	26.47	15.52	14.31	34.92	32.01
480	7.39	17.09	5.34	12.26	35.41	29.28	26.63	33.03	19.60	11.61	38.42	28.63
500	7.56	20.43	5.50	14.56	38.86	30.58	26.57	33.25	18.90	10.98	35.85	26.68
520	11.85	18.27	8.38	12.21	36.32	35.19	26.02	28.69	15.09	13.39	29.29	26.33
540	19.97	14.69	13.15	9.24	31.22	37.21	25.84	24.11	12.19	16.10	23.90	25.70
560	21.07	12.49	12.42	7.38	25.42	29.61	25.68	20.97	10.02	14.36	19.26	22.79
580	15.79	11.56	8.52	6.55	20.02	20.64	23.57	19.09	8.62	10.19	16.12	17.62
600	10.49	11.27	5.18	6.21	16.35	14.82	19.77	18.42	8.03	6.63	14.15	12.65
620	7.74	15.47	3.68	8.41	13.62	10.87	15.48	21.40	8.26	4.50	13.82	9.13
640	5.01	18.63	2.43	10.12	11.17	7.92	11.71	23.57	8.79	3.16	13.94	6.50
660	6.12	24.99	2.95	14.75	16.25	12.47	17.13	30.36	12.89	5.36	15.92	10.51
680	14.42	39.92	7.44	27.44	32.96	28.69	35.61	45.92	24.98	15.56	21.37	25.59
700	31.22	58.63	19.80	47.17	54.70	52.18	58.92	63.26	44.64	35.51	30.82	48.82

Appendix B Continued.

Pair No.	37		38		39		40		41		42	
Sample	mk72	mk73	mk74	mk75	mk76	mk77	mk78	mk79	mk80	mk81	mk82	mk83
Wavelength (nm)												
400	20.13	17.71	12.40	14.41	7.10	7.27	11.43	9.57	10.94	9.83	6.65	5.36
420	23.06	21.84	16.86	15.80	7.38	9.37	13.34	15.11	13.60	15.00	7.88	9.02
440	29.95	26.93	22.74	24.93	15.45	13.33	23.31	23.19	20.75	20.39	15.59	14.13
460	30.67	32.28	27.33	26.35	17.54	17.33	25.20	26.88	19.25	21.08	15.61	14.54
480	27.19	34.81	26.12	21.15	13.14	15.56	18.80	20.91	12.84	15.52	9.73	9.53
500	24.83	32.31	22.08	17.66	10.40	12.44	14.07	15.55	9.17	11.14	6.57	6.57
520	23.75	26.53	16.44	14.97	8.29	8.81	9.51	10.08	6.14	7.02	4.11	4.24
540	23.37	21.92	12.76	13.54	6.94	6.43	6.86	7.07	4.60	4.94	3.00	3.19
560	23.64	18.75	10.08	12.92	5.60	4.42	5.28	5.14	3.95	3.88	2.45	2.63
580	21.45	16.81	8.35	10.70	3.82	3.32	4.28	4.09	3.66	3.49	2.16	2.33
600	16.70	16.09	7.57	7.34	2.43	2.74	3.38	3.68	3.19	3.39	1.86	2.16
620	12.57	18.43	7.75	4.99	1.85	2.59	3.35	3.95	3.73	5.01	1.87	2.21
640	9.35	20.21	8.25	3.50	1.65	2.60	2.74	4.33	3.26	6.40	1.75	2.34
660	14.30	26.50	12.22	6.01	2.25	3.08	4.62	6.89	5.50	10.00	2.45	3.64
680	31.44	41.69	23.96	16.88	6.31	4.81	13.53	15.81	15.44	20.67	7.06	9.45
700	54.45	59.91	43.19	37.03	19.25	8.91	31.91	33.24	34.35	39.25	20.74	23.29

Pair No.	43		44		45		46		47		48	
Sample	mk84	mk85	mk86	mk87	mk88	mk89	mk90	mk91	mk93	mk92	mk94	mk95
Wavelength (nm)												
400	5.07	5.35	23.20	20.39	22.21	18.74	22.34	19.55	8.70	9.25	7.85	5.29
420	5.49	6.53	27.86	24.33	26.24	22.51	27.68	25.36	13.45	13.19	8.36	6.04
440	10.33	8.27	33.76	28.66	32.52	26.80	33.83	30.53	18.29	17.28	10.76	7.81
460	9.67	8.90	33.29	32.92	31.74	31.05	32.50	32.75	17.41	18.64	8.73	10.11
480	5.92	6.62	28.41	34.23	26.38	32.15	26.26	29.53	11.87	14.83	5.84	10.82
500	4.26	4.88	24.98	31.22	22.82	28.84	21.84	24.77	8.67	10.87	4.75	8.70
520	3.31	3.49	22.70	25.91	20.44	23.18	17.93	18.95	6.16	6.92	4.62	5.71
540	2.99	2.96	22.17	21.82	19.81	19.03	15.61	15.10	4.98	4.89	4.95	4.07
560	3.17	2.70	25.67	19.99	22.69	16.95	15.64	13.22	4.53	3.91	6.11	3.44
580	2.90	2.61	29.05	19.56	24.98	16.31	16.10	12.58	4.32	3.59	6.62	3.36
600	2.06	2.47	25.57	19.90	21.27	16.45	15.28	12.71	4.04	3.55	4.77	3.46
620	1.69	2.41	20.63	29.28	16.68	24.53	17.67	19.37	4.17	5.71	3.24	6.92
640	1.57	2.42	16.37	37.03	12.90	31.09	16.04	24.70	4.48	7.67	2.36	8.70
660	1.99	2.84	22.66	45.61	18.62	39.44	22.30	32.34	7.11	11.81	3.87	13.66
680	5.09	4.38	42.37	59.98	37.26	54.75	42.00	47.97	16.15	23.29	11.75	29.92
700	16.45	8.15	63.49	72.58	59.66	69.13	64.15	64.71	33.44	42.14	29.30	52.57

Appendix B Continued.

Pair No.	49		50		51		52		53		54	
Sample	mk96	mk97	mk98	mk99	mk100	mk101	mk102	mk103	mk104	mk105	mk106	mk99
Wavelength (nm)												
400	7.74	7.04	26.75	22.33	20.21	23.87	10.63	13.67	3.08	3.10	25.36	22.33
420	8.84	9.40	31.91	26.41	24.06	29.10	12.11	15.27	3.77	3.49	30.28	26.41
440	12.76	11.30	36.42	30.23	27.60	32.78	13.61	14.51	3.40	3.59	34.52	30.23
460	10.70	10.58	35.60	33.29	30.21	29.87	13.73	11.95	2.42	3.03	33.85	33.29
480	6.63	7.30	31.66	34.92	29.46	23.71	11.39	8.75	1.80	2.14	30.11	34.92
500	4.82	5.51	29.30	34.43	26.11	20.12	9.28	6.99	1.64	1.83	27.76	34.43
520	3.82	4.30	28.86	31.98	21.50	18.01	7.48	6.11	1.58	1.71	27.10	31.98
540	3.59	3.88	29.84	28.64	18.32	17.84	7.11	6.18	1.58	1.71	27.86	28.64
560	4.54	4.19	34.84	27.27	17.53	22.86	7.99	9.06	1.77	2.09	32.86	27.27
580	5.38	4.17	40.23	27.02	18.10	31.73	10.24	14.50	2.93	2.61	38.74	27.02
600	3.98	3.91	37.42	27.80	19.60	31.92	12.69	13.31	3.31	2.69	36.46	27.80
620	2.76	4.03	31.95	40.69	36.84	27.26	14.01	10.51	2.68	2.80	31.23	40.69
640	2.09	4.33	26.79	51.68	60.06	22.47	14.98	6.99	1.97	3.00	26.26	51.68
660	3.28	6.87	34.14	59.91	72.12	29.58	20.38	8.17	2.21	4.78	33.62	59.91
680	9.86	15.67	54.69	69.41	75.62	50.65	34.61	18.14	4.83	11.74	53.89	69.41
700	25.84	32.72	72.48	75.40	76.61	70.55	53.87	37.04	13.65	26.68	70.63	75.40

Pair No.	55		56		57		58		59		60	
Sample	mk66	mk107	mk108	mk61	mk51	mk109	mk110	mk2	mk111	mk4	mk112	mk6
Wavelength (nm)												
400	17.38	13.38	11.57	4.56	5.62	4.74	17.58	14.46	27.05	21.77	8.31	7.03
420	18.58	15.42	10.60	4.80	5.68	4.76	19.00	16.43	31.54	25.34	8.48	8.11
440	22.67	19.05	9.48	6.17	7.09	6.08	22.40	19.76	34.29	29.64	10.75	10.39
460	25.53	24.91	7.84	9.69	10.76	9.86	25.49	24.93	33.86	34.96	12.42	14.18
480	26.63	31.99	6.66	17.09	19.34	20.65	26.25	30.31	31.36	39.57	11.99	17.64
500	26.57	32.46	6.81	20.43	27.43	34.27	24.65	29.59	30.40	38.93	10.42	16.08
520	26.02	27.62	11.30	18.27	39.74	48.36	22.47	24.96	32.26	34.95	8.75	11.80
540	25.84	22.92	21.05	14.69	50.62	49.38	22.28	20.84	35.17	30.81	8.51	8.83
560	25.68	19.47	23.29	12.49	51.10	46.04	24.27	18.75	36.26	28.95	9.40	7.29
580	23.57	17.37	17.53	11.56	44.38	41.03	27.02	18.13	36.99	28.59	10.41	6.79
600	19.77	16.50	11.68	11.27	36.81	36.79	26.83	18.28	36.87	29.12	9.57	6.72
620	15.48	18.48	8.69	15.47	31.79	33.10	22.74	26.80	36.68	41.50	7.13	10.81
640	11.71	20.06	5.65	18.63	25.31	29.33	18.34	33.70	37.01	51.63	4.96	14.23
660	17.13	26.37	6.72	24.99	27.66	36.64	24.84	42.15	39.89	59.74	8.06	20.14
680	35.61	41.79	15.64	39.92	44.23	55.89	45.05	57.15	46.86	69.86	20.99	34.53
700	58.92	60.59	33.38	58.63	64.20	71.69	66.12	70.86	56.60	76.40	42.82	54.29

Appendix B Continued.

Pair No.	61		62		63		64		65		66	
Sample	mk113	mk10	mk114	mk12	mk115	mk14	mk116	mk16	mk117	mk24	mk118	mk43
Wavelength (nm)												
400	9.95	8.84	17.16	14.76	4.33	7.94	7.51	12.27	5.65	5.35	8.26	4.81
420	10.30	10.43	18.38	16.17	4.34	7.72	8.05	12.58	5.69	5.37	8.35	4.83
440	9.23	9.46	20.45	19.04	5.19	6.74	9.59	11.49	6.65	6.30	9.65	6.12
460	6.73	6.45	22.52	23.71	6.60	4.89	11.63	8.99	7.91	7.86	11.55	9.85
480	4.83	3.97	23.34	28.75	7.35	3.55	12.28	6.72	9.04	10.10	13.66	19.91
500	4.40	3.14	23.18	28.87	6.65	3.30	11.02	5.98	9.76	12.13	15.36	30.30
520	5.55	2.93	22.83	26.38	5.66	4.41	9.29	6.87	10.93	14.41	23.58	37.72
540	6.98	3.15	23.60	24.38	5.73	6.71	8.96	8.64	12.02	14.45	41.77	36.79
560	7.72	5.59	27.05	24.97	7.41	11.13	10.14	12.79	16.72	14.59	55.02	37.46
580	8.45	15.47	34.01	27.20	12.14	18.74	13.06	19.16	24.06	14.84	54.29	39.42
600	9.26	25.37	41.06	29.94	18.19	19.06	16.20	17.52	23.85	15.37	50.53	40.91
620	22.29	25.50	43.59	47.05	17.75	16.01	17.85	14.18	19.64	25.70	45.94	55.75
640	46.98	20.37	44.72	65.03	14.27	11.42	18.99	9.80	15.35	36.02	41.10	68.42
660	66.24	22.27	47.76	73.24	19.65	12.94	24.97	11.18	21.23	45.51	48.56	73.65
680	74.38	37.40	54.37	76.72	38.21	25.44	39.91	22.96	40.55	59.60	66.18	76.34
700	77.59	58.29	62.77	78.63	60.19	46.37	58.61	43.46	62.33	71.54	77.30	77.73

Pair No.	67		68		69		70		71		72	
Sample	mk119	mk49	mk120	mk53	mk121	mk55	mk122	mk63	mk123	mk69	mk124	mk71
Wavelength (nm)												
400	11.53	9.70	21.27	17.64	13.33	9.71	4.71	3.04	10.33	11.71	17.84	20.00
420	12.01	10.23	23.13	19.67	13.51	10.38	4.93	3.16	11.75	11.80	21.71	21.77
440	14.26	12.64	25.65	23.45	14.89	12.91	5.85	4.04	14.43	15.57	28.33	30.51
460	18.99	18.24	29.04	30.08	17.15	18.47	6.91	6.56	17.45	14.31	33.24	32.01
480	28.07	30.72	33.35	40.43	20.58	29.94	7.47	12.26	18.55	11.61	34.45	28.63
500	36.51	41.83	36.42	45.20	24.25	38.12	7.76	14.56	17.78	10.98	32.80	26.68
520	46.36	48.64	39.79	44.66	32.21	40.27	9.99	12.21	15.64	13.39	28.02	26.33
540	51.49	47.44	41.55	41.15	39.94	36.94	12.11	9.24	13.43	16.10	23.30	25.70
560	53.39	44.75	44.76	38.43	40.44	32.89	10.05	7.38	11.47	14.36	18.84	22.79
580	49.75	42.01	44.77	36.61	33.54	29.60	7.87	6.55	9.95	10.19	15.24	17.62
600	43.83	40.85	38.96	36.00	25.99	28.12	6.52	6.21	8.56	6.63	13.11	12.65
620	39.16	41.38	34.09	40.21	21.41	28.45	6.14	8.41	8.13	4.50	11.90	9.13
640	32.64	42.52	27.42	43.05	15.92	29.25	6.13	10.12	8.12	3.16	10.61	6.50
660	35.22	49.24	29.83	50.27	17.90	36.02	7.23	14.75	9.47	5.36	15.26	10.51
680	51.72	61.85	46.71	63.45	32.46	51.59	10.63	27.44	13.48	15.56	30.52	25.59
700	68.81	71.88	66.31	73.84	53.82	67.75	17.39	47.17	21.03	35.51	52.22	48.82

Appendix B Continued.

Pair No.	73		74		75		76	
Sample	mk125	mk87	mk126	mk89	mk127	mk101	mk128	mk103
Wavelength (nm)								
400	22.51	20.39	22.40	18.74	24.29	23.87	10.27	13.67
420	27.55	24.33	27.64	22.51	29.41	29.10	11.70	15.27
440	31.03	28.66	31.21	26.80	31.17	32.78	13.37	14.51
460	30.32	32.92	30.66	31.05	28.50	29.87	13.86	11.95
480	26.49	34.23	26.92	32.15	24.31	23.71	11.82	8.75
500	24.05	31.22	24.46	28.84	22.19	20.12	9.72	6.99
520	22.51	25.91	22.77	23.18	21.50	18.01	7.81	6.11
540	22.07	21.82	22.17	19.03	20.40	17.84	7.35	6.18
560	21.67	19.99	21.59	16.95	19.21	22.86	8.07	9.06
580	21.65	19.56	21.41	16.31	18.99	31.73	9.91	14.50
600	21.83	19.90	21.56	16.45	19.53	31.92	11.81	13.31
620	22.55	29.28	22.27	24.53	32.00	27.26	12.89	10.51
640	23.53	37.03	23.24	31.09	44.29	22.47	13.75	6.99
660	30.10	45.61	29.69	39.44	54.11	29.58	18.88	8.17
680	45.86	59.98	45.18	54.75	66.73	50.65	32.72	18.14
700	63.90	72.58	63.07	69.13	75.98	70.55	52.47	37.04

Appendix C.1 Spectral power distribution data for 9 sources, and those abridged at 20 nm intervals for the 7 sources studied.

(a) Raw data of the nine sources measured.

Wavelength (nm)	D65	A	TL84	TL83	WF	WWF	P27	CWF	P30
380	.7002	.1506	.3394	.3831	.4323	.3153	.3900	.4848	.2619
385	.8129	.1119	.2999	.3385	.4882	.3406	.3411	.5847	.2792
390	.9513	.0819	.3100	.3282	.5904	.3980	.3342	.7403	.3330
395	1.1041	.0678	.3391	.3157	.7117	.4707	.2953	.9277	.3815
400	1.9414	.0823	1.1343	1.0358	1.8935	1.3507	1.0842	1.9876	1.1104
405	4.6837	.1279	4.1891	3.8629	5.9328	4.2871	4.3209	5.3431	3.6577
410	1.8995	.2191	1.0170	.6093	1.4096	.9140	.4307	1.8542	.7633
415	2.1502	.3393	1.6034	.8050	1.5485	.9955	.3807	2.1220	.8171
420	2.4342	.4532	2.2324	.9414	1.7688	1.1329	.2953	2.4346	.9313
425	2.7042	.5527	3.0894	1.2171	1.9641	1.2537	.2947	2.7291	1.0549
430	3.0800	.6447	4.0497	1.6054	2.3368	1.4958	.4648	3.1424	1.2739
435	19.9126	.7207	24.2614	21.0291	29.9306	20.7536	20.7642	23.4091	16.0065
440	3.5237	.8112	5.2944	2.0055	2.6089	1.6559	.4404	3.5965	1.3896
445	3.7259	.9057	5.5469	2.0484	2.7097	1.7144	.3758	3.7921	1.4534
450	3.9665	1.0056	5.5861	2.0565	2.8753	1.8159	.3574	4.0341	1.5331
455	4.1988	1.1160	5.3842	1.9941	3.0428	1.9193	.3715	4.2628	1.6161
460	4.3577	1.2230	4.9580	1.8639	3.1618	1.9858	.3716	4.4137	1.6739
465	4.5138	1.3447	4.5623	1.8523	3.2710	2.0535	.4326	4.5676	1.7368
470	4.6340	1.4809	3.9434	1.6289	3.3505	2.1035	.4469	4.6737	1.7780
475	4.6965	1.6089	3.4038	1.4723	3.3990	2.1261	.5039	4.7218	1.8010
480	4.7339	1.7390	4.8532	2.6450	3.4095	2.1367	1.9609	4.7379	1.8136
485	4.7559	1.8910	13.2287	8.4863	3.4077	2.1352	8.0817	4.7192	1.8170
490	4.8160	2.0471	11.2127	6.6517	3.4992	2.1941	6.0688	4.7610	1.8513
495	4.7374	2.2066	7.0280	3.8439	3.3725	2.1053	3.4644	4.6273	1.7977
500	4.6737	2.3313	3.7238	1.9034	3.3434	2.0703	1.5307	4.5262	1.7747
505	4.6514	2.5045	1.5888	.9462	3.3567	2.0645	.6692	4.4690	1.7760
510	4.6305	2.6724	1.1966	.7501	3.3980	2.0910	.4713	4.4412	1.8117
515	4.5902	2.8422	.9875	.6271	3.5157	2.1677	.4053	4.4615	1.8986
520	4.5562	3.0249	.9001	.5798	3.7746	2.3486	.4109	4.6115	2.0837
525	4.4918	3.2119	.9163	.6767	4.2207	2.6628	.5212	4.9018	2.4016
530	4.3920	3.4002	1.4379	1.3279	4.8872	3.1550	1.0053	5.3561	2.8948
535	4.2917	3.5882	7.2926	4.2719	5.7958	3.8557	4.0569	6.0081	3.5870
540	4.2459	3.7926	36.7365	31.6318	7.0278	4.8221	32.2868	6.8761	4.5532
545	11.9088	4.0068	45.6269	38.5168	20.0607	14.3236	40.8892	16.7465	14.8591
550	4.1000	4.2186	15.0835	11.5711	10.0435	7.3535	11.3966	8.9844	7.0484
555	4.0568	4.4371	4.0768	3.6102	11.6794	8.8136	3.4612	10.1037	8.5268
560	4.0500	4.6599	1.9468	2.4897	13.2748	10.3183	2.1970	11.1670	9.9831
565	4.0685	4.8908	1.8001	2.3935	14.6737	11.6810	2.0573	12.0417	11.3433
570	4.0870	5.0980	1.7343	2.2900	15.6771	12.7724	1.9944	12.6402	12.4497
575	5.7661	5.3385	4.3696	5.0233	19.6872	15.4017	5.1943	14.9033	15.0910
580	4.6305	5.5576	9.8958	9.3224	17.5534	14.5504	9.1078	13.5397	14.2677
585	4.2073	5.7566	14.6039	11.9342	16.4496	14.0945	12.2222	12.7078	13.8807
590	4.2275	5.9668	11.3994	9.9982	15.8371	13.7563	10.1919	12.1234	13.5392

Appendix C.1 Continued.

(a) Continued.

Wavelength (nm)	D65	A	TL84	TL83	WF	WWF	P27	CWF	P30
595	4.2380	6.1827	6.3087	7.4222	15.0435	13.1571	7.3570	11.3936	12.9811
600	4.2498	6.4023	4.7523	6.2734	13.9811	12.3295	6.5100	10.5055	12.1736
605	4.2472	6.6002	5.5150	7.0337	12.7617	11.3403	7.5858	9.5336	11.2240
610	4.3179	6.8330	57.0683	69.9523	11.5505	10.3797	79.8583	8.6042	10.2607
615	4.2410	7.0408	15.0503	16.8647	10.2689	9.2363	18.8110	7.6130	9.1633
620	4.1973	7.2768	8.3533	8.5436	9.0484	8.1514	8.8348	6.6768	8.1013
625	4.1399	7.5129	8.5102	9.7064	7.9739	7.1700	10.5072	5.8423	7.1375
630	4.0578	7.7288	8.9225	10.5086	6.9385	6.2308	11.5151	5.0920	6.2073
635	3.9403	7.9365	1.8993	2.3504	5.9773	5.3844	2.3989	4.3791	5.3897
640	3.8315	8.1369	1.8117	1.8877	5.1458	4.6411	1.8998	3.7831	4.6505
645	3.7109	8.3101	1.6251	1.9227	4.4125	3.9736	1.9434	3.2406	3.9894
650	3.5819	8.4962	2.6859	3.5491	3.7701	3.3776	3.7877	2.7655	3.3899
655	3.4461	8.6966	1.3897	1.9630	3.2285	2.8763	2.0134	2.3684	2.8853
660	3.2762	8.9049	2.0243	2.2314	2.7484	2.4340	2.3904	2.0262	2.4532
665	3.0807	9.1959	1.3891	1.3761	2.3433	2.0669	1.4159	1.7374	2.0793
670	2.8900	9.4057	1.0188	1.1438	1.9981	1.7655	1.1458	1.4997	1.7747
675	2.6961	9.6089	.8995	.9602	1.7040	1.4847	.9825	1.2887	1.4969
680	2.5115	9.8944	1.0028	1.0534	1.4535	1.2586	1.1053	1.1243	1.2677
685	2.3444	10.1232	1.8142	2.0603	1.2778	1.0987	2.2697	.9880	1.1030
690	2.2149	10.2561	1.1539	1.3034	1.1965	.9943	1.4365	.9136	.9963
695	2.0413	10.4857	.6225	.7366	1.0706	.8931	.7679	.8552	.8115
700	1.8100	10.6818	.5286	.6612	.7698	.6461	.7402	.6104	.6424
705	1.7123	10.9188	4.4992	5.5582	.7897	.6586	6.3143	.6410	.5669
710	1.5599	11.0741	3.7802	4.6786	.5916	.4849	5.2744	.4796	.4772
715	1.4329	11.2945	.3347	.4266	.5265	.4196	.4549	.4347	.4107
720	1.3140	11.4992	.1965	.2515	.4601	.3640	.2665	.3866	.3625
725	1.2051	11.6884	.1823	.2359	.4383	.3446	.2394	.3753	.3143
730	1.0949	11.8660	.1435	.1853	.3693	.2819	.1947	.3232	.2776
735	1.0450	12.0494	.1513	.1929	.4792	.3709	.1493	.4245	.2453
740	.9117	12.2461	.2341	.2961	.3270	.2435	.3137	.2910	.2194
745	.8289	12.3926	.1477	.1849	.2885	.2090	.1980	.2621	.2012
750	.8583	12.5269	.1928	.2256	.5793	.4582	.1195	.5278	.1792
755	.6651	12.6453	.0650	.0815	.2289	.1659	.3462	.2207	.5658
760	.7472	12.7670	.1927	.2203	.6452	.4700	.6844	.5419	1.1501
765	.5847	12.8545	.1011	.1213	.3107	.2229	.1716	.2815	.2584
770	.5869	13.1178	.1710	.2040	.4608	.3538	.1867	.4056	.2207
775	.4522	13.2754	.0656	.0903	.1874	.1411	.0948	.1901	.1294
780	.4199	13.2659	.0630	.0740	.1804	.1312	.0797	.1804	.1327
785	.3888	13.2946	.0590	.0836	.1763	.1372	.1685	.1769	.2473
790	.3792	13.4676	.0781	.0978	.2078	.1737	.0918	.2154	.1380
795	.4026	13.4884	.1227	.1505	.3240	.2559	.1112	.2952	.1323
800	.4919	13.5559	.2206	.2665	.5775	.4823	.1266	.4968	.1375

Appendix C.1 Continued.

(b) Abridged data of the seven sources investigated.

Wavelength (nm)	D65	A	TL84	TL83	WF	WWF	P27
400	3.0719	.1283	1.0358	1.1280	1.7819	1.6185	1.2137
420	6.0271	.3856	3.9515	2.9302	4.2471	3.6905	2.3488
440	9.8028	.6737	8.4533	6.0563	7.8195	6.7918	4.6669
460	5.9580	1.0239	4.0943	1.5015	2.6924	2.1374	-.1068
480	6.8509	1.4583	6.8055	4.3493	3.3126	2.6611	3.5524
500	6.7957	1.9572	4.8181	3.1322	3.2334	2.5628	2.7695
520	6.3920	2.5227	.2741	.0831	3.5279	2.7805	-.1762
540	8.3799	3.1674	21.0810	19.5512	9.1784	8.1993	20.0425
560	6.7867	3.8889	6.4517	6.6087	13.7963	13.6335	6.5218
580	6.5486	4.6274	6.4620	6.5515	16.7544	17.7951	6.3193
600	6.1208	5.3360	13.9138	18.1398	13.5066	15.3003	19.8663
620	6.0620	6.0740	15.1591	19.9952	8.8349	10.1983	22.2296
640	5.5413	6.7763	2.1398	2.8153	5.0022	5.7707	2.8716
660	4.5838	7.1184	1.3343	1.7852	2.6143	2.9796	1.8429
680	4.1083	9.5992	1.2206	1.4912	1.5973	1.7623	1.5838
700	6.9700	45.2628	2.8050	3.8815	2.1008	2.1184	4.4538

Appendix C.2 Abridged weights of the illuminants and sources studied calculated using the CIE 1964 Supplementary Standard Colorimetric Observer.

(a) Illuminant CIE D65

Wavelength (nm)	Wx	Wy	Wz
400	.2291	.0202	.9789
420	3.2870	.3356	15.6621
440	6.6538	1.1001	34.2479
460	6.0646	2.6070	35.1761
480	1.7330	4.9601	15.9620
500	.0686	8.6833	4.0308
520	2.1823	13.8434	1.0345
540	6.8030	17.3333	.2303
560	12.1692	17.1529	.0020
580	16.4660	14.1494	-.0028
600	17.2296	10.1147	.0000
620	12.8767	6.0141	.0000
640	6.2427	2.5916	.0000
660	2.1148	.8274	.0000
680	.5760	.2230	.0000
700	.1140	.0438	.0000
Sum:	94.81	100.00	107.32

(b) Illuminant CIE A

Wavelength (nm)	Wx	Wy	Wz
400	.0295	.0021	.1163
420	.8038	.0813	3.8363
440	1.8906	.3031	9.7116
460	1.9728	.8558	11.4954
480	.7177	2.1452	6.7802
500	.0418	4.8958	2.3170
520	1.5220	9.6479	.7439
540	5.6764	14.4617	.1965
560	12.4428	17.4758	.0052
580	20.5523	17.5831	-.0025
600	25.3405	14.8981	.0000
620	21.5762	10.0808	.0000
640	12.1740	5.0665	.0000
660	4.6387	1.8194	.0000
680	1.4092	.5461	.0000
700	.3576	.1372	.0000
Sum:	111.15	100.00	35.20

Appendix C.2 Continued.

(c) Source A

Wavelength (nm)	Wx	Wy	Wz
400	-0.0097	-0.0016	-0.0548
420	0.3784	0.0370	1.8073
440	1.1570	0.1829	5.9412
460	1.3696	0.5949	7.9943
480	0.5494	1.6679	5.2410
500	0.0331	4.1204	1.9608
520	1.3635	8.6492	0.6700
540	5.3866	13.7214	0.1873
560	12.4683	17.4920	0.0059
580	21.3961	18.2993	-0.0024
600	26.9732	15.8576	0.0000
620	23.4656	10.9640	0.0000
640	13.4560	5.6022	0.0000
660	5.1669	2.0269	0.0000
680	1.6136	0.6253	0.0000
700	0.4182	0.1605	0.0000
Sum:	115.19	100.00	23.75

(d) Source D65

Wavelength (nm)	Wx	Wy	Wz
400	-0.0812	-0.0185	-0.5188
420	3.5089	0.4115	17.1245
440	9.2449	1.3960	47.0236
460	4.4235	2.0213	25.9808
480	1.5250	4.4000	14.0622
500	0.0795	7.9692	3.7631
520	1.7890	12.1198	0.9339
540	8.3413	20.4367	0.2416
560	11.7490	17.0262	0.0163
580	16.9877	14.5007	-0.0045
600	17.2963	10.1462	0.0000
620	13.1405	6.1384	0.0000
640	6.1856	2.5695	0.0000
660	1.8341	0.7160	0.0000
680	0.3809	0.1470	0.0000
700	0.0520	0.0200	0.0000
Sum:	96.46	100.00	108.62

Appendix C.2 Continued.

(e) Source Philips TL84 (TL84)

Wavelength (nm)	Wx	Wy	Wz
400	-0.1103	-0.0174	-0.5909
420	1.8668	0.2195	9.1392
440	5.8551	0.9165	29.8622
460	2.4770	0.8980	14.2060
480	0.7670	3.6769	8.4049
500	0.0545	3.5109	2.9575
520	-0.2788	0.4217	-0.1587
540	16.5172	38.4428	0.4257
560	6.4270	12.0949	0.0543
580	13.4671	10.6071	-0.0079
600	27.8503	15.7766	0.0000
620	26.5600	12.9352	0.0000
640	1.2528	0.3850	0.0000
660	0.2688	0.0946	0.0000
680	0.0703	0.0270	0.0000
700	0.0275	0.0107	0.0000
Sum:	103.07	100.00	64.29

(f) Source Philips TL83 (TL83)

Wavelength (nm)	Wx	Wy	Wz
400	-0.0826	-0.0138	-0.4511
420	1.3859	0.1741	6.8454
440	4.0606	0.6033	20.5850
460	0.9116	0.3097	5.2706
480	0.4363	2.3136	5.0114
500	0.0447	2.1827	1.9576
520	-0.3299	0.0611	-0.0996
540	14.8702	34.6352	0.3821
560	6.6742	12.0093	0.0497
580	13.1023	10.7248	-0.0072
600	35.2099	19.6277	0.0000
620	34.2000	16.7489	0.0000
640	1.5144	0.4458	0.0000
660	0.3777	0.1348	0.0000
680	0.0742	0.0283	0.0000
700	0.0374	0.0146	0.0000
Sum:	112.49	100.00	39.54

Appendix C.2 Continued.

(g) Source Thorn Polylux 2700 (P27)

Wavelength (nm)	Wx	Wy	Wz
400	-0.0625	-0.0113	-0.3517
420	1.1050	0.1473	5.5037
440	3.0476	0.4281	15.3529
460	0.0211	-0.0627	0.1439
480	0.2794	1.9092	3.6348
500	0.0518	1.8298	1.8137
520	-0.4002	-0.3091	-0.1143
540	14.9146	34.6641	0.3798
560	6.3150	11.5650	0.0510
580	12.4078	10.2022	-0.0073
600	37.5462	20.8170	0.0000
620	37.2248	18.2686	0.0000
640	1.3985	0.3755	0.0000
660	0.3712	0.1313	0.0000
680	0.0756	0.0288	0.0000
700	0.0413	0.0161	0.0000
Sum:	114.34	100.00	26.41

(h) Source Thorn Polylux 3000 (P30)

Wavelength (nm)	Wx	Wy	Wz
400	-0.0518	-0.0100	-0.3026
420	1.3125	0.1634	6.4661
440	3.5630	0.5214	18.0453
460	0.9510	0.4635	5.6622
480	0.3574	1.0286	3.2980
500	-0.0061	1.7895	0.8779
520	0.3440	3.2515	0.2649
540	5.8133	14.1003	0.1584
560	16.9312	23.7028	0.0235
580	31.9610	27.3872	-0.0038
600	30.3124	17.9894	0.0000
620	15.8469	7.3784	0.0000
640	4.6192	1.8924	0.0000
660	0.7907	0.3018	0.0000
680	0.0976	0.0371	0.0000
700	0.0070	0.0026	0.0000
Sum:	112.85	100.00	34.49

Appendix C.2 Continued.

(i) Source Thorn White (W)

Wavelength (nm)	Wx	Wy	Wz
400	-0.0863	-0.0156	-0.4883
420	1.8698	0.2329	9.2141
440	5.0992	0.7462	25.8248
460	1.3722	0.6688	8.1696
480	0.5157	1.4825	4.7548
500	0.0003	2.6076	1.2650
520	0.5767	4.6534	0.3670
540	6.4522	15.7023	0.1811
560	17.2056	24.1043	0.0229
580	30.0548	25.8451	-0.0040
600	26.6073	15.7711	0.0000
620	13.5559	6.3028	0.0000
640	3.9193	1.6047	0.0000
660	0.6757	0.2579	0.0000
680	0.0871	0.0332	0.0000
700	0.0079	0.0030	0.0000
Sum:	107.91	100.00	49.31

(j) Source Thorn Warm White (WW)

Wavelength (nm)	Wx	Wy	Wz
400	-0.0729	-0.0134	-0.4153
420	1.6111	0.2018	7.9462
440	4.3889	0.6402	22.2178
460	1.0763	0.5312	6.4256
480	0.4103	1.1813	3.7830
500	-0.0032	2.0404	0.9981
520	0.4124	3.6195	0.2894
540	5.7116	13.9205	0.1584
560	16.9060	23.6179	0.0221
580	31.6768	27.1654	-0.0037
600	29.8404	17.7074	0.0000
620	15.5129	7.2221	0.0000
640	4.4829	1.8359	0.0000
660	0.7625	0.2909	0.0000
680	0.0944	0.0359	0.0000
700	0.0077	0.0029	0.0000
Sum:	112.82	100.00	41.42

Appendix C.2 Continued.

(k) Source Thorn Cool White (CW)

Wavelength (nm)	Wx	Wy	Wz
400	-0.0618	-0.0128	-0.3747
420	2.0987	0.2495	10.2654
440	5.6065	0.8414	28.4914
460	2.4202	1.1171	14.2403
480	0.8371	2.4038	7.6996
500	0.0183	4.1481	1.9933
520	0.9267	6.7614	0.5186
540	6.8966	16.8764	0.1988
560	16.6619	23.4187	0.0201
580	27.0759	23.2860	-0.0040
600	23.3963	13.8662	0.0000
620	11.6704	5.4207	0.0000
640	3.3454	1.3686	0.0000
660	0.5812	0.2219	0.0000
680	0.0789	0.0301	0.0000
700	0.0079	0.0030	0.0000
Sum:	101.56	100.00	63.05

(l) Illuminant ASTM E308 TL84 (TL84ASTM)

Wavelength (nm)	Wx	Wy	Wz
400	-0.0120	-0.0080	-0.1430
420	1.7460	0.2070	8.5620
440	6.3920	1.0000	32.6050
460	2.4220	0.9090	13.9360
480	0.7220	3.2970	7.7100
500	0.0430	3.3100	2.6740
520	-0.6440	-0.5890	-0.1570
540	17.3240	38.8460	0.3760
560	8.3550	15.8680	0.0750
580	10.2210	7.6350	-0.0110
600	25.8800	14.6180	0.0000
620	29.2460	14.1390	0.0000
640	1.7900	0.6300	0.0000
660	0.2830	0.0980	0.0000
680	0.0660	0.0250	0.0000
700	0.0330	0.0130	0.0000
Sum:	103.87	100.00	65.63

Appendix D.1 Mean visual results (ΔV_T) of 76 metamers under the 7 sources studied: D65, A, TL84, TL83, W, WW and P27.

Pair No.	D65	A	TL84	TL83	WF	WWF	P27
1	3.88	10.00	8.03	9.38	6.59	7.66	9.78
2	3.71	10.73	5.53	6.11	5.17	6.13	7.53
3	3.82	10.73	8.57	9.97	7.55	9.11	10.20
4	1.61	3.98	2.33	1.75	2.64	3.53	2.15
5	1.49	5.84	4.44	3.67	4.99	4.95	3.58
6	2.84	8.28	6.44	6.42	5.67	5.88	8.08
7	1.86	6.81	3.87	4.01	4.14	4.90	4.74
8	2.07	7.43	1.79	2.47	3.45	4.24	3.46
9	2.11	8.72	5.50	6.26	3.58	4.88	6.65
10	2.37	8.89	9.07	10.22	6.06	6.91	9.81
11	3.05	11.03	6.64	8.14	7.11	8.31	9.51
12	2.69	8.45	9.66	11.11	6.85	8.12	12.12
13	2.52	6.92	2.52	2.34	3.74	4.73	3.25
14	1.79	4.86	1.54	1.78	3.32	4.39	2.08
15	1.34	1.38	4.81	3.56	2.28	2.08	3.58
16	1.98	2.65	7.41	6.59	3.98	4.09	6.45
17	2.77	4.57	2.85	2.38	3.11	3.86	3.01
18	2.20	4.42	3.12	2.28	2.65	3.62	2.65
19	2.45	8.79	6.74	8.02	7.06	7.33	8.34
20	1.65	3.89	6.33	7.64	4.67	5.67	7.63
21	1.51	5.61	7.03	8.51	5.18	5.92	7.82
22	2.69	9.06	8.43	9.71	5.92	7.02	10.94
23	2.47	10.41	9.05	10.79	6.07	8.03	10.34
24	2.27	6.80	8.77	9.68	5.45	7.00	10.04
25	1.76	5.59	4.18	5.03	2.73	3.02	4.89
26	1.52	3.71	4.41	4.55	2.21	2.79	5.12
27	2.73	9.33	7.59	8.24	5.35	6.15	8.97
28	2.58	7.69	6.46	7.04	4.30	5.64	7.57
29	3.00	11.02	9.02	10.09	7.53	8.04	11.18
30	4.48	9.12	10.69	10.53	8.49	9.14	11.35
31	3.44	10.61	9.97	10.87	8.11	9.00	11.36
32	3.25	9.59	9.51	11.90	7.34	8.47	10.10
33	2.23	3.19	3.25	3.46	2.55	3.66	4.00
34	1.95	8.05	4.93	5.65	4.11	5.55	5.92
35	3.08	8.24	5.81	7.34	4.79	5.68	7.54
36	1.85	6.02	4.55	5.25	4.00	4.71	5.45
37	1.76	8.05	5.29	6.88	4.90	6.04	6.38
38	1.33	6.03	3.16	4.21	3.29	4.00	4.86
39	1.86	2.43	2.06	2.60	1.83	2.38	3.33
40	1.28	3.46	1.61	1.16	1.13	1.24	1.49

Appendix D.1 Continued.

Pair No.	D65	A	TL84	TL83	WF	WWF	P27
41	1.99	5.87	2.16	2.24	1.67	2.17	2.57
42	1.78	3.46	1.98	2.20	1.62	1.94	1.98
43	2.06	3.69	3.28	3.38	2.40	2.78	4.12
44	2.46	10.34	4.05	5.26	5.23	6.59	6.10
45	2.55	9.83	4.70	5.51	5.16	6.43	7.11
46	1.50	5.01	2.21	1.46	2.20	2.55	1.83
47	1.43	5.12	2.32	2.98	1.60	2.20	3.71
48	2.39	11.00	6.50	8.66	6.35	7.53	8.98
49	1.90	5.56	2.06	2.39	1.57	1.97	3.50
50	2.14	10.22	3.14	3.89	4.69	5.94	5.18
51	1.94	8.25	2.59	2.40	5.14	6.19	3.02
52	1.74	5.67	1.98	2.24	1.96	2.53	2.63
53	1.67	3.30	3.17	2.19	2.31	2.17	2.27
54	1.83	8.96	1.92	2.17	3.82	5.37	3.43
55	2.18	5.74	3.57	4.01	3.93	3.93	4.75
56	2.46	9.77	9.91	10.89	7.84	8.91	11.33
57	2.00	1.52	1.86	1.95	1.39	1.34	2.37
58	3.69	8.92	5.60	5.52	5.56	6.64	6.09
59	2.17	9.26	7.74	7.45	5.28	5.95	8.80
60	3.73	7.56	4.31	4.78	4.84	5.58	5.90
61	3.46	3.76	8.91	7.75	6.36	6.41	8.15
62	2.15	4.73	3.22	2.21	2.71	2.69	2.33
63	2.61	7.03	4.14	4.08	4.82	5.70	3.75
64	2.04	6.77	1.77	1.94	3.67	4.28	2.91
65	1.71	6.85	3.81	2.36	3.70	3.79	2.38
66	2.57	7.42	6.22	7.49	4.63	5.47	8.71
67	1.42	4.60	2.31	2.55	2.04	2.44	3.30
68	1.48	6.03	2.07	2.64	1.83	2.84	3.80
69	1.84	6.86	4.99	5.82	3.49	4.46	6.16
70	1.84	6.24	5.94	7.53	3.46	4.77	7.75
71	2.62	6.91	6.90	6.83	5.87	6.04	7.24
72	1.66	5.05	4.38	4.20	3.69	4.05	4.90
73	2.25	5.77	4.88	5.42	2.95	3.94	5.85
74	2.04	6.02	4.97	5.44	4.07	4.37	5.92
75	2.72	5.52	5.59	4.21	6.15	6.37	4.34
76	2.30	4.28	3.08	2.04	2.29	2.24	3.00

Appendix D.2 Mean visual results (ΔV_1) of 76 metamers under the 3 sources studied: D65, A and TL84.

Pair No.	D65	A	TL84
1	1.65	9.29	6.46
2	2.83	9.20	4.58
3	2.63	9.54	7.68
4	1.26	3.42	2.27
5	.89	5.02	4.36
6	1.71	6.88	6.23
7	1.10	5.81	3.48
8	1.55	7.01	.73
9	1.74	7.85	5.27
10	1.91	8.08	8.45
11	1.66	10.05	6.28
12	1.92	8.15	8.55
13	1.81	5.75	1.80
14	1.10	4.05	1.38
15	.65	.74	4.04
16	1.47	1.73	6.63
17	2.49	4.06	2.41
18	1.62	3.97	2.63
19	1.52	7.85	6.05
20	1.09	3.29	5.90
21	1.39	4.49	6.21
22	2.03	8.22	7.53
23	1.98	9.16	8.18
24	1.97	6.25	7.88
25	.91	4.52	4.17
26	1.23	2.92	3.52
27	2.05	8.41	7.27
28	1.89	7.25	5.54
29	2.07	9.95	8.82
30	3.31	7.35	10.09
31	2.67	8.86	8.91
32	2.44	8.80	8.23
33	1.90	2.72	2.43
34	1.61	6.68	4.82
35	2.10	7.90	5.46
36	1.39	4.81	3.94
37	.37	6.81	4.49
38	.48	4.74	2.70
39	1.16	1.79	1.64
40	1.19	2.55	1.34
41	1.88	5.18	1.76
42	1.39	3.20	1.68
43	1.88	2.93	2.87
44	1.61	9.80	3.92
45	1.42	8.88	4.48

Appendix D.2 Continued.

Pair No.	D65	A	TL84
46	.84	4.21	1.90
47	1.09	4.38	2.07
48	1.54	10.32	5.92
49	1.36	4.91	1.62
50	1.16	8.37	2.69
51	1.18	7.28	2.03
52	.99	4.86	1.25
53	1.20	3.03	2.74
54	.88	7.30	.92
55	1.73	5.01	3.41
56	1.68	8.52	9.40
57	1.41	.92	1.71
58	2.55	7.06	4.94
59	1.58	7.86	7.45
60	2.48	6.40	3.94
61	3.27	2.68	8.89
62	1.64	3.98	2.24
63	2.24	5.75	3.90
64	1.57	5.81	.76
65	.86	5.98	3.30
66	1.86	5.26	5.79
67	.93	3.89	2.22
68	1.09	5.15	1.70
69	1.43	5.40	4.47
70	1.37	4.80	5.03
71	2.15	6.03	6.24
72	1.27	4.20	3.46
73	1.41	5.09	4.45
74	1.18	5.30	4.45
75	2.37	4.01	4.75
76	2.00	3.92	2.54